Identification of Regulators and Effectors of RhoGTPase Signalling in Corneal Epithelial Cells

Stephen James Terry

This Thesis is submitted to University College London for the Degree of Doctor of Philosophy

March 2011

Department of Cell Biology

UCL Institute of Ophthalmology

11-43 Bath Street

London

EC1V9EL

Declaration

I, Stephen James Terry, confirm that the work presented in this thesis is my own. Where information has been derived from other sources, I confirm that this has been indicated in the thesis

London, March 2011

Abstract

Epithelial cells adhere to each other and are connected via a series of junctions. Tight junctions (TJs) are a specific type of junction consisting of heteromeric protein complexes that are linked to the actin cytoskeleton and are important in regulating paracellular permeability and cell polarity. RhoGTPases are small molecular switch proteins that are important regulators of the cytoskeleton and modulators of gene expression. RhoGTPases have thus been identified as being major signalling components associated with TJs. However little is known about how RhoGTPases are regulated to control junction formation and gene expression in corneal epithelial cells. I used a siRNA screening approach combined with functional assays to identify components of RhoGTPase signalling that affect the assembly of junctions and gene expression in Human corneal epithelial cells (HCE). I identified and validated several candidates that regulate junction assembly. One of these candidates was p114RhoGEF, a novel TJ localised guanine nucleotide exchange factor (GEF) important for the assembly of functional TJs. p114RhoGEF is a widely expressed and I discovered its depletion effects junction formation and morphogenesis in three dimensional culture systems in different epithelial cell types. p114RhoGEF is required for activation of RhoA at cell-cell junctions and junctional actinomyosin activity, p114RhoGEF is present in a complex containing Myosin II-A, the RhoA effector Rock II and the junctional adaptor protein Cingulin; indicating p114RhoGEF is a component of a junction associated RhoA-signalling module. p114RhoGEF, thus regulates spatial activation of RhoA at cell-cell junctions and organisation of the junctional cytoskeleton. p114RhoGEF may also have a role in cell migration, as depletion in HCE cells, caused cells to migrate at a

slower rate during wound healing assays. I have also started to explore the function of a putative p114RhoGEF ortholog, cg10188 in *Drosophila melanogaster*. Preliminary experiments have identified cg10188 to be important in larval development.

Contents

List of Figures

CHAPTER 1

CHAPTER 3

CHAPTER 4

CHAPTER 5

CHAPTER 6

List of Tables

CHAPTER 1

CHAPTER 2

CHAPTER 3

List of Abbreviations

α-PIX	PAK interacting exchange factor alpha
AJ	Adherens junction
AP-1	Adaptor protein 1
APC	Adenomatosis polyposis coli
aPKC	Atypical protein kinase C
ATP	Adenosine triphosphate
ATPase	Adenosine triphosphate hydrolysing protein
BBB	Blood brain barrier
BTB	Bric a brac tram track domain
BVES	Blood vessel epicardial substance
Caco-2	Colorectal adenocarcinoma
CaM	Calmodulin-dependent kinase
CAR	Coxsackievirus-adenovirus receptor
Cdc24	Cell division cycle 24
Cdc42	Cell division cycle 42
CDK4	Cyclin dependent kinase 4
CTD	Carboxy terminal domain
Dbl	Diffuse B cell Lymphoma
Dbs	Dbl's Big Sister
DH	Dbl-homologous
DLC	Deleted in Liver cancer
DMEM	DMEM Dulbecco's Modified Eagle Medium
DMSO	Dimethyl sulfoxide
DNA	Deoxyribonucleic acid
dNTP	Deoxynucleotide Triphosphate
DOCK	Dedicator of cytokinesis
DHR	Dock homology regions
E-Cadherin	Epithelial Cadherin
ECL	Enhanced chemiluminescence
EDTA	Ethylenediaminetetraacetic acid
EMT	Epithelial-mesenchymal transition
Erk	Extracellular regulated kinase
ERM	Ezrin radaxin and moesin
FBS	Fetal bovine serum
FRET	Fluorescence energy resonance transfer
GAP	GTPase activating protein
GDI	Guanine nucleotide dissocciation inhibitor
GDP	Guanosine diphosphatase
GEF	Guanine exchange factor

GFP	Green fluorescent protein
GLISA	G-protein linked immunosorbent assay
GPCR	G protein coupled receptor
GSK3b	Glycogen synthase kinase 3 beta
GST	Glutathione S-transferase
GTP	Guanosine triphosphatase
GTPase	Guanosine triphosphatase hydrolysing protein
GuK	Guanylate kinase
HCE	Human corneal epithelial cells
HCL	Hydrochloric acid
HeLa	Henrietta Lacks, cervical immortalised cancer cell line
IgG	IgG Immunoglobulin G
IKK	IκB kinase
IPTG	Isopropyl β-D-1-thiogalactopyranosid
ITSN	Intersectin
JACOP	Junction-associated coiled-coil protein
JAM	Junction adhesion molecules
K-SFM	Keratinocyte serum free media
LARG	Leukemia-associated Rho GEF
LB	Luria-Bertani
MARK	Microtubule affinity-regulating kinase
MDCK	Madin-Darby Canine Kidney
mDia	Mammalian diaphanous
MeOH	methanol
MLC	Myosin II regulatory light chain
MRCK	Myotonic dystrophy related kinase
MUPP1	Multi-PDZ-domain protein 1
MYPT	Myosin phosphatase target subunit
NACos	Localise to nucleus and adhesion complexes
NF-kB	Nuclear factor kappa-light-chain-enhancer of activated B-cells
NTD	Amino Terminal domain
PAGE	Polyacrylamide gel electrophoesis
PAK	p21-activated kinase
PAR3	Partitioning protein 3
PAR6	Partitioning protein 6
PATJ	Pals 1 associated tight junction protein
PBS	Phosphate buffered saline
PCNA	Proliferating cell antigen
PCR	Polymerase Chain Reaction
PDZ	Post synaptic density protein (PSD95), Drosophila disc large tumour suppressor (DlgA), and zonula occludens-1
PFA	Paraformaldehyde
PH	Pleckstrin Homology
PI(3,4,5)P3	Phosphatidylinositol 3,4,5-trisphosphate
PI(3,5)P2	Phosphatidylinositol 3,4-bisphosphate
PI(3)P	Phosphatidylinositol 3-phosphate

PI(4,5)P2	Phosphatidylinositol 4,5-bisphosphate
PI(4)P	Phosphatidylinositol 4-phosphate
PI3K	Phosphatidylinositol 4,5-bisphosphate 3-kinase
PKC	Protein Kinase C
PMSF	Phenylmethylsulfonyl fluoride
Rab	Ras-like protein in brain
Rac1	Ras-related C3 botulinum toxin substrate 1
RGS	Regulator of G protein signalling domain
Rho	Ras homolog
RNA	Ribonucleic acid
RNAi	Ribonucleic acid interference
ROCK	Rho-associated protein kinase
SDS	Sodium dodecyl sulfate
SH3	Src Homology 3
shRNA	Short Hairpin ribonucleic acid
siRNA	Short interfering ribonucleic acid
TCF	T- cell factor
TEM	Transmission electron microscopy
TER	Transepithelial Resistance
Tiam-1	T-cell lymphoma invasion and metastasis-inducing protein
TJ	Tight Junction
TNFα	Tumour necosis factor alpha
UAS	Upstream Activation Sequence
VASP	Vasodilator-stimulated Phosphoprotein
VEGF	Vascular endothelial growth factor
WASP	Wiscott-Aldrich Syndrome Protein
Wnt	Wingless and Int
ZEB	Zinc finger E-box-binding homeobox
ZO	Zona Occludens
ZONAB	(ZO-1)–associated nucleic acid binding protein

CHAPTER 1

INTRODUCTION

Introduction

(Parts of this introduction were published as a review article titled 'Rho signalling and Tight junction functions', see reference [4])

Overview

In multicellular organisms, epithelia consist of specialized cells that form selective barriers controlling the passage of water, ions and other small molecules between different body compartments and the external environment. This requires cells to be polarized, that is, to form distinct membrane domains. An apical side, for facing the lumen of a body cavity or the outside environment and a basal side, adjacent to the underlying tissue. For instance, the epithelial cells lining the intestinal lumen are at the interface between the internal and external environments regulating the absorption of nutrients and water, as well as ion homeostasis. In addition, these cells provide a protective barrier against commensal and pathogenic microorganisms. Epithelial cells have to adhere tightly to each other to form sheets and are connected to each other via a series of intercellular junctions (Figure 1.0). Gap junctions are one class of junction, these are communicating junctions that form intercellular pores between adjacent cells and allow the selective passage of small molecules up to 1kDa. They are composed of twelve connexin subunits, of which six subunits known

as a connexon, are contributed from each adjacent cell [8]. Three other classes of epithelial junctional complex exist, Tight junctions (TJs), Adherens junctions (AJs) and Desmosomes, known collectively as the epithelial junctional complex [9, 10].

These structures consist of heteromeric protein complexes and are linked to different cytoskeletal elements. They mediate cell-cell adhesion to different extents, and play crucial roles in the biogenesis and maintenance of epithelial barriers In epithelial cells, the distribution of TJs and AJs is generally spatially well defined: TJs are typically located at the apical end of the basolateral membrane, where they form an apical ring, while AJs and desmosomes are located more within the basolateral membrane [9]. In contrast, the distribution of junctional complexes in endothelial cells is less defined, with TJs and AJs being more intertwined with each other [11, 12]. TJs and AJs are both linked intracellularly to the actin cytoskeleton, which is often seen to co-localize with junctions to form a “belt like” ring of filaments encircling the perimeter of the cell, sometimes referred to as “perijunctional actin”. In contrast, desmosomes are linked to intermediate filaments of the keratin family and function to confer structural strength to epithelia enabling them to resist pressure, shear stress and friction [13 14]. In epithelia desmosomes appear to be located more basally than TJ and AJ and are distributed along the lateral membrane of adjacent cells. Hemidesmosomes are a special class of junction related to Desmosomes and form along the basal membrane. They are involved in attachment of epithelia to laminin, an extracellular matrix protein of basement membranes [14].

At the electron microscopic level, (Figure 1.1) AJs are present at sites where the two opposing membranes of neighbouring cells are separated by a gap of about 20nm along which the neighbouring plasma membranes appear very parallel over a distance of 0.2-0.5μm [7]. Using deep etching electron microscopy to observe structures within the inter cellular space in this parallel region, AJs were found to be connected to each other by numerous cylinder-like projections, that are thought to be multimeric structures containing the transmembrane components of AJs known as Cadherins and nectins (see molecular composition of AJ). TJs at the resolution of transmission electron microscopy (TEM), appear as sites where there is close apposition of adjacent plasma membranes between neighbouring cells [9] (Figure 1.1). In freeze fracture replicas, these close contact sites are seen as networks of intracellular strands that encircle the cells below the apical surface [15-17] (Figure 1.1). TJs can mediate adhesion, but primarily act as dynamic barriers that selectively regulate the diffusion of water, ions and other small molecules through the paracellular space between neighboring cells. They also function to maintain cell polarity, by acting as a molecular barrier, thus restricting the diffusion of apical and basolateral membrane components. The functional role for AJs is somewhat similar to desmosomes as its name implies they are crucial for the initiation and maintenance of intercellular adhesion. The initiation of adhesion, developmental cell movements, tissue biogenesis and wound repair all require dynamic changes in cell adhesion, AJ complexes provide the strength to maintain stable cell-cell associations in response to external stress caused by tissue

morphogenesis or body movement, thus contributing to embryogenesis and tissue homeostasis.

Aside from the adhesive properties and the classical gate and fence functions, intercellular junctions have emerged to act as dynamic heteromeric signalling complexes. [18] [19]. The signalling at junctions is bi-directional, such that signals are transmitted from the cell interior to forming or existing junctions, to regulate their assembly and function, while junctions coordinately receive and transmit information back to the cell interior to regulate gene expression and subsequent cellular behaviour like proliferation and differentiation. Multiple TJ and AJ components interact with the actin cytoskeleton. These interactions are known to be important to regulate the permeability properties of TJs, mediate the strength of adhesive contacts of AJs and for processes that require junctional reorganization during the initiation of cell-cell adhesion and assembly of junctions. Many studies have implicated both actinomyosin contractility and actin dynamics, such as filament polymerization and turnover, as being important mechanisms in the formation, maintenance and regulation of the permeability properties of junctions [20-27]. Junctions also recruit signalling proteins that regulate gene expression and, subsequently, proliferation and differentiation.

In this introduction, I will first provide a comprehensive overview of the molecular composition of junctions. Introduce small molecular switch proteins known as RhoGTPases that function as important cytoskeletal regulators and modulators of gene expression. I will then discuss how they are regulated and

have recently emerged as being major signalling components associated with junctions.

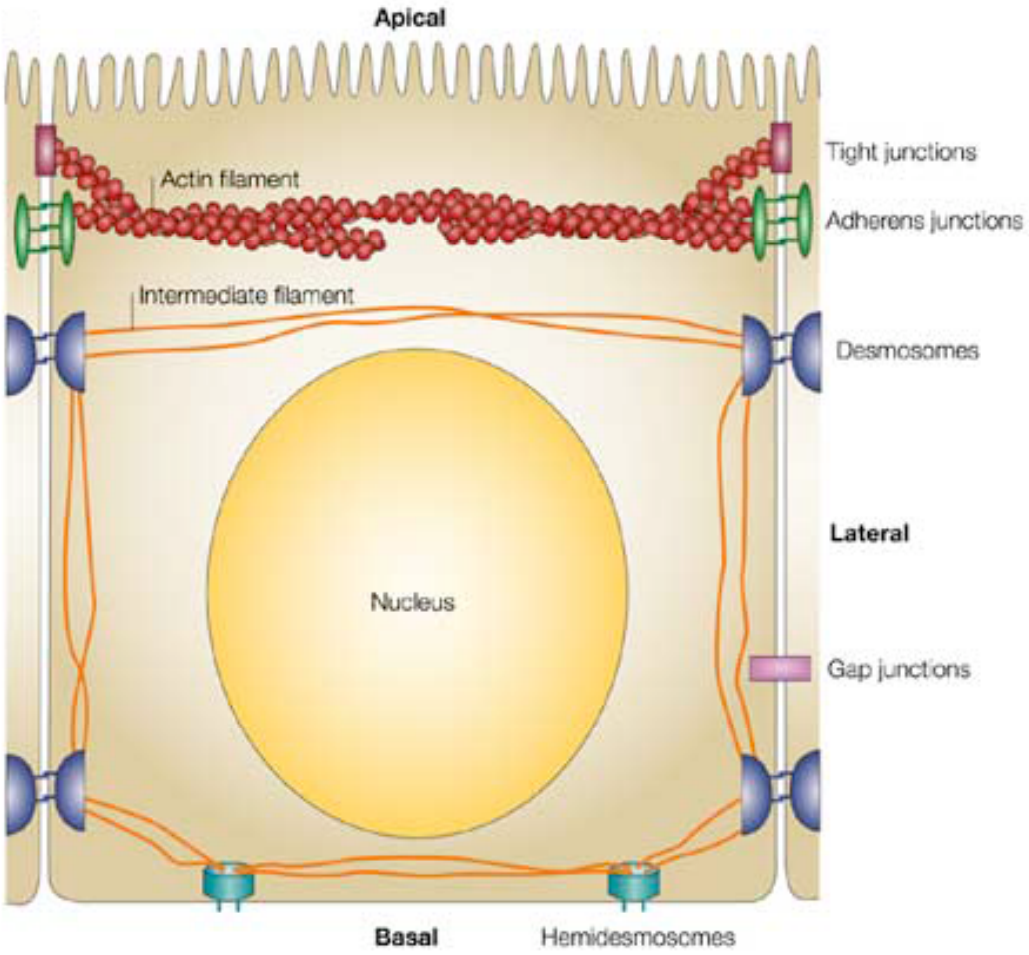

Figure 1.0 Epithelial intercellular junctions.

Schematic representation of a polarized absorptive epithelial cell illustrating different types of intercellular junction. Gap junctions are a type of intercellular junction and form small pores between two adjacent cells and allow the selective passage of small molecules up to 1kDa. Tight junctions, Adherens junctions and Desmosomes form what is known collectively as the epithelial junctional complex. All these types of junction consist of heteromeric protein complexes having similar architecture of transmembrane proteins that are linked to a cytoplasmic plaque of diverse adaptor and signaling proteins. Tight junctions(TJ) are the most apical of this complex whereas Adherenes junctions (AJ) and Desmosomes are located more basally along the lateral membrane. Desmosomes and AJs function primarily in cell-cell adhesion, whereas TJ are known to regulate Paracellular permeability. Both TJs and AJs are linked to the actin cytoskeleton, whereas Desmosomes are linked to Intemediate filaments of the Keratin class. Hemidesmosomes are structures similar to Desmosomes being linked to Intermediate filaments but, Cell-extracellular matrix adhesions. Diagram from [3]

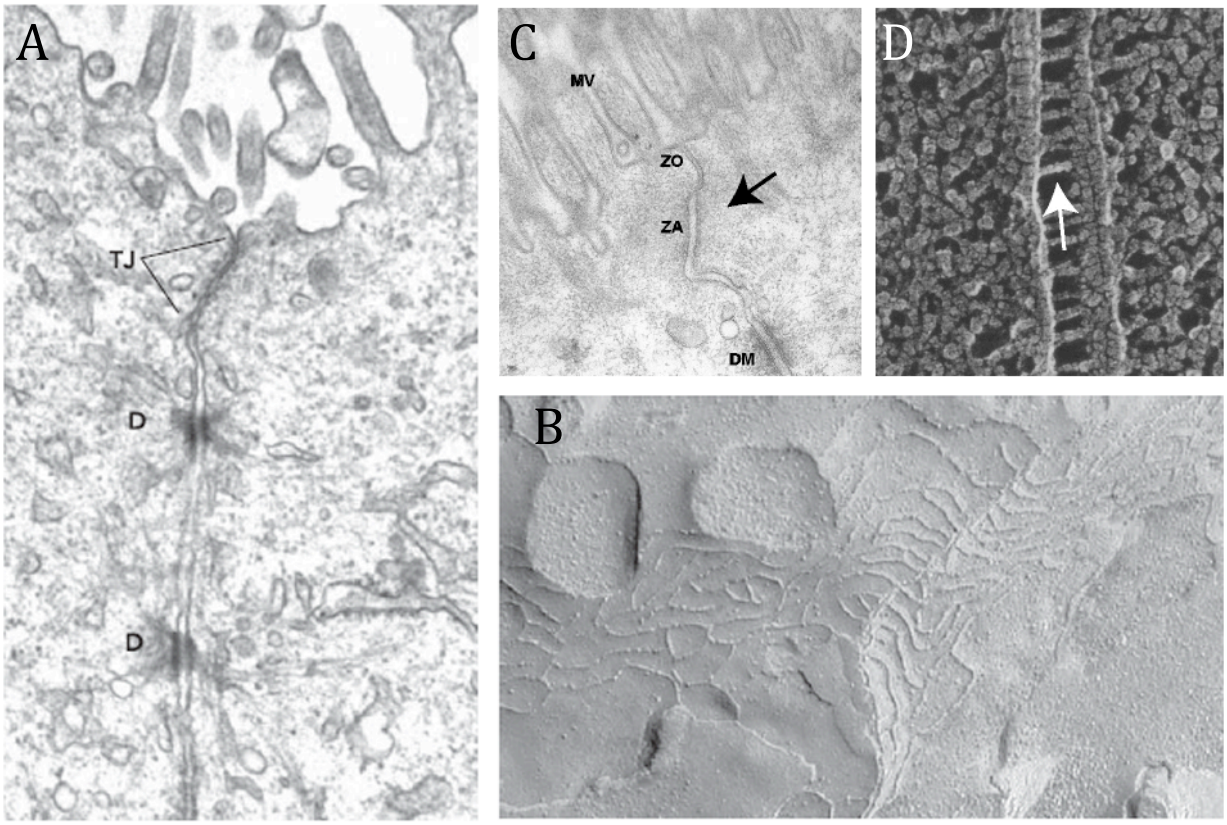

Figure 1. 1 Structure of the Epithelial Junctional Complex.

A Transmission electron micrograph (TEM) of Kidney epithelial cells the apical junctional complex, Tight junctions (TJ) can be seen at sites of close opposition in between opposing plasma membranes of neighbouring cells Desmosomes (D) appear in regions located more basaolateral to the apical TJs [2]. **B** freeze fracture replica of intestinal epithelial cells showing transmembrane based TJ strands. [5] **C** TEM image of apical junctional complex in intestinal cells showing the microvilli (MV) and the position of ZO (zonula Occludins / TJ) Zonula Adherenes (ZA/AJ) , Desmosomes (DM). The arrow marks the site of AJ where the two adjacent plasma membranes of neighbouring cells run very parallel [7]D Quick-freeze, deep-etch image of the AJ between intestinal epithelial cells. White arrow shows the presence of rod-like bridging structures extending between adjacent cells [7]

Molecular composition of Tight junctions

At the molecular level, TJs consist of multimeric protein complexes, having a similar architectural principle as other cell-cell adhesion complexes [7, 28, 29]. The TJ complex is composed of integral membrane proteins linked to a network of adaptor proteins that form a cytoplasmic plaque (Table 1.0). The transmembrane proteins are known to mediate cell-cell adhesion as well as to form the paracellular barrier. The adaptors of the cytoplasmic plaque act as linkers between transmembrane proteins and the cytoskeleton, and as scaffolds, to recruit different types of signalling proteins. The transmembrane proteins of the TJ are often grouped according to the number of times they span the plasma membrane. There are single pass membrane proteins such as JAMs (junction adhesion molecules) [30-32] and CAR, (Coxsackievirus-adenovirus receptor) [33]; three pass membrane proteins such as BVES (blood vessel/epicardial substance) [34]; and four pass membrane domains such as the claudins (24 family members) [17, 35], Occludin [36, 37], tricellulin, a protein enriched at cell-cell contact points between three adjacent cells [38] and the recently identified MarvelD3 [39]. While most of the transmembrane proteins seem to have at least some adhesive abilities, it is the tetraspan membrane proteins that seem to be more directly linked to epithelial barrier functions [17, 40, 41].

The claudins are thought to be the major components of tight junction strands and seem to underlie the different barrier properties of different types of

epithelia due to the tissue-specific expression of different claudins [42, 43]. Aside from being a structural components of the junctional barrier, Claudins are responsible for the ion selectivity of the paracellular pathway, a function that is thought to involve the formation of ion-selective pores or channels. [35, 41, 44-46]However, the molecular structure of these ion-selective pores remains unclear. The role of Occludin in barrier permeability is controversial due to the discrepancy between the Occludin mouse knockout model and the many in *vitro* studies. While the Occludin knockout mouse model exhibited complex phenotypic defects in a range of epithelia, TJs themselves did not appear to be affected morphologically, and, as far as examined, the barrier function of the intestinal epithelium was normal [47, 48]. However, data from cells in culture suggest an important role for Occludin in the permeability properties of TJs [37, 49]. For example, overexpression studies of Occludin in MDCK cells resulted in raised transepithelial electrical resistance (TER), a measure of the instantaneous ionic conductivity properties of an epithelial layer, but also to increased size-selective paracellular tracer permeability, a measure of slow diffusion across junctions [50]. The observation that dominant negative Occludin constructs inhibit paracellular tracer permeability suggests that Occludin promotes permeability [37]. The exact mechanisms behind these observations remain unclear, but these and similar observations suggest that ion conductance and tracer permeation are mediated by distinct molecular mechanisms that can be differentially regulated [37]. When Occludin was depleted by RNA interference in MDCK cells, paracellular permeability was not effected, but a failure to activate the RhoGTPase RhoA in response to certain stimuli was observed [51]. Moreover, a recent study demonstrated Occludin

regulates barrier function in response to pro inflammatory cytokines. Stimulation of MDCK II cells with a combination of pro inflammatory cytokines[52], TNFα and INFγ resulted in increased TER and decreased paracellular permeability. Knockdown of Occludin attenuated the barrier alterations induced by these cytokines, suggesting Occludin contributes to regulating epithelial barrier functions of epithelial cells in response to inflammatory stimuli.

Many of the transmembrane proteins interact with proteins in the cytoplasmic plaque via PDZ(**P**SD/**D**lgA/**Z**O-1)-binding domains present in their cytosolic domains and PDZ domains found on components of the plaque such as ZO-1, ZO-2, and ZO-3 [53-55] ; PAR-3 and PAR-6[56]; Pals1 [57] and PATJ[58], MUPP1[59] and the MAGI proteins [60] . However there are several adaptor proteins that do not contain PDZ domains. Examples are JACOP/ paraCingulin [61, 62] and Cingulin, a protein known to interact with junctional membrane proteins; ZO-1, -2 and -3; as well as F-actin, Myosin II and GEF-H1, a junction associated activator of the RhoGTPases [63, 64].

Scaffolding proteins also mediate interactions with filamentous actin, thus linking the TJ to the actin cytoskeleton, and recruit many different types of signalling proteins to the TJ. These include various protein kinases such as different isoforms of protein kinase C (PKC); protein and lipid phosphatases; small monomeric G proteins such as Rho, Rab and Ras GTPases and their regulators; as well as heterotrimeric GTPases [2, 28, 65]. In addition, transcription factors are also recruited to junctions via scaffolding proteins, which is thought to be important for the regulation of gene expression [66].

The ZO proteins are classic examples of scaffolding proteins of TJs. ZO-1, 2 and 3 have three PDZ binding domains and a single SH3 and GuK domain. The ZO proteins have been shown to interact directly by *in vitro* binding assays with the C terminal domain of Claudins 1-8 through their PDZ1 domains [67]. The ZO-proteins also interact in *vitro* with Occludin. This interaction is mediated between the GuK domain and region in the centre of the C terminal domain of Occludin [68].

The C-terminal region of ZO-1 [69] and ZO-3 [70] are known to bind f-actin in co-sedimentation assays, whereas ZO-2 does not [69, 71]. ZO-1 can also homodimerise and can bind ZO-2 and 3 but, ZO-2 and 3 can not form a complex with each other [71]. They also bind α-Catenin, a component of AJs that binds actin filaments [72]. This interaction between the ZO proteins is thought to provide "fine tuning" of components in junctions to allow different types of scaffold structures permitting, different types of connections to the actin cytoskeleton provide a linking scaffold for signalling crosstalk between components of AJs and TJs.

ZO-1 has been implicated in controlling epithelial cell proliferation and differentiation. One line of evidence comes from experiments where truncated forms of ZO-1 were expressed in MDCK cells and resulted in partial dedifferentiation. [73] ZO-1 and ZO-2 expression can be altered in certain types of tumours[74, 75], suggesting a functional link in the suppression of factors that promote proliferation. For example in colorectal cells, ZO-1 expression is down

regulated where the AJ component β-Catenin is overexpressed.[76] β-Catenin is involved in Wingless/Wnt growth factor signalling and regulates transcription by association with the T cell factor (TCF)/Lef transcription factor. β-Catenin signalling is often deregulated in many cancers, leading to activation of β-Catenin, therefore β-Catenin promotes proliferation [77, 78]. It seems that β-Catenin signalling inactivates the growth suppressive function of ZO-1. An involvement of ZO-1 in nuclear processes has also been suggested, based on reports that show it localised to the nucleus. However this localisation is somewhat controversial, as different laboratories disagree about the nuclear localisation of ZO-1 [79] [80, 81] ZO-1 is known to affect the transcription of several genes [82, 83], however this does not require nuclear localisation of ZO-1, but sequestration of a transcriptional repressor protein known as ZONAB [80].

ZONAB is a protein that is an interesting example of a class of protein termed NACos (localise to nucleus and adhesion complexes) [82]. This type of protein has a dual localisation and provides TJs with a means to directly regulate gene expression and subsequently cellular behaviour, such as proliferation. ZONAB is a Y box transcription factor that binds to the SH3 domain of ZO-1[80]. ZONAB localises to the nucleus where it acts as a transcriptional repressor of the Erb-2 gene and renal differentiation markers [80] and can stimulate transcription of cyclinD1 and PCNA genes [83], which is important in proliferation. ZONAB is known to bind sequences containing inverted CCAAT boxes from several different promoters in vitro [80]. In MDCK (Madin-Darby canine kidney) cells, ZONAB is expressed at high levels during proliferation and is present at TJs

and the nucleus. It becomes down-regulated in mature monolayers, and is no longer present in the nucleus [82]. Experiments in MDCK cells where ZO-1 was over-expressed reduced the nuclear accumulation of ZONAB and inhibited proliferation. This suggested that TJs modulate epithelial proliferation through the sequestration of ZONAB by ZO-1[82]. Further evidence to support the role of ZONAB in proliferation was shown by its ability to directly interact with CDK4, a G1/S phase regulator. CDK4 was shown to localise to junctions and the nucleus. The nuclear accumulation of CDK4, like ZONAB can also be inhibited by over-expression of ZO-1[82]. Several promoters of genes that are G1/S phase regulators have ZONAB binding sites. Cyclin D1 and PCNA (proliferating cell nuclear antigen) and have been demonstrated to be up-regulated in ZONAB over-expressing cells [83]. This evidence demonstrates nuclear accumulation of ZONAB is linked to the regulation cell cycle genes and is a good example of how TJs, can by direct mechanisms regulate gene expression. TJs can thus be seen as actin-bound, multimeric protein complexes that interconnect neighbouring cells that receive and send signals and thereby regulate epithelial barrier functions, as well as epithelial proliferation and differentiation.

Protein	Interacting partners
Tight junctions	
Transmembrane proteins tetraspan	
Occludin	*ZO-1,2,3 JAM-A, Cingulin, MarvelD3,YES,PI3K,ERK1,casenin kinase 1ε PP1,PP2A,itch,F-actin*
Claudins	*ZO-1,2,3,PATJ, MUPP-1,PATJ,WNK4,OAP1,EphA2*
MavelD3	*Tricellulin*[84]
Tricellulin	*ZO-1, MavelD3*
Transmembrane proteins single span	
JAM, CAR,	*Occludin, ZO-1,Cingulin, PAR3,MUPP-1, AF6/afadin*
ESAM,CLMP	*reovirus,adenovirus,coxsackievirus*
BVES	*ZO-1* [34]
CRB3 (crumbs homologue 3)	*Pals1, PatJ and PAR6*
Cytoplasmic adaptor proteins	
ZO-1	*Occludin, Claudins, JAMs,BVES, ZO-1, 2, 3, Cingulin,Tuba,Apg2, f-actin α-Catenin,α-actinin,Afadin,shroom2, connexins*
ZO-2	*Occludin, claudins, ZO-1, F-actin, Cingulin, α-Catenin, f-actin,hScrib, connexin 43,SAFB,Jun,fos,Myc,Csk,AP1*
ZO-3	*Occludin,claudins,ZO-1,Cingulin,PATJ,Afadin,p120Catenin,f-actin*
MAGI-1	*PTEN.JAMs,synaptopodin,MASCOT,α-actinin, Rap GEF2*
MAGI-2	*PTEN,β1-adrenergic receptor*
MUPP-1	*Claudins, JAMs, CAR*
PATJ	*Pals1, CRB3,PATJ,ZO-3,JEAP,angiomotin*
Pals1	*PATJ,CRB3,PAR6,Lin7,MPP4*
PAR-6	*CRB3,PAR3, aPKC, Cdc42,Rac1,Pals1,smurf,Ect2,TGF-β receptors*
PAR-3	*PAR-6,Tiam-1,aPKC,Cdc42,Rac-1,14-3-3proteins*

JEAP	*PATJ*
Cingulin	*ZO-1, -2, -3, JAM, F-actin, Myosin II,GEF-H1*
paraCingulin (JACOP)	*GEF-H1, Tiam-1, f-actin*
Shroom2	*ZO-1,MyosinVIIa*
Amot	*Rich-1,Pals-1, PatJ, Par-3* [85]
Signalling proteins	
aPKC	*Occludin PAR3. PAR6,Cdc42,*
GEF-H1	*Cingulin, ZONAB, RhoA*
CDK4	*ZONAB,D-type cyclins*
G proteins	*ZO-1 Gα12*
PTEN	*MAGI-1,2,3,PAR3*
PP1	*Occludin*
PP2A	*Occludin*
Rich1	*Amot* [85]
Tuba	*ZO-1, Cdc42*[86]
YES	*Occludin*
Rab 3b	*Noc2,plgR,calmodulin*
Rab13	*Protein kinase A, MICAL-L2*
WNK4	*Claudins*
Transcriptional regulators	
ZONAB	*ZO-1, GEF-H1, CDK4, symplekin*
Symplekin	*ZONAB, poly adenylation factor CstF,HSF1*
AP-1	*ZO-2*
HuASH1	*Unknown*

Table 1.0 Molecular components of Tight junctions.

Shown above is list of different classes of protein (Transmembrane, Adaptor, Signalling and transcriptional regulator) that are associated with the TJ complex. Interaction partners are also listed for particular proteins. This is by no means a complete comprehensive list, as many more novel TJ proteins and new associations between them yet to be discovered. Table adapted from [2] [6] where additional information has been added the reference is indicated.

Molecular composition Adherens junctions

AJs are adhesive junctions in epithelial cells. The main adhesion receptors in these junctions are Cadherin family proteins (Table 1.1). E-Cadherin is a member of the Cadherin super-family expressed in most epithelial tissues [87]. E-Cadherin is the most understood of all the Cadherins due to its prominent role as a tumour suppressor and regulator of morphogenesis [19]. E-Cadherin, like all Cadherin proteins, is a single pass transmembrane glycoprotein. It is the extracellular domain of E-Cadherin that forms homotypical interactions with E-Cadherins in neighbouring cells. This interaction is calcium dependent, as calcium is required for the correct comformational organisation of the extracellular domain.[88] Interactions between the cytoplasmic domain of E-Cadherin and other proteins, namely the Catenins, recruit signalling components that are important for linkage to and regulation of the local actin cytoskeleton and also the control of gene transcription. The cytoplasmic domain of E-Cadherin binds directly to Catenin family members β-Catenin and p120 Catenin [89 90]. α-Catenin is known to directly bind to β-Catenin to form a dimmer, resulting in the formation of a Cadherin-Catenin complex. α-Catenin is indispensable for Cadherin-mediated adhesion; absence of α-Catenin disrupts the formation of AJs and the association of the Cadherin-Catenin complex with actin filaments is prevented. α-Catenin binds bundles of actin filaments and actin interacting proteins such as ZO-1, α-actinin, vinculin, ZO-1, formin 1, afadin and Eplin [72, 91-93].

It was thought on the basis of several observations that the α-β-Catenin dimer links the Cadherin complex to the actin filaments and so physically connects the AJ to the actin cytoskeleton, and thus represents a structural component of the assembly, maintenance and function of the AJ complex [94]. However this model is somewhat controversial, and some studies suggest that α-Catenin is not directly involved in the linkage between the E-Cadherin/β-Catenin complex and actin filaments because experiments show that binding of α-Catenin to actin and β-Catenin in *vitro* is mutually exclusive [95, 96]. Alternative models of how E-Cadherin complexes are linked to the actin cytoskeleton suggest other β-Catenin binding proteins [97] or other unknown α-Catenin/actin binding proteins. However a recent study showed that when force was applied to α-Catenin generated from the spatial activation of actinomyosin contraction at the basalolateral membrane, only the stretched region of α-Catenin was able to recruit vinculin, an actin binding protein, resulting in linkage to the actin cytoskeleton and AJ development [98]. This study may offer an alternative explanation for the mutually exclusive binding of α-Catenin to actin and β-Catenin in *vitro* as this could be a reflection of the technical difficulties of isolating this complex just because it does not bind in *vitro* does not mean it never occurs. Indeed, it is possible that when force is applied to α-Catenin it may change its structure to reveal a masked actin binding site when α-Catenin is bound to the E-Cadherin/β-Catenin complex.

Nectins are another class of transmembrane protein associated with AJs [99, 100]. The interactions between Nectin proteins unlike Cadherins is calcium

independent. The cytoplasmic domain of Nectins associates with Afadin, [101] which is known to bind to f-actin [102] and also weakly to α-Catenin [101]. It is thought that via this link Nectin complexes are linked to the actin cytoskeleton. However it still remains unclear how Nectin complexes are physically associated with Cadherins. It is probably mediated via Afadin/ α-Catenin interactions, as Afadin and α-Catenin are known to be essential for this interaction [101, 103], but may involve other unknown intermediate adaptor proteins.

β-Catenin is a multifunctional protein, that is a key component of AJs. β-Catenin is able to interact with multiple binding partners that function in cell-cell adhesion and also translocates to the nucleus, where it can associate with LEF/TCF transcription factors, important for proliferation [104] [105]. The tumour suppressive function of E-Cadherin is partly due to its sequestration of β-Catenin at cell-cell adhesion sites [77]. Overexpression of β-Catenin is also often seen in many cancers [77, 106] [78] and is generally thought to promote proliferation.[107] It is not fully understood how different cellular pools of β-Catenin are regulated and communicate with each other. The Wnt/wingless growth factor signalling pathway is one of the main regulators of β-Catenin [107]. Wnt signalling regulates the activity of glycogen synthase 3β(GSK3β), which in turn controls the phospholyation state of β-Catenin. Phospholyated β-Catenin is present in a complex with adenomatous polyposis coli protein (APC) and axin resulting in ubiquitination and subsequent targeting of β-Catenin to the proteasome for degradation [108]. In the absence of Wnt signalling β-Catenin remains phospholyated and therefore degraded in the cytoplasm. In the

presence of Wnt, GSK3β is inactivated and β-Catenin remains dephosphorylated resulting in an inhibition of degradation, translocation to the nucleus and activation of gene transcription mediated by LEF/TCF [109, 110].

Protein	Interacting partners
Adherens junctions	
Transmembrane proteins	
Cadherins	*Cadherin, β-Catenin, p120-Catenin,Hakai,RapGEF1 (C3G)*
Nectin	*Nectin, afadin, PAR-3*
Vezatin	*Myosin VIIA, Cadherin–Catenin complex*
Cytoplasmic adaptor proteins	
α-Catenin	*β-Catenin, F-actin, ZO-1, Ena-VASP, formin-1, afadin, Zyxin, Spectrin, α-actinin, vinculin, Eplin*
β-Catenin	*α-Catenin, p120-Catenin, Lin-7, IQGAP, fascin, PI3-kinase,RapGEF6*
p120-Catenin	*E-Cadherin, β-Catenin, VAV-2 (Rho-GEF),p190RhoGAP,RhoA*
Afadin	*Nectin, α-Catenin, F-actin, ZO-1, Ponsin, profilin, Bcr, c-Src*
Eplin	*F-actin, α-Catenin*

Table 1. 1 Molecular components of Adherens junctions.

Shown above is list of different classes of protein (Transmembrane, or adaptor) that are associated with the AJ complexes. Shown also are interaction partners of particular AJ components . Table adapted from [2, 6].

AJs aside from regulating β-Catenin mediated transcriptional responses can also regulate the activity of the transcription factor NF-κB. NF-κB regulates genes involved in cell growth and survival [111] [112, 113], pro-inflammatory immune responses [114] as well as genes important for Epithelial to Mesenchymal Transition (EMT) [115].

NF-κB is a structurally conserved family of transcription factors that exist as dimeric complexes. Each monomeric subunit of the dimer contains a N-terminal 300 amino acid sequence termed the Rel homology domain, which contains sequences important for dimerisation, nuclear localization and DNA binding [114]. There are five NF-κB monomeric subunits in mammals; these are p65 a.k.a RelA, c-Rel, RelB, p50 and p52. NF-κB subunits bind DNA target sites upon homo or hetrodimerisation with each other to form transcriptionally active complexes that have varying activities depending on subunit composition [116] . NF-κB complexes are normally sequestered as transcriptionally inactive complexes in the cytoplasm by association of an inhibitory binding protein IkBα that prevents NF-κB from translocaling to the nucleus [116]. In general activation of the canonical pathway involving p65/p50 and c-Rel/p50 NF-κB complexes is preceded by activation of the IKK complex that phospholyates the inhibitory binding protein IkB resulting in its degradation and thus permitting NF-κB to translocate to the nucleus where it mediates transcription of target genes [116].

Many studies have implicated NF-κB transcriptional activity to be required for the maintenance and invasive phenotypes of cancers [115, 117 118]. NF-κB is known to activate several developmentally important transcription factors such as snail, slug, twist, ZEB1 and 2 that are important for promoting EMT by promoting the expression of genes important for maintaining a mesenchymal phenotype such as vimentin fibronectin and metalloproteinases[115], while repressing epithelial phenotype associated genes such as E-Cadherin [119], occuldin and claudins [120]. The snail family of transcription factors is known to regulate EMT during developmental processes as well as to participate in tumour progression. Snail is a direct repressor of E-Cadherin gene transcription [119].

A recent study observed the p65 subunit of NF-κB in association with a complex formed by E-Cadherin/ α,β and p120 Catenins [121]. This E-Cadherin-Catenin-p65 complex was disrupted when AJs were perturbed by K-ras overexpression or E-Cadherin depletion by siRNAs. Furthermore stimulation of basal and TNFα stimulated NF-κB transcriptional activity was also observed when E-Cadherin was depleted, suggesting that E-Cadherin, in a manner analogous to E-Cadherin-β-Catenin interactions, represses NF-κB activation possibly by sequestering it at AJ complexes and thereby suppresses transcription of Snail and other transcription factors important for promoting EMT.

p120 Catenin is a component of AJ showing structural similarities to β-Catenin. p120 like β-Catenin can also bind to E-Cadherin and plays a role in cell-cell

adhesion[122]. Like β Catenin, p120 Catenin can function as a transcriptional regulator, but instead of regulating LEF-1 it is known to regulate another transcription factor called Kaiso that is known to repress transcription of β-Catenin target genes [123].

Studies in a mouse model where p120 Catenin is conditionally knocked out in the epidermis revealed links between p120 Catenin and the regulation of NF-κB signalling in cell proliferation and inflammatory responses [124]. In this study p120 null neonatal epidermis showed no overt disruption in paracellular permeability and adhesion, however older mice started to display epidermal hyperplasia and chronic inflammation. p120 Catenin null epidermal cells were shown to have elevated levels of active NF-κB causing expression of NF-κB target genes such as pro-inflammatory cytokines that were responsible for the inflammation and epidermal hyperplasia observed in older mice. Interestingly the role of p120 Catenin in NF-κB regulation was not dependent upon its function in maintenance of Cadherin-mediated adhesion, but appeared to function to activate NF-κB via the regulation of RhoGTPases. P120 is known to be a negative regulator of the RhoGTPase RhoA, and hence provides an important link between NF-κB signalling and RhoGTPase regulation.

Assembly of apical cell-cell Junctions

Assembly of AJ and TJs has been studied in different experimental systems most extensively in MDCK cells. In this model system it has been determined that junctions assemble in a sequential stepwise manner. Calcium dependent, E-Cadherin mediated cell adhesion is the initial cue that triggers assembly of all junctions [125] [126]. After E-Cadherin engagement the next step seems to be the formation of primordial junctions that contain components from AJ and TJ. Changes in cell morphology and organization of the actin cytoskeleton result in the final step of maturation and polarized cells with distinct AJ and TJs.

De novo junction assembly has also been studied using *in vivo* models during early development [127]. The sequential recruitment of junctional proteins observed in cultured cells, correlates well with the development of functional intercellular junctions in the first epithelial structure to form in the mouse pre-implantation embryo, the trophectoderm. The junctional complex of this epithelium forms as a result of the sequential recruitment of AJs and TJs proteins to cell-cell contacts. Starting with E-Cadherin engagement during compaction of the 8 cell embryo and ending in the recruitment of claudins to produce mature functional TJs in the 32 cell blastocyst [128].

The initiation of cell-cell adhesion is mediated first by the touching of actin based protrusive membrane structures. MDCK cells, for example, form transient lamellipodia, to initiate contact[129, 130]. Whereas keratinocytes use filopodia, to initiate cell-cell adhesion [131].

Initial plasma membrane contact from adjacent cells has been visualized in MDCK cells using GFP-tagged E-Cadherin [129]. This study defined different sequential stages in cell-cell contact development. The first stage showed E-Cadherin distribution changed from a diffuse pool of cell surface E-Cadherin into small punctate clusters upon touching of adjacent plasma membranes. These punta have been observed in different cell types and systems and represent a primodial junctional state, as they are known to contain other proteins associated with AJ and TJs such as Catenins, nectins JAM-A and ZO-1 [129, 131, 132]. These initial punta are stablised by association of actin filaments. The actin cytoskeleton undergoes striking changes during junction formation. During this initial stage of contact, thin actin filaments can be observed branching out from the circumferential ring of actin. These filaments terminate at these punctuate E-cadherin containing complexes and are thought to stabilise them at the plasma membrane[129, 131].

In the second stage, circumferential actin filaments near cell-cell contact sites separate and the two ends of the cable swing outwards towards the perimeter of the contacts. As a result of these actin cytoskeletal changes, E-Cadherin punta spread out to the margins of the contact to form large E-Cadherin containing plaques. One might think of it as a zipper whereby changes in the actin cytoskeleton causes zipping up cell membranes from sites of punctate clustered E-Cadherin complexes into a continuous line that spans the contact surface between the two adjacent cells. This reorganisation results in the formation of the circumferential actin cables that circumscribes both cells and that are linked to the E-Cadherin plaques at the contact zone of neighbouring

cells. Actin polymerization has been suggested to provide the driving mechanical force for this zippering effect, which seals cell membranes together as contacts expand [131]. A number of actin regulatory proteins that promote polymerisation, such as the Arp/2/3 complex[133], formins[134] and members of the Mena/VASP family [135], are all known to be recruited to sites of E-Cadherin contacts and are thought to be important regulators of this stage of junction assembly. The Arp/2/3 complex is known to promote actin nucleation and branched filament polymerization [136]. Arp2/3 is known to be important for the formation of lamellipodia membrane protrusions. Lamellipodia are important for junction formation by permitting neighbouring cells to expand cell-cell contacts along the whole length of touching adjacent membranes [130]. Arp2/3 activity can be inhibited by α-Catenin [96], through a mechanism whereby dimers of α-Catenin bind to actin filaments resulting in a conformational change the three-dimensional structure of the actin filaments. The change in filament structure is enough to prevent Arp2/3 binding, thus preventing filament branching and also protects actin filaments from cleavage from the actin depolymerising factor cofilin (Nelson, W.J 2010 unpublished). This protection of actin filaments by α-Catenin might be important for limiting Arp2/3 activity and so lamellipodia formation to newly contacting membranes, while stabilising older contacts by developing stable un-branched actin filaments.

The final stage of junction assembly is the maturation of this primordial junctional complex into polarized cells with distinct AJ and TJs. ZO-1 and JAM-A are known to be present in primordial E-Cadherin based contacts and are the first TJ proteins to be present at the compaction stage of the 8 cell mouse

embryos [128] . The recruitment of additional TJ proteins then follows, including proteins that are components of polarity complexes, which establish apical /basal polarity, and the transmembrane proteins that are the constituents of TJ strands, such as Occludin and the Claudins.

As junctions mature, there is an elongation of the lateral membrane. The actin cytoskeleton reorganizes to form a perijunctional actin ring. Circumferential actin filaments contract and bundle so that they tightly align with the apical junctional complex [129, 137, 138]. Actinomyosin forces generated by Myosin II activity are required for this actin reorganization and cell shape changes. Inhibition of Myosin II ATPase activity does not prevent E-Cadherin contacts forming, but does prevent formation of the peri-junctional actin ring, TJ formation and cell polarization [137]. Furthermore a recent study has highlighted the role for different isoforms of Myosin II having roles at different stages of junction assembly. [139]. Myosin IIB can compensate functionally for Myosin IIA but not *visa versa*, suggesting a unique functional role for Myosin IIB. Myosin IIA seems to have an essential role in Cadherin clustering and in concentration of Cadherin complexes at forming AJs. In contrast to Myosin IIA, Myosin IIB has been proposed to function at later stages of junction formation by strengthening the perijunctional actin ring, thereby by enabling it to resist orthogonal forces produced when cells form a continuous epithelial sheet. Furthermore Myosin IIA and IIB junctional localization appear to be regulated by different signalling pathways. Myosin IIA is regulated RhoA/ Rock signalling pathway, and IIB by signalling from the GTPase Rap, suggesting they are parts of two distinct functional Myosin II signalling modules. However it remains unknown how the

activity of these modules are coordinated in forming AJs.

The regulation of the actin cytoskeletion dynamics and actinomyosin contractility is critical in the initiation and maturation of cell-cell junctions. The Rho family of small GTPases, are molecular switch proteins that are master regulators of the actin cytoskeleton. It is therefore not surprising that they have emerged as being crucial regulators in the assembly and maintenance of cell-cell junctions. In these next sections I will discuss how Rho signalling is regulated and can be coordinated in a spatial and temporal manner by additional Rho regulatory factors and discuss their regulation in the assembly and function of junctions.

RhoGTPases

The Ras super-family of small monomeric GTPases contains about 150 members in mammals [140]. This super family is further subdivided into five main sub families; Ras, Rho, Rab, Rap and Arf RhoGTPases. Like all Ras family members they are molecular switch proteins that employ a simple biochemical mechanism to control many complex cellular processes. The basis for this mechanism relies on the ability to cycle between On or active (guanosine-5'-triphosphate (GTP) bound), or Off / inactive (guanosine-5'-biphosphate (GDP) bound) states. When GTP bound, considered the active state, the RhoGTPase undergoes a conformational change that allows it to interact with downstream effectors that are often kinases, phosphotases and lipases and so to transduce signals. The activation of RhoGTPases is often regulated by various cell surface

receptors, such as adhesion molecules, cytokine receptors, tyrosine kinases, as well as G-protein coupled receptors.

In mammals the Rho family of GTPases is comprised of 20 members [141]. Most studies have focused on what is termed classically activated Rho proteins, these undergo the normal on /off cycle of activity and include Rac1-3, Cdc42 and Rho A, B and C. However 8 members of the Rho family are considered atypical. These have lost their GTPase hydrolysis activity and remain predominantly GTP bound. Examples are RhoBTBs[142] and Rnds [143]. Atypical Rhos therefore are not regulated by GEFs or GAPs, but by other methods like gene expression, protein stability or phospholyation. RhoGTPases were first indentified as regulators of the actin cytoskeleton [144]. They are also important regulators of gene transcription and contribute to mitogen activated protein kinase cascades and inflammatory signalling. They have been implicated in a diverse array of cellular processes such as cell-cell adhesion, migration, phagocytosis, cytokinesis, cellular morphogenesis, polarization, proliferation and cell survival. [145, 146]

Regulation of RhoGTPases

Cycling between GDP and GTP bound states is tightly regulated by additional protein factors that can be divided into two families. GTPase activating proteins (GAPs) [147], which, enhance the slow intrinsic GTPase activity of the RhoGTPase and Guanine nucleotide exchange factors (GEFs) [148], which catalyse the exchange of GDP by GTP. GEFs are positive regulators and GAP

negative regulators of RhoGTPase signalling. The inactivation of the RhoGTPase by a GAP, is sometimes coupled with its extraction from membranes. Extraction is mediated by Guanine nucleotide dissociation inhibitors (GDIs) [149, 150], which are a third set of regulatory proteins that preferentially bind the inactive, GDP-bound RhoGTPase and prevent GDP dissociation. This is thought to keep the RhoGTPase in an inactive state in the cytosol and prevent delivery of RhoGTPases to membranes where they can become activated by interactions with GEFs. GDIs therefore act to keep RhoGTPases permanently inactive, by sequestering them in the cytosol. However the mechanism for release of the RhoGTPase from GDI is not yet fully understood but may be mediated by phospholyation of the GDI or the RhoGTPase by a number of different kinases.

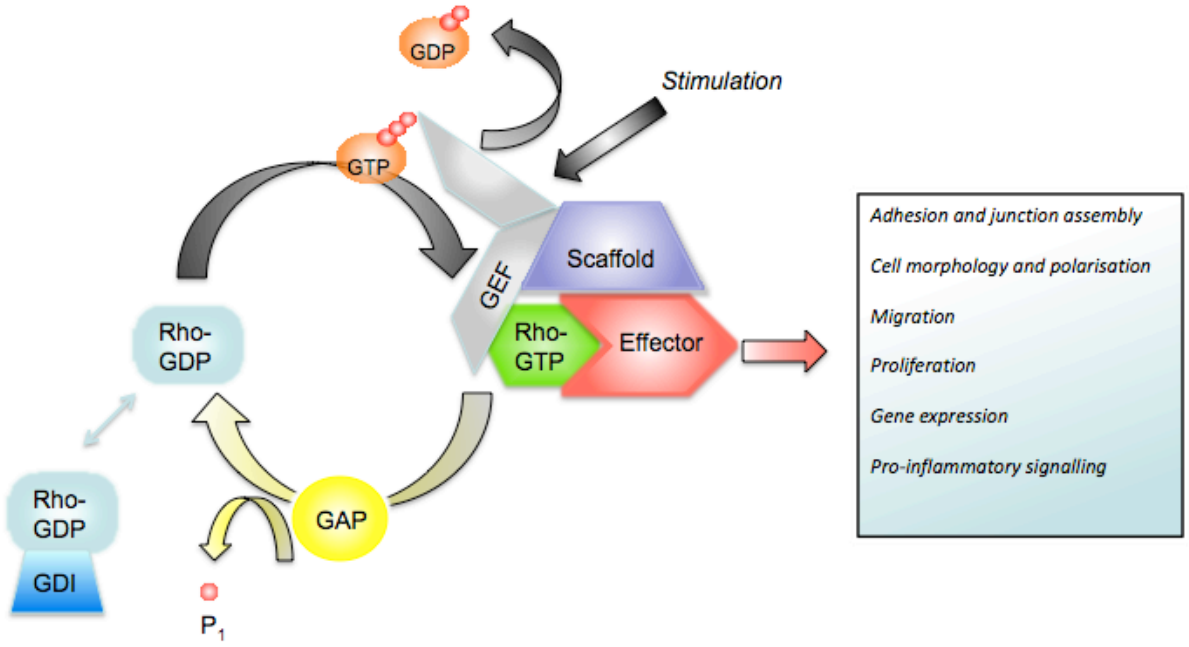

Figure 1. 2 RhoGTPase regulatory cycle

RhoGTPases cycle between inactive (GDP bound) and active (GTP bound) confirmations. Upon conversion from inactive to active states a conformational change occurs exposing structural features required for the recruitment of effector proteins, that transmit downstream effects (see blue box).. Three families of protein factors regulate the activity and subcellular localization of the RhoGTPase. GEFs are positive regulators of RhoGTPases by promoting the exchange of GDP to GTP. GEFs exhibit specificity towards a particular RhoGTPase. Most contain domains that allow interactions with different scaffold proteins and or phospholipids. These interactions may regulate catalytic exchange activity and/or the subcellular localization of GEFs. Some scaffold proteins can also bind RhoGTPase effector proteins. Extracellular or intracellular stimuli may activate the GEF causing activation of the RhoGTPase permitting it to bind and activate effector proteins. Some GEFs can also act as scaffolds themselves. Scaffolds, thus provide a platform for recruitment of GEFs and effectors allowing efficient signal transduction and spatial activation of Rho signalling. RhoGTPases have intrinsic GTPase activity and can hydrolyse GTP to GDP leading to inactivation. GAPs are negative regulators of RhoGTPases by enhancing the intrinsic GTP hydrolysis activity of the RhoGTPase and thereby promote the transfer of the RhoGTPase back to an inactive state. GAPs also exhibit specificity towards a particular RhoGTPase and like GEFs have other domains that can interact with scaffolds (not shown above) permitting tight control of signal transduction pathways linking upstream signalling to inactivation of specific Rho signaling pathways. RhoGTPases are modified post-translationally by the addition of an isoprenyl (geranyl-geranyl) lipid group to cystine of a CAAX motif at the C-terminal region of the GTPase. Inactivation of a RhoGTPase is sometimes coupled with its extraction from a membrane. GDIs sequester the RhoGTPases in their inactive GDP bound form in the cytosol, by masking the C-terminal isoprenyl group preventing its localization to membranes.

Guanine nucleotide exchange factors (GEFs)

The first mammalian GEF to be identified was discovered as a cancer transforming gene from diffuse B-cell lymphoma cells and was assigned the name Dbl [151] [152]. Dbl contains a region of ~240 amino acids residues that has homology to cdc24 a GEF for cdc42 in yeast *Saccharomyces cerevisiae* implicated in cell polarity [153]. Dbl was shown to be a GEF for human Cdc42 and subsequently this Dbl (DH) domain has been found in approximately 70 proteins in humans, which constitute the Dbl family of RhoGEFs [148]. Many of these RhoGEFs have oncogenic activity, which has aided in their identification. Invariably Dbl family GEFs have a DH domain and an adjacent C-terminal Pleckstrin Homology (PH) domain.

The DH domain of ~ 200 amino acids is the minimal domain required for nucleotide exchange activity in vitro. There is low sequence homology between DH domains of different RhoGEFs, but structural studies on a number of GEFs Dbl, Dbs, Vav-1, Tiam-1 [148] [154] have revealed there is conserved tertiary structure. There is extensive contact in the interface between the DH domains of Dbl GEFs and RhoGTPases, structural and biochemical studies, demonstrate large variation of residues amongst different GEF:RhoGTPase complexes important for determining specificity of a GEF towards a specific RhoGTPase. An example of this was from a study where Rac1 was mutated at Trp-56 to Phe. This mutation prevented activation of Rac1 by Tiam-1, yet Rac1 could still efficiently be activated by ITSN-L another GEF that is normally a Cdc42-specific GEF [155]. Similarly a single Leu-Ile mutation in the DH domain of the GEF Dbs

permitted it to have robust catalytic exchange activity for of Rac1, which is not normally its substrate [156].

Crystal structures of DH domains bound to RhoGTPases have been used to discover the mechanism of nucleotide exchange, a process involving remodelling of the switch regions that alters the shape of the nucleotide binding pocket and directly occludes binding of a Mg2+ cofactor causing dissociation of the guanine nucleotide. This leaves the GTPase nucleotide pocket exposed and GTP binds, as its cellular concentration is normally greater than GDP [148].

PH domains of Dbl GEFs are ~100 amino acids in length and are invariable located C-terminally to DH domains in GEFs. Experimental evidence suggests different functional roles of PH domains in different GEFs. The function of the PH domain in certain Dbl GEFs has been linked to a membrane targeting role, whereas in other GEFs the PH domain is thought to contribute to RhoGTPase activation by stimulating nucleotide exchange activity and determining specificity.

Analysis of the structure of Dbs in complex with Cdc42 showed regions of the DH-associated PH domain that are required for effective activation of Cdc42 [157]. However, the structure of Tiam-1 in complex with Rac-1 shows PH domains are significantly removed from the bound GTPase [154], making it difficult to see how they could influence productive interactions required for GTPase activation. PH domains also have been discovered to regulate GEF activity by binding to

phospholipids. For example the exchange activity of P-Rex-1 and Vav1 activators of Rac1 was stimulated in vitro by the addition of soluble PtnIns(3,4,5)P3, presumably by an allosteric regulation of GEF activity, whereas PtdIns(4,5)P2 inhibited Vav1 exchange activity [158]. Experimental evidence also implicates the PH domain in targeting the GEF to membranes [159, 160]. However, the PH domains of Dbl GEFs consistently bind phospholipids with low affinity and little specificity, implying that these interactions may be insufficient for targeting to membranes. Indeed membrane targeting of Dbs, Tiam-1, and Vav-1 does not require the PH domain [160-162], but is mediated by other domains/motifs. Furthermore many other GEFs are not regulated by phospholipid binding, suggesting different functional roles for PH domains [163].

The targeting of Dbl GEFs to specific subcellular sites may however be mediated by interactions of the PH domain with other proteins. For example, the PH domain of Dbl is known to interact directly with ezrin, a linker protein that mediates interactions between the plasma membrane and the actin cytoskeleton [164]. The PH domain of GEF-H1 is known to mediate binding to the TJ adaptor protein Cingulin, resulting in the targeting and subsequent inactivation of GEF-H1 at TJs [64]. Undoubtedly, future work will discover more instances of Dbl GEF -PH- domain interactions with diverse sets of proteins that will link activation of Rho signalling to distinct cellular sites and signalling cascades.

Dock family GEFs

A Second family of Guanine nucleotide exchange factors called the Dock180-realted family of GEFs, also known as the CZH family has been indentified in invertebrates and mammals [165] [166]. They have been shown to be *bona fide* Guanine nucleotide exchange factors proteins, but are unrelated in their sequence homology to Dbl family GEFs, suggesting that they evolved from a different ancestral linage. Dock180 was the first member to be discovered as a binding partner of Crk, a protein involved in receptor tyrosine kinase signalling from focal adhesions [167]. Ced-5 the ortholog of Dock180 in the worm *Caenorhabditis elegans* was shown to be required for cell migration and phagocytosis [167] where as the fly *Drosophila meloanogaster* ortholog myoblast city was identified as a protein essential for myoblast fusion and dorsal closure [168]. Subsequent studies have identified 11 family members in mammals and most show preferential activation towards Rac [165]. However, Dock 9, also known as Zizimin1 preferentially activates Cdc42 [169]. They all lack the typical DH-PH module found in Dbl GEFs, but instead have two conserved Dock homology regions (DHR). The DHR2 region is responsible for nucleotide exchange activity. In contrast to Dbl GEFs, the structure and catalytic mechanism of Dock180 GEFs has not been studied as extensively as Dbl GEFs. However structural studies of DOCK9 complexed with Cdc42 show regions in the DHR2 domain directly insert into Cdc42 nucleotide binding pocket and interfere with Mg2+ binding causing nucleotide dissociation [170].

The DHR1 domain of Dock180 GEFs is known to bind phospholipids analogous to PH domains in Dbl GEFs, that are required for membrane targeting. DHR1 domains binds PtdIns(3,5)-bisphosphate and PtdIns(3,4,5)P_3 in *vitro* and in cells. When the DHR1 in Dock180 was mutated this prevented Rac dependent cell elongation and cell migration even through GTP bound Rac loading was unaffected, suggesting an important difference between activation of Rac and the biological output of Rac signalling [171]. Thus supporting a possible role for the DHR1 domain of Dock180 in Rac signalling by regulating the positioning of Rac signalling at sites of PtdIns(3,4,5)P_3 production.

Rho GTPase activating proteins

RhoGTPase activating proteins (GAP) are considered to be negative regulators of RhoGTPases. Their mechanism of action is to enhance the intrinsic catalytic GTPase activity of the RhoGTPase, resulting in GTP hydrolysis to GDP and thus termination of Rho signalling. Approximately 70 proteins in the human genome contain a RhoGAP domain and to date over just half of these have been characterised [147]. GAP proteins contain a conserved 150 amino acid RhoGAP domain that is essential for GAP activity. RhoGAP domains form a structure containing 9 alpha helixes with a conserved arginine residue in a loop region [172]. Studies where this arginine was mutated to alanine have been shown to prevent GAP activity, and structural analysis of RhoGAP domains in complex with RhoGTPases have revealed this residue to form part of the catalytic active site that promotes GTP hydrolysis by stablising a transition state intermediate of the GTP hydrolysis reaction [173]. The interaction of a RhoGAPs

with GTPases is mediated by the RhoGAP domain. Structural studies revealed the RhoGAP domain interacts with the switch I and II regions of GTPases that undergo conformational shape changes upon GTP binding [172]. RhoGAPs, like RhoGEFs, show specificity for particular RhoGTPases they interact with. Interactions between the RhoGAP and non-conserved regions in the RhoGTPase p-loop region contribute towards a GAP's GTPase substrate specificity.

Regulation of Rho signalling

The number of GEFs and GAPs largely outnumbers the number of RhoGTPases as over 70 Rho GEFs and GAPs are encoded in the human genome [147, 148]. There are a number of possible explanations for this observation. Firstly not all GEFs and GAPs are widely expressed, with some showing tissue specific expression and function. Secondly, specificity towards a particular RhoGTPase could be an explanation; however, in *vitro* binding assays have shown that some GEFs and GAPs regulate the activation state of multiple RhoGTPases. Finally, apart from the conserved catalytic domains, GEFs and GAPs contain a diverse array of different types of protein domains allowing them to interact with phospholipids, signalling molecules such as heterotrimeric G-proteins, tyrosine kinases, adaptor/scaffolding proteins, or also act as scaffolding proteins themselves. All of these types of interactions enable GEFs and GAPs to be regulated in a variety of ways, modulating the spatial and temporal restricted control of Rho signalling pathways in response to diverse extracellular and intracellular stimuli.

Regulation of the catalytic activity of GEFs and GAPs can be controlled directly by post-translational modification such as phosphorylation or indirectly by protein-protein interactions. Many Dbl GEFs are constitutively activated as a result of deletion of domains important for inhibitory intramolecular binding to the DH domain [174] . Mutations resulting in N and C-terminal truncations of Dbl GEFs were discovered in many different cancers. These truncation mutants often have greater transforming oncogenic potential when overexpressed in cultured cells than of the full length forms.

A well characterised example of N-terminal domain regulation, is demonstrated by phosphorlyation of Vav-1 [174] [175]. The N-terminal region interacts with the DH domain to allosterically prevent access by RhoGTPases. Phosphorlyation of Try174 within this N-terminal domain and of other proximal Try residues by various receptor-associated tyrosine kinases, such as Lck [176], opens the DH domain to GTPases by disrupting the inhibitory intramolecular binding of the N-terminal region to the DH domain. However, although many RhoGEFs are phosphorlyated as a result of different stimuli, the consequences of phosphorylation are only beginning to be understood. For example, the Rho GEF Tiam-1 is phosphorlyated on several sites by Calcium/calmodulin-dependent (CaM) kinase II, protein kinase C and Src with varying effects on stimulation or inhibition of GEF activity [177-179]. Furthermore phosphorlyation at residue Thr 678 of the TJ associated RhoA-specific, GEF-H1 by the Erk-1/2 kinase, has been demonstrated to enhance GEF-H1 exchange activity to towards RhoA [180]. However, phosphorlyation of GEF-H1 at Ser 885 by other kinases, such as PAK1 and Aurora [181] [182] and phosphorlyation at Ser959 by

CDK1 [182] resulted in down regulation of GEF-H1 activity by ill-defined mechanisms. The RhoGAP CdGAP is also regulated by ERK-1/2 by phosphorlyation at Thr776 resulting in inactivation of its GAP activity *in vitro* [183]. The post translational modification of GEFs and GAPs by phosphorlyation is clearly important in the regulation of Rho signalling, understanding the mechanism of how phosphorlyation modulates activity is a worthy aim for future investigations.

Several Dbl family RhoGEFs are main points of convergence between signalling cascades originating from heterotrimeric G proteins and those that regulate RhoGTPases. p115RhoGEF, LARG, and PDZ-RhoGEF all contain a highly divergent regulator of G protein signalling (RGS) domain that is typically associated with enhancing the GTPase activity of $G\alpha$ subunits [184, 185]. Purified p115RhoGEF[186] and LARG[185], increase the rate of GTP hydrolysis of $G\alpha_{12}$ and $G\alpha_{13}$ to produce GDP bound and therefore inactive forms of these heterotrimeric G proteins. Furthermore, purified p115RhoGEF and LARG are known to act as exchange factors for RhoA. Their exchange activity can be stimulated by interaction with activated $G\alpha_{12}$ and $G\alpha_{13}$. p115RhoGEF and LARG therefore seem to act as downstream effectors of active GTP bound $G\alpha$ subunits, while simultaneously acting as GAPs to terminate signalling from $G\alpha$ subunits. Regulation between heterotrimeric G proteins and RhoGEF signalling initially seems antagonistic, but permits this system to have an inbuilt signal to noise control. Only signals that produce robust stimulation of GPCR and thus a high concentration of GTP bound $G\alpha$ subunits would activate RhoGEF

signalling, as weaker or spurious signals that activated Gα subunits would be eliminated by the GAP activity of the bound RhoGEF.

Coordination between signalling from heterotrimeric G proteins and RhoGTPases can also be regulated by the interaction of βγ subunits of heterotrimeric G proteins with Dbl family GEFs. For example the RhoGEF P-Rex-1 activates Rac in response to a synergistic stimulation by βγ subunits PtdIns(3,4,5)P_3. [187]. Additionally, interaction of βγ subunits with the DH-PH domain of p114RhoGEF was demonstrated to enhance RhoA mediated SRE-driven gene transcription [188].

Regulation of GEFs and GAPs by subcellular sequestration

Regulation of the subcellular localisation of GEFs and GAPs is often mediated by domains outside of their conserved catalytic domains. This provides a common means of restricting the spatial and temporal regulation of Rho signalling in response to different stimuli. For instance the RhoGEFs Net 1 and Ect2 both contain nuclear localization sequences that target them to the nucleus, where they are sequestered and prevented from interacting and activating their substrate RhoA [189, 190]. Ect2 is known to be important in cytokinesis, and it is held inactive in the nucleus during interphase. When mitosis occurs the nuclear envelope breaks down and Ect2 is released where it associates with microtubules as well as to the cleavage furrow during subsequent different phases of cell division where it is thought to activate

RhoA[190]. GEF-H1 interacts directly with microtubules resulting in inhibition of its nucleotide exchange activity towards RhoA at the plasma membrane [191]. The Dbl RhoGEF Tiam-1 is know to be recruited to cell-cell contacts through its association with the TJ adaptor protein Par3 via a N-terminal region of Tiam-1[192]. In Par-3 depleted cells Tiam-1 activity is not restricted to this site and results in aberrant activation of Rac preventing cell-cell junctions from forming correctly [193]. Furthermore, the Cdc42 RhoGEF Tuba is localised to TJs by interaction between its C-terminal SH3 domain and the TJ adaptor protein ZO-1 [86]. This localisation is presumably important for the spatially restricted activation of Cdc42 and the effector N-WASP, as depletion of Tuba effects TJ assembly via organization of the peri-junctional actin cytoskeleton. The Cdc42 GAP Rich-1 is localised to TJs by interaction with the TJ adaptor protein Amot, via coiled coil regions of Amot and the BAR domain of Rich-1. Amot/Rich 1 complex seems to function to modulate Cdc42 activity at TJs by regulating intracellular protein trafficking of polarity complex containing Pals1, PatJ and Par-3 [85]. Many RhoGEFs contain evolutionary conserved C-terminal PDZ binding motifs that enable them to interact with proteins containing PDZ domains, a common domain often found in adaptor proteins of the cytoplasmic plaque of junctional complexes [194]. For example, binding of the Cdc42 GEF βPIX to the polarity protein Scribble is mediated by the PDZ domains of Scribble. βPIX promotes regulated exocytosis by Cdc42 activation. Scribble is thought to mediate membrane localization of βPIX an essential requirement in this process [195].

GEFs can act as scaffolds to recruit RhoGTPases effectors proteins enabling them to provide a platform for efficient transduction of RhoGTPase signalling. GEFs, by binding the downstream RhoGTPase effectors are able to activate RhoGTPases and effectors in close proximity to each other, thus providing a mechanism for permitting efficient and spatially restricted control of Rho signalling. The interaction between active RhoGTPase effector and GEF can create in some instances a feed back loop to further enhance signals or suppress activating signals. For example, the GEF α-PIX has an important role in coordination the activation of Cdc42 with GPCR-mediated signals crucial to chemotaxis [196]. Upon activation of chemoattractant receptors the βγ subunits of the stimulated heterotrimeric G protein binds to the Cdc42 effector protein p21 activated kinase (PAK), which also associates with α-PIX. This results in an enhanced activation of Cdc42 by α-PIX. Active Cdc42 can then activate the highly concentrated local PAK. Essentially α-PIX is acting as a scaffold to coordinate signals from GPCRs with the activation of Cdc42 and subsequent downstream activation of high local concentrations of PAK. This system may have inbuilt negative feed back, as activation of PAK has been demonstrated to inhibit binding to PIX isoforms α and β [197]. The Cdc42 specific GEF, ITSN-L shows enhanced nucleotide exchange activity on binding to the SH3 domain of the Cdc42 effector (WisKott-Aldrich syndrome protein (WASP) [198]. Activated GTP bound Cdc42 and ITSN-L probably functionally compete for binding to available amounts of WASP. With lower amounts of WASP available for binding to ITSN-L when Cdc42 is activated, an increase in the pool of basally repressed form of ITSN-L would occur, that would feed back to shut down levels of active Cdc42. Interestingly the Cdc42 specific GAP CdGAP also binds to ITSN-L [199]

and may also play a role an additional control to tightly regulate WASP activation. ITSN-L itself is therefore acting in a negative feed back loop to allow fine-tuning of Cdc42 activation. ITSN-L may also act as a scaffold to recruit protein factors that add an additional tight regulation of Cdc42 activation.

In summary GEFs and GAPs permit RhoGTPase regulation to be linked to diverse types of upstream stimuli to allow for Rho signal specificity, to permit the coupling of upstream signals with the correct type of downstream effector to produce appropriate cellular responses. The examples discussed demonstrate RhoGEFs and GAPs can be activated in a variety of ways by direct phospholyation or by interaction with phospholipids. Aside from their catalytic domains RhoGEFs and GAP contain a diverse set of protein domains that enable them to link activation of Rho signalling to different upstream signalling cascades. Different protein domains also permit RhoGEFs and GAPs to be sequestered at different subcellular sites. This is often mediated by interaction with adaptor/ scaffold proteins that also bind RhoGTPase effectors thus coordinating spatial activation of RhoGTPases with a specific type of effector. RhoGEFs and GAPs may also behave as scaffolds themselves by binding RhoGTPase effectors, a function that in part determines Rho signalling specificity and can lead to autonomous feedback loops that allow tight control of Rho signalling.

RhoGTPases and their regulation in the assembly and function of junctions

A role for small GTPases in junction formation was first demonstrated using a non-hydrolysable GTP analogue, GTPγS, which inhibited junction formation in

calcium switch experiments [200]. The calcium switch technique is a method to study *de novo* junction formation. It involves culturing cells in a medium that contains low calcium, preventing formation of cell-cell junctions; addition of calcium to the medium then triggers junction formation [201]. The use of C3 transferase, which inactivates RhoA-C (referred to as Rho), but not Rac or Cdc42, was also shown to inhibit junction assembly as well as to affect the permeability properties of TJs; similar observations were made when mutant Rho GTPases were expressed in epithelial and endothelial cells [202-206]. In rat brain endothelial cells, C3 transferase was reported to inhibit lymphocyte transmigration, indicating that Rho is required for junction dynamics [207]. Overall, these studies suggest that activities of Rho family GTPases need to be finely balanced in order to obtain optimal junction integrity.

Despite the clear importance of RhoGTPases in the assembly and function of TJs, how their activities are controlled in a TJ specific context is less clear. Heterotrimeric G-proteins have been implicated in Rho activation as well as in the regulation of TJs and hence might represent a functional link [200, 208, 209]. For example, when the prostaglandin EP3β receptor, which is coupled to Rho activation via heterotrimeric G proteins, was transfected and activated in MDCK cells, an increase in TER as well as an increase in paracellular tracer mannitol was observed [210]. This suggests that Rho activation by heterotrimeric G proteins could be one of the mechanisms that regulate TJ permeability. However, the molecular mechanisms mediating G protein-induced Rho activation at TJs is not known. Several Rho GEFs can interact with

heterotrimeric G proteins (see section Regulation of Rho signalling), which results in their activation, but none of them is known to localize to TJs.

Currently, only two TJ-associated GEFs for RhoGTPases have been identified and functionally linked to TJs. Tuba, an activator for Cdc42, has only recently been shown to be recruited to TJs in ZO-1-dependent manner and to regulate junction assembly in a Calcium-switch experiments [86]. Despite affecting junctional configuration and Cdc42's importance for polarization, Tuba does not seem to play an important role in establishing polarized epithelial cells in standard cultures. As ZO-1 depletion also only affects epithelial morphogenesis in three-dimensional cultures [211], it would be important to test the importance of tuba in more complex tissue culture systems.

The second TJ-associated Rho GEF is GEF-H1, an activator of RhoA [212]. GEF-H1 regulates paracellular permeability in epithelial and endothelial cells, as well as disassembly of junctions in response to calcium removal [27, 212 , 213]. At TJs, GEF-H1 interacts with Cingulin, a junctional adaptor, resulting in inhibition of its exchange factor activity [64]. However, Cingulin depletion does not induce increased permeability despite increased Rho activation [64, 214], suggesting that compensatory mechanisms might counteract prolonged RhoA activation. Moreover, GEF-H1 also interacts with JACOP/paraCingulin, which also affects junctional recruitment of GEF-H1 [62], suggesting that Cingulin and JACOP/paraCingulin may have overlapping functions. Nevertheless, the GEF-H1/Cingulin complex represents an important Rho signalling pathway in

epithelial cells as it stimulates epithelial proliferation by regulating G1/S phase transition and gene expression [64, 215].

GEF-H1 is known to interact with various different cellular components in different cell types, which includes microtubules and various protein kinases [180-182, 191, 216]. In the context of TJs and regulation of epithelial permeability, most of these interacting proteins have not been analyzed in great detail. Some of them, however, are likely to play important roles in epithelia if analyzed under appropriate conditions as they also associate with epithelial junctions. Examples include 14-3-3 proteins, which bind GEF-H1 in a PAK-1-regulated manner [181], and Par1/MARK kinases, which are known to regulate epithelial morphogenesis [215, 217]. Moreover, ERK1/2 phosphorylates GEF-H1, a necessary event for the induction of cellular responses including proliferation and motility [180]. GEF-H1 is also a target of TNFα signalling in endothelial and epithelial cells, resulting in Rho signalling and stress fiber induction [215, 218] and inhibition of Erk1/2 prevents TNFα-induced stimulation of paracellular permeability [219]. GEF-H1 may thus represent a Rho signalling activator that receives input from different types of upstream pathways to regulate junction function, as well as assembly and disassembly of the junction.

RhoGTPase effector pathways and regulation of paracellular permeability

Multiple RhoGTPase effector pathways target the actinomyosin cytoskeleton, which is thought to play a central role in the regulation of paracellular

permeability [18, 26, 203, 212, 213, 218, 220, 221]. On one hand, interactions between TJ proteins - such as Occludin, Cingulin and the ZO proteins - and, actin filaments are thought to stabilize the junction and might also provide a means to transmit force to alter protein-protein interactions within TJs, resulting in increased paracellular permeability (Figure 1.3). However, there is currently scant experimental proof that any of these actin-binding functions indeed plays a direct role in the regulation of permeability. However a recent study has shown for the first time that ZO-1 provides a direct link between TJ permeablity barrier function and the peri-junctional cytoskeleton [222] . Nevertheless, the C-terminal domain of Occludin, which is important for the regulation of paracellular permeability [50], interacts via multiple adaptor proteins and with F-actin [28, 49, 223, 224]; hence, functionally important actin-binding proteins might be difficult to identify because of functional redundancy.

Nonmuscle Myosin heavy chain II isoforms seem to be major players in Rho-regulated junctional regulatory mechanisms. Myosin IIA and IIB have been linked to cell-cell adhesion in mouse knockout models [225, 226]. Downregulation of Myosin-IIA, but not of IIB or IIC, expression in SK-CO15 colonic epithelial cells resulted in profound changes of cell morphology and cell-cell adhesion [227]. Myosin II associates with the actin cytoskeleton underlying the apical junctional complex and recruitment has been proposed to be mediated by ZO-1 and ZO-2 [228]. However, the data supporting the importance of ZO proteins for junctional recruitment of Myosin are controversial. In some cell types, depletion of ZO-1 is sufficient to inhibit junctional recruitment of Myosin II and in others it favours

junctional accumulation [86, 222]. It is thus unlikely that ZO proteins play a direct role in Myosin II recruitment.

Regulation of Myosin activity seems to play a major role during junction assembly and disassembly, as well as for the regulation of paracellular permeability. ROCKs (Rho associated kinases) are Ser/Thr kinases that are important Rho effectors that regulate TJ permeability [26, 229]. ROCKs are known to stimulate the activation of Myosin by regulating the phosphorylation state of the regulatory light chain (MLC2) [230]. ROCKs also phosphorylate and inactivate the Myosin phosphatase target subunit (MYPT), leading to inactivation of the phosphatase and, hence, increased Myosin activity [231].

Myosin phosphorylation is also mediated by Myosin light chain kinase (MLCK), and pharmacological inhibition of MLCK prevents both MLC2 phosphorylation and regulation of TJ barrier function in response to physiological and pathophysiological stimuli, such as Na+-nutrient co-transport, bacterial infection or proinflammatory cytokines [232-235]. Overexpression of MLCK in mature monolayers further supports a role of MLCK in the regulation of permeability and suggests that MLC2 phosphorylation alone is sufficient to induce TJ regulation in the absence of any upstream stimuli [236]. However, it has been suggested that at least in endothelial cells the gradual increase in permeability induced by TNF-alpha does not reflect contractile mechanisms mediated by Rho, ROCK, and MLCK, but involves long-term reorganization of tight junction proteins [218].

Apart from the non-muscle heavy chain Myosin II pathway, TJ permeability may be controlled by other Rho effectors such as the mammalian Diaphanous-related formin (mDia), which promotes actin nucleation and filament polymerization and is known to represent an opposing Rho effector to ROCK in the regulation of AJ formation and actin dynamics [237]. In endothelial cells, for example, angiopoietin-1 prevents VEGF-induced endothelial permeability by sequestering Src through mDia [238]. ROCK may also regulate TJ permeability by regulating actin filament stability. Another known substrate for ROCK is LIM kinase; activated LIM kinase phosphorylates and inactivates cofilin, an actin-depolymerizing factor, and therefore acts to stabilize the junctional actin cytoskeleton [239, 240]. The importance of cofilin-based mechanisms is also supported by the observation that capsaicin-induced cofilin activation in an intestinal epithelial cell line resulted in a decrease in TER as well as changes in the localization of TJ proteins and altered the f-actin structure [241]. Furthermore, LIM kinase 1 promotes endothelial barrier disruption and neutrophil infiltration in mouse lungs [242]. In agreement, m-Calpain, a cysteine protease, which can inhibit RhoA activation, antagonizes overactivation of RhoA/ROCK/LIMK2 signalling and subsequent cytoskeletal rearrangement in endothelial cells, which leads to barrier enhancement [243]. The fact the TJ-associated polarity protein Par-3 mediates the inhibition of LIM kinase 2 to regulate cofilin phosphorylation and tight junction assembly [244] further supports a role of LIM kinases in TJ dynamics and adds an additional level of complexity in the understanding of the regulation of paracellular permeability by actin rearrangements.

An alternative mode of regulation of TJ by Rho may involve direct modifications of junctional membrane proteins. When a constitutively active form of RhoA was over-expressed in MDCK cells, Occludin phosphorylation was increased, suggesting that Rho signalling can directly affect TJ proteins [245]. When Rho was stimulated with either LPA or histamine in endothelial cells, phosphorylation of the carboxy terminal domain of Occludin increased, which is thought to regulate the interaction of Occludin with the junctional actin cytoskeleton and, hence, paracellular permeability [229]. Direct phosphorylation of Occludin and claudin-5 by ROCK has been reported in brain endothelial cells, correlating with diminished barrier tightness and enhanced monocyte migration across BBB induced by human immunodeficiency virus-1 encephalitis [246]. It thus seems that Rho signalling can affect paracellular permeability by different molecular mechanisms ranging from regulation of actinomyosin contraction and actin polymerization to direct regulation of junctional membrane proteins (Figure 1.3).

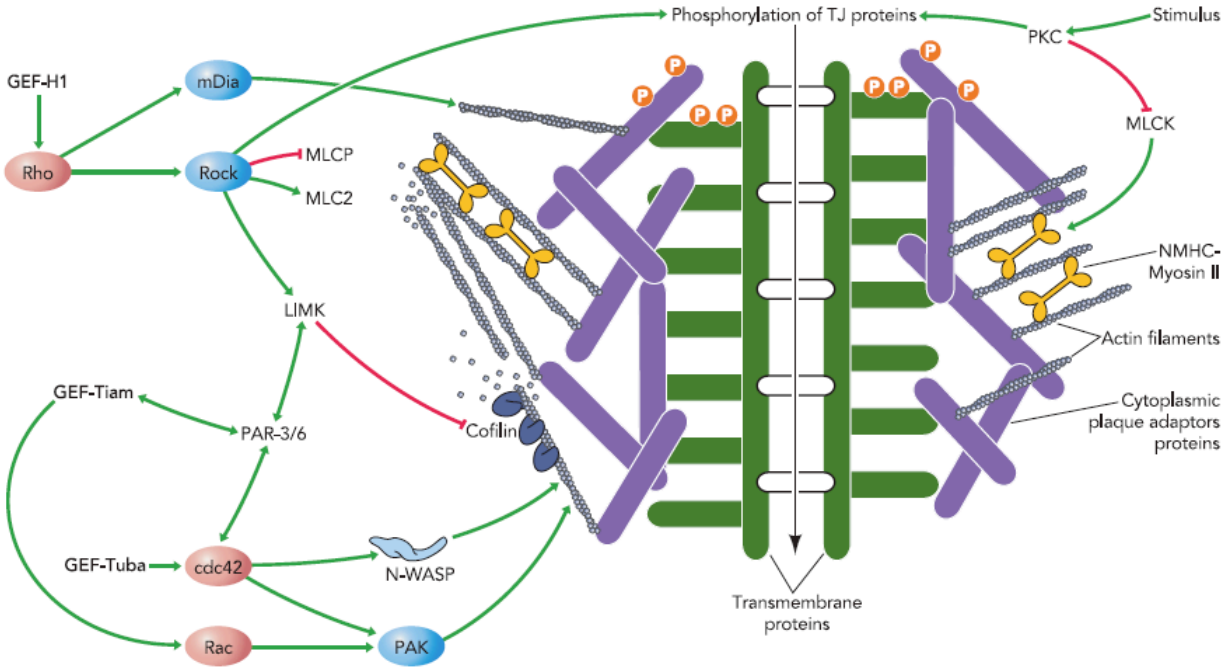

Figure 1. 3 RhoGTPases and regulation of paracellular permeability

Different signaling proteins have been implicated in the regulation of TJ paracellular permeability. The left hand side represents how TJ permeability may be regulated by RhoGTPase signaling. The transmembrane proteins (dark green) represent Claudins, Occludin and Tricellulin as these components are known to regulate paracellular permeability. The cytoplasmic adaptors proteins (purple) represent proteins such as ZO-1, -2 and -3, which act as linkers to the actin cytoskeleton. Stimulation of Rho by GEF-H1, a TJ associated guanine nucleotide exchange factor, results in activation of Rho specific effectors such as Rho kinases (ROCKs). ROCKs phosphorylate and inactivate MLCP (Myosin light chain phosphatase), but phosphorylate and activate MLC2 (Myosin light chain II), leading to activation of actinoMyosin contractility and increased paracellular permeability. A Rho effector that contributes to actin filament nucleation is mDia. Rac and Cdc42 have also been linked to actin cytoskeleton, cell polarity and paracellular permeability regulation. Possible Rac and Cdc42 effectors in actin rearrangement and paracellular permeability are PAKs and N-WASP. Alternatively, ROCK can directly phosphorylate TJ proteins such as Occludin and Claudin-5. Different PKC isoforms (represented on the right) are also known to phosphorylate TJ proteins, and MLCK which is known to contribute to the regulation of TJ permeability. Diagram used with permission from American journal of physiology [4].

Tight junction and regulation of gene expression by RhoGTPases

Different molecular mechanisms that regulate gene expression have been associated with TJs [66]. These include factors that may regulate chromatin structure (e.g., SAF-B), polyadenylation (i.e., symplekin), as well as various transcription factors that associate with junctional proteins (e.g., AP-1, Myc); generally, these associations are thought to be part of regulatory mechanism [81, 247, 248].

Only one TJ-associated signalling pathway has thus far linked RhoGTPase signalling to gene expression. This mechanism is based on ZONAB, a Y-box transcription factor that binds to the SH3 domain of ZO-1 (Figure 1.4). ZO-1 binding inhibits ZONAB by cytoplasmic sequestration [80]. The ZO-1/ZONAB pathway regulates cell proliferation and, in a three-dimensional culture system, epithelial morphogenesis [82, 211]. ZONAB function can be activated by the heat shock protein Apg-2, which binds to ZO-1 and thereby stimulates ZONAB dissociation, which also influences proliferation and epithelial morphogenesis [249, 250]. Furthermore, RalA, a member of the Ras superfamily of small GTPases, inhibits ZONAB transcriptional activity in a cell density dependent manner and expression of oncogenic Ras alleviates transcriptional repression by ZONAB in a RalA-dependent manner [251].

A second mechanism of ZONAB stimulation has recently been identified that is based on Rho signalling [215]. ZONAB activity is Rho-dependent, and the transcription factor forms a complex with the TJ-associated Rho activator GEF-

H1. Modulation of GEF-H1 activity by depletion or overexpression consequently inhibits or stimulates, respectively, transcriptional activity of ZONAB. Both GEF-H1 and ZONAB regulate G1/S phase transition, and GEF-H1 stimulated expression of cyclin D1, a cell cycle regulator and key target of RhoA signalling, is at least in part mediated by ZONAB [215].

GEF-H1 is regulated by different mechanisms and some also affect regulation of gene expression, such as Cingulin [64, 214]. However, it is not known whether any of those genes are indeed ZONAB target genes. An additional complication is that not all mechanisms that stimulate GEF-H1 also activate ZONAB. For example, stimulation with TNF-α activates GEF-H1 [215, 219], but does not stimulate ZONAB activity [215]. This suggests additional mechanisms that modulate ZONAB activity in different cellular and regulatory contexts. For example, RalA, another small monomeric GTPase of the Ras superfamily, is known to be activated by TNFα [252], and active RalA binds and inhibits ZONAB activity [251]; therefore, RalA might inhibit ZONAB in response to TNFα.

Although ZONAB represents a first direct mechanism that links Rho GTPase signalling at TJs to the regulation of gene expression, it is likely that different mechanisms exist and it will be important to identify these pathways and determine how they interact with each other. Moreover, there is still very little known about the pathological relevance of these mechanisms. ZONAB and GEF-H1 expression is deregulated in different types of tumours [191, 253-255]; however, whether this is a cause or a consequence of tumourigenesis is not known.

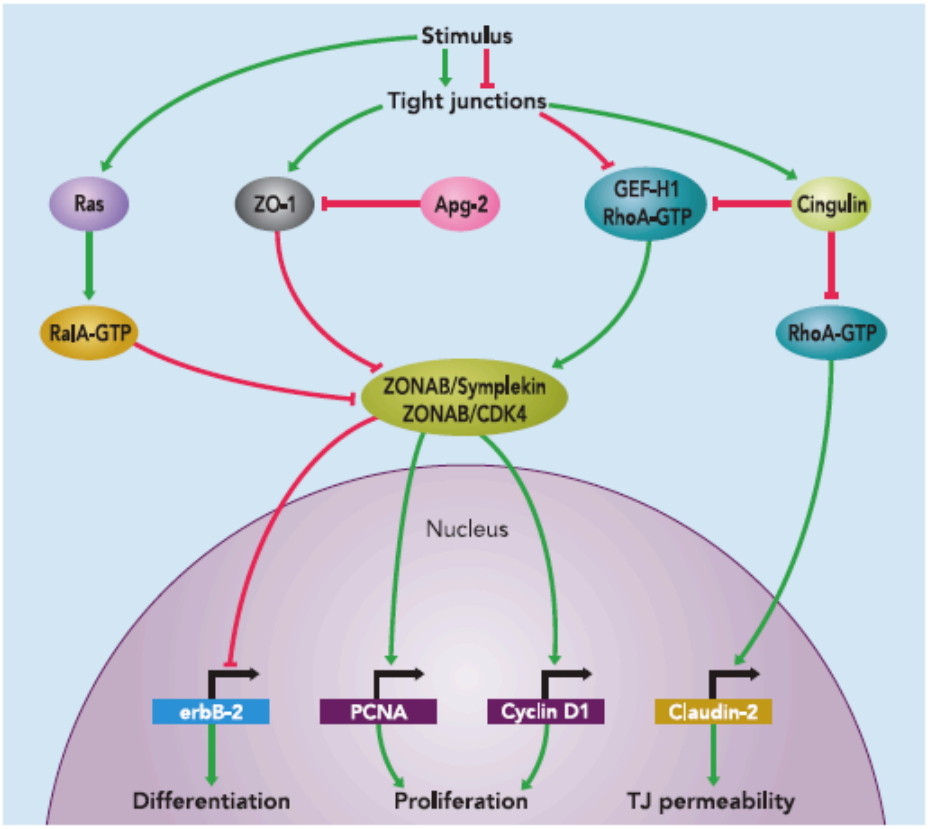

Figure 1. 4 Tight junction and regulation of gene expression by RhoGTPases

Indicated are the main transcriptional pathways involving TJ associated proteins linked to expression of genes that regulate proliferation, differentiation and TJ permeability in response to Rho signaling. Arrows represent activation and T shaped lines represent inhibition. If such lines and arrows are in red, they represent a direct interaction. ZONAB forms complexes with both symplekin and CDK4, but it is not known whether these three proteins form a tripartite complex. ZO-1, by regulating ZONAB localization, has been linked to suppression of erbB-2 expression and increased expression of PCNA and cyclin D1. RalA/ZONAB association in a GTP-dependent manner inhibits transcription of an erbB2 reporter promoter, which is also suppressed by symplekin via interaction with ZONAB. Symplekin and ZONAB have also been linked to the stimulation of cyclin D1 expression. ZONAB-dependent expression of cyclin D1 is also activated by GEF-H1-stimulated Rho activation. Cingulin regulates claudin-2 expression by a RhoA-dependent transcriptional mechanisms. Cingulin also interacts with GEF-H1 and inhibits its activity; however is unknown whether GEF-H1 is involved in claudin-2 expression. Although one might expect significant cross-talk between the different regulatory mechanisms that target ZONAB, how far that indeed occurs is not known. Note, not all mechanisms that target GEF-H1 also regulate ZONAB in a corresponding manner, suggesting that GEF-H1 may be part of different pathways or that other regulatory mechanisms can counteract Rho stimulation of ZONAB (e.g., inhibition by RalA). Diagram used with permission from American journal of physiology [4] .

RhoGTPases are crucial components of signalling mechanisms associated with TJs. It is clear that they are major factors in regulating TJ permeability and in transmitting signals from TJs that regulate gene expression and thus control cellular behaviour including proliferation and differentiation.

RhoGTPase dependent regulation of the actin cytoskeleton is very important for processes requiring junction dynamics, such as assembly and the regulation of paracellular permeability. The available evidence suggests that a major pathway by which RhoGTPases regulate permeability of TJs involves GEF-H1 and RhoA that leads to ROCK activation and regulation of non-muscle Myosin II activity, resulting in actinomyosin contractility. It seems, however, that alternative RhoGTPase dependent mechanisms that regulate actin filament dynamics may also play an important role in the regulation of TJ permeability. Activation of RhoGTPase signalling may also result in the direct modification of TJ transmembrane proteins by inducing phosphorylation and, thereby, resulting in altered permeability.

TJs can also regulate gene expression via RhoGTPase signalling. The interaction between activators of RhoA, such as GEF-H1, and the transcription factor ZONAB provide a mechanism by which TJs are linked to RhoA signalling and gene expression of proliferative genes. However, our knowledge about the spatial and temporal regulation of RhoGTPase activity and the interactions with different effector pathways is still limited. The identification of RhoGTPases regulatory and effector pathways in a TJ-specific context in response to

physiological and pathophysiological stimuli to control cell behaviour remain a crucial challenge for the future.

Structure and function of the Cornea

The cornea is an important component of the eye. It functions as an optical lens that transmits light clearly with a marked refractive power and also contributes to the rigid structure of the eyeball. The cornea is unlike most other organs in the body as it is avasular and transparent. It possesses a relatively simple anatomical structure consisting of three main layers. The outmost of these being the corneal epithelium followed by the stroma and lastly the endothelium see Figure 1.5.

The corneal epithelium serves as an important barrier to protect the eye from the outside environment. Its integrity is essential for the maintenance of corneal transparency. The corneal stroma is populated by cornea fibroblasts and consists of highly order arrays of collagen fibrils. The ordered arrangement of collagen fibers is essential for corneal transparency [256]. This arrangement is maintained by the tight regulation of water content of the stroma through the ion pumping activity of the endothelial layer. The endothelium consists of monolayer of cells abundant in mitochondria that are located at the posterior surface of the cornea and faces the anterior chamber of the eye. [257] Its physiological function is to control the transport of solutes and nutrients from the aqueous humor across to the posterior surface of the cornea and transport

excess water back to the aqueous humor to maintain the cornea in a slightly dehydrated state that is essential for its optical transparency [257].

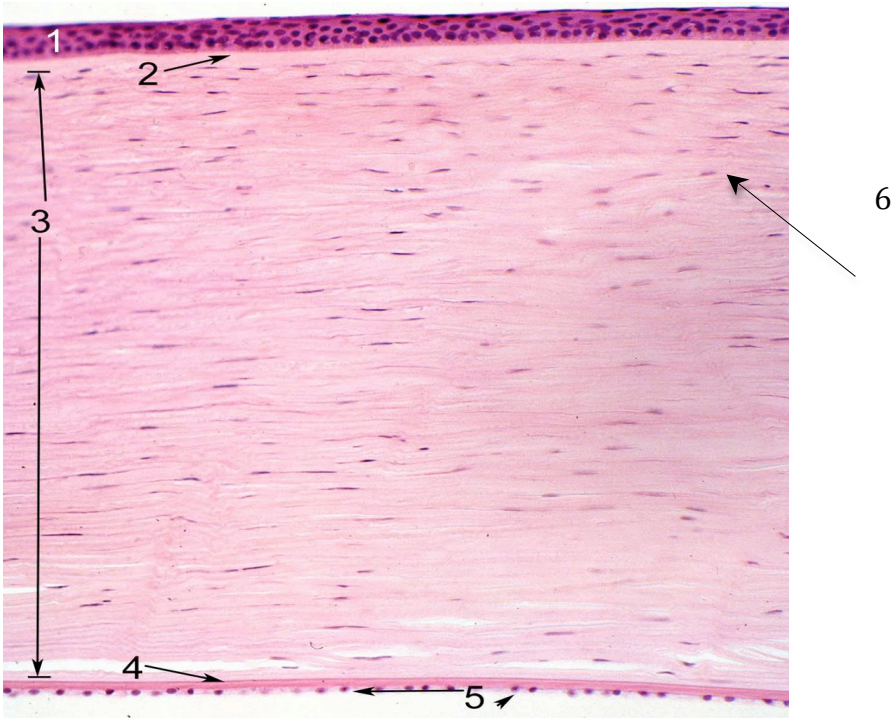

Figure 1.5 Structure of the Cornea

Above is a histological section of Human Cornea that consists of five different layers . (1) The Corneal epithelium is the outer most layer and consists of five-six cell layers thick. The most basal layer is composed of cells that have a cuboid morphology. Above the basal layer are two additional layers of cells known as wing cells because of their wing-like morphology, above these are two layers of more flattened differentated epithelial cells that from the external surface of the corneal epithelium. (2) The corneal epithelium sits on thin basement known as Bowma's layer membrane consisting of collagen fibrils. This membrane separates the epithelium from the stromal layer beneath. (3) The largest layer of the cornea is the stroma it consists of regular parallel arrays of collagen filaments that permit scattered light to be eliminated by destructive interference, thus allowing the cornea to appear transparent and permit the efficient transmission of light to the lens. (4) Below the stroma is basement membrane known as Descement's membrane this membrane is produced by the endothelial layer and consists of a different type of collagen (collagen type VIII) than the stroma. (5) The most basal layer of the cornea is the a single layer of endothelia cells Its physiological function is to control the transport of solutes and nutrients to and from the cornea to maintain the water homeostasis of the stroma that is essential of for the optical transparency of the cornea (6) The stroma of the cornea is often populated by corneal fibroblasts of which the nuclei can be seen stained purple.. Picture adapted from http://www.images.missionforvisionusa.org/anatomy/2005_10_01_archive.html .

Corneal epithelium biogenesis and repair.

The corneal epithelium is in constant state of healing and renewal, cells are constantly shed from the surface and replenished from cells moving centripetal from the limbus and then anteriorly from the basal layer of the epithelium. [258] The limbus is located on the border of the cornea and the sclera (the white of the eye)[1]. The current prevailing theory is that the self–renewing properties of the cornea are reliant on a small population of stem cells located in the basal region of the limbus in a specialised area or niche known as the palisades of Vogt [1, 259]. These stem cells can divide symmetrically to renew themselves or asymmetrically to produce transiently amplifying cells that migrate centripetally to populate the basal layer of the corneal epithelium [1] (Figure 1.6). The corneal epithelium is a dynamic barrier that protects the eye from the environment. It is constantly assaulted from an external maelstrom of environmental insults, such as chemical, physical and microbial damage. It is estimated that the cornea epithelium renews its entire surface every 7-10 days [258]. For the corneal epithelium to be able to maintain a state of equilibrium the rate of proliferation of basal corneal epithelium cells plus the rate of proliferation and centripetal migration must equal the rate of epithelial cell loss from the surface [260].

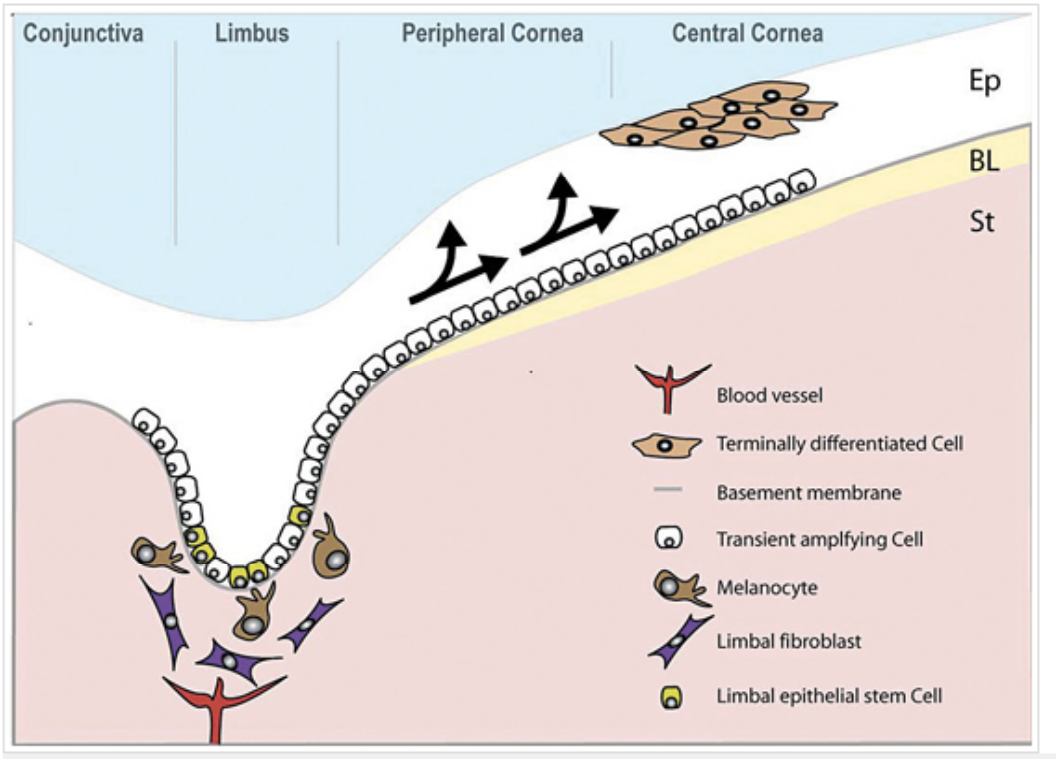

Figure 1.6 The human limbus a site of corneal epithelial stem cells.

Limbal epithelial stem cells reside in the basal layer of the epithelium (Ep), which undulates at the limbus. Transient amplifying cells (TACs) divide and migrate towards the central cornea (arrowed) to replenish the epithelium, which rests on Bowman's layer (BL). The stroma (St) of the limbal epithelial stem cell niche is populated with fibroblasts and melanocytes and also has a blood supply. Diagram from [1].

The coordinated regulation of cell proliferation, cell-matrix and cell-cell adhesions are crucial to the corneal wound healing response [261]. The first phase of the wound healing response is a migration of epithelial cells over the affected area. This requires cells to attach to the underlying matrix and spread over it. Experiments from corneal wound healing experiments in rats show this movement is in two phases [262]. Shortly after wounding there is an initial ruffling and sliding of the basement monolayer (sheet like migration) followed by a mass movement of the above layers. During the sheet like movement the basement monolayer of epithelial cells have to detach from the remaining stratified epithelium a process that involves the disassembly of hemi-desmosomes (structures linking the cells in the basement monolayer to the stratified layers above) [263] and a spreading out over a wide area using lamellipodia projections. Attachment to the extracellular matrix ECM is mediated by family of receptor proteins known as Integrins [264], which are localised in the plasma membrane to form structures known as focal adhesions that are structures that are somewhat similar to cell-cell junctions, in that they act as platforms for intercellular signaling molecules and are also linked to the actin cytoskeleton [264]. Intergrins exist as heterodimmers consisting of α and β subunits. A large variety of different Integrin subunits are expressed in the corneal epithelium [265] .

Different matrix substrates are found in the corneal epithelium basement membrane (see Figure 1.5), often collagen type I being the predominant matrix component, but also collagen type IV, fibronectin and laminin [261]. Adhesion to ECM has to be tightly regulated as if the adhesions are too strong then cells will not be able to migrate. It is therefore proposed that cell movement is likely to

depend on a cycle of adhesion and de-adhesion of the cells to the ECM. This cycle is likely to depend on degradation of different ECM substrates and Intergrin receptors. For example injury to the cornea often results in the destruction of the basement membrane exposing the stroma to the outside environment. Corneal epithelial cells are able to migrate over the stroma in the absence of the basement membrane. During this initial stage of wound healing, fibronectin is synthesised by the epithelial cells and deposited at the site of injury and therefore serves as a temporary matrix for epithelial cells to migrate over [266]. However after the wound is completely healed the expression of fibronectin is down regulated and normal complement of matrix proteins is restored [266].

Cell-cell adhesion also plays an important role in corneal wound healing. Like with cell-matrix interactions, cell-cell adhesion needs to be tightly regulated, for example if cells adhere too tightly to each other they might not be able to migrate to repair the damaged area. Desmosomes are a type of cell junction that contribute to the physical mechanical strength of a tissue as discussed previously. Immunostaining experiments observing Desomsomal transmembrane proteins, Desmoglein 1 and 2 has been demonstrated that they are present in the wing cell layers of rat corneal epithelium [267]. After injury induced by photoablation of a section of the corneal epithelium, Desmoglein 1 and 2 proteins were no longer apparent in migrating epithelial cells, however expression of these proteins was present after a period of three days after photoablation. Thus demonstrating cell-cell contacts in corneal epithelial cells need to be able to go through cycles between of adhesion and de-adhesion in

order to migrate correctly to produce an effective corneal wound healing response.

The rapid reformation of TJ is important in the corneal wound healing response. Studies have demonstrated that TJs are the first junctions to form most rapidly after wounding of the corneal. Other studies have shown the TJ protein Occludin is expressed in the uppermost superficial and sub-superficial layers of cells [267]. In addition injury of corneal epithelium by chemical removal of the superficial cells caused an increase in expression of ZO-1 in sub-superficial cells [268]. These observations might suggest that the expression of TJ proteins in sub-superficial layers permits a rapid response to restore barrier function to prevent exposure and activation of the mesenchymal tissue from environmental stimuli.

Damage to the cornea often leads to the release of many different cytokines and growth factors that influence cell proliferation and migration [269]. For example EGF and TGFβ are known to enhance corneal epithelial cell migration [270]. Whereas pro-inflammatory cytokines, such as TNFα and IL-1α to also have been shown to enhance cell corneal migration, but only in in vitro assay systems when cells are plated on fibronectin [271].

Under certain clinical conditions healing of the cornea is delayed [272]. Thus understanding how corneal epithelial biogenesis and repair is regulated is not

only of biological interest, but also of clinical relevance for the treatment of diseased corneas.

RhoGTPase signalling as discussed previously can regulate cell-matrix and cell-cell junction formation, migration and proliferation. RhoGTPase are also the major downstream targets of physiological and pathological signalling pathways, activated by growth factors and inflammatory signals. Several studies have demonstrated the importance of the Rho signalling for wound healing in corneal epithelial cells by regulating migration, junction formation and proliferation [273, 274]. However how RhoGTPase signaling is regulated in a co-orditained manner to control corneal biogenesis and repair remains largely unknown.

Experimental aims and plan

Aims

The corneal epithelium forms a barrier to protect the surface of the eye from the external environment. For normal vision corneal integrity must be maintained; corneal integrity can be compromised by certain diseases, injury or drug treatments. It is of clinical and biological interest to understand how corneal biogenesis and repair is regulated in health and disease. As discussed RhoGTPases are molecular switches that are involved in epithelial differentiation, cell-cell adhesion, migration, as well as epithelial proliferation. They are major targets of junctional regulatory mechanisms and are also major downstream targets of physiological and pathological signalling pathways, activated by growth factors and inflammatory signals. It is therefore of importance to determine the complex molecular mechanisms present between junction assembly and regulation and RhoGTPases, in order to understand corneal epithelial biogenesis and repair, in health and disease. The aim of this project is to identify regulators and effectors of RhoGTPases in corneal epithelial cells that regulate cell adhesion and junction formation, as well as Rho regulated signalling pathways that regulate gene expression using a siRNA based functional screening approach.

Plan

The primary aim of this project will be achieved using a custom-made siRNA library that contains pools of siRNAs to genes that are regulators or downstream effectors of RhoGTPases. Using this library, functional siRNA screens will be performed to observe junction formation and assembly, as well as gene expression. The screen will be performed in human corneal epithelial cells (HCE), an immortalised SV40 T antigen transformed cell line. HCE cells form functional adherens and tight junctions and spontaneously differentiate, if grown in keratinocyte serum free medium.

To observe junction assembly, immunofluorescence microscopy will be used. Cells will be grown on glass cover-slides and transfected with individual components from the siRNA library. This will be performed in duplicate to allow staining with two sets of antibodies to membrane and cytosolic components of junctions, as well as Golgi complex and DNA markers, to asses the effect on junction assembly and cell morphology. Luciferase based reporter assays will be used to monitor the effect on gene expression. The siRNA screen will focus on identifying candidates that have an effect on the transcriptional regulator NF-κB, a transcription factor regulated by different RhoGTPases and an important mediator of cell survival and the inflammatory response.

Candidates identified in the junction assembly screen will be validated using individual siRNAs, derived by deconvolution of the original siRNA pool. Due to the time limits of this project it may not be possible to validate all candidates from the junction assembly and NF-κB activation screens. However priority will be given to first validating targets that affect junction assembly. Because of constraints on time for this project one or two of the validated candidates will be fully characterised using biochemical and cell biological assays for RhoGTPase signalling and epithelial cell behaviour; Rho-activation assays to determine RhoGTPase specificity, calcium switch assays to observed *de novo* junction formation and effects on permeability, techniques for observing protein-protein interactions such as co-immunoprecipitations and GST pull down assays and as well as effects on cell migration using wound healing assays.

CHAPTER 2

MATERIALS AND METHODS

Materials and Methods

All chemicals are from Sigma unless otherwise stated.

DNA methods

Bacterial transformation

$CaCl_2$ competent bacteria (*E.Coli* strain DH5α) were thawed on ice. 1.7μl of a 1.4M β-mercaptoethanol was added to 100μl of bacteria and incubated for 10 minutes. 10ng of the appropriate plasmid DNA was added to each 100μl and mixed by pipetting up and down once. The bacteria were left to incubate on ice for 30 minutes and then heat shocked for 45 seconds at 42°C, after which they were immediately put back on ice for 3 minutes. 900μl of LB medium was added and the tube was incubated for 45 minutes at 37°C. 100μl of the LB bacteria suspension were plated onto LB agar plates containing 100μg/ml Ampicillin or 50 µg/ml Kanamycin. The plates were placed at 37°C and the bacteria left to grow overnight.

Plasmid DNA Mini/ Midi preps

A single bacterial colony transformed with the appropriate plasmid was picked using a sterile pipette tip and placed into 5ml of LB containing 100μg/ml Ampicillin for Mini or 200ml for Midi preps. This was left to grow overnight in an incubator at 37°C with shaking at 225rpm. The following day the bacteria were centrifuged at 5000rpm for 30mins and processed according to the standard Qiagen Mini and midi prep protocols. The plasmid DNA was re-suspended in 10mM Tris pH 8.5 0.1mM EDTA. Concentration and purity of plasmid DNA

samples were obtained by using a spectrophotometer (Themo Scientific Helios β) to measure the absorbance of samples at wavelengths of 260nm and 280nm.

DNA agarose gel electrophoresis

A 1 % agarose gel was prepared by dissolving 1 g of agarose (Invitrogen) in 100 ml of TAE buffer (40 mM Tris-acetate, 1 mM EDTA pH8.0) Ethidium bromide (1µg/ml) was added prior to gel prior to pouring. 6X DNA loading buffer (30% glycerol (v/v), 0.25% bromophenol blue (w/v), 0.25% xylene cyanol (w/v)) was added to DNA samples to achieve a final concentration of 1X DNA loading buffer. Samples were typically were run at 100 V for approximately 1 hr. DNA bands were visualized using a UV transilluminator.

Polymerase Chain Reaction (PCR)

Standard PCR to amplify fragments for sub-cloning was carried out using 100ng of template plasmid DNA and 100pmol of each primmer (Eurofins/MWG see table) reactions were carried out in 50µl total volume using 1 µl (2.5Units) of expand high fidelity polymerase (Roche Applied Science) and 5mM of dNTP mix (Roche Applied Science) where necessary 10% DMSO was added to the reaction mix. Reactions were carried out in a PCR machine using a typical programme.

1 94°C for 2 minutes

2 94 °C for 30 seconds

3 50°C for 45 seconds

4 72°C for 1kb/minutes

5 Step 2 for X29 cycles

6 72°C for 10 minutes

Restriction enzyme digests, DNA purification and ligations

Typically 5µg plasmid DNA or PCR products were digested in a final volume of 30µl, using 0.5µl of the appropriate restriction enzymes (New England Biolabs) in the provided buffer solutions. Reactions were incubated at 37°C for 1 hr. Digested DNA fragments were purified by running on agarose gels, excising the appropriate bands under a long wave length UV translumintor, and purifying the DNA by adding 1ml of 6M solution of Sodium Iodide and melting the agarose at 70°C for 10 minutes, allowing to cool and incubating with 50µl silica beads (Sigma) for 10 minutes. Samples were then washed twice with silica wash buffer (50mM NaCl, 10m|M Tris HCL pH 7.5 2.5mM EDTA, 50% v/v Ethanol). DNA was eluted from the beads in 30µl of 10mM Tris pH 8.5 0.1mM EDTA. Ligations were carried out using a 1:3 molar ratio of Vector: Insert in a final volume of 10µl, using 1 µl (5 units) of T4 ligase (Roche) in the provided buffer. Reactions were incubated overnight at 4°C and the entire volume used to transform 100µl DH5a *E.coli*.

Site directed mutagenesis

Site directed mutagenesis was performed to generate p114RhoGEF mutants. PCR was performed as stated in PCR methods above, but using 2.5 Units of Pfu turbo,(Stratagene), 200ng of template DNA and double the normal dNTP concentration (see Table 2.0 for template and primer sequences used), using the following PCR program ;

1 94°C for 3 minutes

2 94 °C for 30 seconds

3 48°C for 1 minute

4 68°C for 17.5minutes

5 Step 2 for X 29 cycles

6 68°C for 17 minutes

25μl of this PCR reaction along with 200ng of template DNA as a control was digested in 50μl with DpnI (New England Biolabs) for 1.5 hours to digest the original methylated template. Samples were heated for 20 minutes at 80°C to inactivate DpnI. 4μl of this digest was used to transform 100μl of *E.coli* DH5α and transformed as for normal protocol apart from reducing the recovery time in LB broth to just 15 minutes before plating onto LB agar. Several colonies were picked and plasmid DNA obtained and sequenced to confirm the mutation.

DNA constructs

All DNA constructs used in this study are listed below in Table 2.0

Plasmid name	Description and Source /Construction
pCDNA3- Myc- p114RhoGEF	N-terminal myc tagged p114RhoGEF kind gift from [188]
pCDN4-TO-VSV	Mammalian cell expression vector allows either constitutive or Tetracycline inducible expression of C-terminal VSV tagged protein. (Matter Lab) made from pCDNA4-TO (Invitogen).
pCDNA4-TO-VSV-GEF-H1	C-terminal VSV tagged full length GEF-H1 (Matter lab) [64]
pCDNA4-TO-Myc Cingulin	C-terminal Myc tagged full length Cingulin (Matter lab) [64]
pCDNA6-TR	Tetracycline repressor (Invitrogen)
pCDNA4-TO-VSV p114RhoGEF FL	C-terminal VSV tagged full length p114 made by PCR using pCDNA3 Myc p114RhoGEF as template using primers 5'GCCTATCTTAAGGGTATGACGGTCTCTCAGAAAGGG3' 5'GCTATT-CCGCGG-AA-GAAGAAGATGACGTCTTCTTTGC3' Cloned into pCDNA4TOVSV using AflII and Sac II sites
pCDNA4-TO-VSV p114RhoGEF Δ DH	C-terminal VSV tagged p114 with deleted DH domains made by PCR using pCDNA3 Myc p114RhoGEF as template using primers 5'GCAATACTTAAGGGTATGGAGTGTGAGAAGGGCCAGCGCC3' 5'GCTATT-CCGCGG-AA-GAAGAAGATGACGTCTTCTTTGC3' Cloned into pCDNA4TOVSV using AflII and Sac II sites
pCDNA4-TO-VSV p114RhoGEF CTD	C-terminal VSV tagged p114 with deleted DH and PH domains made by PCR using pCDNA3 Myc p114RhoGEF as template using primers

	5'GCCATTCTTAAGGGTATGCAAAGGGCTGTGGAGAGCTGCC3' 5'GCTATT-CCGCGG-AA-GAAGAAGATGACGTCTTCTTTGC3' Cloned into pCDNA4TOVSV using AflII and Sac II sites
pCDNA4-TO-VSV p114RhoGEF Y260A	C-terminal VSV taggedp114 with catalytically dead GEF activity made using single step PCR site directed mutagenesis template pCDNA4TOVSV p114RhoGEF FL primers 5'CATAACCAAAGCCCCAGTGCTGG3' 5'CCAGCACTGGGGCTTTGGTTATG3'
pGEX43T	Bacterial protein expression vector for making N-terminal GST tagged fusion proteins (GE Lifesciences)
pGEX43T-p114RhoGEF FL	N-terminal GST tagged p114 full length fusion protein made by PCR using pCDNA4-TOVSV p114RhoGEF FL as a template using primers 5'AAAAAA GAATTCCATGACGGTCTCTCAGAAAGGG3' 5'AAAAAACTCGAGTTA-GAAGAAGATGACGTCTTCTTTGC3' Cloned into pGEX43T using EcoR1 and XhoI sites
pGEX43T-p114RhoGEF NTD 1-321	N-terminal GST tagged p114 fusion protein containing N terminal domain 1-321bp fragment made by PCR using pCDNA4-TOVSV p114RhoGEF FL as a template using primers 5'AAAAAA - GAATTC-C-ATGACGGTCTCTCAGAAAGGG3' 5'AAAAAACTCGAGTTA-GAAGAAGATGACGTCTTCTTTGC3' Cloned into pGEX43T using EcoR1 and XhoI sites
pGEX43T-p114RhoGEF PH	N-terminal GST tagged p114 fusion protein containing PH domain 958-1416bp fragment made by PCR using pCDNA4-TOVSV p114RhoGEF FL as a template using primers 5'AAAAAAGAATTCCTCTTCCAGCAAACTCAAGAACG 3' 5'AAAAAACTCGAGTTAGAAGAAGATGACGTCTTCTTTGC3' Cloned into pGEX43T using EcoR1 and XhoI sites

pGEX43T-p114RhoGEF CTD	N-terminal GST tagged p114 fusion protein containing 1308-3051bp fragment made by PCR using pCDNA4-TOVSV p114RhoGEF FL as a template using primers 5'AAAAAA GAATTCCCAAAGGGCTGTGGAGAGCTGCC3' 5'AAAAAACTCGAGTTAGAAGAAGATGACGTCTTCTTTGC3' Cloned into pGEX43T using EcoR1 and XhoI sites
p NF-κB	Contains the NF- κB promotor region of ICAM-1 upstream of firefly luciferase
pTCFwt	B-Catenin/TCF reporter (Matter lab)
pTCFmut	B-Catenin/TCF protor containing mutated TCF binding sites (Matter lab).
pRLEBN	Minimal erb2-b promotor that lacks ZONAB binding, driving renilla luciferase expression [251]
pIkBα S 32,34 A	Contains mutant non phosphorylatable IkBα that acts as a NF-κB repressor (Matter lab)
p-Raichu-RhoA	Allows active RhoA levels to be monitored spatially in live cells. Contains YFP fused to the Rho binding domain of PKN fused to RhoA-CFP (kind gift from M.Matsuda, Osaka University Japan) [275]
shRNA p114 plasmids 1 and 2	Expression of shRNA duplexes against p114RhoGEF shRNA the sequences 5'-AAGACACGTCGGGACGCTTG-3' and 5'-AACTACGTCATCCAGAAAATC-3' were cloned into plasmid containing a tetracycline regulated mouse U6 promotor [64].

Table 2.0 DNA constructs

All DNA constructs used and made are listed above, where a construct has been made shown are the original template as well as the primer sequences used restriction enzyme sites or where sites of point mutations are highlighted in red. All constructs when appropriate were confirmed by sequencing by (Eurofins/MWG).

Protein techniques

Preparation of polacylamide gels

Polyacrylamide gels of the required percentage were prepared a day before use, using a MightySmall minigel electrophoresis system.

Separating gel (100ml)	12%	10%	8%	6%
1.5M Tris pH 8.8	25ml	25m	25ml	25ml
Acrylamide/Bisacylamide mix 30%/ 0.8%	50ml	33.4ml	26.6ml	20ml
Distilled water	23ml	39.4ml	46.4ml	53ml
10% SDS	1ml	1ml	1ml	1ml
10% APS	1ml	1ml	1ml	1ml
TEMED	0.04ml	0.04ml	0.04ml	0.04ml

5% Stacking gel	50ml
0.5 M Tris pH 6.8	6.25ml
Acrylamide/Bisacylamide mix 30%/ 0.8%	8.5ml
Distilled water	34ml
10% SDS	0.5ml
10% APS	0.5ml
TEMED	0.05ml

Running

Protein samples were prepared for SDS/PAGE analysis by washing cells twice with 1XPBS and then adding directly to the cells, one part 3X sample buffer (6%SDS, 30%glycerol, 0.003% bromo-phenol blue, 0.3M DTT, 0.1875M Tris/ pH6.8) and 2 parts distilled water to give a final 1X concentration of sample buffer. Samples were heated at 70°C for 10 minutes and passed 3 times through a 23 gauge micro-needle before loading. Gels were placed into a running tank filled with running buffer (25mM Tris, 250mM glycine pH 8.3 0.1%SDS) samples were loaded and gels were run at constant current of 25mA per gel for 1 hour.

Transferring /staining

Polyacrylamide gels were carefully removed from the running apparatus and left to soak in transfer buffer (25mM Tris, 250mM glycine pH 8.3 0.1%SDS, 20%MeOH) along with the nitrocellulose membrane (LI-COR) and Whatman paper for 30 minutes. Gels were transferred using a wet transfer apparatus (BioRad). Gels were transferred, typically two gels per tank for 2 hours at 4°C at 100V constant and restricting the current to a maximum of 0.45mA. The efficiency of the transfer was assessed by staining the membrane with Amido black dye 0.1% for 30 seconds. Then de-staining with (20% MeOH 7.5% acetic acid) for 15 minutes.

Immunoblotting

The Amido black stained membrane was washed 2 times for 1 minute in PBS, then incubated in blocking solution (5% milk or 5%BSA in PBS 0.1%Tween-20 0.1%NaN_3) for 30 minutes with agitation. The membrane was then incubated overnight at 4°C with agitation with the appropriate primary antibody, diluted in the blocking solution. The next day the membrane was washed three times for 10 minutes with PBS 0.1% Tween-20 solution and then incubated with the appropriate secondary antibody diluted in PBS 0.1% Tween-20 for 1 hour. The membrane was washed twice for 10 minutes with PBS 0.1% Tween-20 solution and then once with PBS for 10 minutes. Specific proteins were detected with horseradish peroxidase conjugated secondary antibodies using enhanced chemiluminescence detection system (ECL, Amersham, Corp. Arlington Heights, IL), or detected using an Odyssey detector and IRDye-680- and IRDye-800CW-conjugated secondary antibodies (LI-COR).

Immunoprecipitations

For immunoprecipitations, a confluent 14cm plate of cells was extracted by using a cell scraper at 4°C with 2ml of Triton X100 0.5%PBS or GB buffer (10 mM Hepes (pH 7.4), 150 mM NaCl, 1% Triton X-100, 0.5% sodium deoxycholate, 0.2% SDS. A cocktail of protease inhibitors, 10 µg/ml leupeptin, 10µg/ml aprotinin, 10µg/ml pepstatin A 50µg/ml benzamide and 1 mM PMSF and phosphatase inhibitors, 10mM sodium fluoride (NaF), 10mM sodium pyrophosphate and 4mM sodium orthovanadate (Na_3VO_4) was added to both buffers prior to extraction. 1ml of extract was pre-adsorbed with 100µl of

inactive sepharose beads for 15 minutes on ice prior to incubation with 1.5μg of antibody conjugated overnight to Protein G sepharose beads for 2 hours at 4°C. Samples were washed twice with 1ml of 0.5% triton X100 PBS and once with PBS while being kept at 4°C before adding 60 μl SDS-PAGE sample buffer boiling for 10 minutes at 70°C and running 15μl on and SDS-PAGE gel.

Expression of GST fusion proteins

BL-21 pLysS *E.coli* (Invitrogen) were transformed with the appropriate plasmids and were plated onto LB agar plates containing 100μg/ml Ampicillin 34μg/ml chloramphenicol. The plates were placed at 37°C and the bacteria left to grow overnight. A single colony was picked per construct into 150ml of LB broth containing 100μg/ml Ampicillin 34μg/ml chloramphenicol and grown overnight at 37°C with agitation at 225rpm. The following day bacteria were centrifuged at 5000rpm for 15 minutes and re-suspended in 500ml of LB broth containing 100μg/ml Ampicillin and 0.5mM mM IPTG and placed at 25°C with agitation at 225rpm for 2 hours to allow protein expression. Bacteria were centrifuged at 5000rpm for 15 minutes and re-suspended in 30ml of cold GST protein Lysis buffer (PBS /Triton x100 0.5%) containing 1mM DTT and protease inhibitors 10 μg/ml leupeptin, 10μg/ml aprotinin, 10μg/ml pepstatin A 10μg/ml benzamide and 400 μM PMSF and incubated on ice for 30 minutes. The samples were then sonicated 3 times for 30 seconds on ice and centrifuged at 10000rpm for 10 minutes. 15μl (0.5%) of sample was run on a 12% polyacryimide gel and stained with Coomassie blue to observe expression levels. Samples were used immediately or frozen at -80 °C for long-term storage.

Purification GST fusion proteins

For purification of GST fusion proteins, bacterial lysates were thawed on ice and the extract was adjusted with lysis buffer to give 30 ml fresh protease inhibitors (as stated above) were added and the whole 30ml was incubated with 1.5ml of 30% Glutathione-agarose beads (Sigma) for 2 hours on a rotor at 4°C. The solution containing beads was loaded into a Pierce protein column (Thermo Scientific) equilibrated with lysis buffer. The column was washed twice with cold lysis buffer and twice with cold PBS. Fusion proteins were eluted with 25mM reduced Glutathione in 50mM Tris pH 8. Fractions were pooled and dialysed in dialysis tubing (8000MW: BioDesignDialysis tubing) overnight at 4 °C and then again for 5 hours at 4 °C against PBS. Protein concentration was quantified on SDS-PAGE gels stained with Coomassie blue and by using a spectrophotometer (Themo Scientific Helios β) to measure the absorbance of samples at wavelengths of 280nm.

GST pull-down assays

For GST pull-down assays cells were extracted in the same buffer and preadsorbed with inactived beads as described above for immunoprecipitations. 15μg of GST fusion protein extracts were incubated with 50μl of 30% Glutathione-agarose beads (Sigma) and washed twice with cold GST lysis buffer and once with cold PBS. Cell extracts were incubated with the washed 50μl of Glutathione-agarose beads coated with fusion proteins and incubated

for 2 hours at 4°C before washing and running on a SDS-PAGE gel as described above for immunoprecipitations.

Lipid-protein binding assay

For Lipid –protein interaction assays PIP strip membranes (Echelon Biosciences Inc) were blocked in 1% milk PBS for 2 hours at room temperature prior to incubation with 1μg/ml of the appropriate fusion proteins ; GST alone, the C1 and PH domain of GEF-H1, the PH domain of P114RhoGEF, as well as PIP2 Grip^{tm} containing the PH domain of PLCδ for a positive control (Echelon Biosciences Inc) in 1% milk PBS overnight 4°C with agitation. Membranes were washed three times for 10 minutes with PBS 0.1%Tween-20 solution and then incubated with the GST antibody 1:2000 in 1% milk PBS 0.1% for 2 hours at room temperature. Membranes were washed 3 times as described above before adding the secondary antibody diluted in 1% milk PBS 0.1% Tween-20 for 1 hour. The membrane was washed and specifically bound proteins detected as according to immunoblot protocol.

RhoGTPase pull-down activation assay GLISA

For RhoGTPase activation assays cells were transfected with the appropriate siRNAs in 12 well plates, after 72 hours protein was harvested and analysed for levels of active RhoA, Cdc42 and Rac1 using the respective GLISA assay kit from Cytoskeleton Inc. Protein concentrations were equilibrated before incubation with the coated 96 well plates. HRP conjugated secondary antibodies were used for detection measuring absorbance at 490nm using a

FLUOstar OPTIMA microplate reader (BMGLabTech, Offenburg, Germany) samples of cell extracts were immunoblotted for the GTPases to exclude altered expression levels.

Cell culture

Cell lines

Human adenocarcinoma Colon cells (Caco-2) [276], Human corneal epithelial cells (HCE) transformed with SV-40 T antigen (Gift from Chang. M.S Vanderbilt University Nashville Tennessee)[34] and Madin-Darby Canine Kidney cells (MDCK) were cultured in DMEM media containing 10% heat inactivated FBS (20%FBS for Caco-2) with 100μg/ml streptomycin and 100μg/ml penicillin (PAA cell culture) at 37°C with 5% CO2. Cells were cultured on tissue culture plastic plates or glass cover-slides for immunostaining. MDCK cell lines expressing Tetracycline inducible p114RhoGEFP were made by calcium phosphate transfection of 10μg/ml of Tet repressor pCDNA6-TR and the appropriate p114RhoGEF plasmids. Cells were selected for 10 days in media containing 5μg/ml Blasticidin and 200μg/ml of Zeocin (Invitrogen). The GEF-H1 expressing cell line was made as previously described [64].

MDCK and Caco-2 cysts

Three dimensional cultures of MDCK cells were generated as previously described. [211] and for Caco-2 cells a recently described method was used [277].

Freezing cells

A single well of a 6 well dish containing 80% confluent cells were trypsinsied for 15 minuites at 37°C with 2ml of 2 times Trypsin EDTA (PAA cell culture), 5ml of DMEM was added to inactivate Trypsin. The cells were centrifuged at 1000rpm for 5 minutes. The supernatant was then discarded and the cells re-suspended in freezing media (DMEM containing 10% DMSO 20% FBS). 1ml of cell suspension was added to each cryotube and placed in -80°C freezer for one day and then transferred to liquid nitrogen for long term storage.

DNA transfection methods

Calcium phosphate

For transfections using calcium phosphate, confluent layers of cells were trypinised for 15 mins at 37°C and plated out at the appropriate density. The appropriate plasmid DNA was precipitated by mixing 10μg/ml of plasmid DNA in 2XHEPES buffer, (280mM NaCl, 50mM HEPES, 1.5mM $NaPO_4$, pH 7.1) with an equal volume of 0.25M $CaCl_2$ added drop-wise, shaking vigorously after each drop. The precipitate was allowed to form by leaving the tube for 30 minutes at room temperature. The precipitate was vortexed once, added to cells where the media was aspirated beforehand and incubated for 15 minutes at 37°C, before an additional volume of media was added and left overnight at 37°C. For a 96 well plate 20μl of precipitate and 80μl of media. The following

day the media was removed, the cells were washed once with PBS and fresh media was added before leaving the cells for 24-48 hours in the incubator.

Lipofectamine

For transfections using Lipofectamine, confluent layers of cells were trypsinised for 15 minutes at 37°C. Cells were plated so that they were 90-95% confluent the next day in DMEM without antibiotics. For example, 0.5ml a 10ml suspension derived from one well of a fully confluent 6 well plate was used for 1well of 24 well plate. In one tube 0.9μg of plasmid DNA was added to OptiMEM medium (Gibco/Invitrogen) to make total volume of 50μl. In another tube 4μl of Lipofectamine 2000 reagent (Invitrogen) was added to 46μl of OptiMEM, both tubes were left at room temperature for 5 minutes. The contents of both tubes were mixed together and left for further 20 minutes at room temperature. The 100μl of DNA-lipofectamine mixture was added directly to each well of cells containing 0.5ml of the appropriate media and left to incubate for 4h at 37°C. The media was then removed and replaced with 0.5ml of fresh media. Cells were left typically between 24-48 to allow expression of protein before being processed.

JetPEI

For transfections using JetPEI a single well of a 6 well plate of 90 -100% confluent cells were trypsinised and diluted into 35ml of DMEM without antibiotics. 0.5ml/per well of cells were plated into a 48 well plate and left for no longer than 20 hours before transfection. Cells were transfected with the

appropriate DNA using JetPEI transfection reagent (Polyplus transfection). JetPEI and 150mM NaCl were votexed and warmed to room temperature, in one tube 0.5μg/48 well of plasmid DNA was mixed with 25μl of 150mM NaCl and vortexed, in another tube 1μl of JetPEI was diluted in 25μl of 150mM NaCl and vortexed and added to the first tube containing the DNA. This was left at room temperature for 15 minutes during this time the media on the cells was discarded and replaced with 250μl of DMEM with no antibiotics. The Transfection mix was then added to the cells and the plate was gently shaken to mix, before cells were placed back in the incubator. Cells were fixed or protein extracted typically after 24 hours.

RNAi

For RNAi experiments siRNAs were transfected into cells using Dharmafect or Interferin transfection reagents (see below for tranfection details). Individual or pools of siGenome or On-Target plus siRNAs for targeting specific genes, as well as non-targeting control siRNA were purchased from Thermo Scientific, Dharmacon.

Sequences for individual p114RhoGEF siGenome siRNAs were 5'-UCAGGCGCUUGAAAGAUA-3' and 5'-GGACGCAACUCGGACCAAU-3'

Sequences for p114RhoGEF ON-Target plus siRNA used as pool were

5'-UCAGGGCGCUUGAAAGAUA-3', 5'GCAGUGACCGGAAUUAUGU-3,'

5'-CACAACGCAUAACCAAAUA-3' ,5'-GGACGCAACUCGGACCAAU-3'

For the expression of shRNA duplexes in MDCK cells, the sequences 5'-AAGACACGTCGGGACGCTTG-3' and 5'-AACTACGTCATCCAGAAAATC-3' were targeted using a plasmid with a tetracycline regulated mouse U6 promotor [64].(For complete list of siRNA sequences using in RhoGTPase Library see Appendix section)

Transfection of siRNAs using Dharmafect

The day before transfection confluent layers of cells were trypsinised for 15 minutes at 37°C. Cells were plated in medium without antibiotics and at an appropriate density, so that they were 50% confluent the next day. siRNAs were purchased from Dharmacon as pools of 4 different siRNAs targeting a specific gene a non specific control siRNA was also purchased from Dharmacon. siRNAs were prepared to a stock concentration of 20μM, by dissolving in 1XsiRNA buffer (Dharmacon). For a transfection per well of a 48 well plate: In one tube 1μl of 20μM siRNA (100nM final siRNA concentration) was mixed with 19μl of 1XsiRNA buffer and 20μl of DMEM without antibiotics. In another tube 1μl of DharmaFECT solution 4 (Dharmacon) was mixed with 40μl of DMEM. Both tubes were left at room temperature for 5 minutes, before being mixed together and left for further 20 minutes at room temperature. 120μl of DMEM without antibiotics was added to the mixture and this was added to the cells and left overnight.

Transfection of siRNA using INTERFERin

For siRNA transfections using INTERFERin a single well of a six well plate of cells were cultured to approximately 80% confluent trypsinised and diluted in 1/50ml 1/100ml, 0.5ml per single well of 48 well plate of cells were plated. Transfection was performed no longer than 20 hours after plating. siRNA was transfected using INTERFERin (Polyplus transfection). INTERFERin was votexed and the desired amount of OPTimen was taken from the stock, both were left to stand to reach room temperature. All values are for 48 well plates using a final siRNA concentration of 40nM. In a tube 0.5μl of 20mM siRNA was added to 50μl of OPTimen and left for 5 minutes at room temperature 1μl of INTERFERin was added and the mixture was pipetted up and down once to mix and left for 10 minutes at room temperature. Media on cells was discarded and replaced with 200μl of DMEM containing no antibiotics. The transfection mixture was added to the cells and shaken to mix. Media was changed the next day and cells were fixed or lysised after a further 72 hours.

Luciferase Reporter assays

A single well of a six well plate that was one hundred percent confluent was trypsinised and diluted in 40ml of DMEM. In a 96 well plate, 100μl of diluted cells were plated per well. The following day a calcium phosphate transfection was performed, using 10μg/ml of one of three different firefly luciferase reporter plasmids (pNF-κB (NF-κB reporter), pTCFwt (beta Catenin reporter) and pXB1EBS (ZONAB reporter)) and 10μg/ml of control Renilla luciferase plasmid pRLEBN. Transfections were performed in quadruplicate, using final volume of

20μl /well of precipitate. A further 80μl of DMEM was added to each well and the cells were left overnight. The following day cells were washed with PBS (200μl /well), fresh media was then added to cells (100μl/well) and left in the incubator for one further day. The next morning the cells were washed once with PBS (200μl /well) and lysed, in 1X passive lysis buffer (20μl /well) from Dual luciferase Kit (Promega). Lysates were incubated on a shaker for 20 minutes at room temperature, before performing a Luciferace assay, using a Dual luciferase Kit (Promega) according to manufacturers protocol, using 12μl of protein extract and 30μl of substrate solutions.

Antibodies

All antibodies used for this study are listed in the Appendix section

Immunostaining and Microscopy

Cells were grown typically for 4 days after plating on glass cover slides in 24 or 48 well plates. Cells were fixed by the addition of cold methanol (-20°C) (0.5ml/well of 24 well plate) and transferred immediately to the freezer for 5 minutes. The methanol was discarded and the cells were re-hydrated with 1XPBS for 5 minutes at room temperature. The fixed cells were blocked prior to staining in PBS-0.5%BSA -0.1%NaN_3 for 30 minutes. Cells were also fixed with 3% PFA /PBS pH 7.4 (0.3ml/well) for 20 minutes at room temperature, permeabilised with 0.3ml/well of 0.3%triton 0.3% BSA for 5 minutes at room temperature then washed twice with 0.5%BSA 20mM Glycine PBS and left to

stand for 30 minutes before discarding solution and adding blocking solution 0.5% BSA, 0.1% NaN_3 PBS. The appropriate primary antibodies was added to cells at the appropriate dilution in the blocking solution 0.5%BSA, 0.1%NaN_3 PBS and incubated for 2 hour at room temperature or overnight at 4°C. The cells were washed three times for 10 minutes with blocking solution and incubated with the appropriate fluorescent secondary antibody conjugated to either FITC, Cy3, Cy5 or AMCA (Jackson ImmunoResearch Inc.) diluted 1:300 in blocking solution or incubated with either FITC or TRITC conjugated Phalloidin 1:2000 (Sigma) or DNA stain Hoechst 33258 1:4000 (Invitrogen) for 1 hour. The cells were washed twice for 10 minutes in blocking solution and given a final wash for 10 minutes in PBS. Cover slides were mounted onto microscope slides in ProLong gold antifade mounting media (Molecular probes/Invitrogen). Slides were observed under a Leica DMIRB fluorescent microscope or a LSM Zeiss 510 and LSM 700 confocal laser scanning microscope using 63x immersion oil lens. Images were acquired using simple PCI and LSM510 and ZEN operating software and processed (i.e., adjustment of brightness) with Adobe Photoshop ver 7.0.

Fluorescence Resonance Energy Transfer (FRET)

For FRET experiments, siRNA transfected cells were plated into ibid multi-well chamber slides and then transfected with p-Raichu-RhoA. The FRET analysis was performed at 37°C with a Leica SP2 microscope using the manufacturer's software measuring donor recovery after acceptor bleaching (YFP was

bleached to 30%). FRET efficiency maps were then produced with the Lecia software. For quantification, CFP images were subtracted and then quantified with ImageJ calculating the ratio of ($CFP_{\text{after bleaching}} - CFP_{\text{before bleaching}}/CFP_{\text{after bleaching}}$). For each image, all cell-cell contacts were quantified and as many internal areas; averages of all cell-cell contacts and all internal areas then gave one value each per image, and these values were used for the final statistical analysis. Normalisations were performed by dividing obtained values for specific fields by values obtained for the entire field imaged.

RhoGTPase siRNA library screen

RhoGTPase library

The siRNA library used in this study contains siRNAs from custom made libraries that target specific classes of genes. It contains siRNAs to 207 RhoGTPase regulators or downstream effectors of RhoGTPases. In addition it also contains 58 siRNAs from a library containing, actin regulatory and binding proteins. The siRNAs in the library contain double stranded RNAs that are made up of pools of 4 different individual siRNAs per gene, at a final concentration of 20μM to total siRNA. The library was made by Dharmacon (siArray siRNA libraries) and uses siGENOME siRNAs. For complete list of genes and siRNA sequences used in the library see appendix section

Junction assembly screen

For the siRNA screens, HCE cells were plated out the day before transfection on glass coverslides in 48 well plates for the immunofluorescent screen and 96 well plates for the NF-κB reporter assay, in medium without antibiotics. They were plated at the appropriate density so that they were 50% confluent the day of the transfection. HCE cells were plated out on glass cover slides in 48 well plates. The following day cells were transfected with 100nM of each siRNA pool from the library the transfection was performed in duplicate to allow staining of two cover-slides with different sets of antibodies. The siRNA library was transfected by mixing in individual wells of a 96 well plate. 1μl of each siRNA pool of the library, 19μl of 1XsiRNA buffer and 20μl of DMEM without antibiotics. This was left at room temperature for 5 minutes. In another tube 300μl of DharmaFECT solution 4 (Dharmacon) was mixed with 12ml of DMEM without antibiotics and was left at room temperature for 5 minutes. 41μl of the DharmaFECT solution 4/DMEM mix was added to each well of the 96 well plate and left for further 20 minutes at room temperature. Then 120μl of DMEM without antibiotics was added to the mixture in each well and 201μl of this mixture was added to the cells in the 48 well plates and left overnight. Cells were grown a further 72 hours and then fixed with methanol. One cover slide for each transfection was stained with Set 1 antibodies (β-Catenin, ZO-1 and Giantin (Golgi)) and the other cover slide was stained with Set 2 antibodies (Occludin, α-Catenin and Hoechst (DNA)).

NF-κb reporter assay screen

HCE cells were plated out in 96 well plates. The following day cells were transfected with 100nM of each siRNA pool. The siRNA library was transfected in triplicate, a 3X mix was made by mixing in individual wells of a 96 well plate. 1.2μl of each siRNA pool of the library, 22.8μl of 1XsiRNA buffer and 24μl of DMEM without antibiotics. This was left at room temperature for 5 minutes. In another tube 1.2μl of DharmaFECT solution 4 (Dharmacon) was mixed with 48μl of DMEM without antibiotics and was left at room temperature for 5 minutes. 49.2μl of the DharmaFECT solution 4/DMEM mix was added to each well of the 96 well plate and left for further 20 minutes at room temperature. Then 48μl of DMEM without antibiotics was added to cells in each well and to this 32.4μl of the siRNA mixture was added to the cells in each well of the 96 well plates and left overnight. The following day a calcium phosphate transfection was performed (see Calcium phosphate transfection for details) to transfect 10μg/ml of pNF-κB (NF-κB reporter) plasmid and 10μg/ml pRLEbn plasmid. As a control for NF-κB inhibition 10μg/ml of IkBα S32,34A plasmid was also transfected. Cells were left a further 48 hours, before performing a Dual luciferase reporter assay. The amount of firefly luciferase activity was divided by the amount of renilla luciferase activity to standardise results for differences in cell density. An average of this ratio was calculated from triplicate plates and from this the fold difference from control (non targeting siRNA) was calculated.

TER and permeability assays

Caco-2 cells were cultured in normal calcium media conditions, transfected with the appropriate siRNAs and plated onto glass cover slide for immunofluorescence or on filters for TER and permeability measurements in low calcium medium (Sigma spinner culture medium with 2 mM glut / 1 mM Na-pyruvate / PenStrep 10% dialyzed FCS) (Sigma) and left for 24 hours before the addition of normal calcium media. Samples were fixed at various time points for immunostaining or TER measurements were taken using a AC square wave current of ± 20 μA at 12.5 Hz with a silver electrode and measuring the voltage deflection elicited with a silver/silver-chloride electrode using an EVOM (World Precision Instruments, Sarasota, FL), as previously described [278] over a period of 48 hours after which the permeability of 4 kDa FITC- conjugated Dextran and 70kDa Rhodamine B (REF company) conjugated dextran tracer were measured using a FLUOstar OPTIMA microplate reader (BMGLabTech, Offenburg, Germany)

Wound healing assays

For wound healing assays a single well a six well plate of cells grown to 80% confluence was trypsinised and diluted into 30 ml and plated onto 12 well plates 1ml /well. The following day siRNAs were trasfected using INTERFERin (see siRNA transfection using INTERFERin) for 1 well used 2μl of siRNA 20mM stock 4μl INTERFERin in 200μl of OPTImem. The next day 3 wells for each siRNA were trypsinised with 0.4ml of trypsin and combined into one tube to give 1.2ml, this was centrifuged in bench-top centrifuge for 5 minutes at 3000rpm.

The trypsin was discarded and cells carefully resuspended in 600μl of DMEM. 80μl of cells were plated in each side of the insert of a culture –insert plate from Ibidi. Cells were left overnight or until confluent before generation of the wound by removal of the insert. Images were taken at the start and at various times after to monitor wound closure. The percentage of the area of the wound was quantified from the images using Image J.

Statistical analysis

Mean averages and Standard deviation were calculated using standard formulae for calculation of statistical significance between two different data sets a two tailed students t-set was used.

Drosophila fly stocks

Flies were kept under standard conditions. y,w,hsflp122;Tub>GFP>GAL4 expressing heat shock inducible flip recombinase and GFP from a minimal tubulin promotor (kind gift from Gary Struhl). y^1,w;P{Act5C-GAL425FO1}/CyO,y^+ Permits ubiquitous expression of GAL4 driven from an actin promoter. (Bloomington Stock number 4412) (flybase.org). RNAi stocks containing shRNA to cg10188 under the control of a yeast UAS promoter were obtained from the Vienna Drosophilla RNAi center VDRC. Transformant ID numbers 18029 and 103391 both contain different shRNA sequences that target cg10188.

Immuno-staining of Imaginal discs

Larvae were heat shocked at 37°C for 30 minutes to induce expression of flip recombinase and drive expression of cg10188 specific shRNA. Lavrae were left for a further 48 hours before imaginal discs were dissected and fixed at room temperature for 20 minutes in 4%PFA /PBS. Discs were washed three times 30 seconds with PBST (1XPBS + 0.3% Triton x100) before incubation overnight at 4°C with primary antibodies. The next day discs were washed as above in PBST and incubated with fluorescent secondary antibodies or TRITC conjugated Phalloidin for 5 hours in the dark at room temperature before three further washes with PBST for 30 seconds and a final wash for 1 hour, before mounting discs on slides with Vector shield mounting media (Vector labs).

CHAPTER 3

Functional siRNA screen for regulators and effectors of RhoGTPases required for Junction formation, and pro-inflammatory gene expression in Corneal epithelial cells.

Chapter 3 –Functional siRNA screening for regulators and effectors of RhoGTPases.

Overview

This chapter contains the results from a functional siRNA screen to identify regulators and effectors of RhoGTPases in human corneal epithelial cells that regulate cell adhesion and junction formation, as well as Rho regulated signalling pathways that regulate gene expression. The screen was performed using a siRNA library containing 265 siRNA pools that specifically target proteins that are regulators or downstream effectors of RhoGTPases, including the 20 known RhoGTPases.

HCE cells were chosen as a model epithelial cell line to study regulation of RhoGTPase signalling in junction formation because they form functional epithelial junctions and express many of the major junctional and polarity markers. HCE cells can be grown in sufficient quantities for a short space of time on glass cover slides. They can be efficiently transfected with siRNA to perform RNAi experiments and can be transfected with different firefly luciferase constructs to perform gene reporter assays, thus making them an ideal model for functional siRNA screening. I transfected the siRNA library into HCE cells grown on glass cover slides fixed and immuno-stained cover slides with two different sets of antibodies/fluorescent dyes for markers that stained specific structures associated with polarity, such as the Golgi complex along with

several components of Tight and Adherens junctions and observed if polarity and junction morphology was perturbed.

To identify components of RhoGTPases that have effects on gene regulation, firefly luciferase based NF-κB, TCF/β-Catenin reporter assays were optimised for use in HCE cells. However due to time constrains of this project only a RhoGTPase siRNA screen for components that affected NF-κB activity was performed.

By performing the siRNA screen to observe effects on epithelial junction morphology I identified 26 components that had strong and 36 that had weaker effects on junction morphology. We also indentified a number of components of RhoGTPase signalling that regulate NF-κB reporter activity by identifying several candidates that had strong inhibitory or stimulatory effects on constitutive NF-κB activity. I discovered the RhoGTPases, RhoA and Cdc42 had the strongest effects on junction formation, with Rac1 seeming to give a weaker effect in HCE cells. I also identified a number of GEFs, GAPs and downstream effectors of both RhoA and Cdc42, as potential candidates that regulate junction formation from the screen. I validated a subset of these candidates, as well as several candidates that were identified as having effects on junction formation, from a similar screen performed in Caco-2 cells (Matter 2007 unpublished results), by de-convolution of the siRNA pool into individual siRNAs. I chose to fully characterise the function of one of these validated candidates, p114RhoGEF. This analysis is presented in chapter 4.

Establishing HCE cells as a model epithelial cell line for performing functional siRNA screening.

HCE cells are an immortalised SV40 large T–antigen transformed human corneal epithelial cell line. When cultured in *vitro,* HCE cells assemble functional adherens and tight junctions and spontaneously differentiate when grown in serum free keratinocyte growth medium [34]. HCE cells express many of the known major structural and regulatory components of tight and adherens junctions (Occludin, ZO-1,2,3 Cingulin, Claudin 4, ZONAB, GEF-H1, E-Cadherin, β-Catenin and α-Catenin as well as conserved polarity genes Crb 2 and 3 and the components of the PAR3/6/aPKC complex [34, 279] (Matter 2007 unpublished results), making them suitable for use as a model for early junction assembly and differentiation. To establish the culture conditions needed to test the suitability of HCE cells for functional siRNA screening, I needed to establish if they could be grown on glass cover slides at a relatively low confluence to permit efficient siRNA transfection. Starting at a low confluence would allow sufficient time for discreet junctions to form, as well as enabling a robust knockdown of the target protein. Establishing if RNAi could be performed efficiently in HCE cells by transfection of siRNAs was addressed using a β-Catenin siRNA pool as a control.

Figure 3.0 shows β-Catenin protein levels are reduced 72 hours post transfection of β-Catenin siRNA pool compared to non-targeting control siRNA. Immunostaining for β-Catenin and ZO-1 was performed on non-targeting and β-

Catenin siRNA transfected cells (Figure 3.0). In the control (non-targeting siRNA), there was recruitment of ZO-1 and β-Catenin to distinct junctional complexes. Control cells appeared to have a normal morphology indicating the transfection reagent used (Dharmafect solution 4) was not toxic and the non-targeting siRNAs did not effect morphology or junction formation of HCE cells. Transfection with β-Catenin siRNAs led to a clear reduction in β-Catenin at cell-cell junctions and the appearance of large spread cells, indicating RNAi is working efficiently to repress β-Catenin expression. However ZO-1 recruitment to junctions seemed to remain unaffected indicating that β-Catenin is not required for ZO-1 recruitment to junctions.

Before I performed the functional siRNA screen I stained HCE cells grown for 4 days with two different sets of antibodies. Figure 3.1 clearly shows HCE cells form distinct tight and adherens junctions within 4 days of culturing, making them suitable to screen for genes regulating the early stages of junction formation. Furthermore the combinations of two different sets of antibodies can be used as markers in the screen, as they all work in methanol fixed cells and no cross reactivity was observed between the different antibodies.

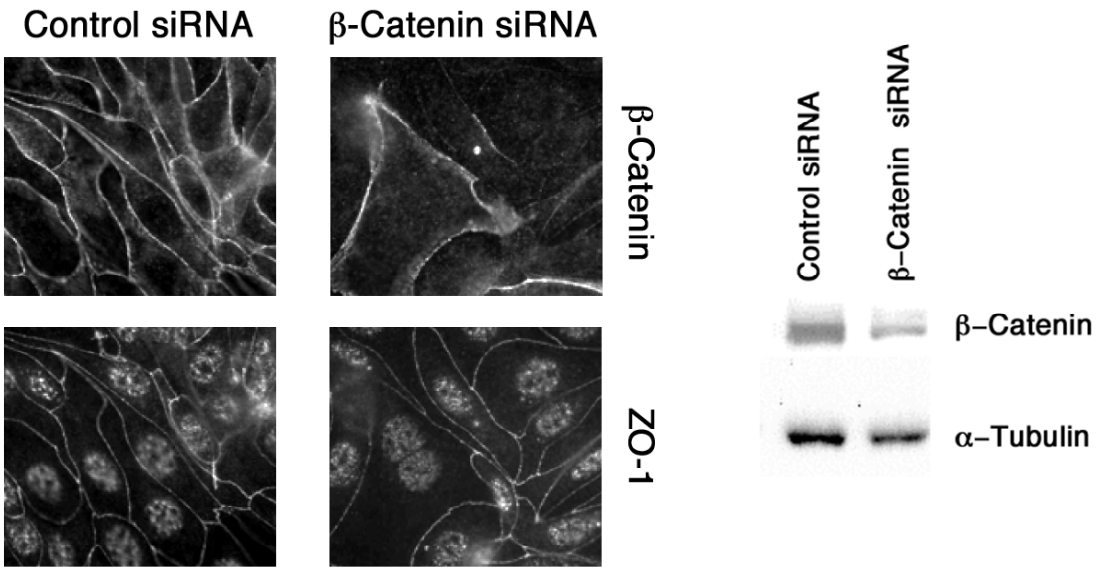

Figure 3. 0 RNAi can be efficiently performed in HCE cells using siRNAs.

HCE cells cultured in DMEM 10%FBS were transfected with 100nM of non-targeting control or a pool of β-Catenin siRNAs using Dharmafect solution 4. The efficiency after 72 hours of siRNA mediated, knockdown of β-Catenin was assessed by Immunoblot using a β-Catenin specific antibody and immunoblotting for levels of α-tubulin as a loading control. Immunofluorescence staining with β-Catenin and ZO-1 antibodies in methnol fixed HCE cells transfected as above is also shown with control non targeting or β-Catenin siRNAs.

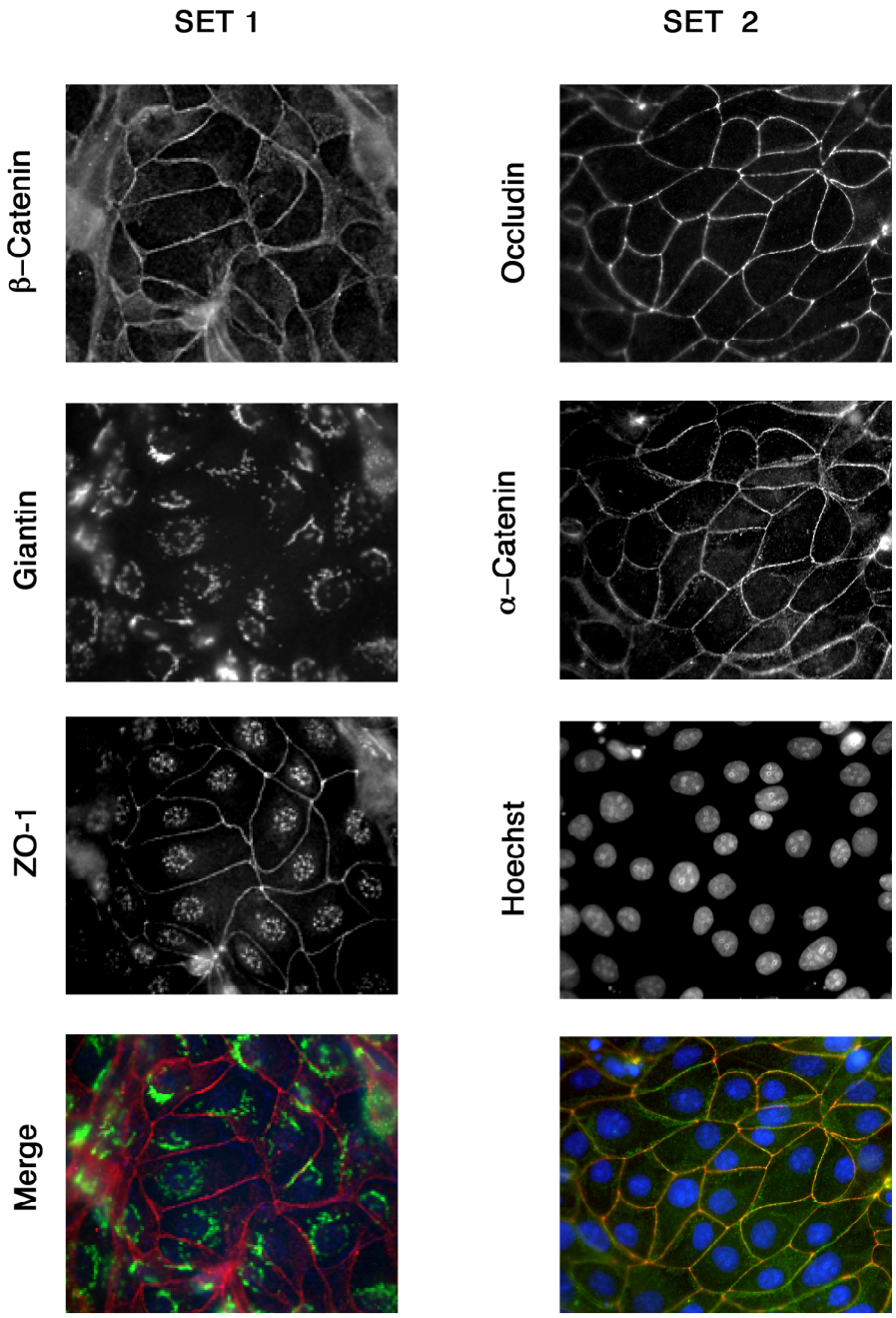

Figure 3.1 HCE assemble distinct Tight and Adherens Junctions.

HCE cells cultured on 10mm glass cover-slides in DMEM 10% FBS, fixed with methanol and stained with two different sets of antibodies/markers SET1: β-Catenin, Adherens junction marker (red), Giantin, Golgi marker (green) and ZO-1, Tight junction marker (blue). SET 2: α-Catenin, Adherens junction marker (red), Occludin, Tight junction marker (Green), Hoechst 33258, DNA stain (blue).

Establishing luciferase based reporter gene assays to monitor NF-κB and β-Catenin/TCF activity in HCE cells.

To study the effects RhoGTPase signalling has on gene expression pathways in the corneal epithelium, lucfierase based reporter assays of three transcriptional regulators, (NF-κB and TCF/β-Catenin) were optimized for use in HCE cells. NF-κB is a transcription factor important in mediating pro-inflammatory responses, cell growth and survival [111, 124], as well as genes important for EMT [115]. NF-κB activity can be regulated by components of junctions, such as E-Cadherin and p120 Catenin [121, 124]. Many growth factor and cytokine induced signalling cascades also result in the activation of NF-κB. Signalling that activates pro-inflammatory responses often results in increased paracellular permeability or even disassembly of cell-cell junctions. RhoGTPases are crucial regulators of junctions and are important regulators of NF-κB signalling. I wanted to investigate how RhoGTPase signalling regulated NF-κB activity in HCE cells. I performed NF-κB reporter assays in HCE cells grown in normal serum (DMEM/10%FBS) or serum free conditions (K-SFM), as Fetal bovine serum contains a complex mix of growth factors that alter NF-κB activity. I performed the NF-κB reporter assay in these two conditions and indeed detected constitutive activation of NF-κB when the assay was performed in the presence of serum. This level of activity was not seen in serum free conditions (Figure 3.2).

To test if the constitutive activity could be inhibited a plasmid containing a mutant non-phosphorylatable form of IkB S32 34A, a strong inhibitor of NF-κB activation was co-transfected. The dominant mutant inhibited NF-κB activity by about 2 fold. It was also tested if the low basal NF-κB activity in serum free conditions could be induced by TNF-α, a pro-inflammatory cytokine and potent stimulator of NF-κB. This activity was induced about 5 fold, by stimulation with 20ng/ml of TNF-α for 5 hours (Figure 3.3 B). This inducible activity could be inhibited by the expression of IkBαS32,34A. These experiments demonstrate, NF-κB activity can be measured by reporter assays in HCE cells as either constitutive or TNF-α induced activity.

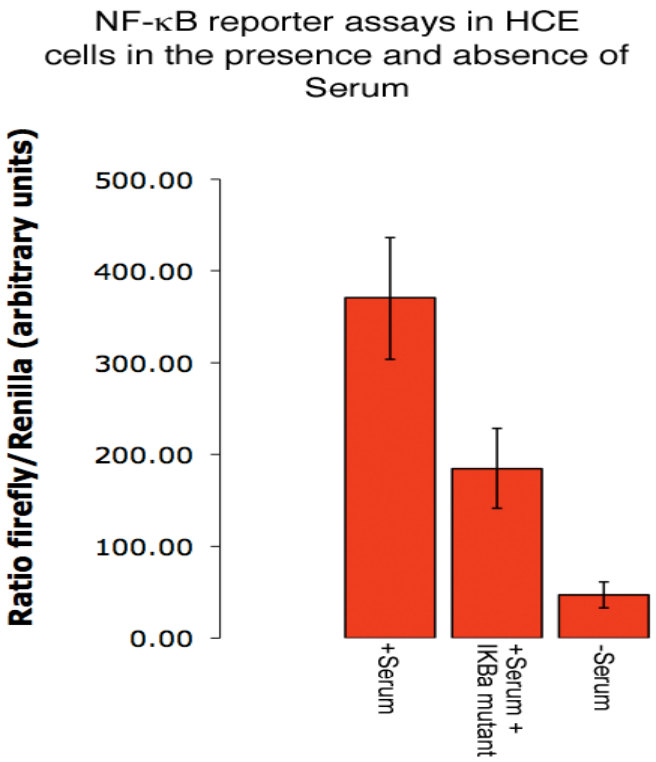

Figure 3.2 NF-κB reporter assay performed in HCE cells.

NF-κB reporter assay was performed in HCE cells in DMEM 10%FBS (+serum) or in K-SFM (-serum). Constitutive activation of NF-κB in serum conditions can be inhibited by transfection of 10μg/ml of inhibitory IkBα S32 34A protein. Values are plotted as a ratio of firefly luciferase activity divided by Renilla luciferase. Bars represents mean average from quadruplicate wells. Error bar represent +/- 1 standard deviation.

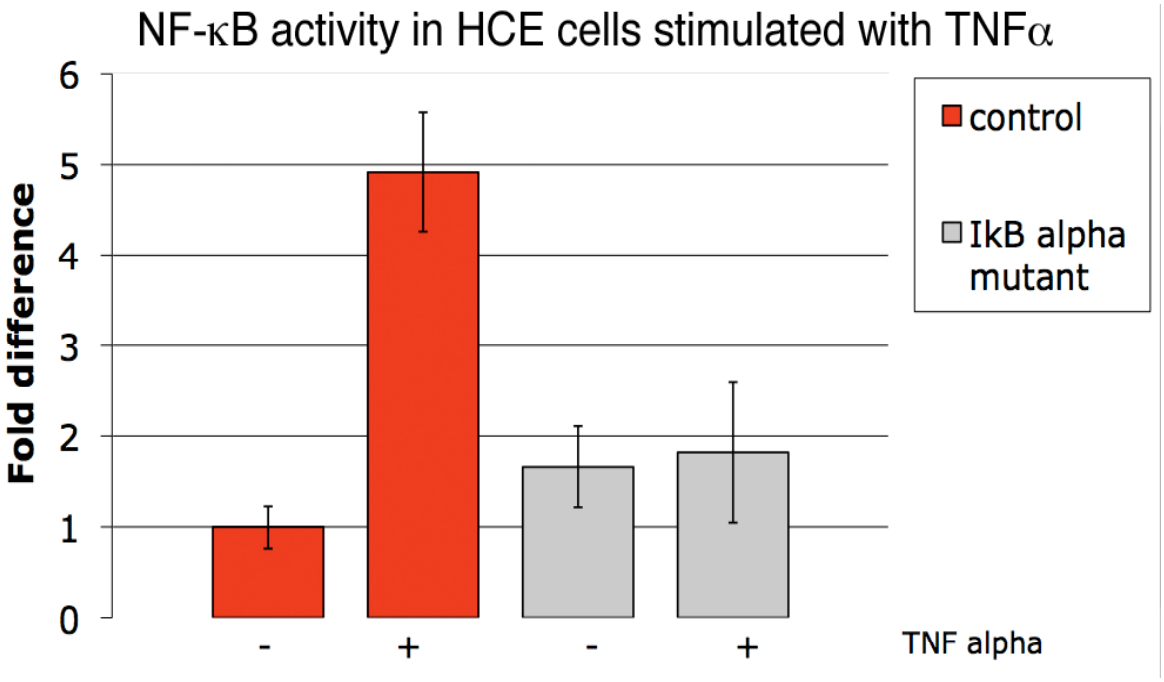

Figure 3.3 NF-κB activity can be induced in HCE cells with TNFα stimulation

NF-κB reporter assay was performed in HCE cells in serum free conditions without or after 5 hours stimulation with 20ng/ml of TNFα (shown on graph as - or +). Stimulation with TNFα caused a 5 fold increase in activity which can be inhibited by transfection of 10μg/ml of inhibitory IkBα S32,34A protein. NF-κB reporter activity was calculated as a ratio of firefly luciiferase divided by Renilla lucferase. Results were normalised to control experiments. Bars represent mean of quadruplicate wells. Error bars represent +/- 1 standard deviation.

Next, I adapted two assays for transcription factors known to be regulated by cell-cell adhesion. β-Catenin is a multifunctional protein that is a key component of AJs and is known to interact with multiple binding partners that function in cell-cell adhesion and transcriptional regulation [106]. In epithelial cells β-Catenin recruitment to AJs is thought to result in inactivation of its transcriptional role by preventing it from translocating to the nucleus. However when cell-cell contacts are forming or disrupted it is thought that more cytoplasmic β-Catenin is present. This shift in the equilibrium of cytoplasmic β-Catenin, permits greater amounts to translocate to the nucleus, where it associates with LEF/TCF transcription factors leading to their activation and transcription of genes required for proliferation.

First I performed a β-Catenin/ TCF reporter assay in the presence of serum. (Figure 3.4). The reporter assay was performed after transfection with control, non-targeting and β-Catenin siRNAs. A three fold reduction was observed in cells transfected with β-Catenin siRNA, providing evidence that the activity observed was specifically dependent on β-Catenin. A control plasmid was also transfected along with control siRNAs. This plasmid contained a version of the β-Catenin/ TCF promoter that had its TCF binding sites deleted rendering it non functional. This construct gave no observable activity.

In summary NF-κB and β-Catenin/TCF activity can be measured by reporter assays in HCE cells. In addition, depletion of these two transcriptional

regulators can be obtained by transfection of specific siRNAs. Thus the conditions for performing siRNA mediated depletion of specific proteins to observe effects on NF-κB and β-Catenin/TCF activity by reporter assays, are now optimized for use in HCE cells. The initial aim of this study was to use these three assays to perform siRNA screens using the RhoGTPase siRNA library to observe changes in β-Catenin/TCF and NF-κB activity and thus identify components of RhoGTPase signalling pathways important for gene expression. However due to the limited time and resources for this study the RhoGTPAse siRNA screen was only performed for NF-κB activity and not β-Catenin/TCF activity.

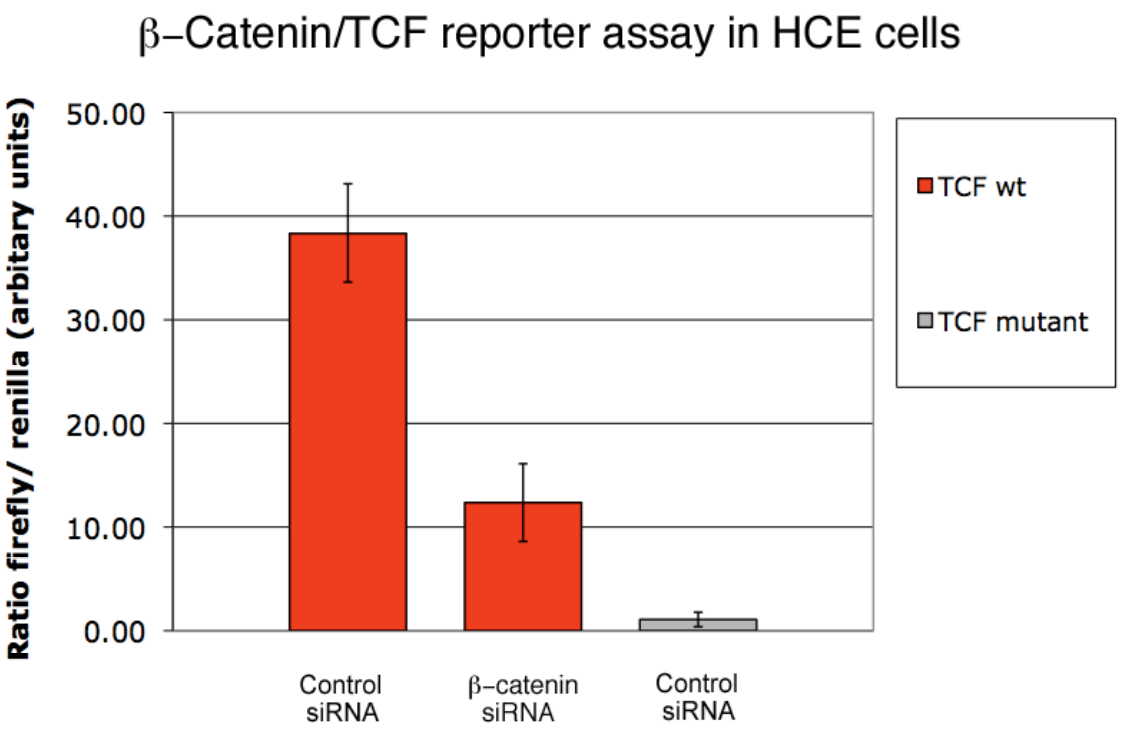

Figure 3.4 Establishing β-Catenin/TCF reporter assays in HCE cells

Luciferase based β-Catenin/TCF reporter assays performed in HCE cells in serum conditions. Non-targeting control and β-Catenin siRNA pool were transfected into HCE cells, luciferase activity β-Catenin/TCF reporter was measured 72 hours post siRNA transfection. Knockdown of β-Catenin resulted in a 3 fold reduction of β-Catenin/TCF activity. To test the specificity of the assay, a construct containing mutations in the TCF promotor binding site (TCF mutant) was transfected and demonstrated to give very low luciferase activity. Values are plotted as a ratio of firefly luciferase activity divided by renilla luciferase activity. Bars represent mean average from quadruplicate wells. Error bars represent +/-1 standard

siRNA screen for regulators and effectors of RhoGTPases that effect junction formation.

Using the conditions established for performing RNAi in HCE cells (Figure 3.0), I performed a siRNA RhoGTPase library screen to identify regulators and effectors of RhoGTPases that effect junction formation. The screen was performed on HCE cells grown on glass cover slides in 48 well plates, pools of 4 siRNAs to each target protein in the library were transfected in duplicate to allow staining with two different sets of antibodies (Figure 3.1). A total of 63 candidates were identified with 26 being classified as having a strong effect and 37 having weaker effects on junction formation (Table 3.0). I defined a strong effect as broken or discontinuous junctions in most of the cells observed compared to control (see Figure 3.5, RhoA and Cdc42 and p114RhoGEF for examples) and weak effects, when a smaller proportion of cells had broken or discontinuous junctions (see Figure 3.5, Rac1).

Strong	Weak	
AHRGEF12, LARG	AKAP13, LBC	PARD6G
ARHGD1B	ARHGAP20	PIK3R1
ARHGEF18, p114RhoGEF	ARHGAP22	PLEKHG3
CDC42	ARHGEF16	PLEKHG5
CDC42BPA, MRCK alpha	ARHGEF6	PLEKHG6
CDC42BPB,MRCK beta	ARHGEF7	PLXNA1
CTNNA1	BCR	RAC1
DEPDC1B	CTNNA3	RALBP1
DOCK4	DLC1	RHOBTB1
FGD5	DOCK10	RHOG
ITSN1	DOCK2	TIAM2
ITSN2	DVL2	TRIP10
MAP4K1	INpp5B	
OBSCN	MAP4K2	
OCRL	MAP4K5	
PIK3R2	MCF2L	
PLEKHG1	MLK3	
PLEKHG2	MYLK2	
RACGAP1	MYO1C	
RAD51L3	MYO7B	
RHOA	MYO9A	
RHOBTB3	NGEF	
SPATA13	PAK1	
STARD13, DLC2	PAK7	
STARD8,DLC2	PAK7	
TINK	PARD6A	

Table 3.0 siRNA screen results for regulators and effectors of RhoGTPases that effect junction formation.

A total of 64 candidates were identified from the siRNA screen, 26 candidates had a strong effect on junction formation shown in red and 38 had a weaker effect, shown in grey.

RhoA and Cdc42 are essential for junction formation and polarity in HCE cells.

Cdc42, Rac1 and RhoA are the three most well characterised family members of RhoGTPases [144] , all three have been identified to have crucial roles in epithelial junction formation and the maintenance of polarity [18]. The siRNA screen identified Cdc42 and RhoA as having strong effects on junction formation (Figure 3.5). The effects observed on junction morphology with the RhoA specific pool of siRNAs were validated to control for off target effects by de convolution of the siRNA pool into four individual siRNA. All four RhoA siRNAs gave the same phenotype as the RhoA pool (Figure 3.9), validating the importance of RhoA for junction formation.

Depletion of both of these RhoGTPases prevents normal TJ formation (Figure 3.5), as ZO-1 a marker for TJs appeared broken and discontinuous at cell-cell contacts. AJs were also effected, demonstrated by β-Catenin staining at cell-cell contacts being broken and having a more undulating appearance than control cells. Cdc42 depletion severely effected cell polarity, as the appearance of the Golgi looked fragmented and disorganised. However Rac1 appeared to have a weaker effect on junction formation than Cdc42 and RhoA, with AJs remaining largely unaffected, but ZO-1 recruitment to cell-cell contacts was perturbed in some small patches (Figure 3.5). Rac1 is known to be critical for the initial stages of assembly of cell-cell contacts, becoming activated upon E-Cadherin engagement [130, 280]. Its weaker effects observed in the screen could be

explained simply by a less efficient knockdown of Rac1 levels. Alternatively its functional role in early junction formation may occur before time has elapsed to give a sufficient knockdown of Rac1 levels, explaining the appearance of a weaker phenotype. Furthermore it is possible that Rac1 is not as important in HCE cells as in the other epithelial models in which it was studied. The importance of Cdc42, RhoA and to a lesser extent Rac1 in junction formation in HCE cells (Figure 3.5), confirms established roles of these RhoGTPases in cell-cell adhesion, polarization and differentiation and support the aim of the screen to identify novel regulators of Rho signalling.

RhoA and Cdc42 had the strongest effects in the screen therefore we focused on sorting the hits based on evidence from the literature into GEFs, GAPs and downstream effectors of these two RhoGTPases (Table 3.1). GEFs and GAPs, are reported sometimes to activate/inactivate more than one RhoGTPase. For example the GAPs DLC2 and 3 identified in this screen were shown in *vitro* to have GAP activity for Cdc42 and RhoA, but not Rac1 [281] [282], therefore it is present in both Cdc42 and RhoA tables.

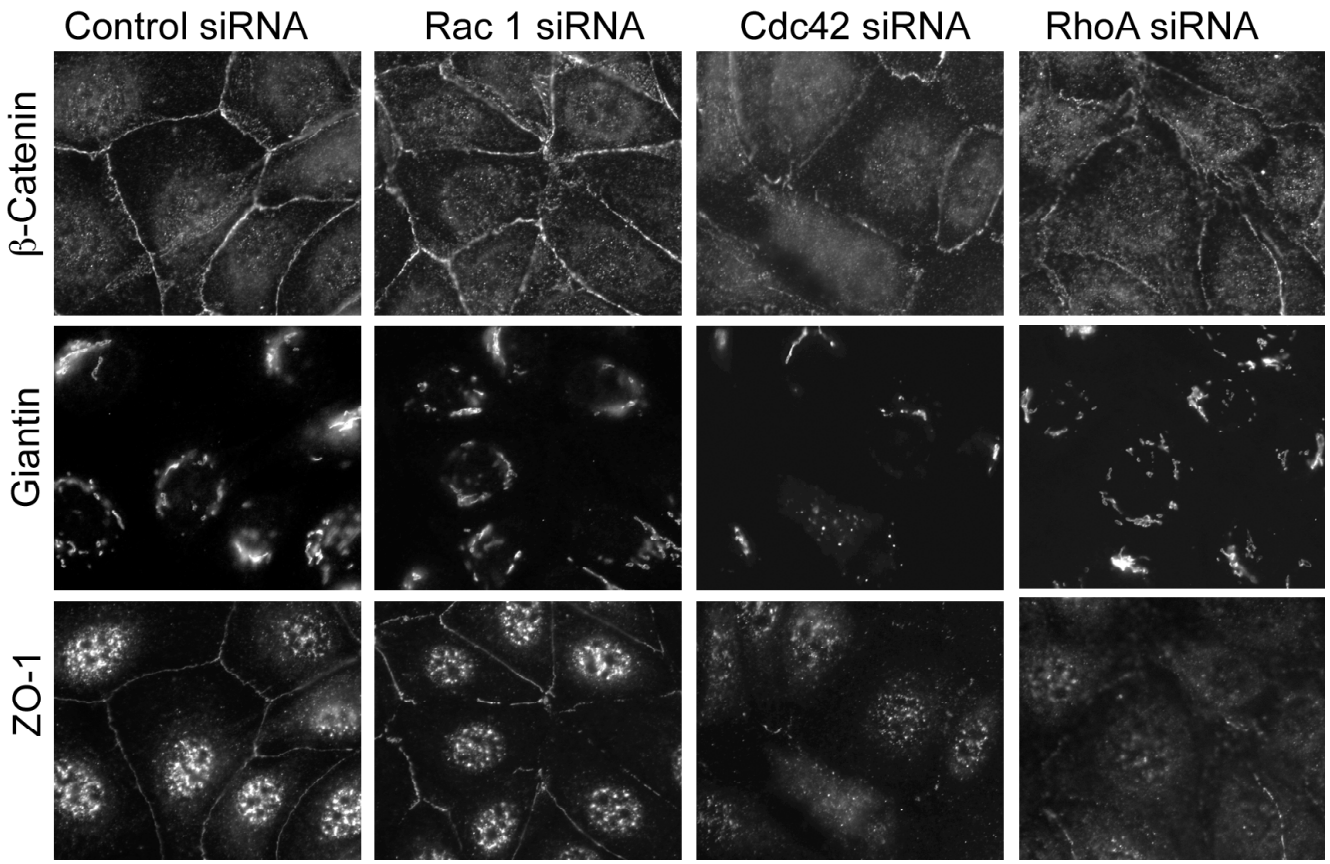

Figure 3.5 RhoGTPases Cdc42, RhoA, and Rac1 all affect junction formation.

HCE cells transfected with non-targeting control siRNA or a pool of 4 siRNAs specific to Cdc42, RhoA and Rac1. Cells were methanol fixed 72 hours after RNAi, cells were immunostained with ZO-1, β-Catenin and Giantin (golgi marker). Note Cdc42 and RhoA are good examples of strong effects, whereas Rac1 is an example of a weak effect.

Morphology
CDC42
GEFS
ARHGEF6 / a-PIX / cool 2
BCR
DOCK10
FGD5
ITSN1 /Intersectin-1
PLEKHG2, Clg
MCF-2L, Dbs
GAPs
RALBP1
RACGAP1
SPATA13
STARD13, DLC2
STARD8, DLC3
Effectors
CDC42EP2 / MSE55 / Borg5
CDC42BPA; MRCKalpha
CDC42BPB / MRCK2 (beta)
PAK7
PARD6G
PARD6A
TRIP10 /CIP4

Morphology
RhoA
GEFS
ARHGEF/18/p114RhoGEF
ARHGEF12 LARG
NGEF/ephexin-1
FLJ10665 /PLEKHG6
KIAA0720 /PLEKHG5
MCF-2L, Dbs
GAPs
STARD12/DLC1
STARD13/DLC2
STARD8/ DLC3

Table 3.1 Candidates grouped into RhoA or Cdc42 specific regulators or downstream effectors.

Candidates were grouped into two lists according to if they were a GEF or GAP or downstream effector of RhoA or Cdc42 based on literature and predictive methods. Candidates that had a strong effect are highlighted in red and candidates that had weak effects highlighted in grey. It is worth noting there is some degree of promiscuity of GEFs and GAPs as to which RhoGTPase they preferentially activate/ inactivate. For example, DLC2 and 3 appear both as RhoA and Cdc42 GEFs.

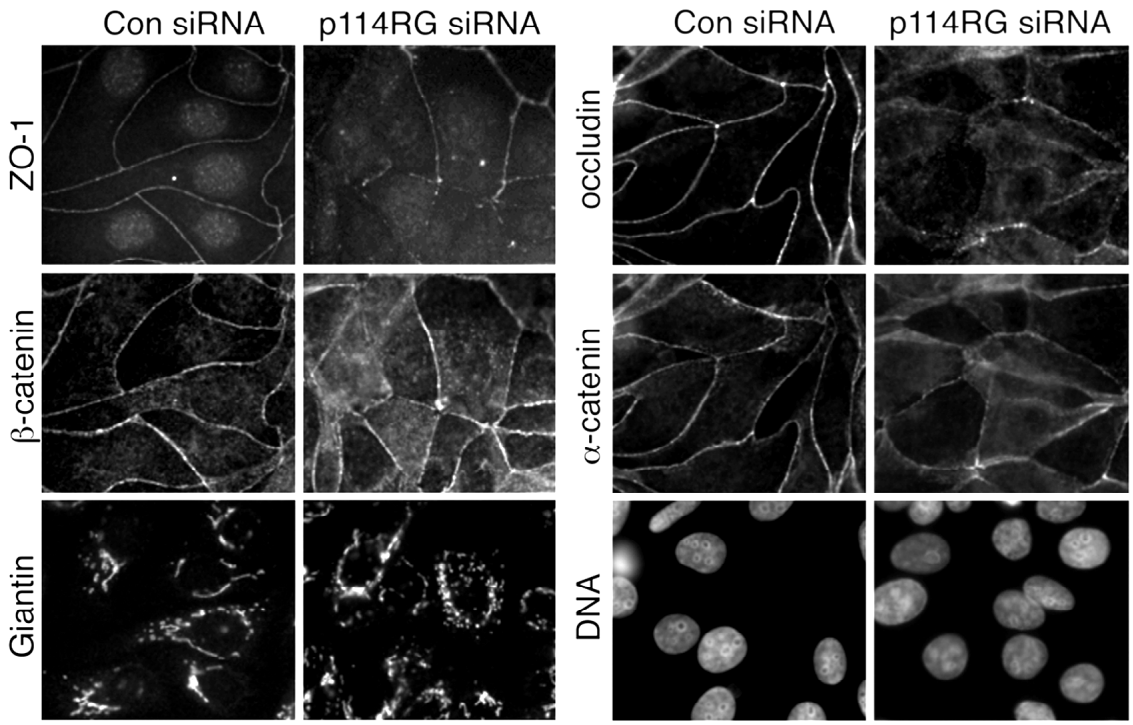

Figure 3.6 p114RhoGEF was identified from the siRNA screen as strongly affecting TJ formation.

HCE cells transfected with non-targeting control or a pool of 4 siRNAs specific to p114RhoGEF. Cells were methanol fixed after 72 hours RNAi, cells were immunostained with ZO-1, β-Catenin, Giantin (golgi marker), Occludin, α-Catenin and DNA stain, Hoechst 33258.

siRNA screen for regulators and effectors of RhoGTPases that effect NF-κB activity

RhoGTPases are major targets of junctional regulatory mechanisms and are also major downstream targets of physiological and pathological signalling pathways, activated by growth factors and inflammatory signals. NF-κB is a transcriptional regulator mediating transcription of genes associated with pro inflammatory responses and cell survival as well as genes important for epithelial to mesenchymal transition (EMT) [111, 113, 115, 117, 283, 284]. I wanted to indentify components of Rho signalling pathways that regulate NF-κB activity in HCE cells.

I performed a screen using the siRNA RhoGTPase library to observe the effects on NF-κB activity in HCE cells grown in the presence of serum. I decided to perform the screen in serum conditions as it was technically difficult to achieve robust knockdowns of target proteins in HCE cells using serum free conditions. The fold difference in activity from control (non targeting siRNA) was calculated for all candidates (Figure 3.7). Potential candidates were sorted, based on having a stimulatory or inhibitory effect on NF-κB activity. As a control for repression of NF-κB activity the dominant negative IkB mutant was also transfected and suppressed activity by 60%. Candidates that gave a strong or weak effect on morphology, identified in immunofluorescent screen are also merged with the data shown in Figure 3.7. Using these data I plotted the results in a Venn diagram (Figure 3.8). The results show very little correlation between

proteins that regulate junction formation and regulate NF--κB activity, however as the screen was performed in the presence of serum, which causes constitutive NF-κB activity I felt candidates that produced inhibitory effects, rather than stimulatory effects maybe more valid to study. MAP4K1, RacGAP1 and OBSCN were all candidates that had a strong effect on morphology and strong inhibitory effects on NF-κB activity. Two candidates MCF2L and RhoBTB1 had weaker effects on morphology, but also gave strong inhibitory effects on NF-κB activity. Validation of these candidates will need to be performed by repeating NF-κB reporter assays with individual siRNAs derived by deconvoluting the pool of siRNA used in this screen to each potential candidate. Due to time constraints candidates were only validated from the junction morphology screen. However, it will be important to validate hits in the future to understand the involvement of Rho signaling in NF-κB activation in HCE cells.

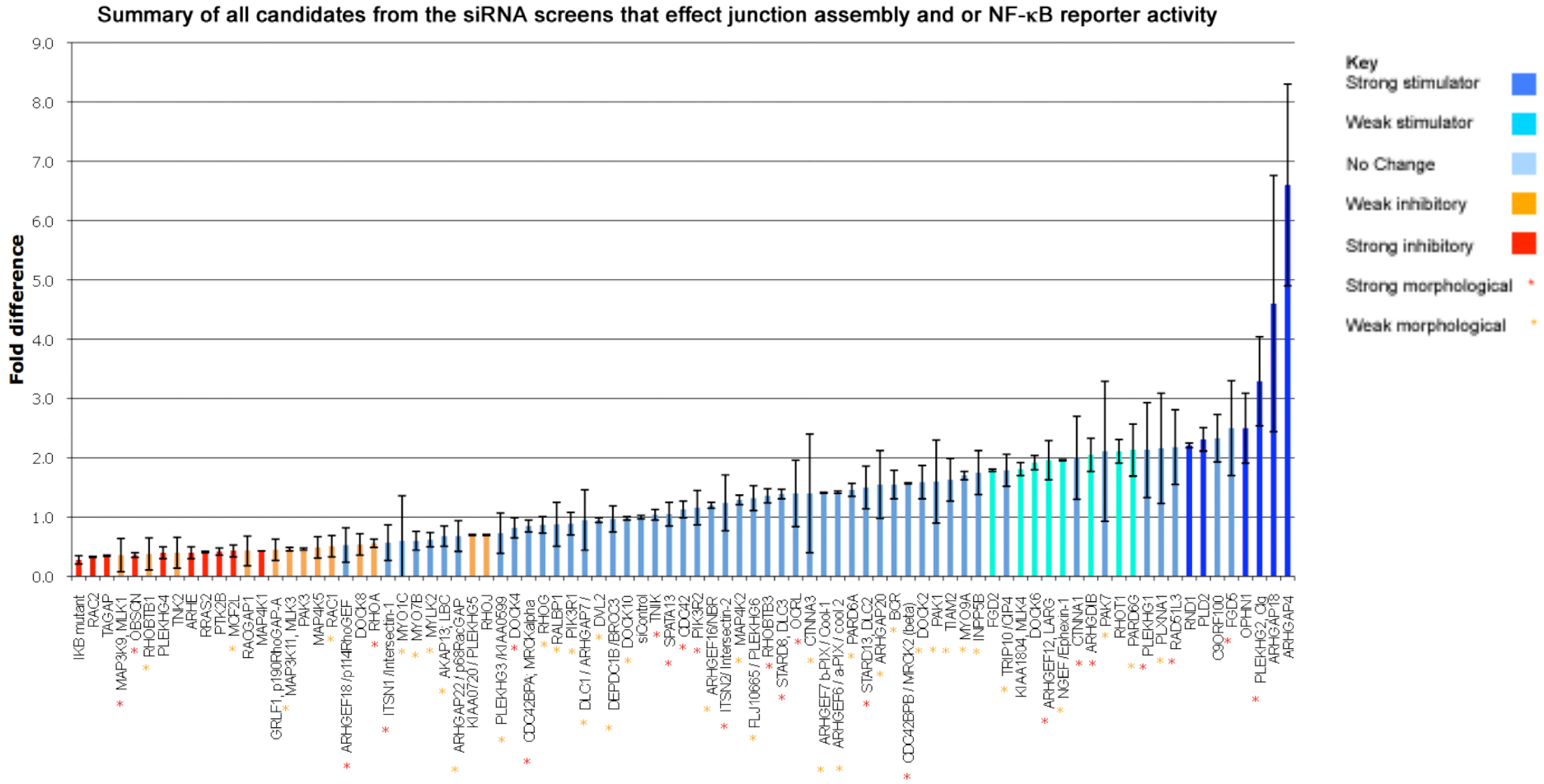

Figure 3.7 siRNA RhoGTPase library screen for proteins that effect NFκB activity in HCE cells.

Luciferase based NFκB reporter assays were performed after transfection of siRNA Rho library in HCE cells grown in the presence of serum. Results are plotted as fold difference from non-targeting siRNA control. As a control for inhibition cells were transfected with 10μg/ml of a dominant negative mutant IkBαS32,34A. Candidates were sorted based on if they had a strong stimulatory effect >2 fold (dark blue), weak stimulatory 1.8-2.0 (turquoise), no change 0.8-1.8 (blue), weak inhibitory 0.7-0.5 (orange), Strong inhibitory >=0.4 (red). * Represent candidates that have strong effect on morphology * represents weaker morphological effect. Bars and error bars represent mean and +/- 1 SD of triplicate experiments.

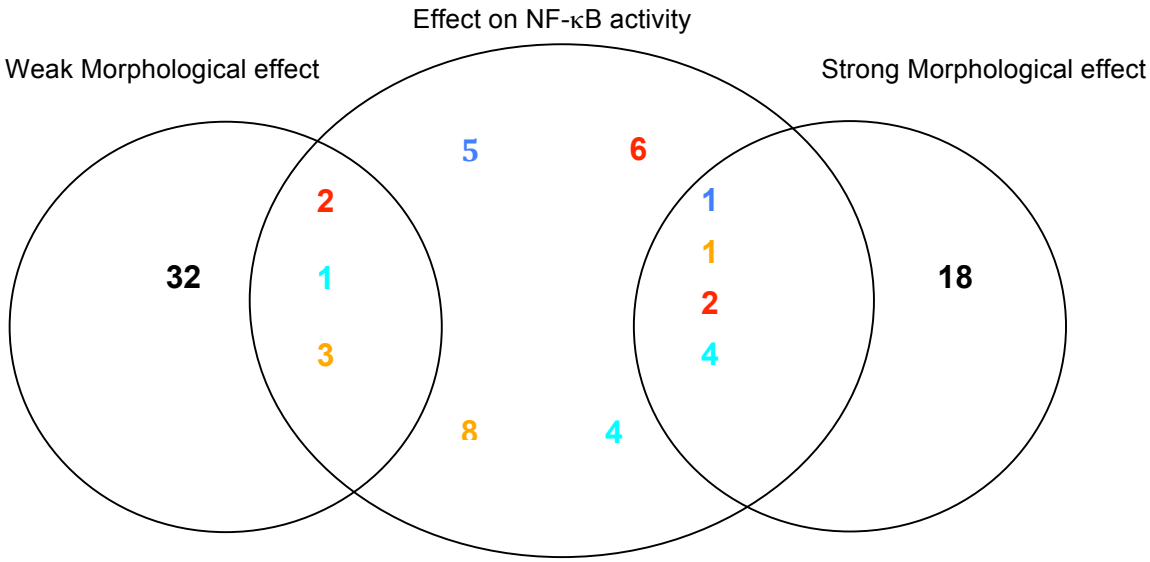

Figure 3.8 Summary of potential candidates from Immunofluorescent screen correlated with the data from screen for NF-κB activity.

A total of 85 Candidates were grouped into three categories represented by circles. Weak effect on morphology (left), effect on NF-κB activity (centre) or strong effect on morphology (right). Numbers represent candidates that fall into particular categories. The colours represent effect on NF-κB activity Red= strong inhibitory effect. Blue= Strong stimulatory effect. Orange=weak inhibitory effect. Turquoise=weak stimulatory effect. Black = no effect.

Validation of Candidates from junction formation screen.

To validate potential candidates from the primary screen for junction formation, pools of siRNAs were deconvoluted into individual siRNAs. Candidates were validated by transfecting individual siRNA and testing for their ability to reproduce the phenotype observed in the initial screen. This was to control for "off target" effects produced by pools or specific siRNAs. The initial aim was to validate hits from both junction formation and NF-κB activity screens, however due to the time constraints of this project I focused on just validating hits that effected junction morphology. Validation was performed for example for RhoA (Figure 3.9), with all four individual siRNAs producing the same phenotype when using the RhoA siRNA pool and hence confirmed the effect targeting of RhoA has on junction formation.

p114RhoGEF was validated as knockdown of p114RhoGEF by two different individual siRNAs, derived from the pool in the initial screen produced the same phenotype of disrupted TJs observed in the initial screen. A pool of these two individuals also produced the same phenotype as well as, a pool containing On-target plus siRNAs that had different p114RhoGEF specific siRNA sequences to the original siGenome pool of siRNAs (Figure 3.11). Knockdown experiments using these individual and pools of siRNA, produced similar phenotypes and seemed to affect the formation of TJ in Caco-2 cells. However unlike in HCE cells, TJs were warped and gave an uneven appearance, reminiscent of phenotypes caused by the manipulation of Myosin II activation or if actin

dynamics are pharmacologically perturbed [236]. Immunoblotting, HCE and Caco-2 cell lysates revealed that efficient knockdown of p114RhoGEF was achieved using two different individual siRNAs, as well as a pool of the two individuals siRNAs. (Figure 3.10). I also validated the effects observed on junction assembly of a subset of candidates. I confirmed as valid candidate by two or more individual siRNAs reproducing the same effect on junction morphology (Table 3.2). Examples are shown for effects on Junction formation for the Cdc42 and RhoA GEF, MCF2L a.k.a Dbs (Figure 3.12), and two Cdc42 effector proteins MRCKα and β (Figure 3.13-14).

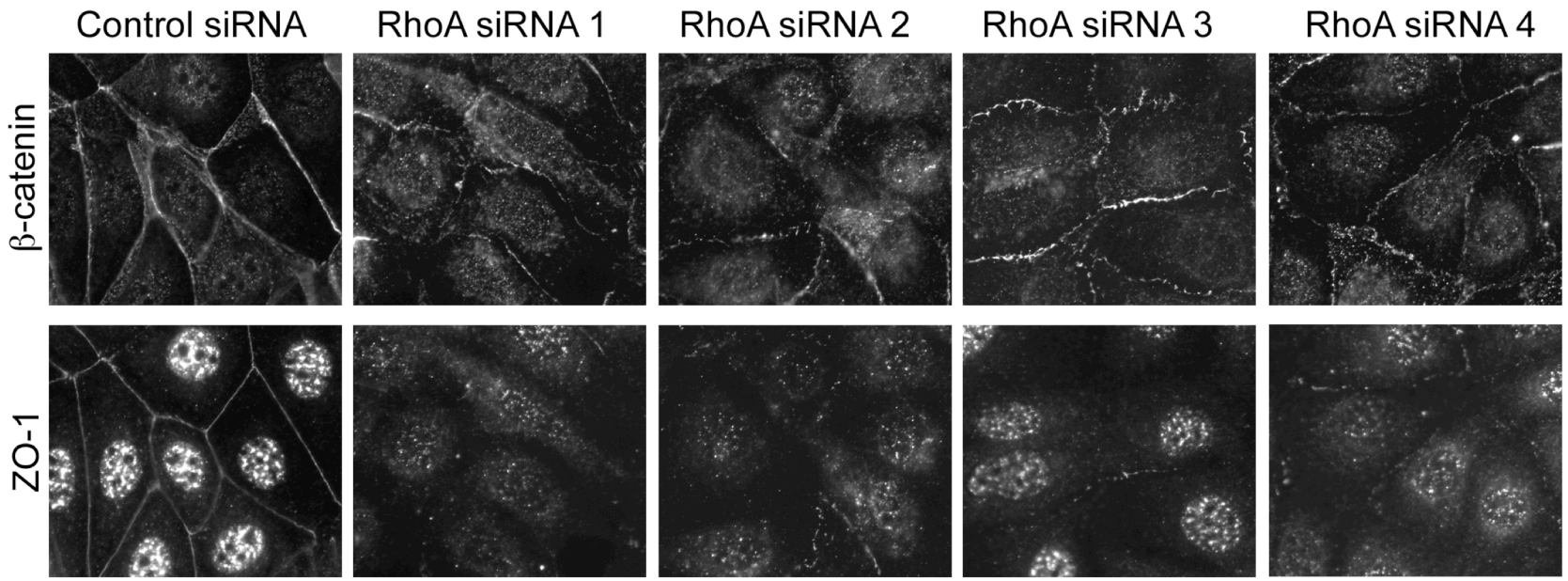

Figure 3.9 Validation of RhoA RNAi using individual siRNAs

HCE cells transfected with non-targeting control siRNA or with four different individual siRNAs specific to RhoA. Cells were methanol fixed 72 hours after RNAi, cells were immunostained with ZO-1 and, β-Catenin.

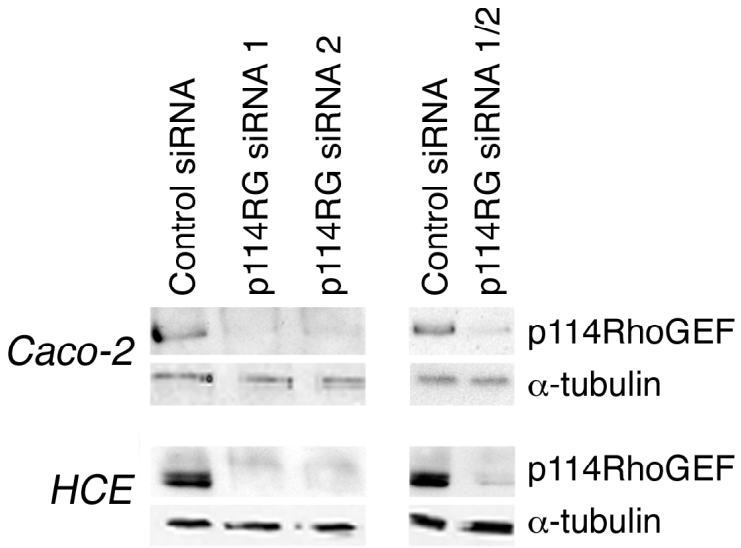

Figure 3.10 siRNAs efficiently knockdown p114RhoGEF in HCE and Caco-2 cells.

Immunoblot of HCE and Caco-2 cells lysates 72 hours after siRNA transfection of control non targeting siRNA or two different individual p114RhoGEF specific siRNAs (siRNA 1 and 2), as well as a pool of the two individual sequences (siRNA1/2). Membranes were blotted with p114RhoGEF and α-Tubulin as a loading control.

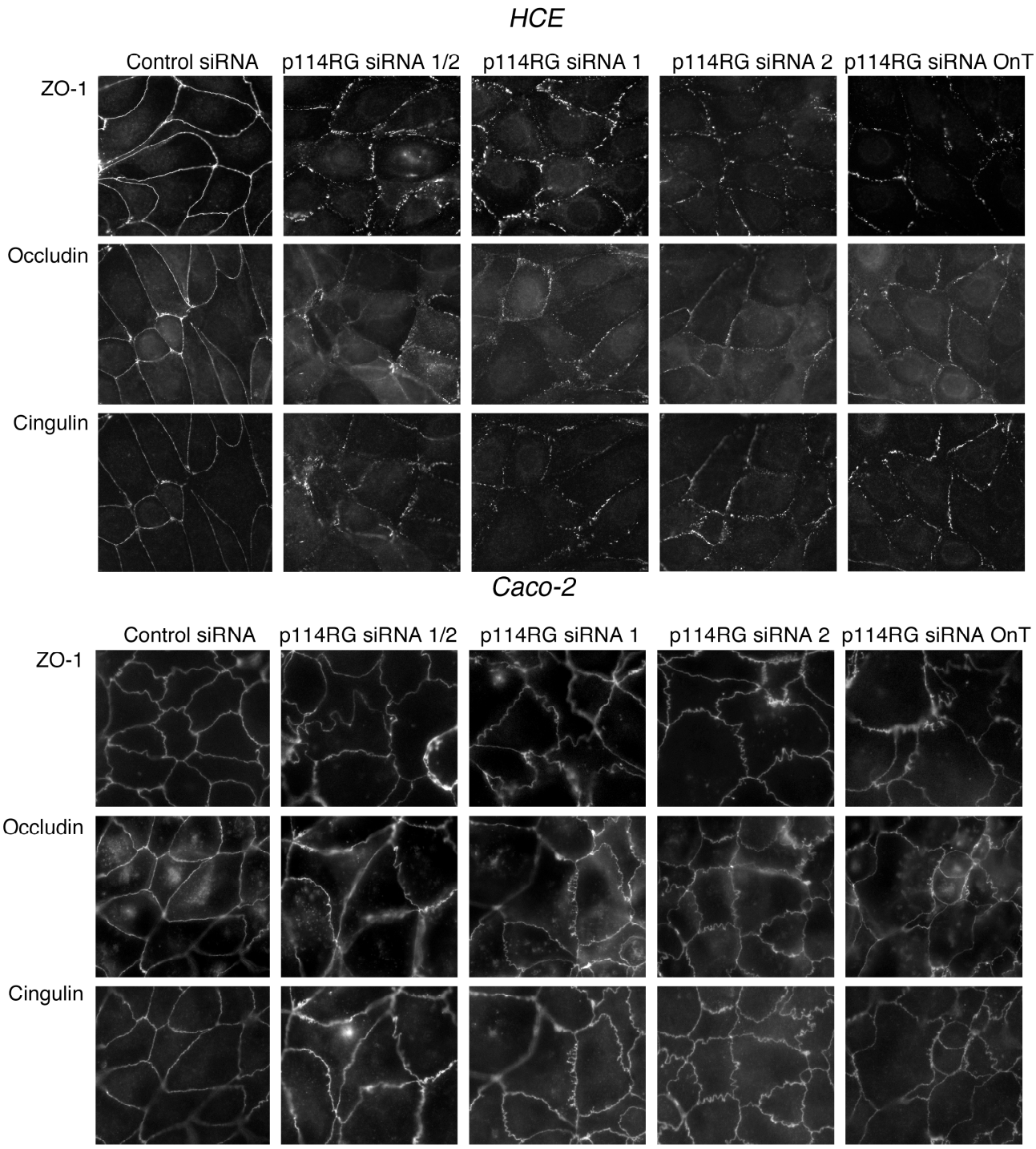

Figure 3.11 Validation of p114RhoGEF siRNAs in HCE and Caco-2 cells.

HCE and Caco-2 cells methanol fixed and immunostained with TJ marker proteins ZO-1, Occludin and Cingulin, 72 hours after transfection with control non targeting, or two different individual p114RhoGEF specific siRNAs (siRNA 1 and 2) as well as a pool of the two individual sequences (siRNA1/2) and an on target plus pool of p114RhoGEF siRNAs (siRNA OnT)

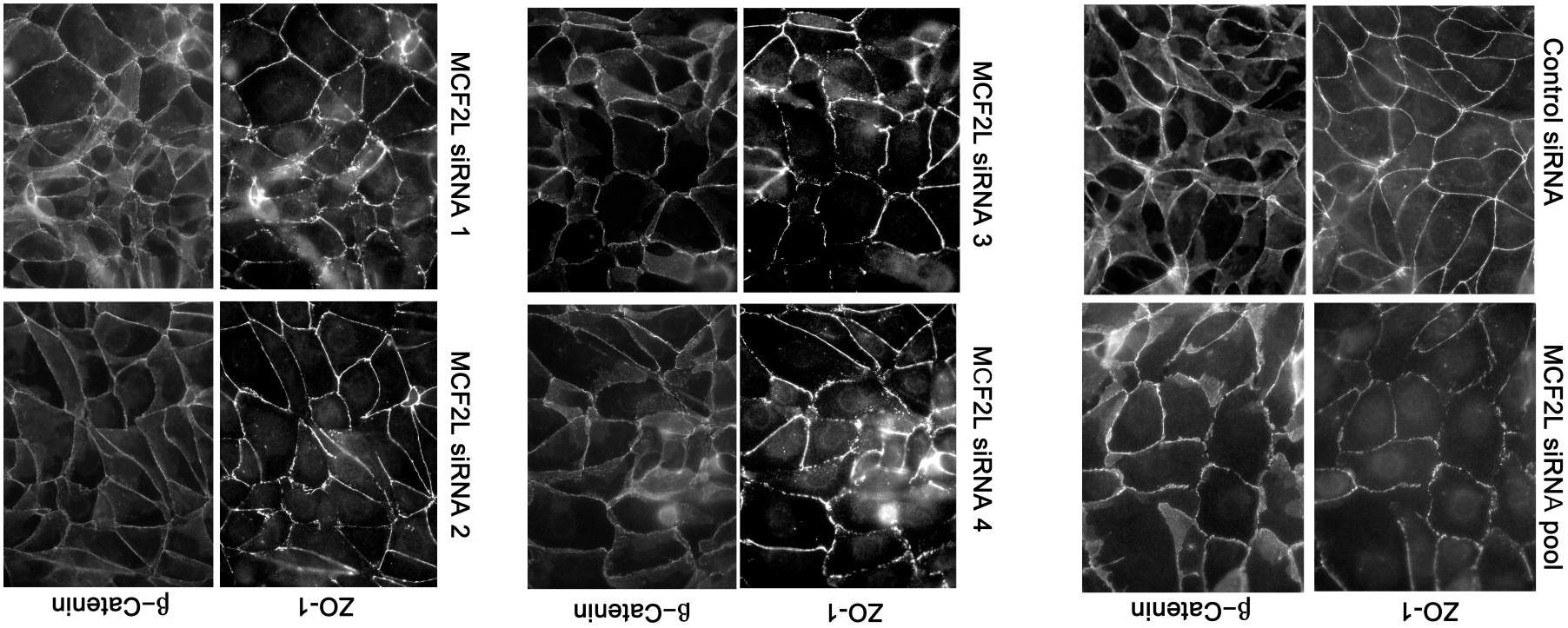

Figure 3.12 Validation of MCF2L in HCE cells.

HCE cells methanol fixed and immunostained with TJ marker proteins ZO-1, and AJ marker β-Catenin, 72 hours after transfection with control non targeting, or siRNA or a pool of 4 MCF2L specific siRNAs. Effects on Junction formation were validated using 4 different individual MCF2L specific siRNAs (siRNA 1 - 4).

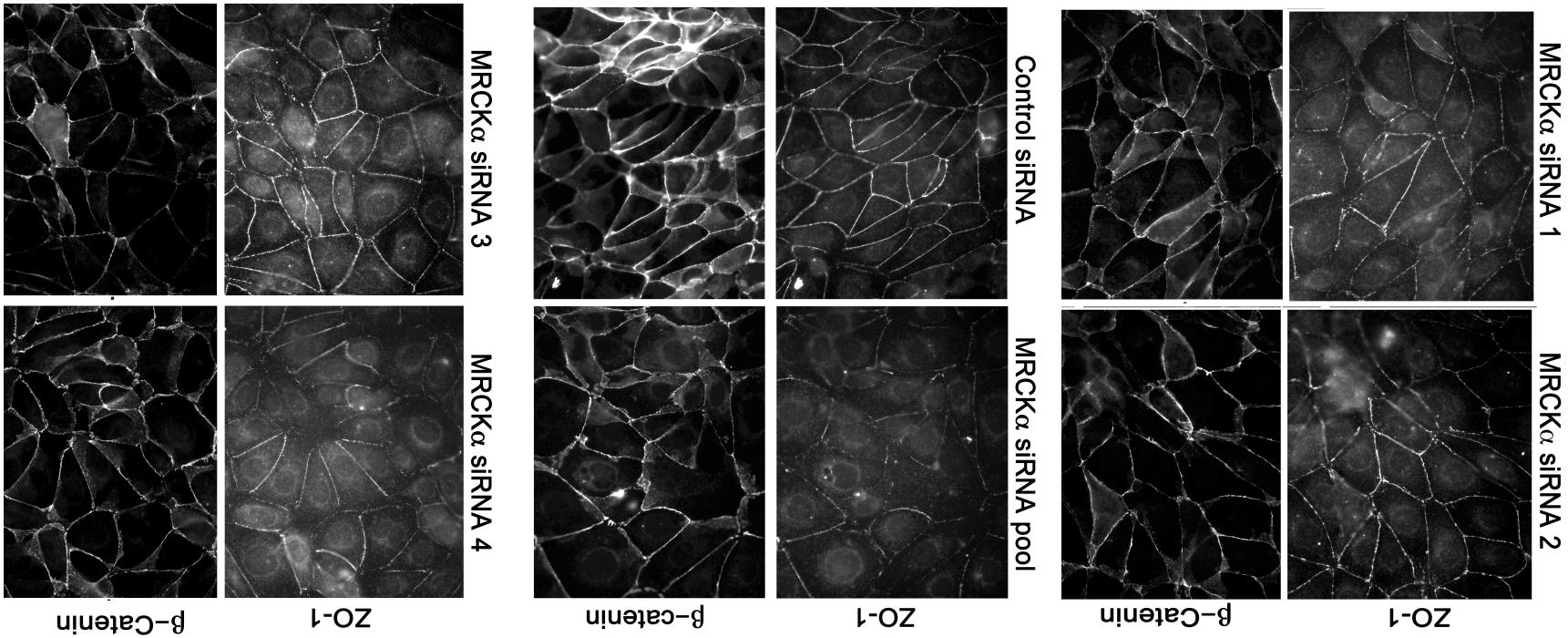

Figure 3.13 Validation of MRCKα in HCE cells.

HCE cells methanol fixed and immunostained with TJ marker proteins ZO-1, and AJ marker β-Catenin, 72 hours after transfection with control non targeting, or siRNA or a pool of 4 MRCKα specific siRNAs. Effects on Junction formation were validated using 4 different individual MRCKα specific siRNAs (siRNA 1 - 4).

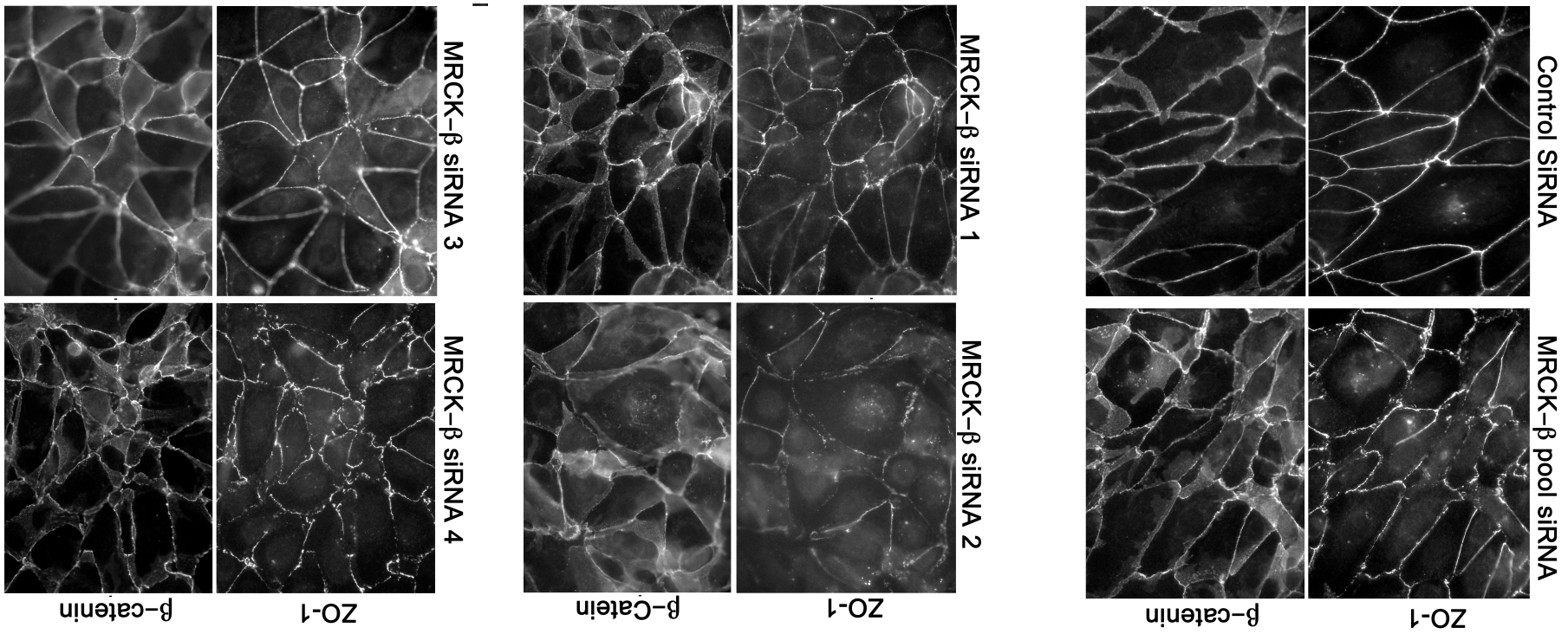

Figure 3.14 Validation of MRCKβ in HCE cells.

HCE cells methanol fixed and immunostained with TJ marker proteins ZO-1, and AJ marker β-Catenin, 72 hours after transfection with control non targeting, or siRNA or a pool of 4 MRCKβ specific siRNAs. Effects on Junction formation were validated using 4 different individual MRCKβ specific siRNAs (siRNA 1 - 4).

Candidate	*Effect on junction morphology*	*Class of protein*	*RhoGTPase*
RhoA	Strong disruption of TJ and AJ junctions very disordered	RhoGTPase	-
P114RhoGEF	Strongly disrupted broken TJs, weaker effect on AJs	GEF	RhoA
MCF2L/Dbs	Weak disruption of both TJs and AJs junctions broken, cells appear flatter	GEF	RhoA/Cdc42
DLC1	Strong disruption of TJs broken discontinuous, weaker effect on AJs	GAP	RhoA
DLC2	Weak disruption on TJs weak effects on AJs	GAP	RhoA / Cdc42
DLC3	Strong disruption of TJ and AJ very disordered	GAP	RhoA / Cdc42
MRCKα	Weak disruption of TJs, cells appear flatter, weak effect on AJs	Effector	Cdc42
MRCKβ	Strong effect on TJ broken disordered AJs very disordered look irregular	Effector	Cdc42
Obscurin/OBSCN	Strong disruption of TJs, weaker effect on AJs, cells appear flatter.	GEF	Not determined
OPHN1	TJs broken discontinuous cells appear larger and flatter weaker effect on AJs	GAP	RhoA
PLXNA1	TJ broken discontinuous weak effect on AJ, Cells appear flat and larger	Semaphorin Receptor	-
PLXNB1	TJ broken and discontinuous, weaker effect on AJs, cells appear large and very flat	Semaphorin Receptor	-
TC10/RhoQ	TJ broken disorganised, AJ appear disordered, cells appear flatter	RhoGTPase	-
Trio	Strong effect on TJs broken discontinuous no effects on AJs	GEF	Rac1/ RhoA
Vav3	Strong effect on TJs broken discontinuous, increased cytoplasmic distribution of TJ components, disorganized AJs, cells appear flatter	GEF	RhoG/ RhoA, possible Rac1

Table 3.2 Summary of validated candidates

A subset of candidates were validated by deconvolution of the siRNA pool used in the primary screen. Individual siRNAs deconvoluted from this pool, were used to confirm if the same phenotypes on junction morphology observed with siRNA pools could be reproduced. Shown is a short description of the effect on junctions, the class of protein they are GEF/GAP etc. and what RhoGTPase they are known to regulate or be an effector of. Note several of the candidates shown here PLXNA1, PLXNB1, TC10, Trio and Vav3 were not identified in the primary screen in HCE cells, but were known to effect junction formation in Caco-2 cells (Matter 2007 unpublished results) these proteins were also validated with individual siRNAs and gave effects on Junction formation in HCE cells.

Chapter 3 – Discussion

In this study I set out to identify novel regulators and effectors of RhoGTPase signalling that regulate junction formation and gene expression in HCE cells. To do this I used a RhoGTPase siRNA library, combined with functional assays to observe junction formation gene expression. Effects on junction formation were observed using immunofluorescent microscopy with antibodies to known junctional components and effects on gene expression were measured using a luciferase based reporter assays to observe constitutive NF-κB activity. In this discussion I will primarily focus on candidates identified from the siRNA screen that effected junction formation, as a subset of these were validated in contrast to the non-validated candidates identified from the siRNA screen that effected NF-κB activity.

A total of 63 candidates were identified from this initial screen as having effects on junction morphology. Candidates were sorted into different bins according to if there was a strong or weak effect on junction morphology. A total of 26 candidates were classified as having strong effects on junction formation. Amongst the strong category in the junction assembly screen were the RhoGTPases RhoA and Cdc42. It was unsurprising that these two RhoGTPases had strong effects on TJ, AJ and polarity, as they both have established crucial roles in epithelial junction formation and the maintenance of polarity [18]. However the RhoGTPase, Rac1 gave weaker effect on junction

formation. This is a surprising result as Rac1 is known to be critical for junction formation, specifically in the initiation of adhesion [280]. This discrepancy could be simply explained by less efficient suppression of Rac1, but alternatively maybe due to insufficient suppression of Rac1 at the early stages of junction formation were it is known to play a prominent role.

In addition to the RhoGTPases, RhoA, Cdc42 and Rac1, the RhoGTPase RhoBTB3 also had effects on junction formation. RhoBTBs are atypical GTPases that are thought to be constitutively active by binding GTP. This means it is not regulated by GEFs or GAP proteins, but by protein expression phosphorylation [142]. The RhoBTB family consists of three members RhoBTB 1 and 2 and 3 all contain a characteristic BTB (Bric-a-brac, tramtrack, Broad complex) domains. RhoBTB 1 and 2, are most similar and have been identified as tumour suppressor genes, with RhoBTB2 having been shown to be downregulated in several tumour types [285]. RhoBTB3 has recently been shown to be involved in retrograde trafficking from endosomes to Golgi trafficking acting as a downstream effector of the RabGTPase, Rab9 [286]. Interestingly this study identified RhoBTB3 to bind and hydrolyse ATP rather than GTP. This ATPase activity was thought to be important for the release of cargo from endosomes to permit efficient docking and fusion to the Golgi. Rab13 has been linked to the recycling of tight junctional protein Occludin [287] and has been proposed to play a role in TJ development in the trophectoderm of the mouse blastocyst [288]. It is possible that RhoBTB3 together with Rab9 forms a new

pathway that is critical for junction formation and maintenance, by recycling junctional though endosomes back to the membrane.

The screen identified a number of GEFs and GAPs and downstream effectors of the RhoGTPases RhoA and Cdc42. These two RhoGTPases clearly gave the strongest effects on junction morphology. I therefore decided to sort candidates into two lists based on known information from the literature, about which RhoGTPase they are known to regulate or are a downstream effector for. Several of these candidates from this list (Table 3.1) along with several additional candidates not identified from the primary screen in HCE cells, but identified in an identical screen in Caco-2 cells (Matter 2007 unpublished results), were chosen for validation using individual siRNAs derived from the de-convolution of the original siRNA pool used in the screen. A complete list of validated candidates was produced (Table 3.2) I will now focus this discussion on a few examples of these validated candidates (Dbs, MRCKα and β and p114RhoGEF).

The GEF MCF2L a.k.a Dbs was one of these validated candidates; absence of Dbs caused junctions to form with broken discontinuous lines and cells also appeared flatter. AJ and TJ seemed affected as both had perturbed morphology. Dbs was discovered in a screen for cDNAs that had transforming ability when overexpressed in fibroblasts [289] Dbs is known to stimulate nucleotide exchange for Cdc42 and RhoA in *vitro* [290, 291]. However RhoGTPase specificity seems to be cell type dependent [156, 292]. The PH domain of Dbs binds

to phosphoinositide lipids, and lipid binding is known to be required for its transforming activity. Interestingly the PH domain also mediates binding to the active, GTP bound Rac *in vitro,* suggesting Dbs can act as a Rac effector [292]. Dbs was also indentified as inhibiting constitutive NF-κB activity in HCE cells suggesting a role in proliferation /cell survival. However, this result has not yet been validated using individual siRNAs, but this result is in agreement with a previous study that demonstrates that Dbs promotes growth by activation of transcription from the cyclin D in an NF-κB dependent manner [291]. Further studies will need to be performed to confirm its RhoGTPase specificity in HCE cells and other epithelia. This will require investigations that dissect the molecular mechanisms involved in spatially coordinating RhoGTPase signalling during junction assembly and proliferation.

Two other candidates MRCKα and β were also validated for their effects on junction assembly. Absence of MRCKα caused flatter cells with broken and discontinuous TJs, but had weaker effects on AJs causing them to appear more undulated than straight AJs in control transfected cells. MRCKβ seemed to cause a stronger phenotype than MRCKα with TJs and AJs appearing broken and very warped and undulated. MRCKs are both known to be effectors of Cdc42 and regulate cytoskeletal reorganization though several mechanisms. MRCKs are related to the Rho kinases ROCKs, sharing high sequence identity in their kinase domains, and act on similar substrates, but contain different RhoGTPase binding domains to ROCKs [293]. MRCKs can phospholyate MLC leading to Myosin II activation, in a manner that is independent of RhoA/Rock or

MLCK signalling. MRCKs can also phospholyate ERM proteins, that contribute to the cytoskeletal organization that directs filopodia formation [294]. Evidence from several studies has also demonstrated MRCKs to have important roles in cell migration contributing to the invasive properties of cancer cells [295] [296]. During cell migration MRCKs are involved in regulating actin retrograde flow, a process whereby actin filaments flow from the front to the back of the extreme margin of the cell lameliipodia in a Myosin II dependent manner [296]. It will be interesting to investigate the molecular mechanisms, whereby MRCK α and β regulate the junction associated actin cytoskeleton.

One possibility for the function of MRCKs in junction formation is via actinomyosin contractility of the perijunctional actin cytoskeleton during the later stages of junction maturation. Calcium switch experiments will need to be performed to identify the precise stages of junction formation that MRCKs regulate. However there is a large amount of evidence that implicates RhoA signalling to regulate actinomyosin contractility during junction formation. Interestingly a recent study highlighted the role of different isoforms of Myosin II play during junction assembly [139]. Myosin IIA is regulated by a RhoA/ Rock signalling pathway, and IIB by signalling from the GTPase Rap. Activation of Rap1 could lead to activation of Cdc42 [297], that may result in Myosin IIB activation via MRCK. Dissecting out the contribution of RhoA/ Rock and Cdc42 MRCK mediated Myosin activation in junction assembly and how these two pathways coordinately regulate different Myosin II isoforms remains a challenge for future experiments.

p114RhoGEF was the final candidate to be validated. Its absence predominately affected TJ formation in HCE and Caco-2 cells. p114RhoGEF was previously reported to be an exchange factor for RhoA[188] In the next chapter (Chapter 4). I greatly expand on the function of p114RhoGEF in epithelial cells, and identify the molecular mechanisms that underlie its function in junction formation.

CHAPTER 4

Spatially restricted activation of RhoA by p114RhoGEF drives epithelial junction formation and morphogenesis.

Chapter 4 -Spatially restricted activation of RhoA by p114RhoGEF drives epithelial junction formation and morphogenesis.

The results in this chapter have been accepted as a manuscript in November 2010 titled 'Spatially restricted activation of RhoA signalling at epithelial junctions by p114RhoGEF drives junction formation and morphogenesis' to the Journal Nature Cell Biology

Overview

This chapter contains a full detailed analysis of p114RhoGEF a candidate from the siRNA screens, that upon depletion inhibits the assembly of tight junctions in different epithelial cell types. p114RhoGEF is a gene that is widely expressed in different tissue types [188] and belongs to the family of Dbl GEF proteins having a characteristic tandem DH-PH domains. It is known to function as a specific activator of RhoA in *vitro* and to induce the formation of stress fibres and activating serum response element mediated gene transcription [298]. Here I greatly expand on the function of p114RhoGEF in epithelial cells, by identifying it as a novel tight junction-associated activator of RhoA that regulates epithelial differentiation, barrier formation and epithelial three-dimensional morphogenesis in MDCK and Caco-2 cultures. I demonstrate that p114RhoGEF drives the spatial activation of RhoA at cell-cell contacts and subsequently the

activation of the junctional actinomyosin cytoskeleton, ultimately regulating the organisation of the junctional cytoskeleton during junction assembly. I discovered mechanistic evidence for p114RhoGEF being part of a junction-associated Rho signalling module formed by p114RhoGEF, Myosin IIA, Rock II and the junctional adaptor protein Cingulin. I show that the formation of this complex is dependent on the assembly of cell-cell junctions and that junctional adaptor Cingulin is required for efficient recruitment of p114RhoGEF to cell-cell junctions.

Localisation of p114RhoGEF in epithelial cells

I investigated the cellular localisation of p114RhoGEF in HCE and Caco-2 cells and discovered it localised to apical cell junctions, but also had a diffuse cytoplasmic distribution (Figure 4.0). By performing p114RhoGEF RNAi using a pool of p114RhoGEF specific siRNAs, I observed a reduction in the cytoplasmic and junctional staining in p114RhoGEF knockdown cells compared to the control. This established that the staining observed was specific for p114RhoGEF (Figure 4.0). I wanted to establish if p114RhoGEF was localised specifically to TJs in HCE cells by observing if p114RhoGEF co-localised with Occludin a protein known to localise to TJs, or more with E-Cadherin, an integral transmembrane protein associated with AJs (Figure 4.1). I found it difficult to determine if p114RhoGEF was localised to TJs in HCE cells as TJs and AJs appeared difficult to resolve clearly as they form a flatter monolayer than Caco-2 cells, that have a more columnar shape and TJs and AJs can be more clearly resolved. In Caco-2 cells p114RhoGEF localisation demonstrated

clear co-localisation with Occludin and very little co-localisation with E-Cadherin (Figure 4.1), thus demonstrating p114RhoGEF is present at TJs.

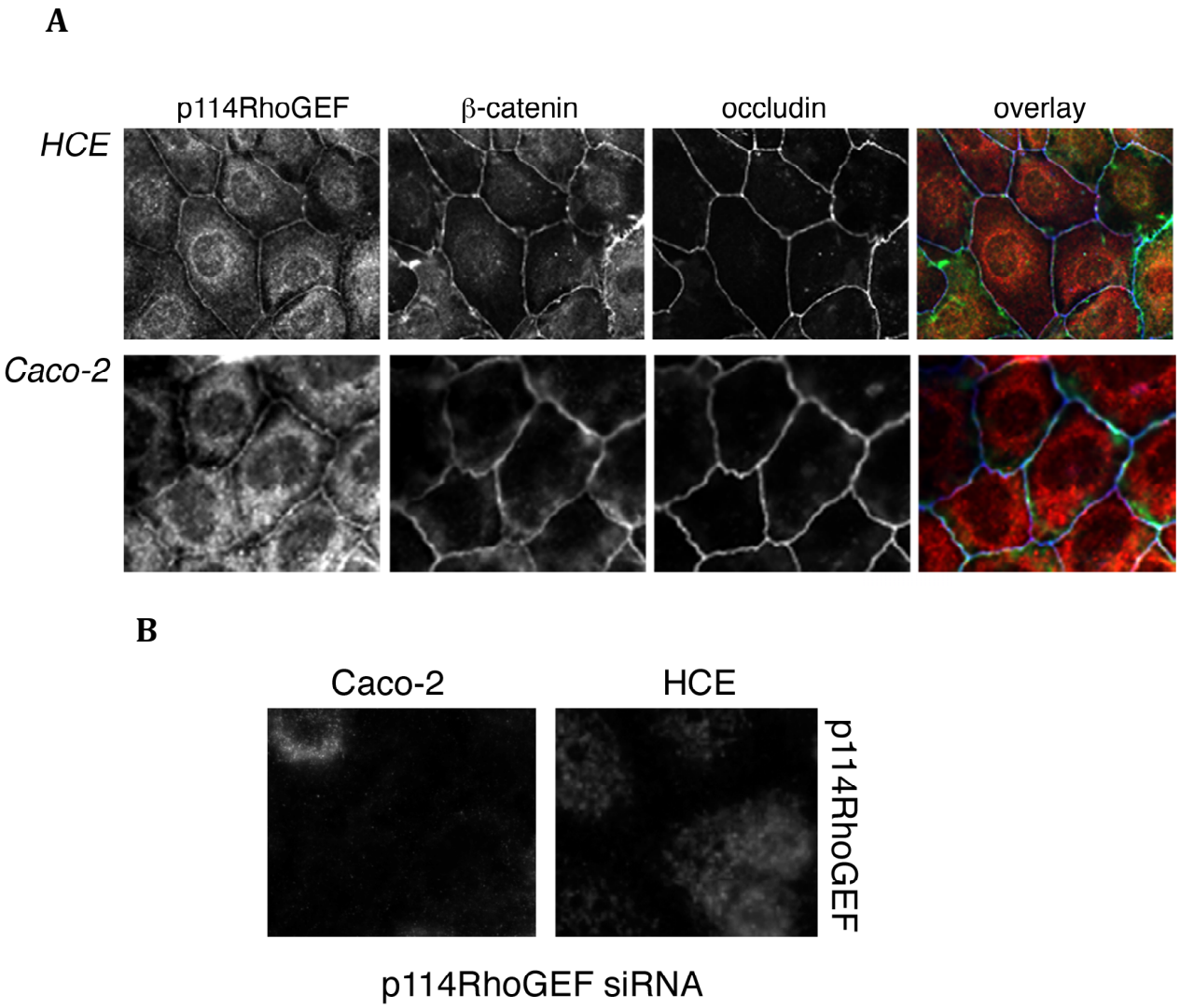

Figure 4.0 p114RhoGEF is localised to apical cell junctions and the cytoplasm.

A HCE and Caco-2 cells immunostained with p114RhoGEF (red), β-Catenin (green) and the TJ protein Occludin (Blue) **B** HCE and Caco-2 cells fixed with methanol and immunostained for p114RhoGEF after 72 hours transfection with control non targeting and pool of p114RhoGEF siRNAs.

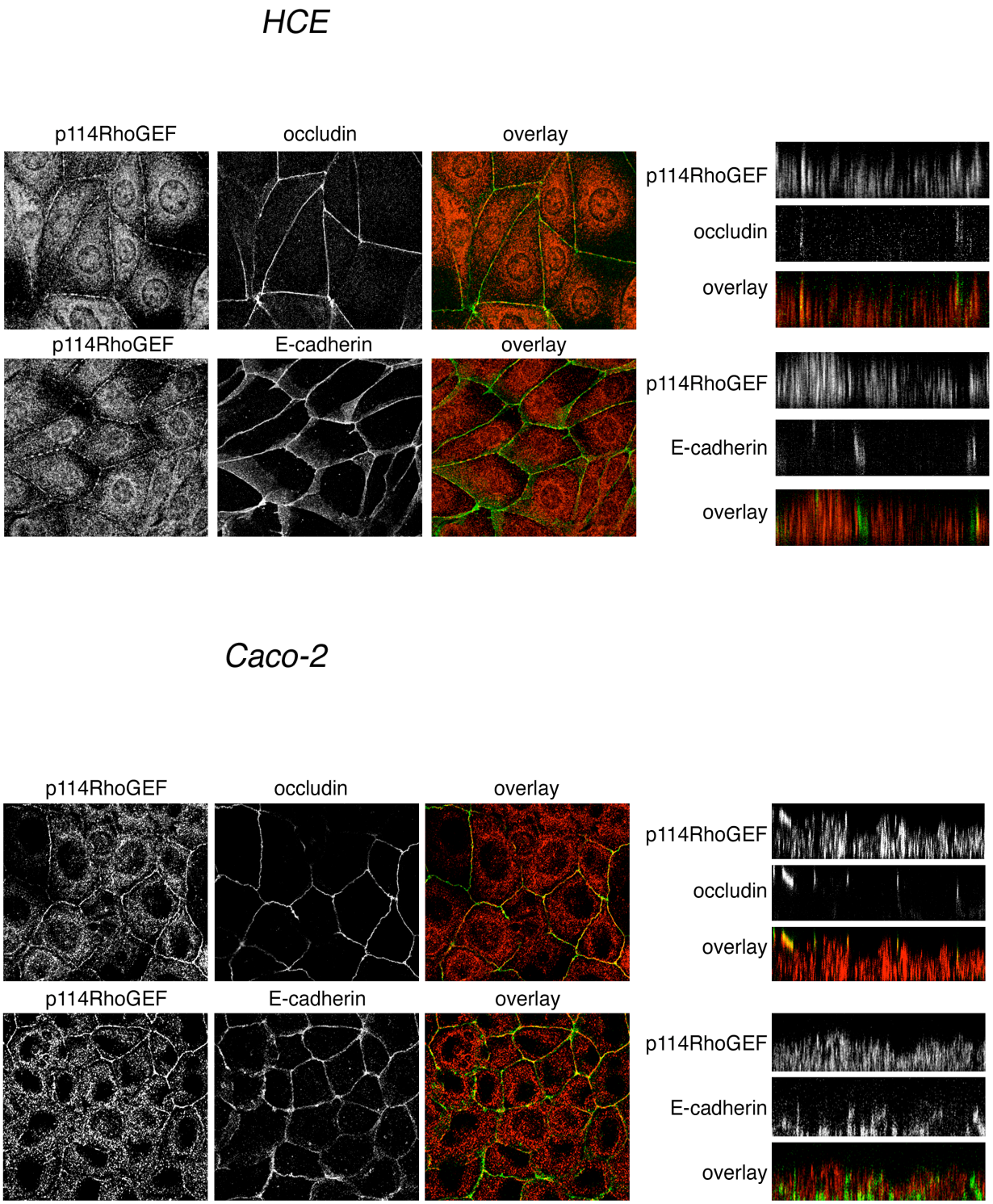

Figure 4.1 p114RhoGEF is localised to TJs

A single confocal x/y section of HCE(top panels) and Caco2 cells (bottom panels), immunostained with p114RhoGEF (red) and the TJ protein Occludin (green) on the left is a slice through the z axis

RhoGTPase specificity of p114RhoGEF

p114RhoGEF had been characterised previously as being a GEF for RhoA, but also Rac1, but not Cdc42 [298]. To investigate the RhoGTPase specificity of p114RhoGEF in HCE cells. I suppressed levels of p114RhoGEF by transfection of two individual siRNAs, as well as a pool made up of these two individual siRNAs. I measured active levels of the three main RhoGTPases RhoA, Rac and Cdc42, using a RhoGTPase activation assay (GLISA). I discovered that depletion of p114RhoGEF specifically reduced active RhoA, but not Rac or Cdc42, suggesting that it is mainly required for RhoA activation (Figure 4.2).

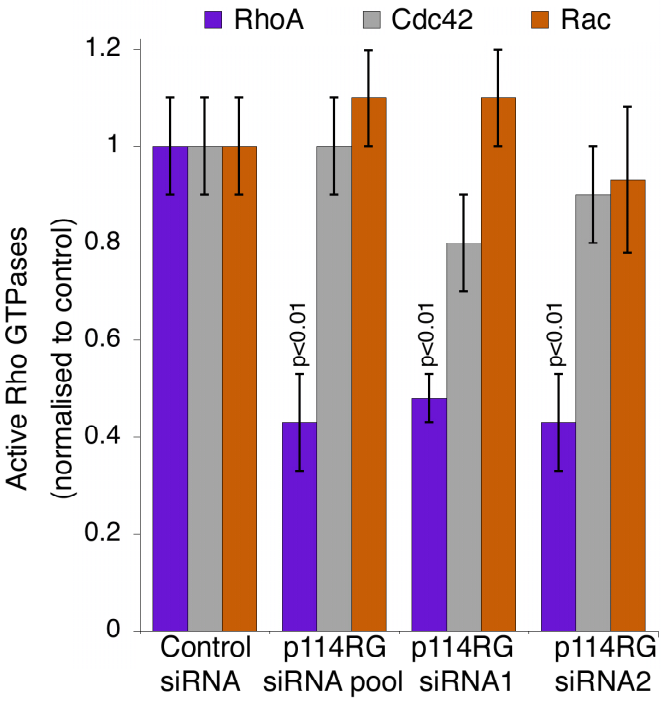

Figure 4.2 p114RhoGEF specifically activates RhoA.

GLISA assay performed in HCE cells 72 hours after transfection with control non-targeting siRNA or with two different individual p114RhoGEF siRNAs or a pool of both the individuals. Levels of active RhoA, Cdc42 and Rac are shown normalised to control levels. Bars represent mean average of triplicate experiments. Error bars represent +/-1 SD.

p114RhoGEF is required for the assembly of functional epithelial barriers

I investigated if epithelial cells depleted of p114RhoGEF can form functional epithelial barriers, by testing the permeability properties of TJs. To observe *de novo* junction formation, I performed a calcium switch assay in Caco-2 cells depleted of p114RhoGEF, using two different siRNA pools (si-Genome and On-Target plus), I measured the TER (a measure of the instantaneous ion conductance of an epithelial sheet) over a period of 48 hours to follow barrier formation (Figure 4.3). There was a clear impairment of TER development in p114RhoGEF depleted cells, having a 3 fold lower TER compared to controls, indicating increased permeability of the epithelial barrier to ions (Figure 4.3). Permeability after 48 hours in normal calcium medium of the epithelial monolayer to two different sizes of dextran tracers, was found to be greatly increased in p114RhoGEF depleted cells (Figure 4.3), indicating TJs were permeable to hydrophillic tracers. These experiments thus provide strong evidence that p114RhoGEF is essential for the formation of functional epithelial barriers. Levels of active RhoGTPases were measured 20 hours after the restoration of normal calcium conditions in Caco-2 cells. A clear reduction of active RhoA, but not Cdc42 and Rac1 was observed (Figure 4.4) providing supporting evidence that p114RhoGEF acts specifically to activate RhoA during the assembly of junctions.

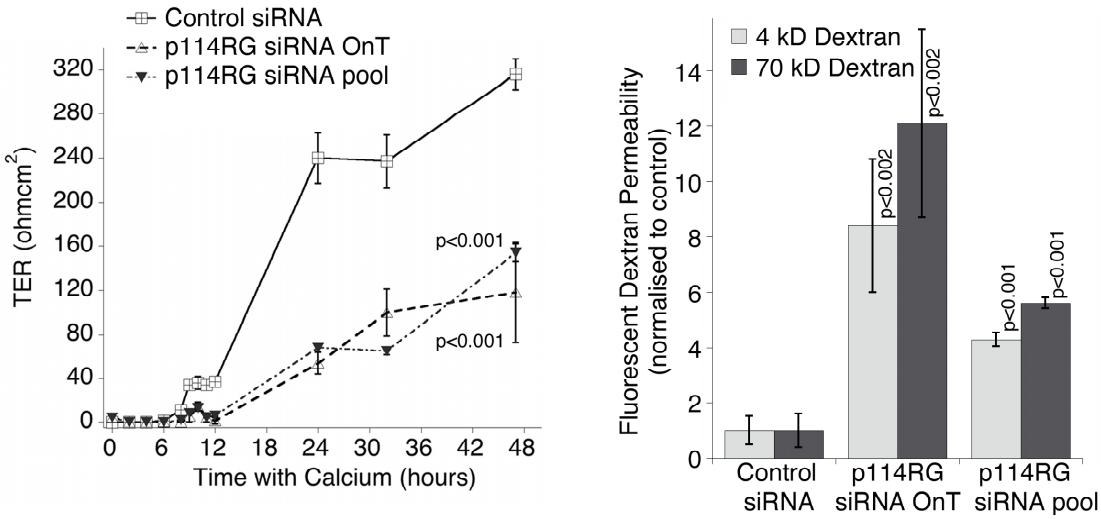

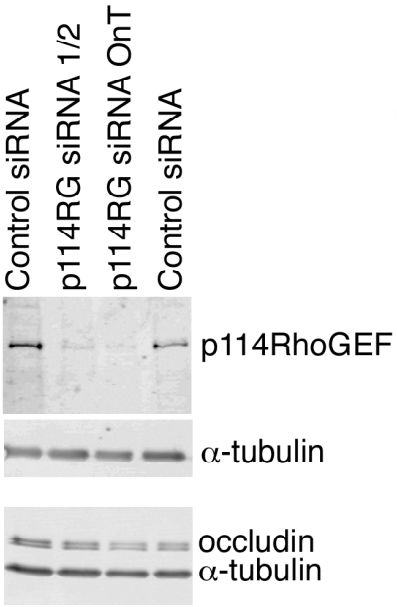

Figure 4.3 p114RhoGEF regulates epithelial barrier formation.

Caco-2 cells transfected with control (non targeting) or to two different pools of p114RhoGEF specific siRNA (siRNA 1/2 (a pool of two individual siGenome siRNAs and On Target plus pool) were trypsinised and plated onto filters in low calcium media for 24 hours to prevent formation of cell-cell contacts. Normal calcium media was added and cell-cell contact formation was monitored during the next 48 hours by measuring Trans epithelial resistance (TER). Shown are mean averages and SD of triplicate experiments. Paracellular tracer permeability after 48 hours was determined using two different sizes of fluorescently labelled dextrans. Bars represent mean averages and error bars SD of triplicate experiments. Expression of p114RhoGEF and other junction proteins (GEF-H1 and Occludin), as well as α-Tubulin as a loading control were assayed at the end of the experiment by immunoblot.

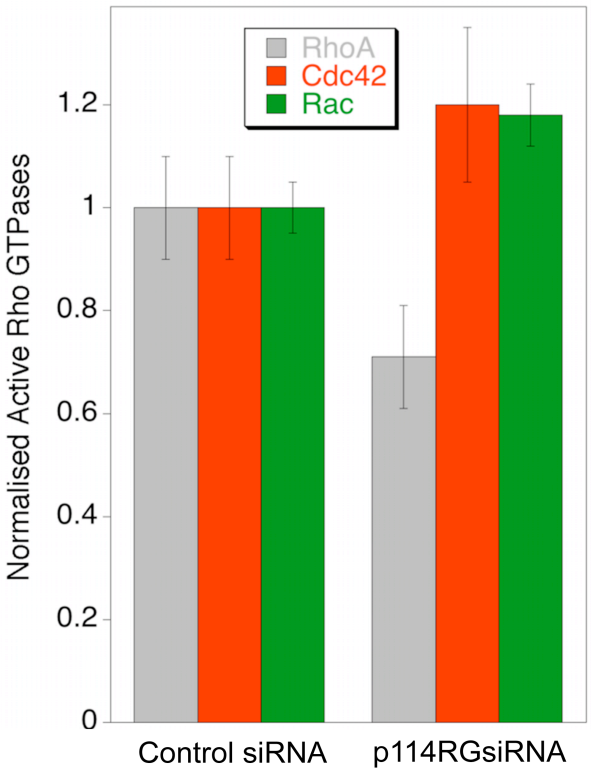

Figure 4.4 p114RhoGEF specifically activates RhoA during junction assembly.

G-Lisa assay performed in Caco-2 cells depleted of p114RhoGEF. After depletion Caco-2 cells were trypsinised and plated out in low calcium media for 24 hours to prevent formation of cell-cell contacts. Normal calcium media was added to induce cell-cell contact formation for 20 hours, after which levels of active RhoGTPases RhoA, Cdc42 and Rac were determined. Bars represent mean averages and error bars SD of triplicate experiments.

Morphological analysis of cells incubated at different times after calcium replenishment revealed p114RhoGEF depletion did not affect initial cell spreading and the initiation of cell-cell contacts, as ZO-1 accumulation was observed at forming junctions, already after 1 hour and f-actin staining revealed well spread cells. (Figure 4.5). However ZO-1 staining remained discontinuous after 24 hours. Similar observations were made with other junctional markers after 4 hours, (Figure 4.7). As a control for the specificity of the impaired junctional formation effects of p114RhoGEF depletion, I reduced levels of GEF-H1, another TJ associated RhoA specific GEF. As expected with previously reported results [64] GEF-H1 depleted cells spread more slowly with "roundish" looking cells being detected 1 hour after calcium replenishment (Figure 4.6). However, GEF-H1 depleted cells did established morphologically normal junctions. p114RhoGEF and GEF-H1 seem to function at different stages of junction formation. In agreement with previous observations GEF-H1 is not required for junction formation, but to regulate the early stages of cell spreading and the initial stages of cell contact formation [212, 255, 299], whereas p114RhoGEF functions at a later stage of junctional maturation.

I discovered p114RhoGEF to be recruited to cell-cell junctions already after 1 hour of junction reformation (Figure 4.8). Myosin IIA, a downstream target for RhoA activation in junction formation [300] [280], also associated with junctions at this early time point; however, it was not recruited to cell-cell junctions in p114RhoGEF depleted cells and instead localised to intense actin stress fibre arrays at the base of cells (Figure 4.8). GEF-H1 was not recruited to the forming junctional complex in p114RhoGEF depleted cells where it normally would be

inactivated, therefore GEF-H1 may contribute to activation of RhoA and lead to the increase in the basal stress fibres (Figure 4.9).

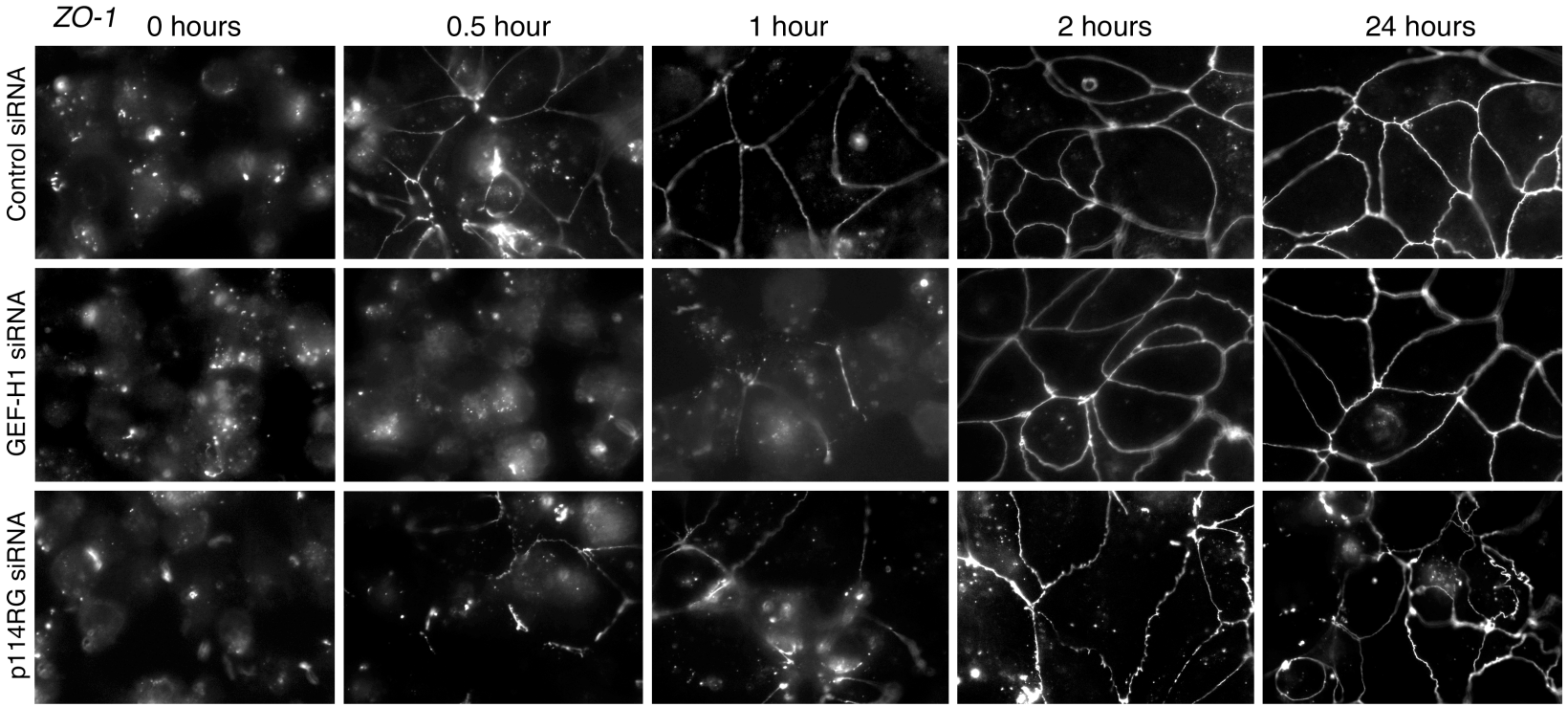

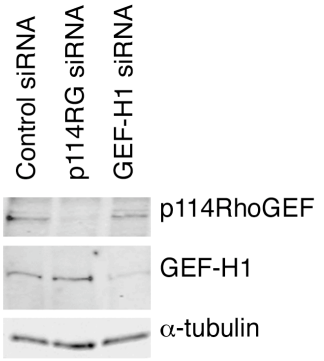

Figure 4.5 p114RhoGEF is involved in junction maturation as opposed to GEF-H1 that regulates cell spreading and early adhesion.

Caco2 cells transfecfected with control non-targeting, p114RhoGEF and GEF-H1 specific pools of siRNA were plated in low calcium. Cells were fixed at various times indicated in hours after the replenishment of calcium and immunostained for the TJ protein ZO-1. Expression of p114RhoGEF, GEF-H1 and α-Tubulin as a loading control were assayed at the end of (24 hours after calcium replenishment) the experiment by immunoblot.

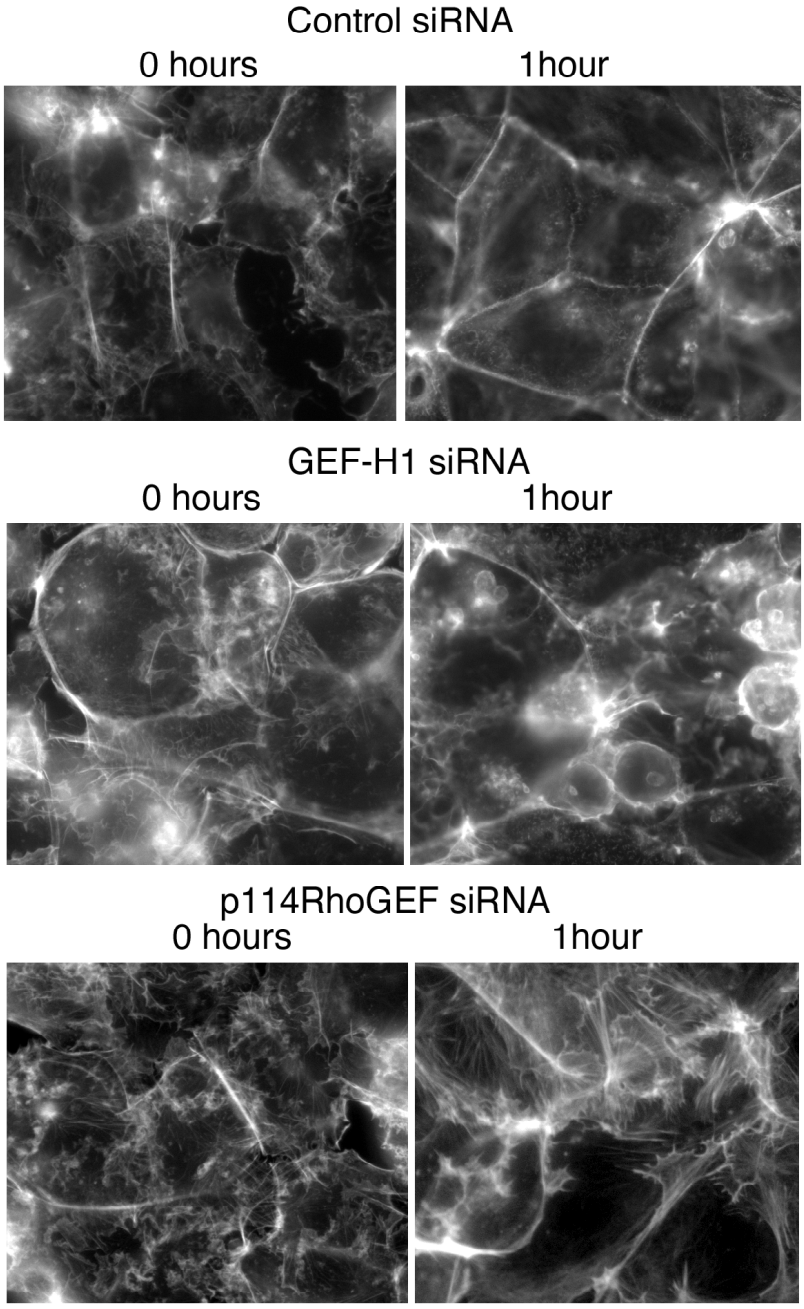

Figure 4.6 Cell morphology during junction reformation in p114RhoGEF and GEF-H1 depleted cells.

Caco-2 cells depleted of GEF-H1 and p114RhoGEF were trypsinised and plated onto glass for 24 hours in low calcium media (0 hours). The media was replaced with normal calcium media for 1 hour before being fixed and stained for f-actin with TRITC conjugated phalloidin. Note, rounded appearance of GEF-H1 depleted cells after 1 hour.

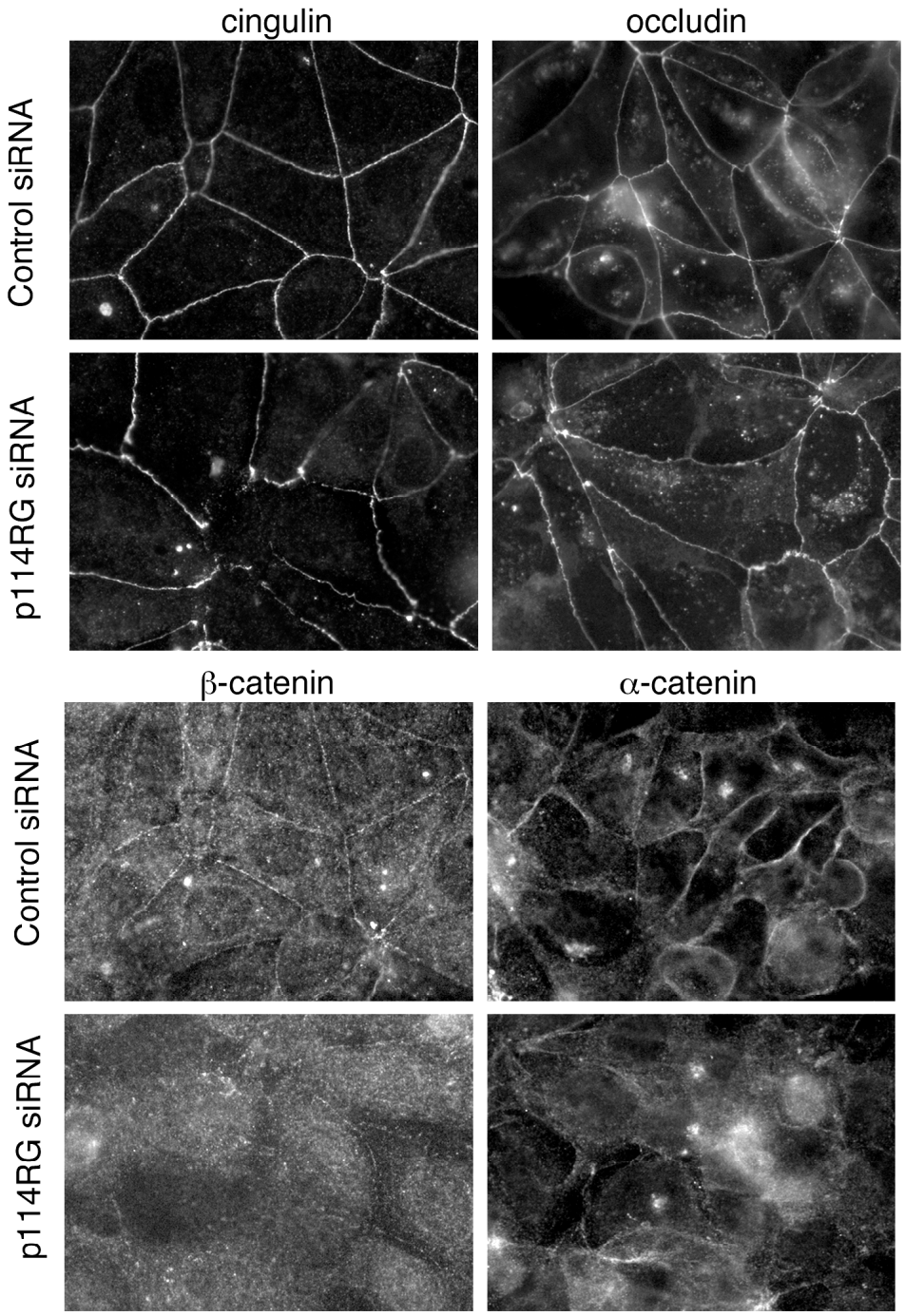

Figure 4.7 Recruitment of different junctional proteins to reforming juctional complexes in p114RhoGEF depleted cells.

Caco-2 cells depleted of p114RhoGEF were trypsinised and plated onto glass for 24 hours in low calcium media (0 hours). The media was replaced with normal calcium media for 4 hours before being fixed and stained for TJ markers Cingulin, Occludin and AJ markers α and β-Catenin.

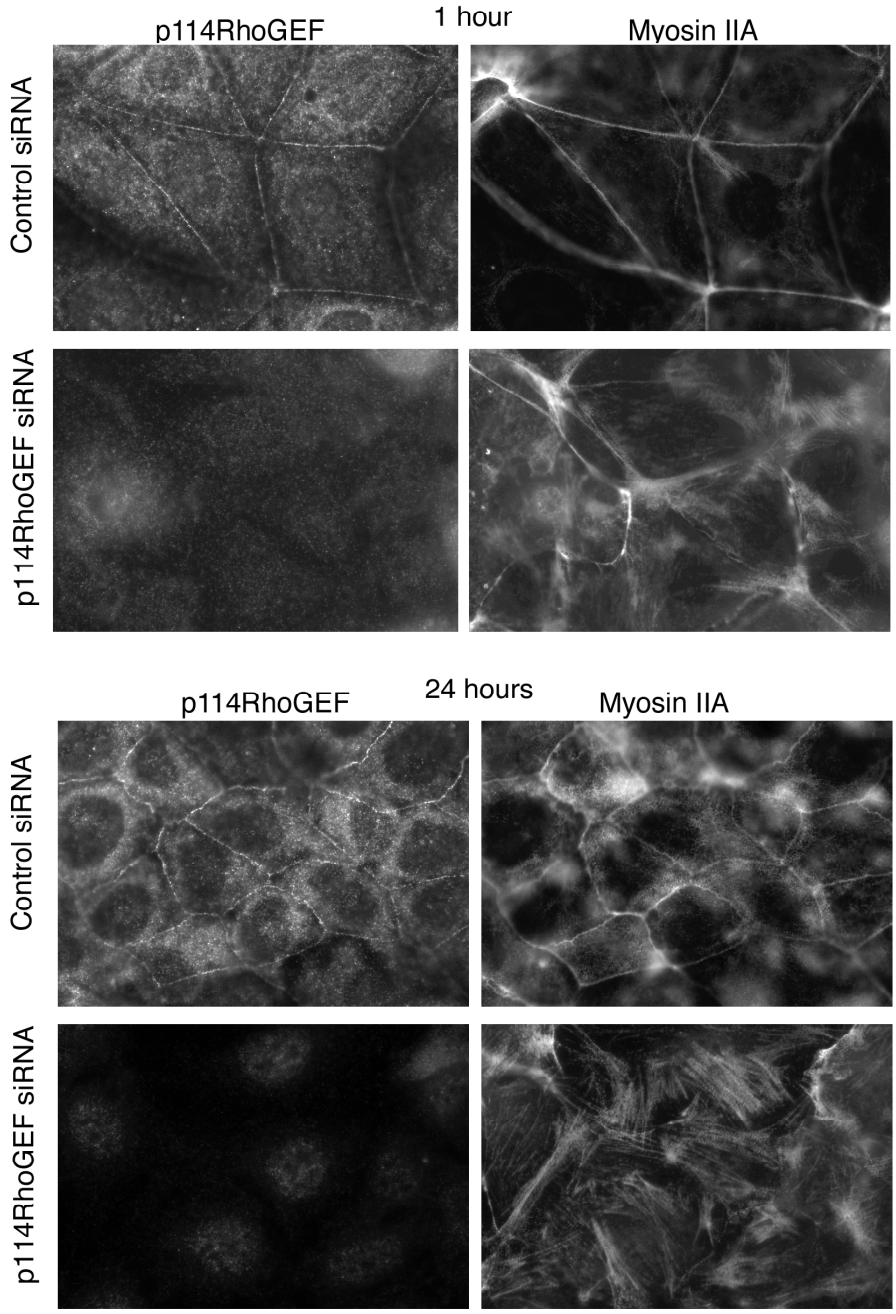

Figure 4.8 p114RhoGEF is recruited to junctions early and its absence causes redistribution of Myosin IIA from forming junctions to basal stress fibre arrays.

Caco-2 cells depleted of p114RhoGEF were trypsinised and plated onto glass for 24 hours in low calcium media before the media was replaced with normal calcium media. Cells were at fixed at 1 hour and 24 hour time points and stained for Myosin IIA and p114RhoGEF.

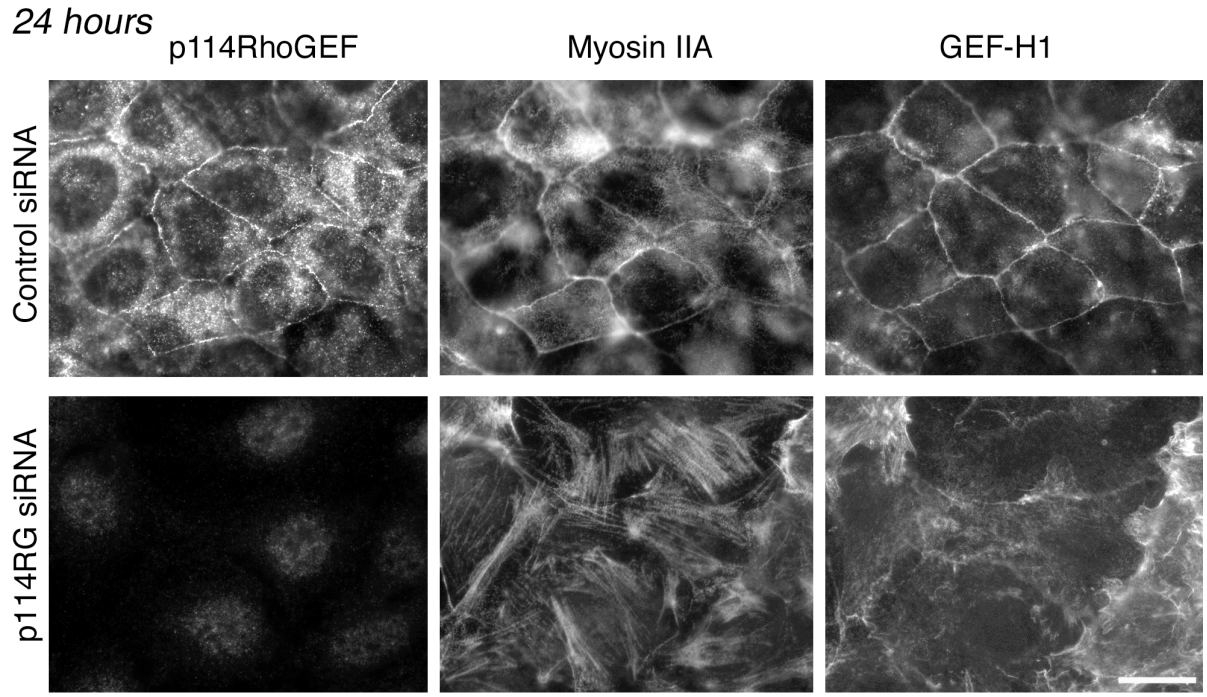

Figure 4.9 Absence of p114RhoGEF causes redistribution of Myosin IIA and GEF-H1

Caco-2 cells depleted of p114RhoGEF were trypsinised and plated onto glass for 24 hours in low calcium media before the media was replaced with normal calcium media. Cells were at fixed at 24 hour time point and stained for Myosin IIA and p114RhoGEF and GEF-H1.

p114RhoGEF regulates epithelial morphogenesis in three dimensional cysts.

I wanted to analyze if p114RhoGEF was a regulator of epithelial morphogenesis by using a three dimensional culture system that allows the formation of polarised cysts with a central lumen [301]. p114RhoGEF was depleted in Caco-2 cells by siRNA transfection of a p114RhoGEF specific siRNA pool and in MDCK cells by expression of p114RhoGEF specific shRNAs(Figure 4.10). Depletion affected both cell types and resulted in cysts that had a disorganised appearance often having multiple lumens (Figure 4.11-12). Confocal microscopy revealed an irregular distribution of ZO-1. However, podocalyxin an apical marker in MDCK cells still accumulated in lumens, suggesting absence of p114RhoGEF does not cause a loss of polarity, but a disorganised cyst structure, possibly due to a perturbation of actinomyosin tensile forces required to maintain normal cyst morphology.

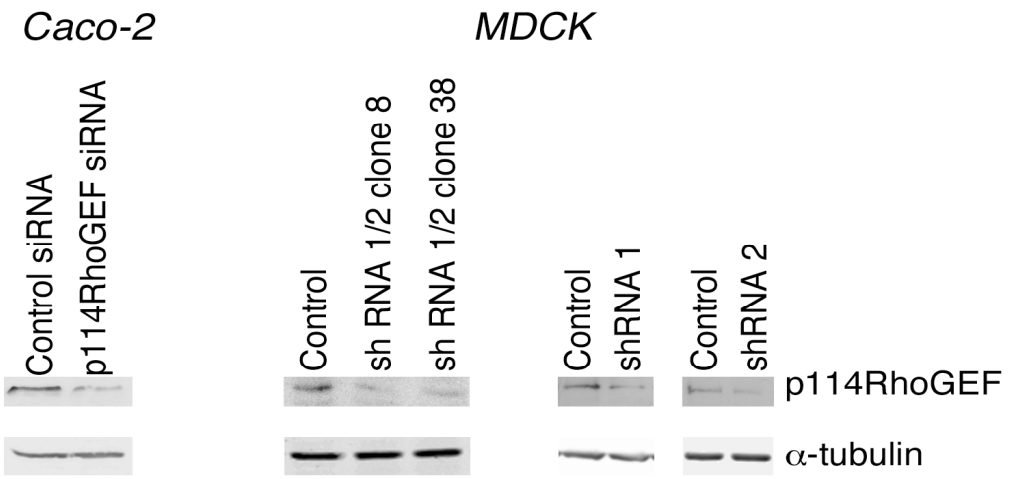

Figure 4.10 Efficiency of p114RhoGEF in 3D MDCK and Caco-2 Cysts.

For Caco-2 cyst cultures p114RG was depleted using pool of p114RG specific siRNA. For MDCK cyst cultures stable cells lines expressing control, non targeting shRNA, two different individual p114RG shRNAs (shRNA1 and shRNA2) and another expressing both shRNA (shRNA1/2 two different clones shown 8 and 38). Depletion of p114RhoGEF in cyst cultures was analysed by Immunobloting membranes with p114RhoGEF and with α-Tubulin as a loading control.

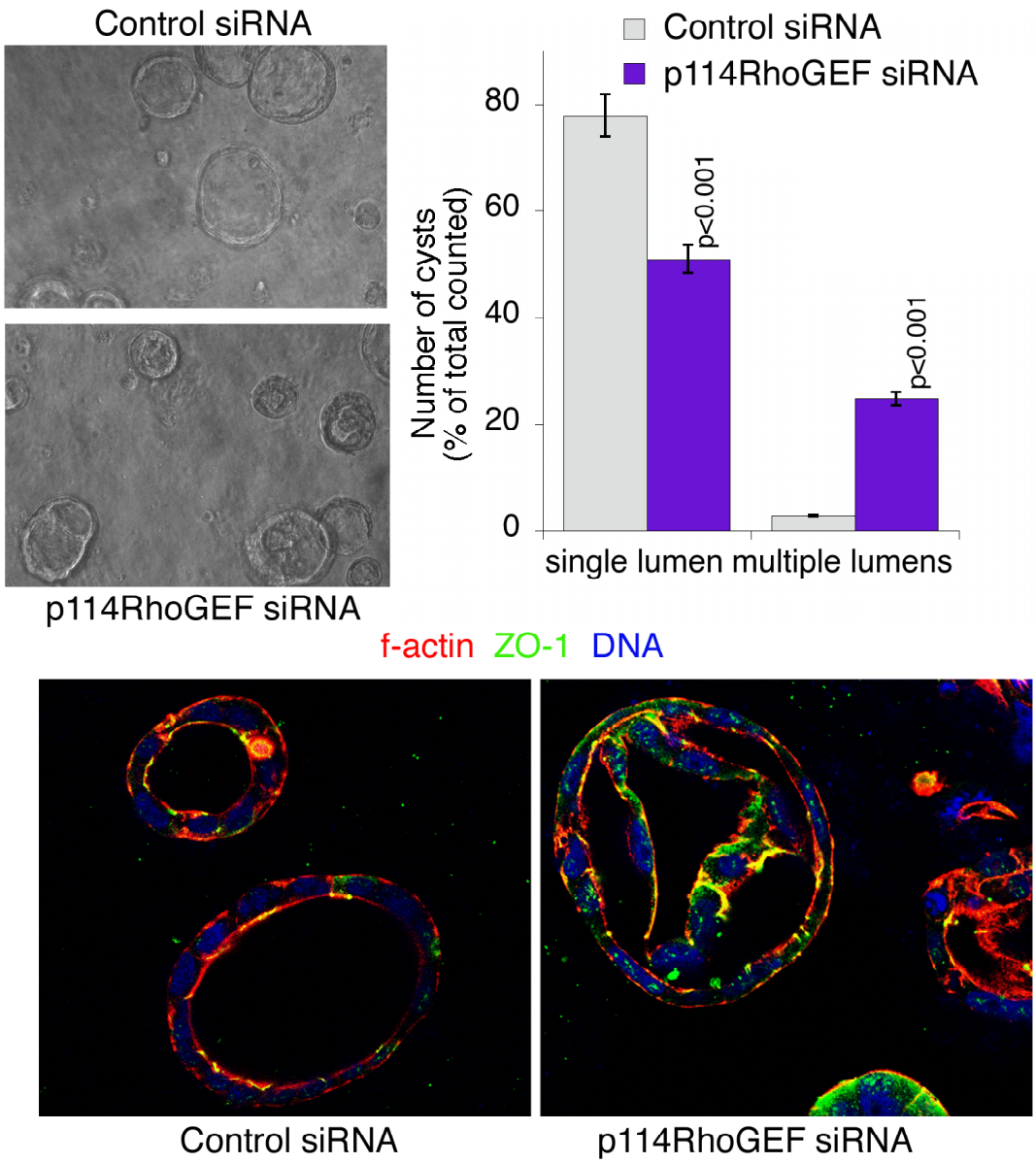

Figure 4.11 p114RhoGEF regulates epithelial morphogenesis in Caco-2 3D cyst cultures.

p114RG was depleted in Caco-2 cells by transfection of p114RG specific siRNAs. After 5 days control (non targeting) transfected siRNA and p114RG depleted cultures were analysed by Phase contrast microscopy and quantified by counting the number of cysts that had a single lumen or structures that had disorganised appearance or multipliable lumens, the mean and SD+/- are shown for n=3.The cultures were then fixed and stained and processed for confocal microscopy using staining for ZO-1 (green) f-Actin (red) and DNA (blue). Scale bar represents 10μm.

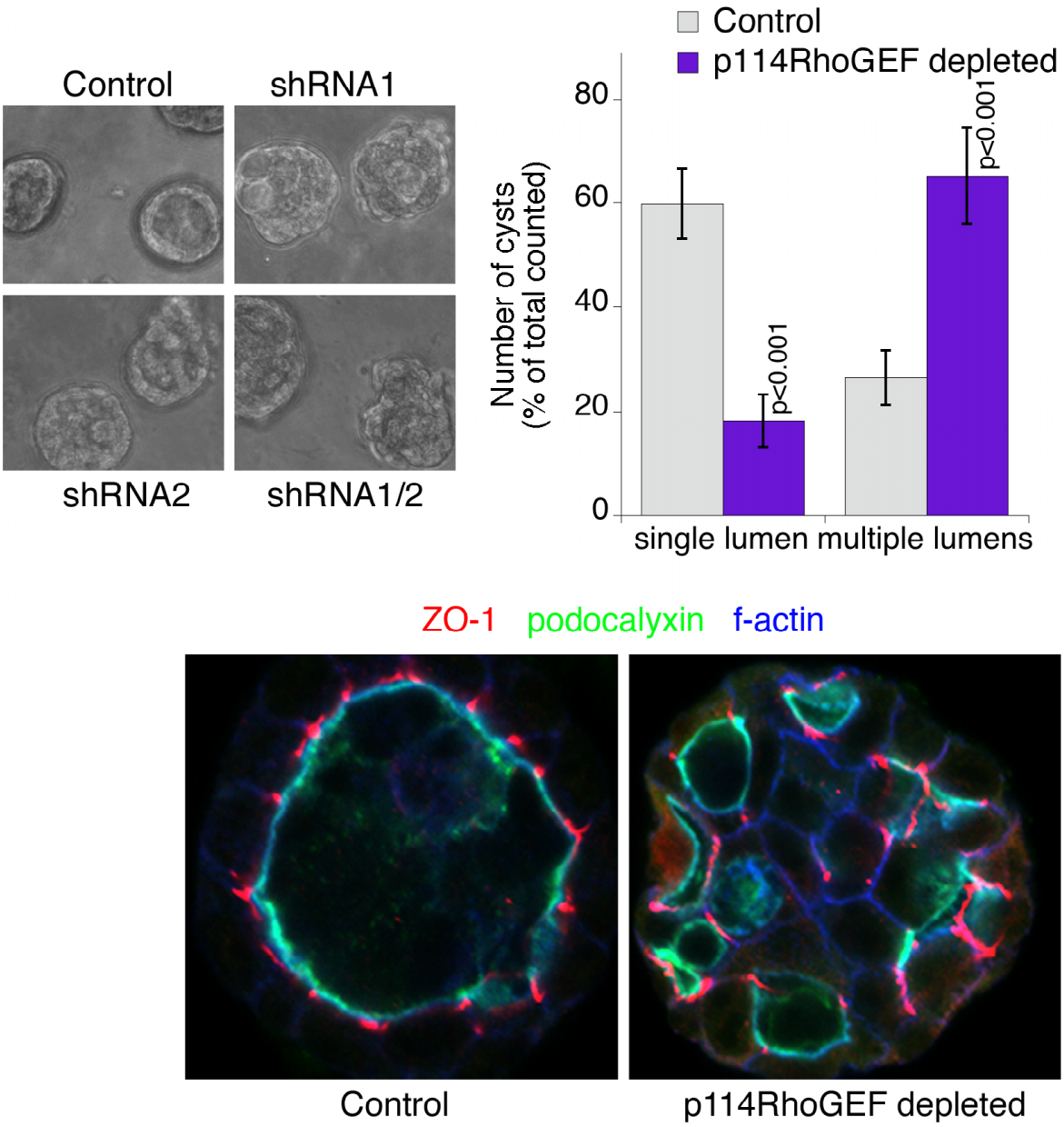

Figure 4.12 p114RhoGEF regulates epithelial morphogenesis in MDCK 3D cyst cultures.

p114RG was depleted in MDCK cells by generating cell lines expressing shRNAs to p114RG. After 5 days control (non targeting) shRNA expressing and p114RG depleted cultures were analysed by Phase contrast microscopy and quantified by counting the number of cysts that had a single lumen or structures that had disorganised appearance or multipliable lumens. Mean and SD are shown for n=3. The cultures were then fixed and stained and processed for confocal microscopy using staining for ZO-1 (red) f-Actin (blue) and polarity marker podocalyxin (green). Scale bar represents 10μm.

Spatially restricted activation of RhoA and subsequent Myosin II activation is regulated at cell-cell contacts by p114RhoGEF

The localisation of a RhoGTPase to a specific membrane domain or compartment, where a specific GEF is recruited or resides is thought to be essential to the spatially restricted control of a RhoGTPase. The recruitment of p114RhoGEF to junctions and the apparent effects of its depletion on Myosin recruitment and distribution suggested that p114RhoGEF, may stimulate Rho signalling at the junctional complex in a spatially restricted manner. I wanted to investigate if this was a function of p114RhoGEF by using a FRET (Fluorescence Resonance Energy Transfer) –based RhoA biosensor to visualise active RhoA in live cells after depletion of p114RhoGEF and as a control of another specific RhoA GEF, GEF-H1 (Figure 4.13).

In control cells transfected with non-targeting siRNA the most intense FRET signal, indicating active RhoA, localised along cell-cell junctions. There was also a small amount of less intense FRET signals distributed throughout the cytoplasm. Depletion of p114RhoGEF led to a dramatic redistribution of the intense FRET signal away from cell junctions and was increased throughout the cells including the basal domain. Depletion of GEF-H1 did not change distribution of the FRET signal indicating these effects were specific to p114RhoGEF. I quantified the amounts of FRET signal at cell-cell junctions and at internal areas (Figure 4.14) and discovered the change in the distribution of the FRET signal at cell-cell junctions and internal regions in p114RhoGEF

depleted cells vs that of control or GEF-H1 depleted cells was statistically significant. I performed the FRET experiments in Caco-2 and HCE cells and found comparable results, indicating that p114RhoGEF is required for spatially restricted activation of RhoA at cell-cell junctions.

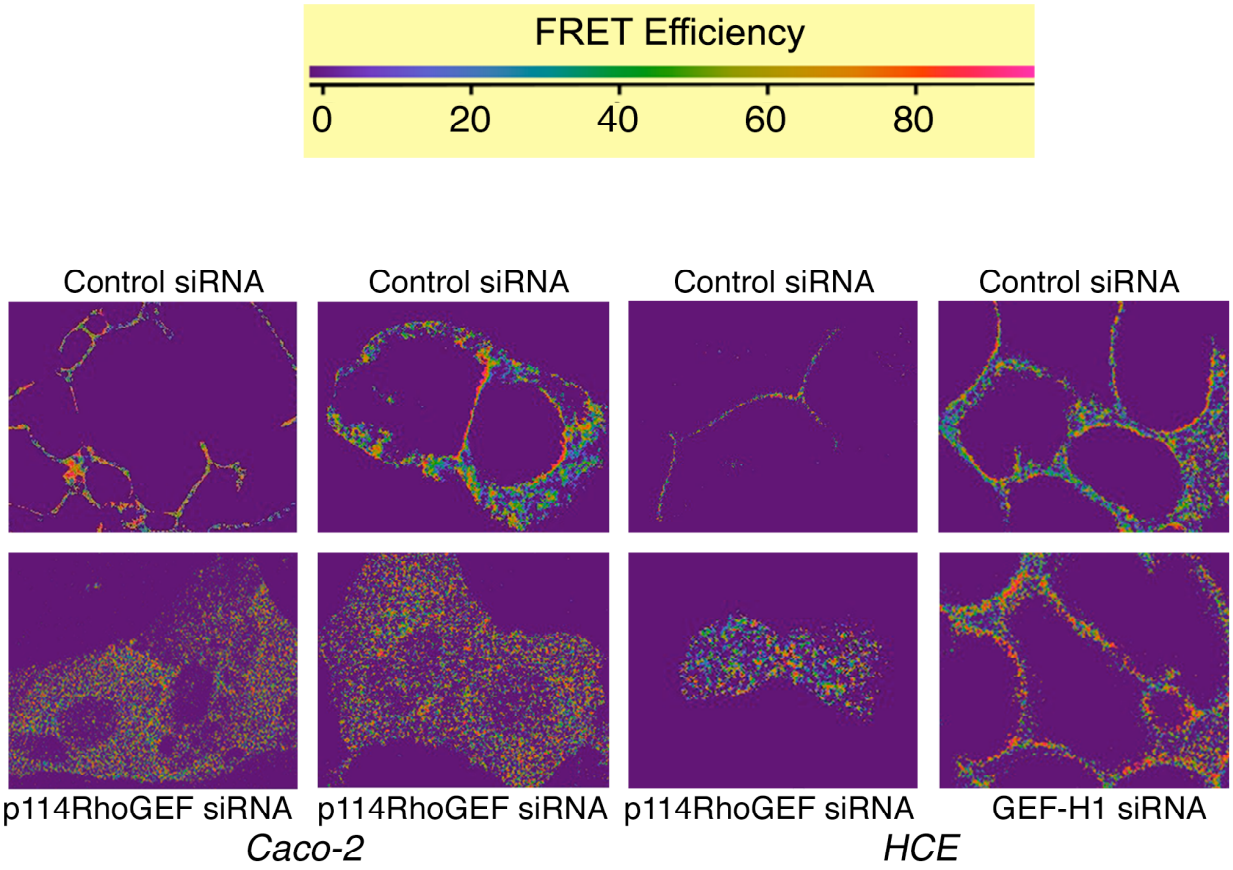

Figure 4.13 p114RhoGEF regulates spatially restricted activation of RhoA signalling at cell junctions.

Caco-2 and HCE cells were transfected with control non-targeting and p114RhoGEF and GEF-H1 specific siRNAs, then 2 days after with a plasmid containing the FRET RhoA biosensor. RhoA activity was imaged by gain of CFP fluorescence after acceptor bleaching, displayed as the level of FRET efficiency. Shown are images of control, p114RhoGEF and GEF-H1 depleted cells.

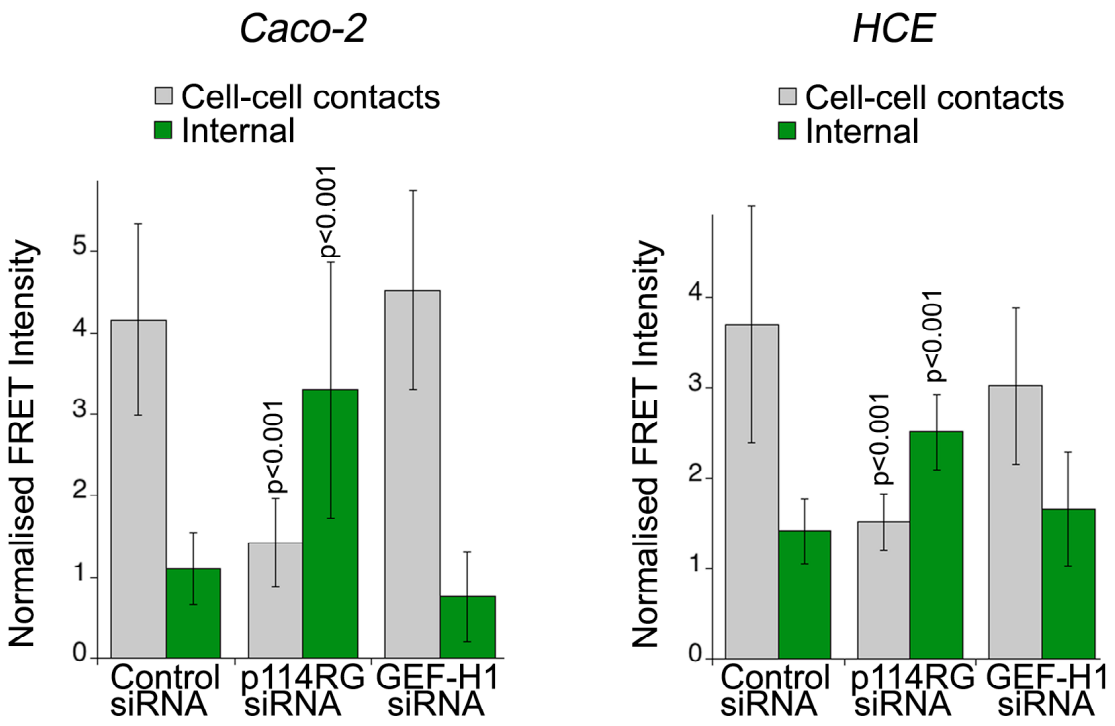

Figure 4.14 Quantification of FRET signal at cell-cell contacts and Internal areas in Caco-2 and HCE cells.

Images were quantified by normalising FRET efficiency in specific cellular regions (cell-cell contacts (grey bars) or internal cytoplasm (Green bars)), against the total FRET efficiency in the quantified fields of view. Bars represent mean of 12 images, error bars = +/- 1 SD.

p114RhoGEF regulates active Myosin IIA distribution

RhoA is an important regulator of cytoskeletal dynamics. One of the main targets of RhoA signalling is the phospholyation of the regulatory light chain of Myosin II (MLC) at Threonine 18 and Serine 19, leading to Myosin activation, and actinomyosin contraction. Based on the evidence that p114RhoGEF activates RhoA at cell-cell junctions and its effect on Myosin distribution, I wanted to observe the effects on the organisation of the actin cytoskeleton and Myosin activation in p114RhoGEF depleted cells.

I found a disruption of the actin cytoskeleton in p114RhoGEF depleted cells, with peri-junctional f-actin appearing reduced and more loosely bundled compared to control cells. I also surprisingly observed an increase in the formation of stress fibres at the base of cells (Figure 4.15). In control cells Myosin II and MLC were distributed along the junctional complex and to a lesser extent along the basal membrane in Caco-2 and HCE cells (Figure 4.16-17). In the absence of p114RhoGEF there was a dramatic redistribution of Myosin IIA and MLC from junctions to stress fibres (Figure 4.16-17). This reflected redistribution of active Myosin, as phosphorylated MLC was located along junctions in control cells (in Caco-2 cells in a punctuate manner and HCE cells, in a more continuous distribution) and redistributed to stress fibre arrays in p114RhoGEF depleted cells. Total levels of phosphorylated MLC remained unchanged in Caco-2 cells and were slightly reduced in HCE cells. In addition levels of phospholyated (inactive) Myosin phosphatase target subunit (MYPT) a substrate of ROCK, that functions to inactivate Myosin II via dephospholyation

of MLC, also remained unchanged (Figure 4.18). This suggests that the increase in active Myosin observed on basal stress fibres may compensate for loss of active Myosin II at junctions. Thus total levels of phospholyation of these two Myosin regulators appear unchanged.

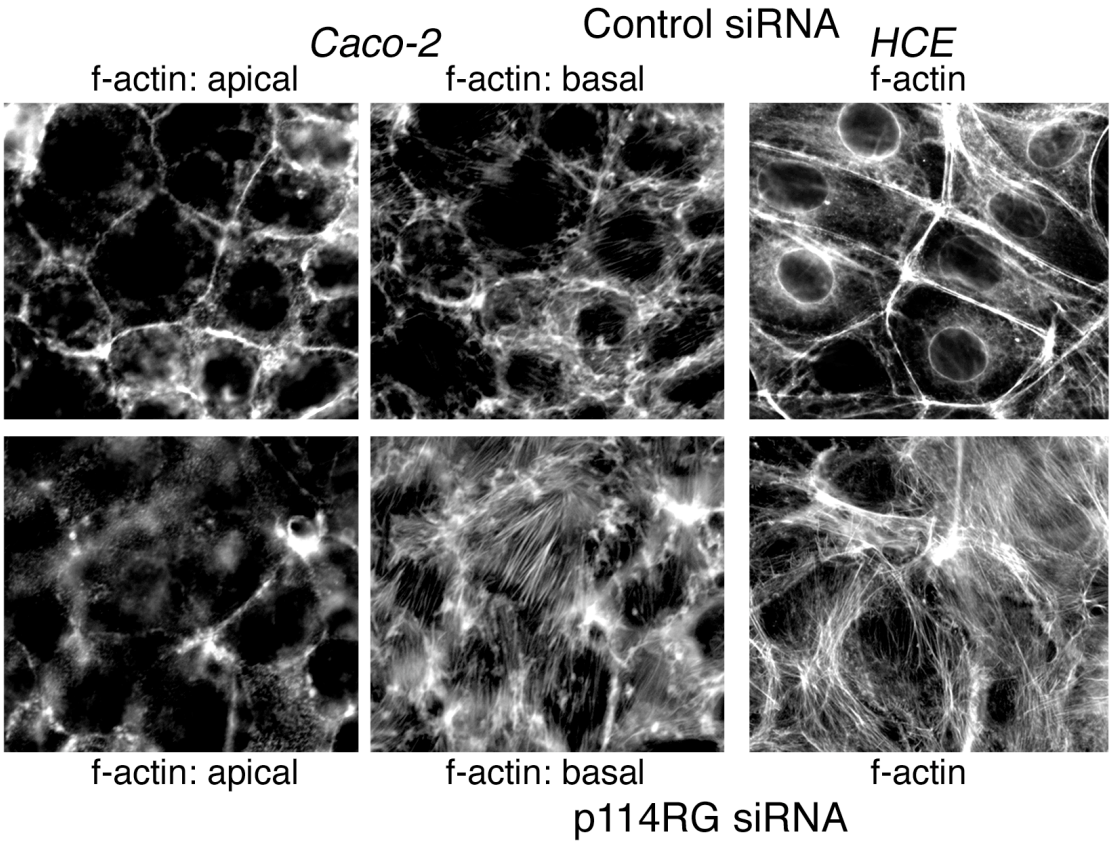

Figure 4.15 p114RhoGEF depletion causes disorganisation of peri-junctional actin and leads to increase in stress fibres.

Caco-2 and HCE cells were depleted of p114RhoGEF by siRNA for 72 hours (bottom pannels) after being fixed and stained with TRITC- conjugated phalloidin to visualise f-Actin. For Caco-2 cells two fields of view were taken an apical (left) and basal (middle).

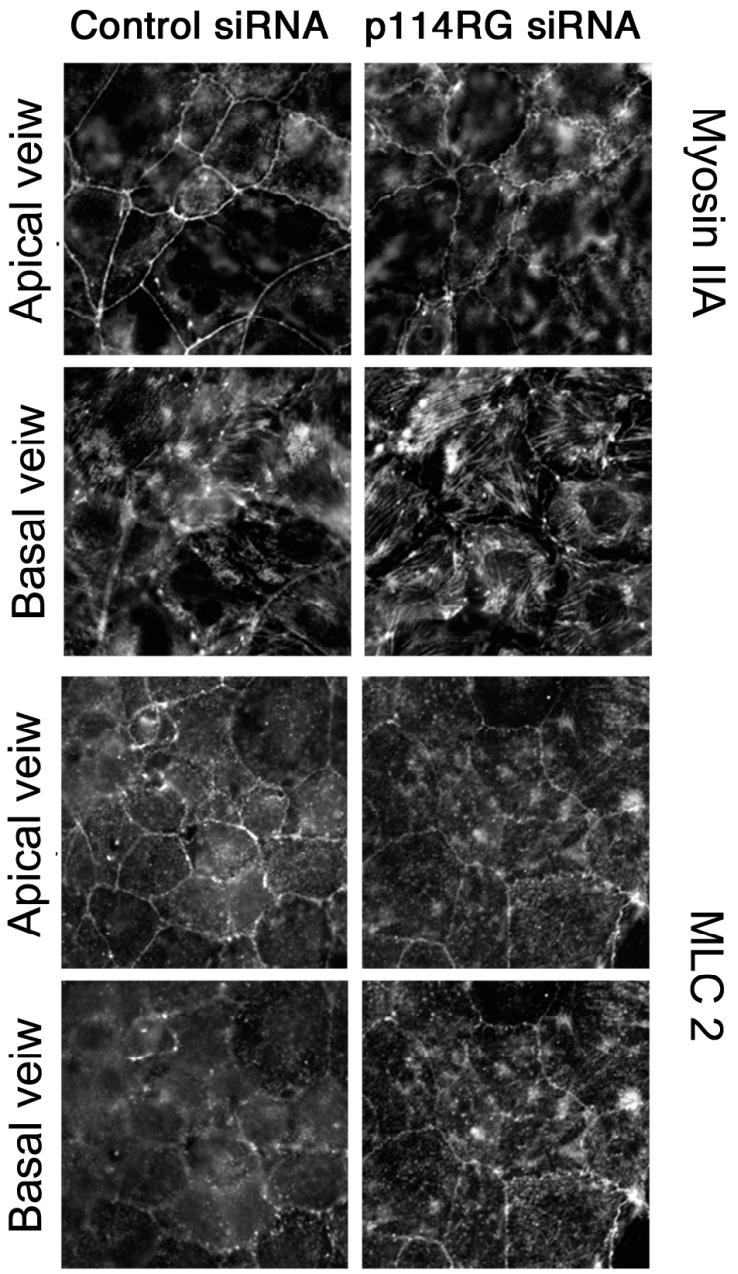

Figure 4.16 Absence of p114RhoGEF causes redistribution of Myosin IIA from cell-cell contacts to basal stress fibre arrays.

Caco-2 cells were depleted of p114RhoGEF using siRNA for 72 hours after being fixed and immunostained with Myosin IIA and Myosin light chain (MLC2) antibodies. Apical and basal fields of view are shown for each antibody stain.

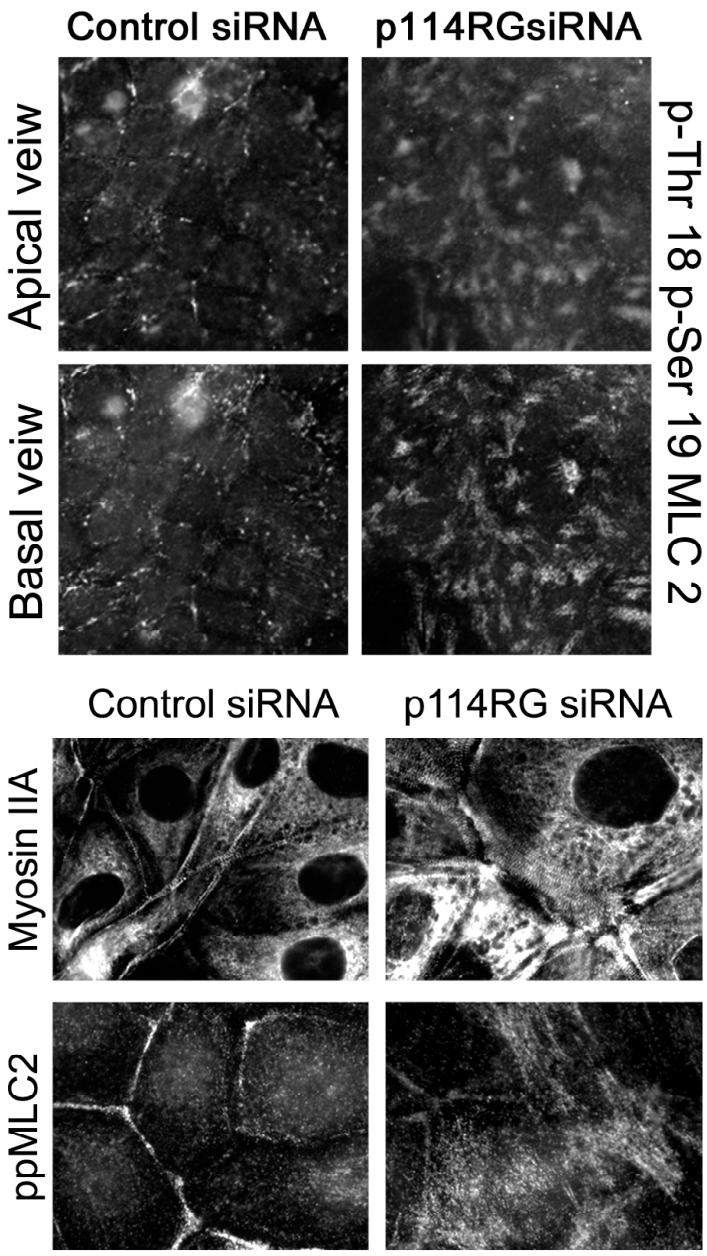

Figure 4.17 Active Myosin II is redistributed from cell-cell junctions to stress fibres in Caco-2 and HCE cells.

Caco-2 and HCE cells depleted of p114RhoGEF by siRNA for 72 hours after being fixed and immunostained with an antibody that recognises phospholyated Myosin light chain (pThr18p-Ser19MLC2 and ppMLC2). For Caco-2 cells two fields of view are shown apical and basal (top panel). For HCE cells Myosin IIA staining is shown in addition to active Myosin IIA.

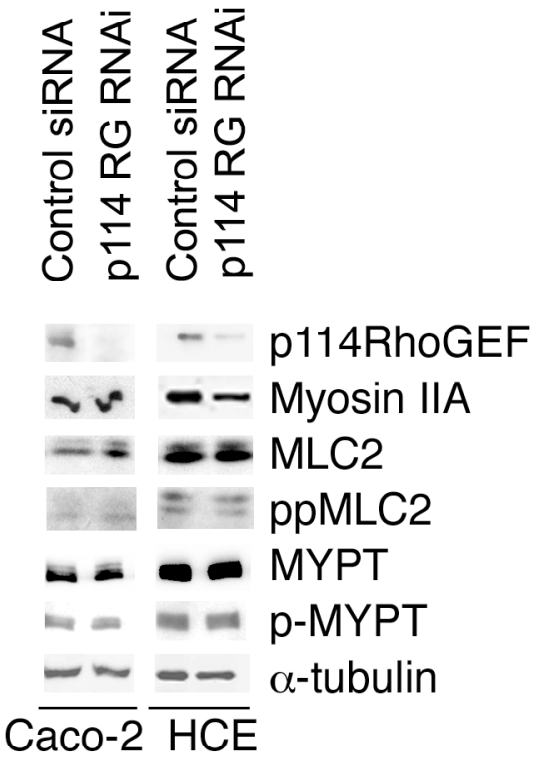

Figure 4.18 Levels of active Myosin II and Myosin phosphatase remain unchanged in p114RhoGEF depleted cells.

Whole cell lysates from Caco-2 and HCE cells transfected with control non targeting siRNA or p114RhoGEF specific siRNAs. After 72 hours RNAi were immunobloted for p114RhoGEF , Myosin IIA, Myosin light chain (MLC2), active phospholyated MLC2 (ppMLC2), Myosin phosphatase target subunit MYPT, inactive phospholyated MYPT (p-MYPT) and α- tubulin to assess total protein levels.

In summary these observations suggest p114RhoGEF is required for spatially restricted control of RhoA and subsequent activation of Myosin at cell-cell junctions. Its absence leads to defective junction assembly, cell spreading and increases in RhoA signalling along the basal domain of cells leading to the formation of stress fibres decorated with activated Myosin II.

Overexpression of p114RhoGEF induces, junctional actinomyosin contraction

If p114RhoGEF regulates the activation of junction associated Myosin, overexpression may induce junctional actinomyosin contraction. To test this hypothesis, I made C-terminally VSV tagged expression constructs of p114RhoGEF to study the effects of its exogenous expression on actinomyosin contraction.

Indeed cells expressing VSV tagged p114RhoGEF caused cells to have an apically contracted, rounded morphology and increased peri-junctional actin filaments (Figure 4.19-21). In HCE cells compaction was very striking with overexpressing cells greatly increased in height and adopting an elongated "dome like" appearance compared to normal relatively flat non-transfected cells. (Figure 4.20). To determine if these morphological effects required RhoA activation, I mutated a highly conserved tyrosine residue to alanine (Y260A) present in the DH domain of 114RhoGEF. Analogous mutations were previously shown to inactivate the GEF activities of GEF-H1 and Lbc [302, 303]. I

tested if the Y260A mutation was able to inhibit p114RhoGEF catalytic ability to activate RhoA by making stable MDCK cell lines to allow inducible expression of wild type and mutant p114RhoGEF. Overexpression of the Y260A mutant did not activate RhoA levels, compared to that of wild type p114RhoGEF, validating its use as a catalytically inactive mutant (Figure 4.22). Expression of the Y260A mutant severely abrogated cell elongation with the majority of overexpressing cells having a normal relatively flat morphology (Figure 4.20), demonstrating RhoA activation is required for this effect. Overexpression of GEF-H1, a RhoA specific exchange factor that is not active at junctions [64], did not induce contraction of the perijunctional actinomyosin ring, indicating that the phenotype observed is specific for p114RhoGEF and not a general effect of transfection of a RhoA GEF (Figure 4.21). In stably transfected MDCK cells up-regulation of the active p114RhoGEF GEF led to increased f-actin and phospholyated MLC at cell junctions, as well as ROCK-dependent rounding and monolayer contraction. (Figure 4.22-23). Furthermore, I found increased total levels of phosphorylated MLC, in addition to increased phospholyated levels of cofilin (Figure 4.25), a protein that is inactivated by phospholyation and that functions to disassemble actin filaments [304] [241], indicating the inactivation of cofilin may have a role in the enrichment of peri-junctional actin in p114RhoGEF over-expressing cells.

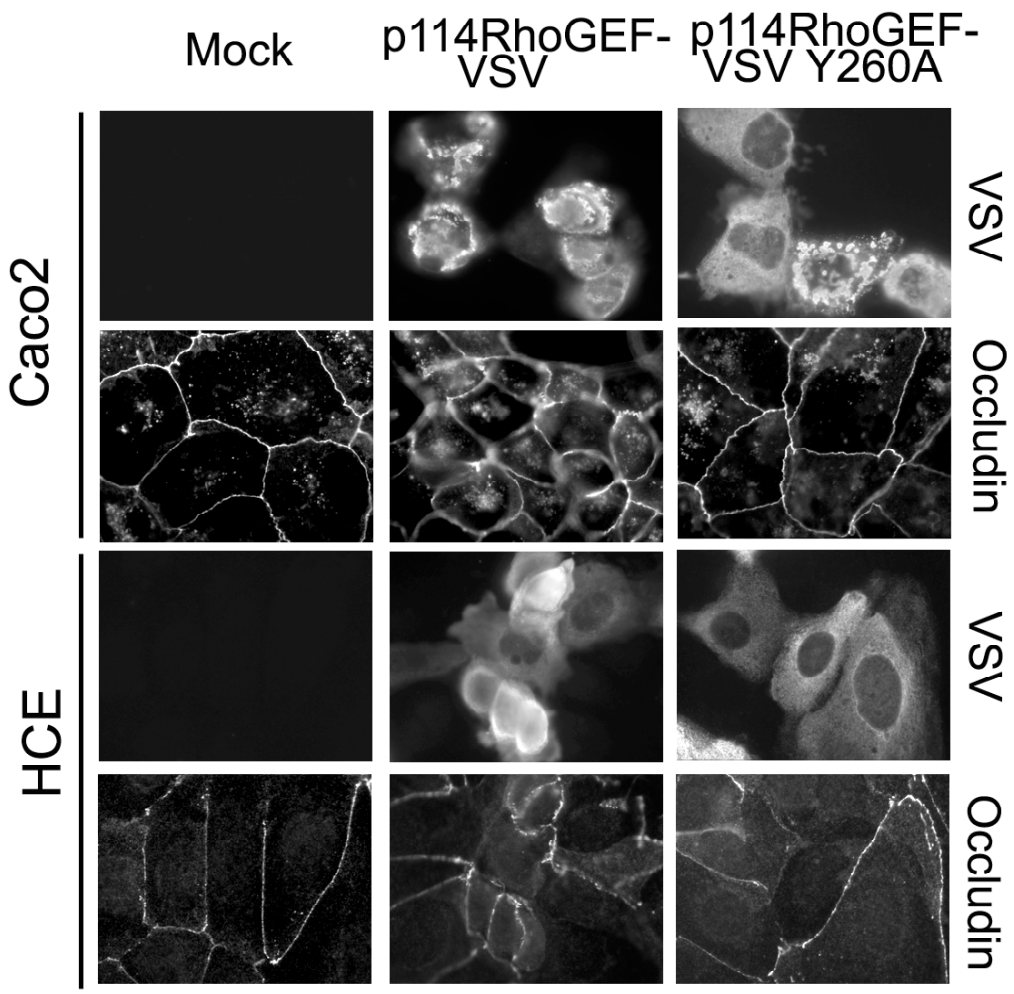

Figure 4.19 Changing of cell morphology in response to p114RhoGEF overexpression.

Caco-2 and HCE cells were transfected with cDNAs encoding C-terminal tagged VSV p114RhoGEF (p114RhoGEFVSV) and catalytically inactive mutant p114RhoGEF (p114RhoGEF Y260A-VSV). Cells were left to express the proteins for 20 hours before fixation and processing for immuno fluorescent staining with VSV and Occludin antibodies.

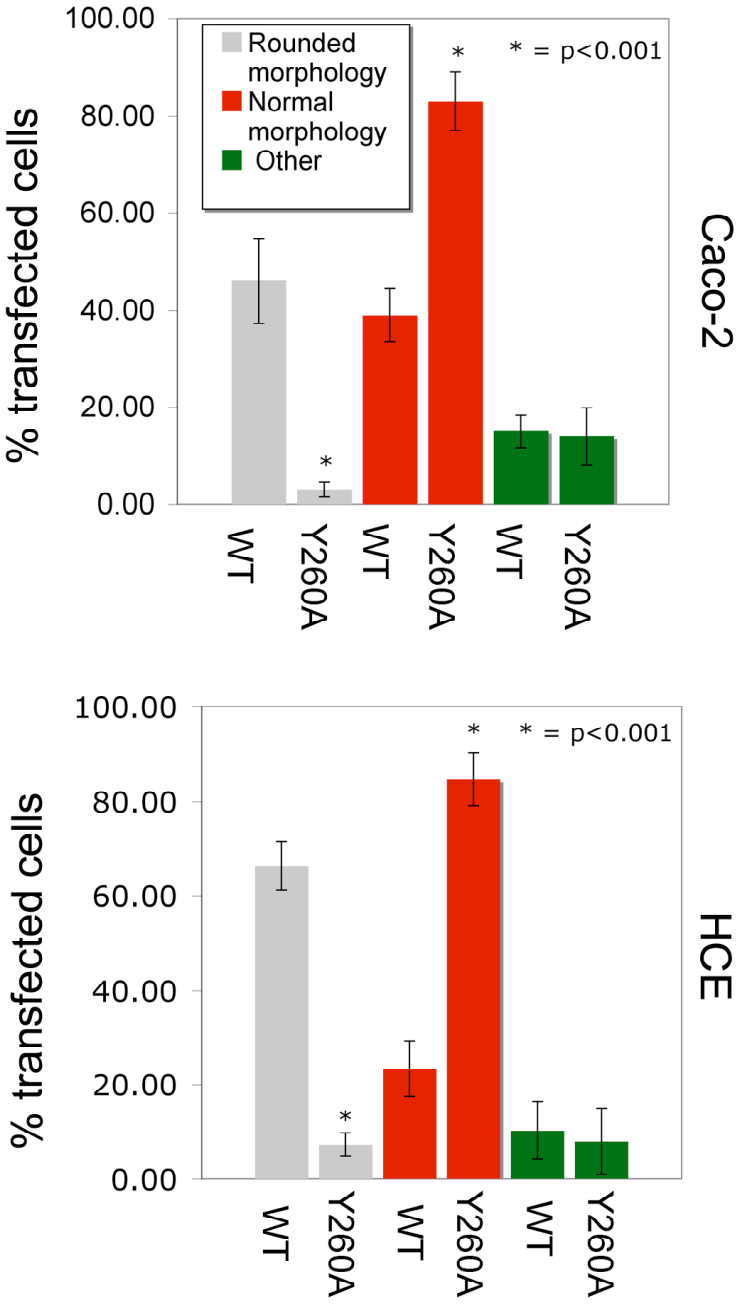

Figure 4.20 Quantification of change in cell morphology caused by overexpression of active p114RhoGEF.

Images shown in figure 4.18 for HCE and Caco-2 cells expressing wild type p114RhoGEF(WT) or inactive mutant p114RhoGEF(Y260A) were quantified by counting transfected cells with a rounded/contracted morphology (grey bars), normal/ flat cells (red bars) as well cells having abnormal morphology apart from rounding (green bars). Bars represent mean of 3 experiments. 100 cells counted per experiment. Error bars represent +/- 1 SD.

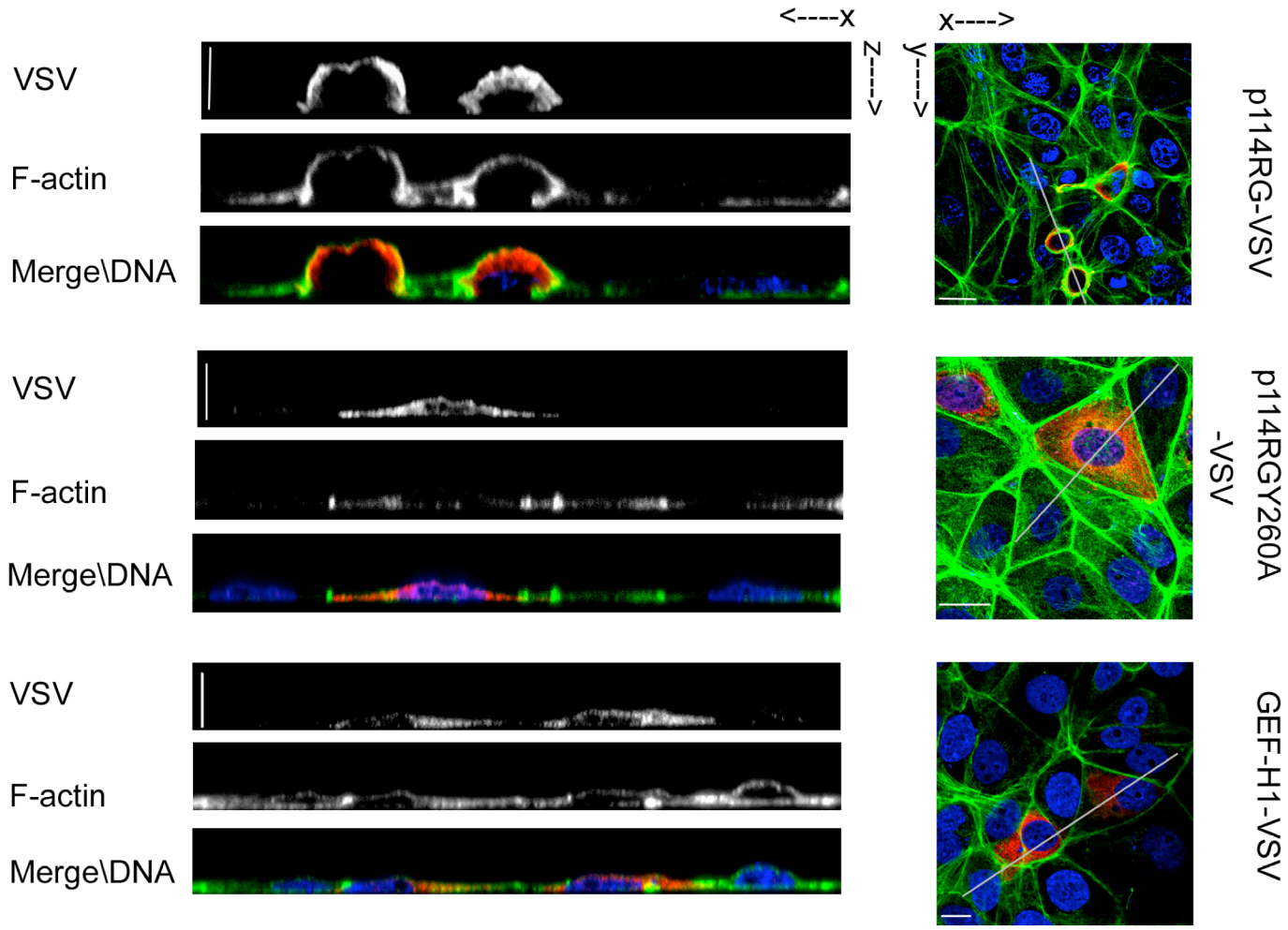

Figure 4.21 Overexpression of p114RhoGEF causes cell elongation

HCE cells were transfected with cDNA containing p114RhoGEF-VSV, mutant p114RhoGEFY260A

and GEF-H1-VSV. Proteins were expressed for 20 hours and fixed and processed for immuno fluorescent staining using FITC-conjugated phaloidin to visualise f-actin (green) VSV antibody (red) and DNA stain Hoechst 33258(blue). Shown are z line scans and xy sections grey lines on xy section represent were z line was taken. Note the contracted appearance of cells expressing active p114RhoGEF; scale bars in grey represent 10μm.

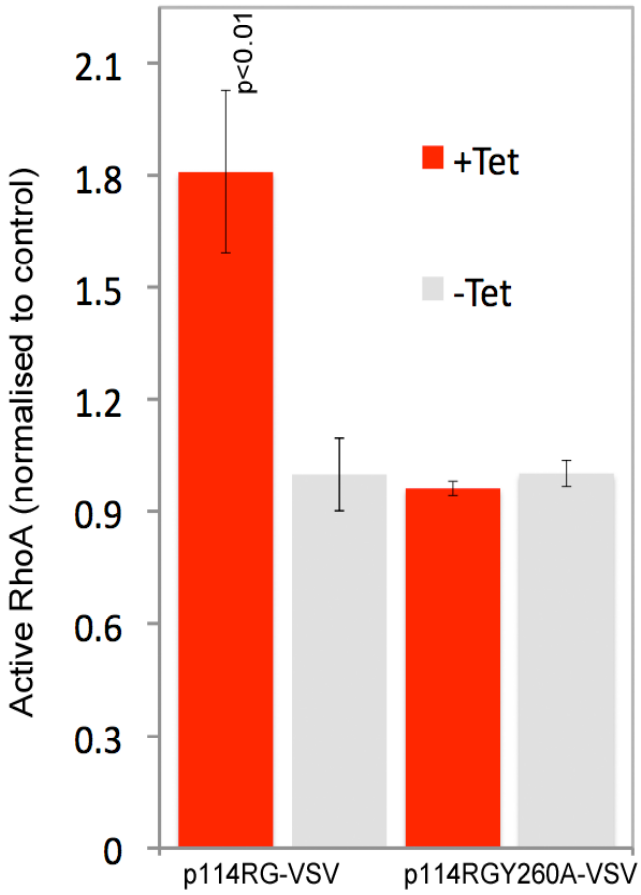

Figure 4.22 Levels of active RhoA in stable MDCK cells overexpressing p114RhoGEF-VSV and p114RGY260A-VSV

Expression of p114RhoGEF and p114RhoGEFY260A was induced by tetracycline in stable MDCK cells lines for 24 hours before performing GLISA assay to observe levels of active RhoA. Note inactive mutant p114RhoGEFY260A does not increase activate levels of RhoA when overexpressed, whereas wild type p114RhoGEF does. Bars represent mean average of 3 experiments normalised to p114RhoGEF –tet control, error bars +/- 1 SD.

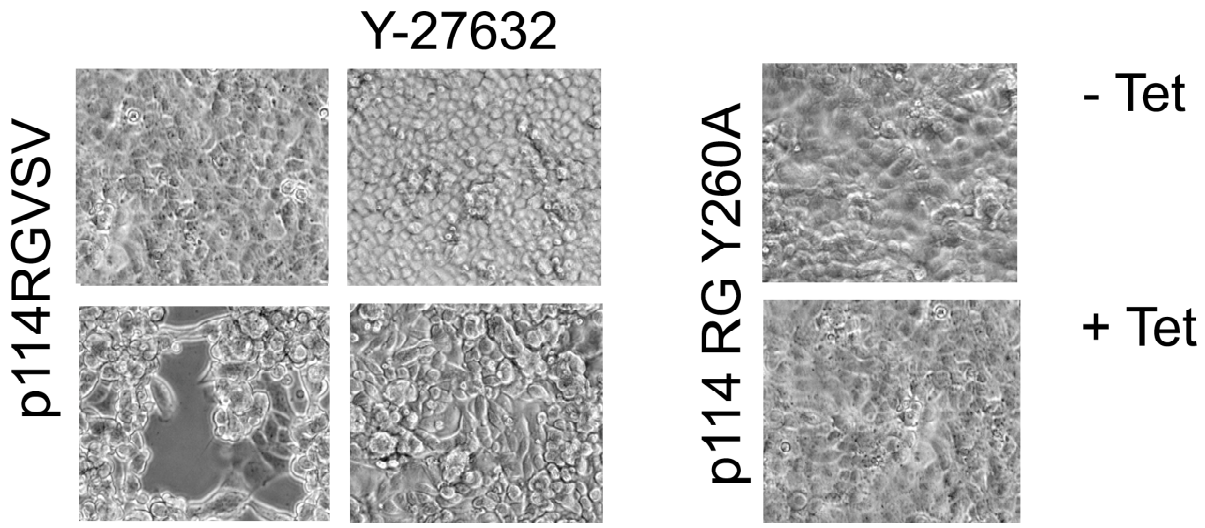

Figure 4.23 Overexpression of p114RhoGEF causes ROCK dependent cell rounding and monolayer contraction.

MDCK cells induced for stable expression of VSV tagged p114RhoGEF or inactive mutant p114RhoGEFY260A by Tetracycline for 24 hours, fixed and imaged using phase contrast microscopy. Note that only overexpression of active p114RhoGEF-VSV causes cell rounding and monolayer contraction, an event that is Rock dependent as addition of the Rock inhibitor Y-27632 at the time of induction attenuates this effect.

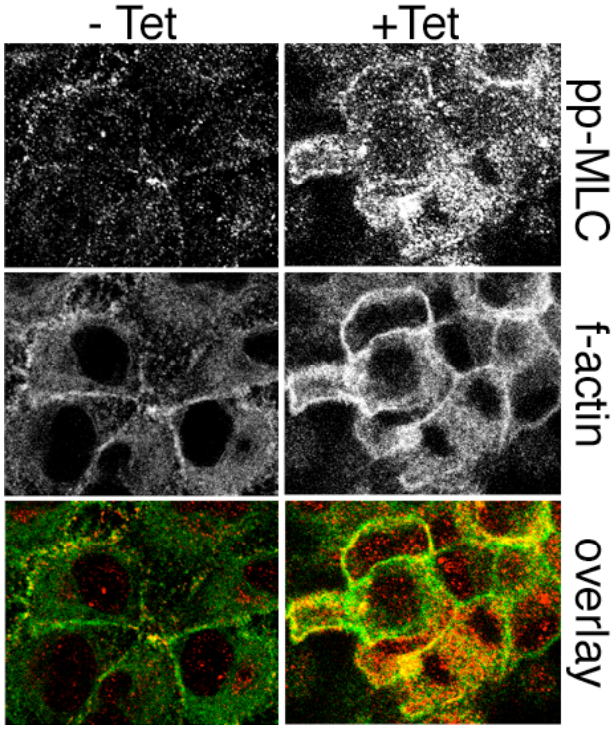

Figure 4.24 Peri-juctional actin and active Myosin are increased in MDCK cells stably expressing p114RhoGEF.

MDCK cells induced for stable expression of VSV tagged p114hoGEF by Tetracycline for 24 hours before fixing and immunostaining with FITC-conjugated phaloidin (green) and active phospholyated MLC (ppMLC), (red)

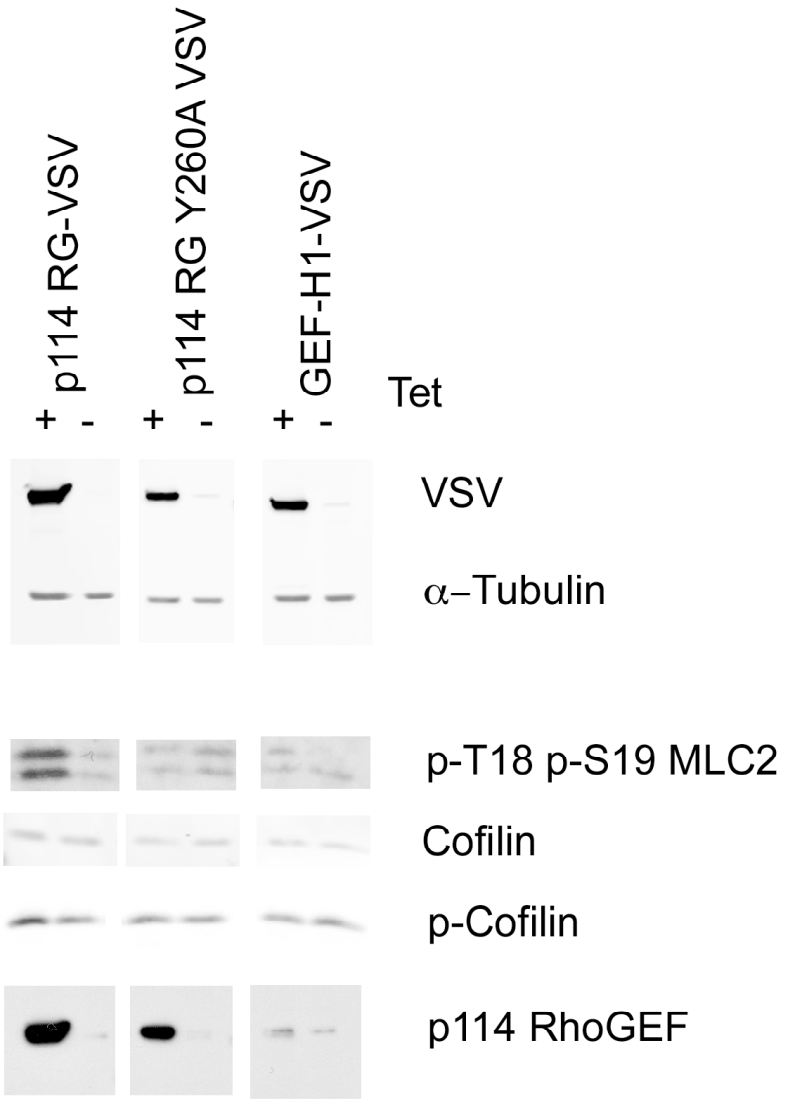

Figure 4.25 Overexpression of p114RhoGEF in MDCK cells causes increases in levels of phospholyated MLC and Cofilin.

Stable MDCK cells lines expressing VSV tagged proteins p114RhoGEF, p114RhoGEF Y260A and GEF-H1 were induced for expression for 24 hours by the addition of Tetracycline before protein was extracted and immunoblotted with specific antibodies to VSV, phospholyated MLC (p-T18 p-19MLC2), Cofilin phospholyated Cofilin (p-Cofilin), p114RhoGEF and α-Tubulin as a loading control.

p114RhoGEF forms a complex with Myosin II, Cingulin and the RhoA effector Rock II.

As p114RhoGEF was known to regulate the junctional recruitment of Myosin, I investigated whether the two proteins were part of a common complex by immunoprecipitation. Indeed, p114RhoGEF immunoprecipitates contained Myosin IIA, as a control for the specificity of this interaction no Myosin IIA was detected in immunopreciptates of the negative control (goat IgG). For efficient signal transduction, RhoGTPases are often in a complex with the GEF that activates them, as well as downstream effectors [148]. We tested if this was the case for p114RhoGEF and discovered the RhoA effector, Rock II, but interestingly not Rock I was present in p114RhoGEF immunoprecipitates. (Figure 4.26). Cingulin a tight junction-associated adaptor known to form a complex with Myosin [63, 305] and regulate RhoA signalling [64], was also immunoprecipitated with p114RhoGEF, but not in negative IgG controls, suggesting that it might function in p114RhoGEF recruitment (Figure 4.26). Cingulin can also bind GEF-H1; however, co-immunoprecipitation of the two GEFs or Myosin or Rock II with GEF-H1 was not observed suggesting they are part of different complexes.

To give mechanistic insight into how p114RhoGEF complexes containing Myosin, Cingulin and Rock II form, I repeated the immunoprecipitation experiments in cells plated in low calcium media to prevent the formation of cell-cell junctions. I observed Myosin II, Cingulin or Rock II was not detected in

p114RhoGEF immunopreciptates (Figure 4.25), indicating the requirement of cell-cell junctions for all members of this complex to form.

I used GST fusion proteins of p114RhoGEF to map the domain of p114RhoGEF required for these interactions (Figure 4.27). I found full-length p114RhoGEF pulled down Myosin IIA, Cingulin and Rock II; however, the efficiency of pulldown was low, possibly reflecting the need for activation of many GEFs before they can bind signalling partners. This may be the case for p114RhoGEF as much of its cellular pool is located in the cytosol (Figure 4.0), possibly requiring activation for an efficient complex formation at cell junctions. The Pleckstrin Homology (PH) domain pulled down Myosin and Cingulin most efficiently out of all the GST- fusion proteins tested; however, it is difficult to make a direct comparison to the full-length protein as it has a weaker expression than the different p114RhoGEF fragments. Pull down of Rock II was less efficient, suggesting that Rho activation might be needed for efficient complex formation.

The PH domain of some Dbl GEFs can bind to specific phosphatidylinositol lipids that can regulate the recruitment of the GEF to specific membrane sites [160] and can also influence the activity of the GEF by the nature of the phosphatidylinositol lipid that is bound [158]. I tested if the PH domain of p114RhoGEF bound to any specific lipids by performing a lipid-binding assay using a recombinant GST- PH domain fusion protein of p114RhoGEF (Figure 4.28). I discovered the PH domain of p114RhoGEF did not bind to any lipids, as a control I used the C1 domain of GEF-H1, which was known to bind to

Phosphatidylinositol phospholyated at the 3,4 or 5 position (PI(3)P, PI(4)P, or PI(5)P). I also used the PH domain of GEF-H1 and demonstrated this did not bind any lipid either Indicating that the PH domains in these two GEFs, may function in protein-protein rather then lipid binding.

I investigated if Cingulin was a factor required for the recruitment of p114RhoGEF to cell-cell junctions. Indeed depletion of Cingulin by siRNA in Caco-2 cells inhibited the association of p114RhoGEF to TJs. In HCE cells Cingulin was required for tight junction formation: as depletion lead to a loss of junctional staining of Occludin and ZO-1, but not E-Cadherin a component of AJs, thus producing a phenotype reminiscent of cells depleted of p114RhoGEF (Figure 4.29 and 4.7). Cingulin and p114RhoGEF co-localised by confocal microscopy (Figure 4.30) and overexpression of Myc tagged Cingulin resulted in a redistribution of p114RhoGEF and Myosin IIA from the cytosol to peri-junctional areas where the overexpressed Cingulin was localised(Figure 4.31-32), further supporting evidence for a role of Cingulin in the recruitment of p114RhoGEF to TJs.

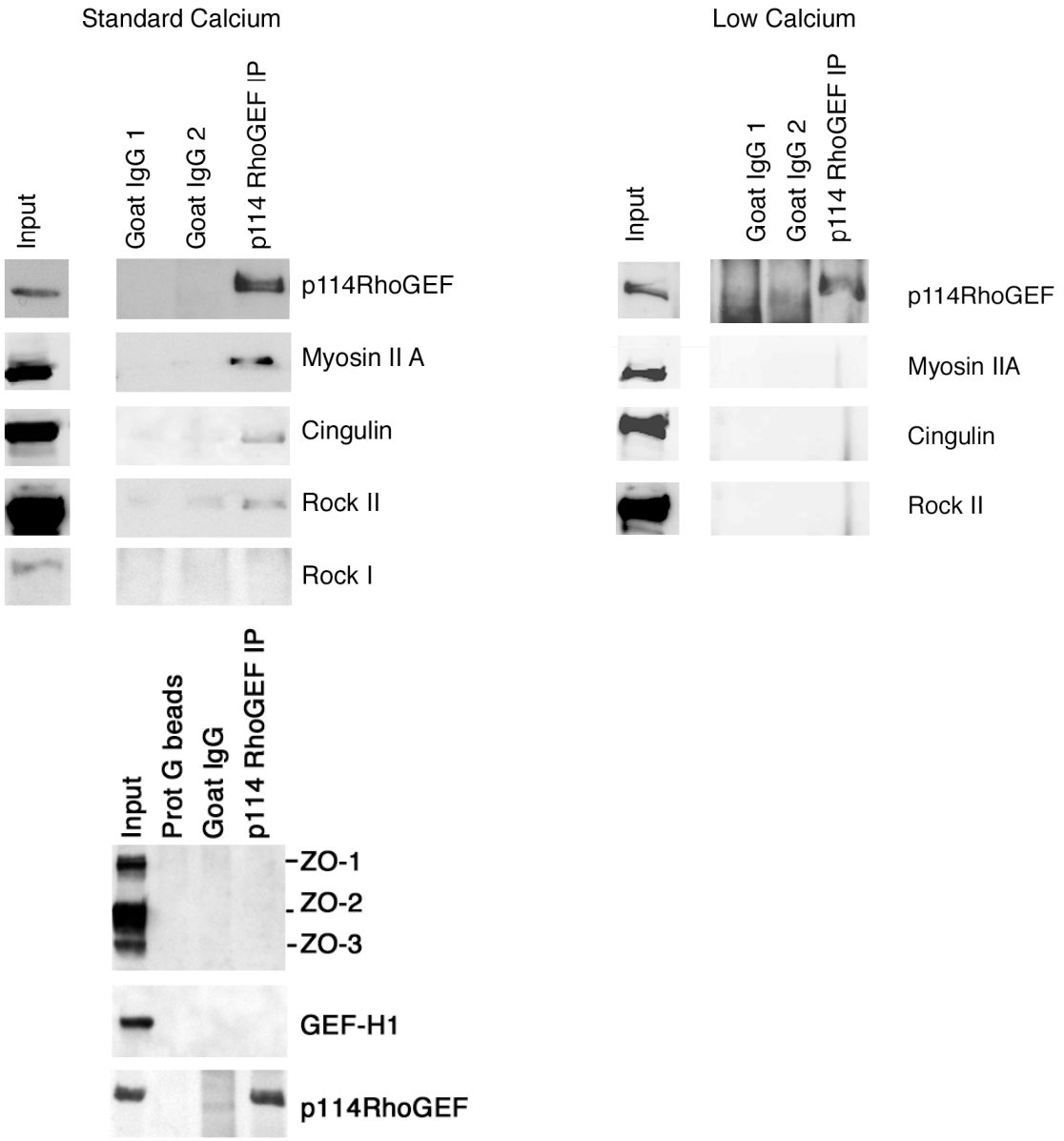

Figure 4.26 p114RhoGEF forms a complex with Myosin IIA, Cingulin and Rock II when cell-cell junctions are present.

p114RhoGEF was immunopreciptated from Caco-2 cell extracts in cells grown in media containing standard amount of calcium or cells grown in media containing low calcium to prevent the formation of cell-cell junctions. Two different goat IgGs were used as a negative control. Co-Immunoprecipitating proteins were analysed by immunoblotting with the antibodies described above. Note: Myosin IIA, Cingulin and Rock II do not form a complex with p114RhoGEF in the absence of cell-cell junctions. And ZO-1,2,3 and GEF-H1 do not Coimmunopreciptate with p114RhoGEF.

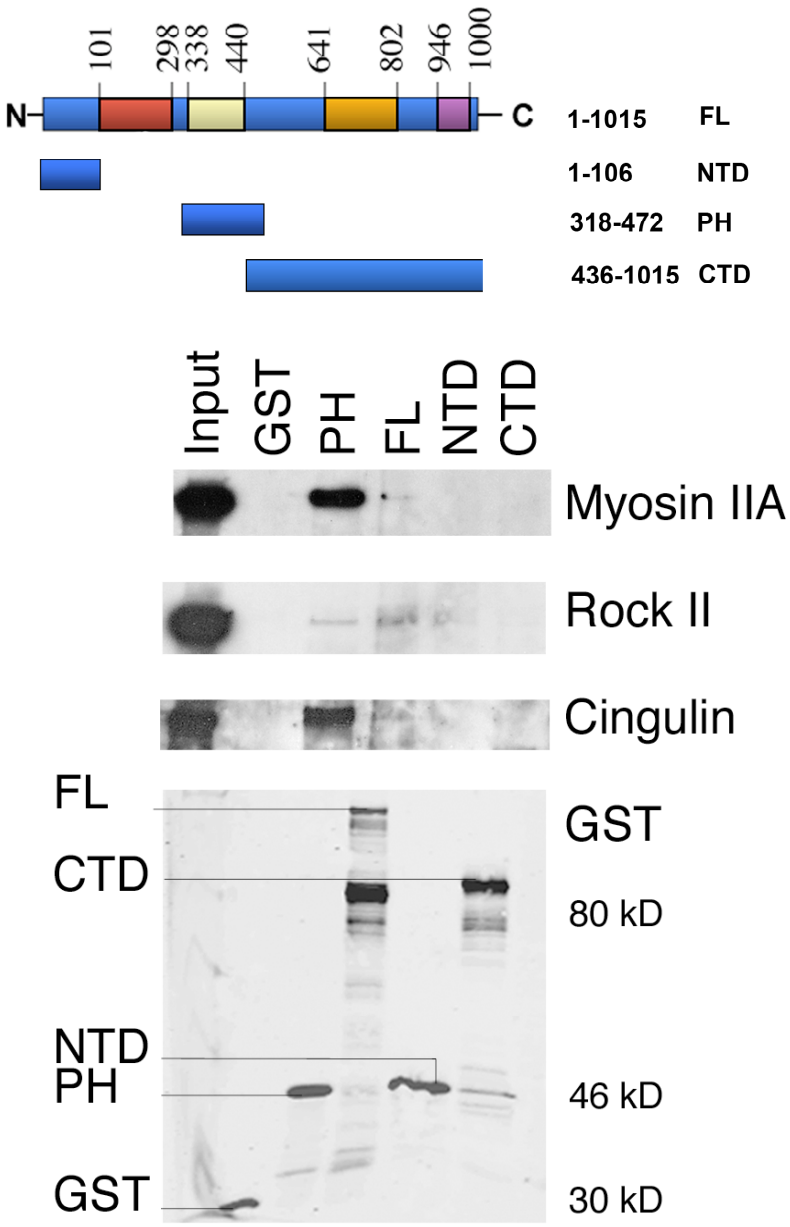

Figure 4.27 Myosin II, Cingulin and Rock II are pulled down using p114RhoGEF-GST fusion proteins.

A schematic representation of p114RhoGEF (top) showing following domains DH (red) PH (yellow) coiled coil (orange) proline rich (puple). GST fusion proteins containing full length and different domains indicated, in the schematic above were bound to beads and used for pulldown experiments in Caco-2 cells. Pulldowns were analysed via immunoblot for Myosin IIA, Cingulin, Rock II and GST to observe amounts of fusion protein added.

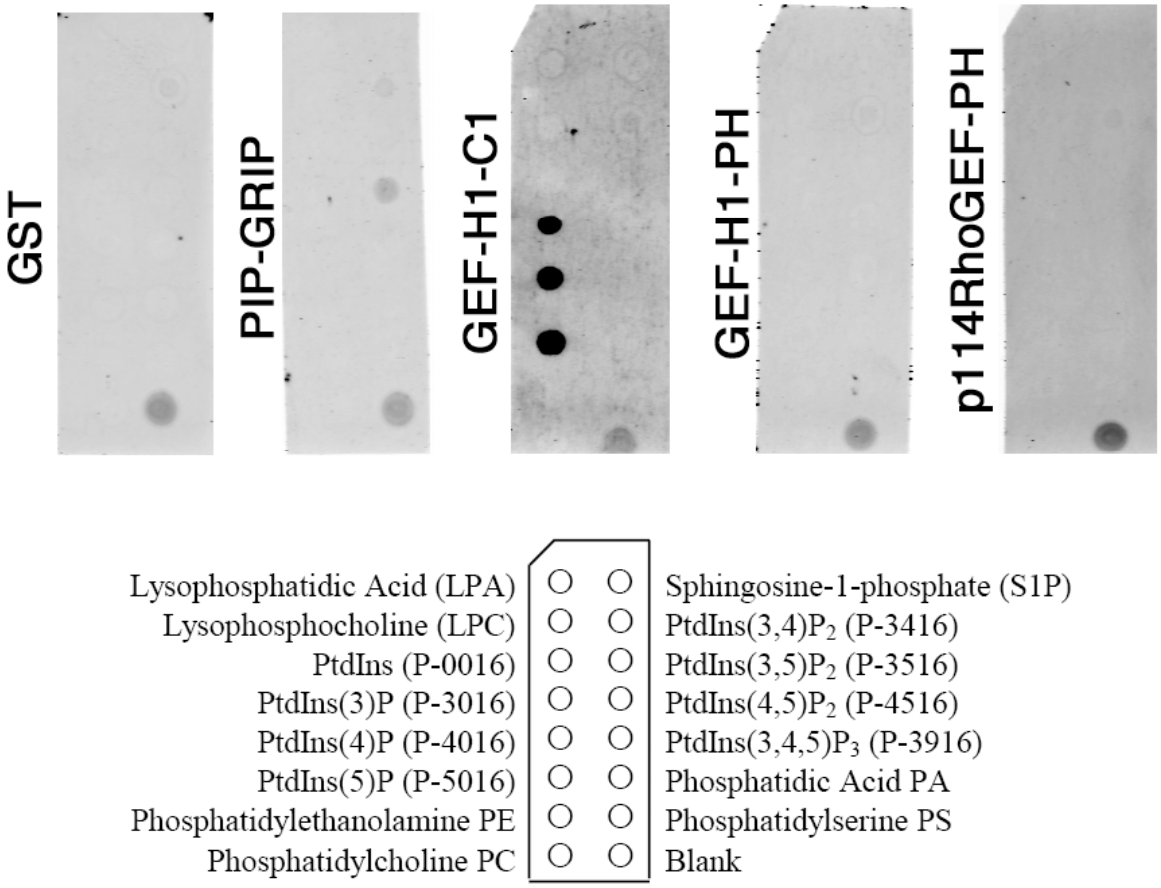

Figure 4.28 The PH domain of p114RhoGEF does not bind phospholipids.

A lipid binding assay was performed by incubating membranes containing different types of immobilised lipids with 1 μg/ml of different recombinant GST fusion proteins. Lipid binding was detected by incubating the membrane with GST antibody. Positive controls for protein that bind different lipids were the C1 domain of GEF-H1 and PIP GRIP (containing the PH domain of PLCδ), GST was used as a negative control. Note no lipid binding was observed using the PH domains of p114RhoGEF and GEF-H1.

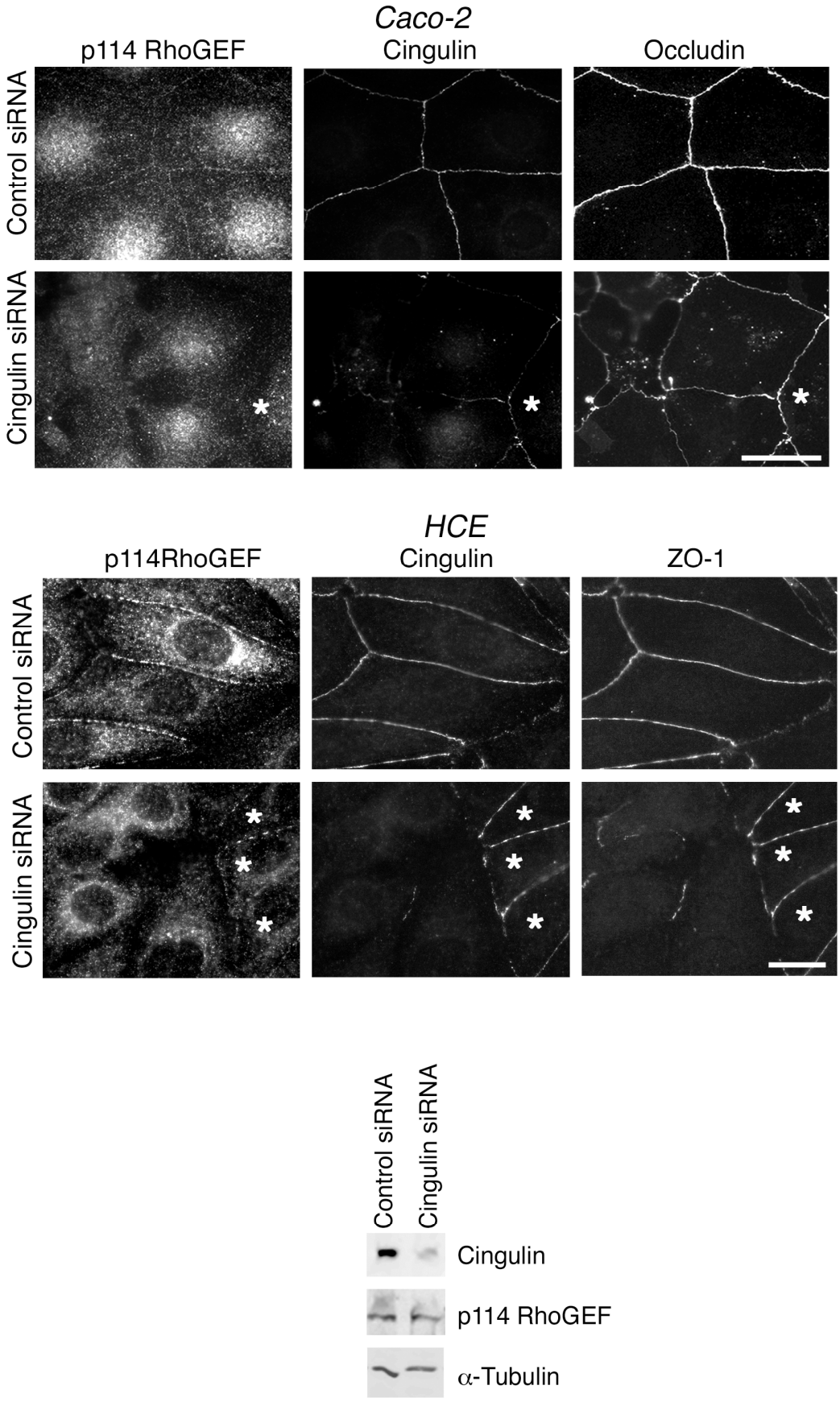

Figure 4.29 Cingulin is required for efficient recruitment of p114RhoGEF to junctions.

Caco-2 and HCE Cells depleted of Cingulin by transfection of siRNAs. After 72 hours cell lystates were immunoblotting with Cingulin, p114RhoGEF and α-Tubulin in Caco-2 cells, or cells were fixed for immunostaining with Cingulin, p114RhoGEF and Occludin antibodies. Stars show cells that have more Cingulin due to less efficient knockdown. Scale bar represents 10μm.

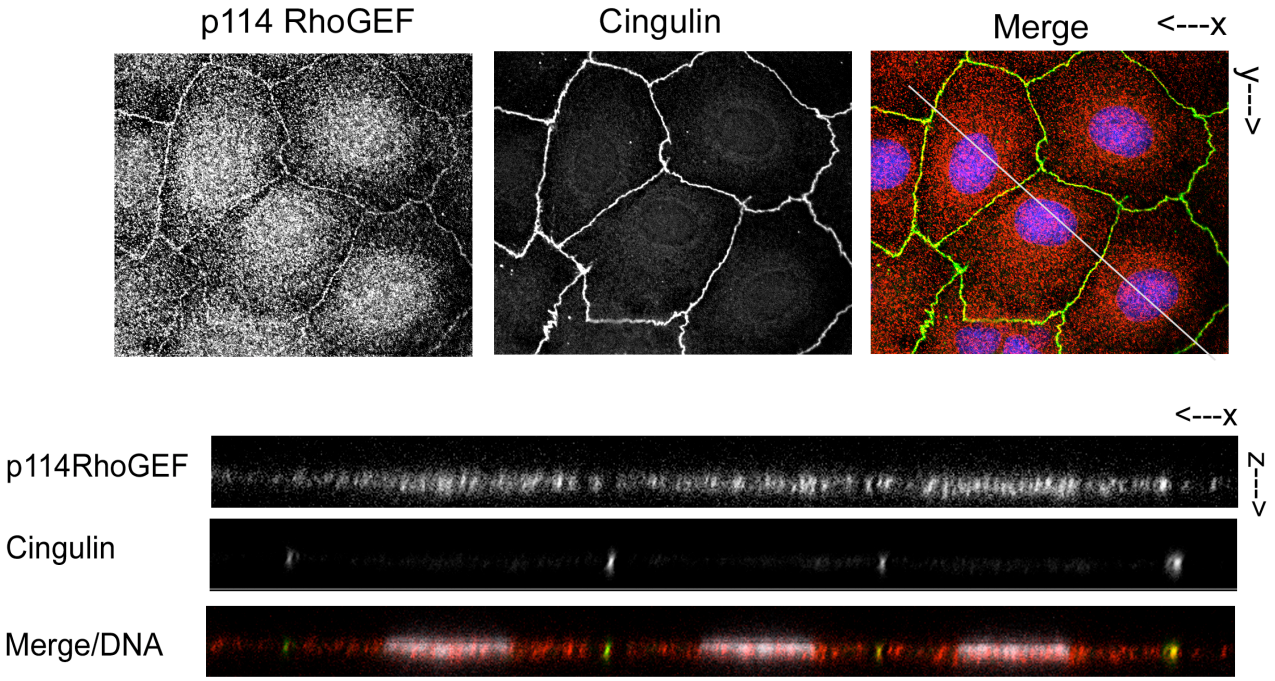

Figure 4.30 Cingulin and p114RhoGEF colocalise with each other at apical cell junctions.

Caco-2 cells immunostained with p114RhoGEF (red) and Cingulin (green) and the DNA stain Hoechst 33258 (blue) were imaged using confocal microscopy. Shown are z line scan and xy sections. The grey line on xy section represent were a z line was taken. Scale bars in grey represent 10μm.

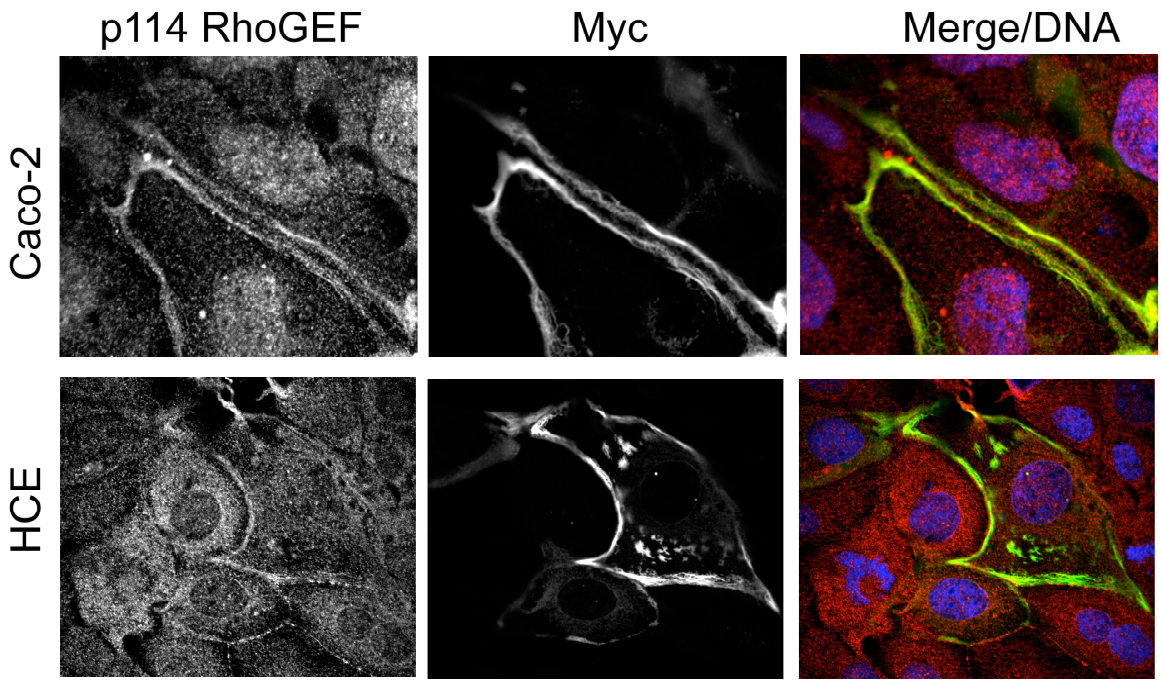

Figure 4.31 Overexpression of Cingulin causes redistribution of p114RhoGEF

Myc-tagged Cingulin was overexpressed in Caco-2 and HCE cells for 24 hours before cells were fixed and immunostained with p114RhoGEF (red), Myc (green) antibodies and the DNA stain Hoechst 33258 (blue) Note overexpression of Cingulin causes redistribution of p114RhoGEF from the cytosol to cell-cell iunctions.

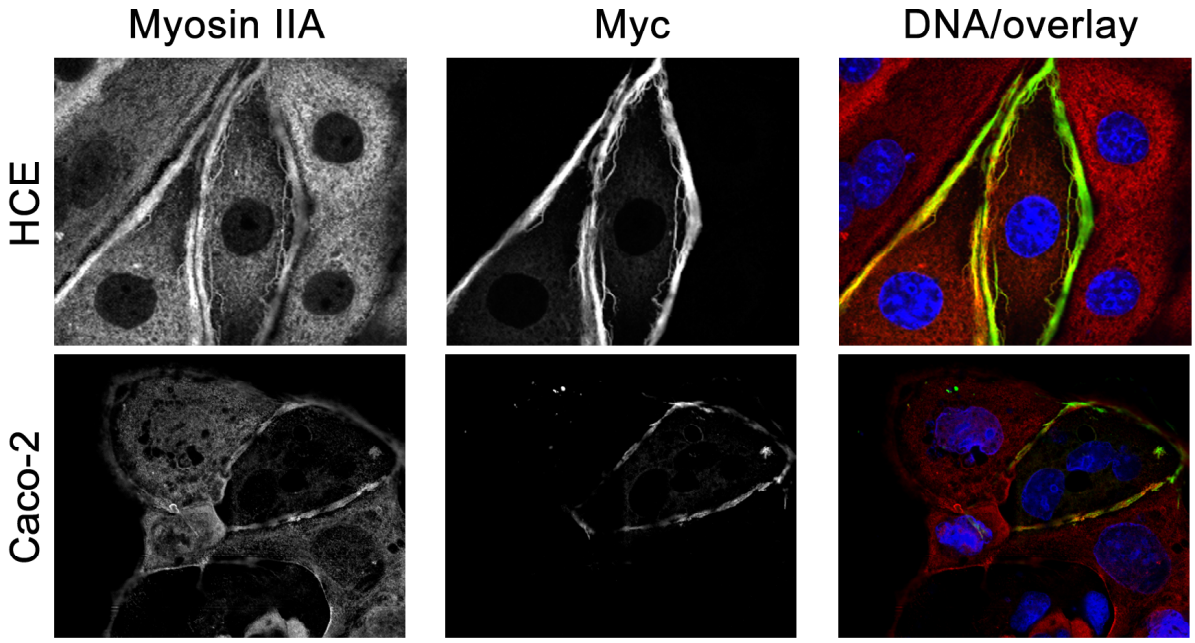

Figure 4.32 Overexpression of Cingulin causes redistribution of Myosin II

Myc-tagged Cingulin was overexpressed in Caco-2 and HCE cells for 24 hours before cells were fixed and immunostained with Myosin IIA (red), Myc (green) antibodies and the DNA stain Hoechst 33258 (blue) Note overexpression of Cingulin causes redistribution of Myosin IIA, observed more clearly in Caco-2 cells from the cytosol to cell-cell junctions.

Chapter 4 –Discussion

Here I have presented results showing p114RhoGEF a GEF identified from a siRNA screen for junction assembly, regulates spatially restricted activation of RhoA at epithelial junctions, driving junction assembly and junctional actinomyosin activation. RhoA signalling is well established to be crucial in the regulation of junction assembly and function [4] however the identification of the GEF that activates RhoA at cell-cell junctions had been unknown until now.

p114RhoGEF forms a signalling module complex containing the Rho effector Rock II and Myosin II two proteins known to regulate junctional dynamics [299]. Interestingly the RockI isoform was not part of this complex. This is in agreement with previous studies that support evidence for Rock II to have a more predominant role in junctional dynamics [299]. Junctional recruitment of p114RhoGEF requires Cingulin a TJ adaptor protein has been previously linked to RhoA signalling via interaction with GEF-H1 [64]. Cingulin is present in a complex with p114RhoGEF Myosin and Rock II. I have shown evidence for this by demonstrating p114RhoGEF and Cingulin co-localisation by confocal microscopy and by showing that repressing levels of Cingulin prevents p114RhoGEF from being recruited to TJ. In complete contrast, when Cingulin is overexpressed levels of p114RhoGEF and Myosin II are redistributed and enriched at cell-cell contacts. Cingulin is also known to bind to GEF-H1; however, no coprecipitation of p114RhoGEF and GEF-H1 was observed, suggesting that they are part of distinct complexes. The formation p114RhoGEF /Myosin II/Rock II/ Cingulin complex seems to be dependent on cell-cell

junctions being present. As no interactions were observed when co-immunopreciptation experiments were performed in cells devoid of cell-cell junctions, suggesting that this complex forms during the stages of junction formation. This is supported by the observation that p114RhoGEF and Myosin II are recruited at similar time to forming junctions during Ca switch experiments. The domain of p114RhoGEF important for mediating interactions with Myosin II, Cingulin and Rock II was mapped to the PH domain. PH domains of some GEF are known to bind specific phospholipids. PH domain/lipid interactions are known to be able to regulate activity of some GEFs[158] or their subcellular localisation [306]; however, no lipid binding was observed with the PH domain of p114RhoGEF. The PH domain pulled down Rock II less efficiently than Myosin II or Cingulin suggesting that Rho activation may be required for efficient Rock II recruitment. The interaction of PH domain of p114RhoGEF with Myosin II and Cingulin could be important in mediating recruitment, but also in stimulating its GEF activity towards RhoA.

p114RhoGEF regulates spatially restricted RhoA activation at cell-cell contacts in different epithelial cell types. In agreement with previous studies GEF-H1 was not found to be required for junction formation or RhoA activation at junctions. [64] Absence of GEF-H1 seemed to retard the initial stages of junction formation, by regulation of cell spreading and initial cell shape changes, but did not affect formation of junctions as such. This was in direct contrast to p114RhoGEF, where its absence did not affect early adhesion and cell shape changes, but did prevent junction formation by effecting contraction of the actinomyosin belt and junctional maturation. p114RhoGEF and GEF-H1 therefore seem to represent

two opposing pathways of RhoA regulation at cell junctions. p114RhoGEF is recruited to the forming junctional complex where it promotes junctional maturation via actinomyosin contractility whereas, GEF-H1 is recruited and inactivated to forming junctions, contributing to inhibition of RhoA signalling that promotes proliferation and cell morphological changes at low cell confluence .

Depletion of p114RhoGEF did not only inhibit RhoA activation at cell junctions, but caused increased non-junctional RhoA activation and increased MLC phospholyation along the basal domain. As counterintuitive as this may seem this evidence supports the specificity of p114RhoGEF for spatial activation of junctional RhoA signalling and its importance for junction formation. RhoA activity is well known to be down regulated in response to cell confluence, thus interfering with junction formation stimulates RhoA signalling in different spatial areas of the cell. GEF-H1 is not recruited normally to junctions in p114RhoGEF depleted cells giving a more diffuse cytoplasmic distribution, and hence may contribute to overall activation in these cells. GEF-H1 is known to induce stress fibres in response to stimuli such as TNFα [215] [219]. Other unidentified RhoA specific GEF proteins that are inhibited by junction formation may also contribute to non-junctional RhoA activation. However there are other mechanisms that contribute to the inhibition of RhoA activity as cells reach confluence, such as the regulation of p190RhoGAP [307] or possibly the junction associated GAP Myosin-IXb [308].

The junction associated actinomyosin cytoskeleton is critical for the formation and function of junction dynamics, and also drives processes in tissue

remodelling during development, such as apical constriction [309-312]. Overexpression of p114RhoGEF induces actinomyosin contraction, causing cells to greatly increase in height and adopting an elongated "dome like" appearance. Overexpression of active p114RhoGEF led to increased f-actin and increased activated Myosin II at cell junctions and ROCK-dependent rounding and monolayer contraction in MDCK cells. This evidence correlates with the loss of active Myosin II at junctions when p114RhoGEF levels are suppressed. p114RhoGEF is a critical factor required for epithelial morphogenesis. Depletion of p114RhoGEF in three dimensional cyst culture systems of two different epithelial cell types resulted in cysts that had a disorganised appearance with multiple lumens. However some degree of polarity was maintained. The disorganized cyst appearance is possibly as a result of the loss of actinomyosin tensile forces required to maintain normal cyst morphology[313]. Supporting evidence, comes from a recent study that identified p114RhoGEFregulating epithelial morphogenesis in an siRNA screen in three dimensional MDCK cultures [314].

This evidence supports a model (see Figure 4.33), where p114RhoGEF associates with and activates a Rho signalling module that is central to activate actinomyosin contractility and drives epithelial junction formation and morphogenesis. Given the physiological roles of junctional RhoA signalling, p114RhoGEF represents a regulator of central importance. It will be important to identify the signalling components that stimulate p114RhoGEF during physiological and developmental processes to drive spatially restricted Rho signalling and Myosin activation at cell junctions. Additionally it will also be

important to identify if the p114RhoGEF- RhoA Myosin II signalling module is important for different epithelial processes other than cell-cell adhesion, such as cell migration. In Chapter 5, I present some preliminary data that suggests a role for p114RhoGEF in wound healing induced cell migration.

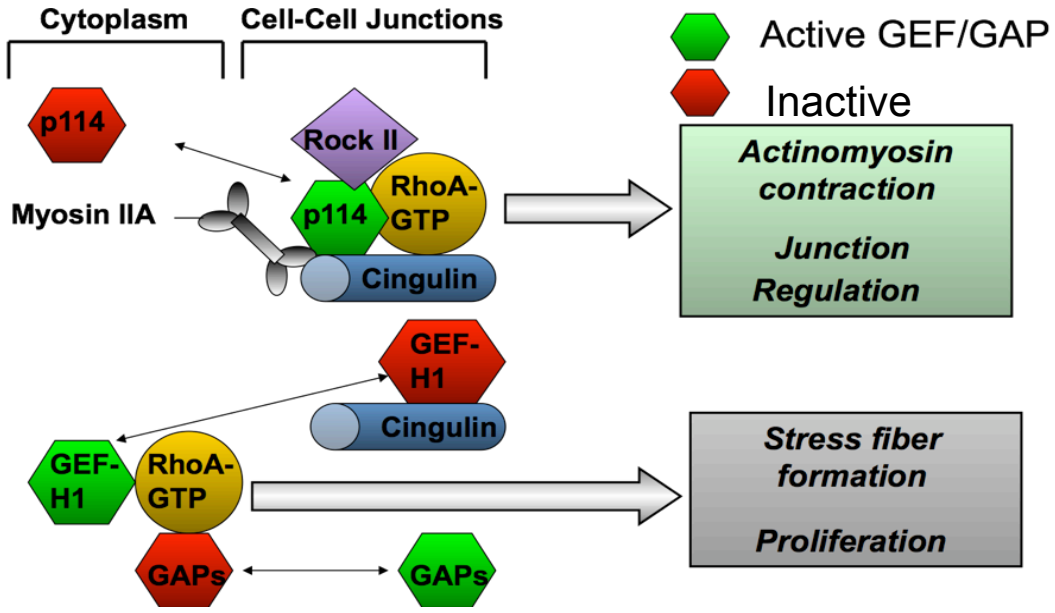

Figure 4.33 Regulation of epithelial morphogenesis by the reciprocal spatial activation of RhoA by two different Tight junction associated GEFs.

p114RhoGEF is recruited from an inactive state in the cytoplasm to TJs by the adaptor protein Cingulin as junctions are assembling, where p114RhoGEF forms a complex with Myosin IIA and the RhoA effector Rock II. p114RhoGEF activates RhoA leading to Myosin II activation and subsequently, ActinoMyosin contraction, thus driving junction formation and epithelial morphogenesis. GEF-H1 is also recruited to junctions by Cingulin as they are assembling, but is in a different complex to Cingulin /p114RhoGEF/ Myosin IIA and Rock II. GEF-H1 Guanine nucleotide exchange ability is inactived by its interaction with Cingulin. At low cell confluence, where junction are not established, GEF-H1 is active in the cytoplasm where it activates RhoA and contributes to stress fiber formation and proliferation. Certain junction associated GAPs, such as p190RhoGAP or Myosin IXb may also contribute to active levels of non-junctional RhoA activation.

CHAPTER 5

p114RhoGEF regulates cell migration

Chapter 5- p114RhoGEF regulates cell migration

Overview

Cell migration requires dynamic and spatially coordinated changes to the actin cytoskeleton and cell adhesion. RhoGTPases as important regulators of the cytoskeleton are crucial in coordinating cellular responses required for cell migration. Before cell migration occurs, cells have to first establish a front –rear asymmetry or polarise, this is then followed by membrane protrusion from the front leading edge and retraction at the trailing rear. This process occurs through the coordination of cytoskeletal dynamics and intergin mediated attachments to the substratum [315, 316].

Early studies demonstrated RhoGTPases Rac and Cdc42 function to produce different types of actin based protrusive membrane structures [144]. Active Rac is known to produce lamellipodia, a protrusive sheet like structure containing a mesh of branch like actin filaments, whereas active Cdc42 causes formation of filopodia, finger-like actin-rich protrusions. In contrast active RhoA leads to stress fibre formation and regulates actinomyosin contractility. This has lead to a generally proposed model that Cdc42 and Rac function at the leading edge to organise cell polarity, induce formation of lamellipodia in the formation of new adhesions to the substratum and RhoA functions towards the rear to mediate cell body contraction and tail detachment. However, recent studies using FRET based biosensors of active RhoGTPase have enabled insight into their spatial activation during cell migration [317]. Several of these studies suggest RhoA is

activated at the trailing end of migrating cells where it regulates cell body contraction and detachment of the trailing end, but may also play a role at the leading edge of cells [317] [318]. One of these studies[317] that employed simultaneous visulisation of active RhoA and Rac1 or RhoA and Cdc42, revealed that activation of RhoA was synchronous with leading edge extension and Cdc42 and Rac1 were found to be activated a short time after and 2μm behind the leading edge. Suggesting Rho has a role in the initial events of protrusion whereas Cdc42 and Rac1 function downstream of the initial burst of RhoA activation.

It is well established that GEFs are known to have important roles in activation of different RhoGTPases during cell migration For example the RhoA GEFs p115RhoGEF/lsc and GEF-H1 have both have been shown to regulate cell migration in neutrophills[319] and in HeLa cells [320] respectively. The Cdc42 GEF Pixα regulates directional cell migration in chemotaxic leukocytes [196] and Tiam - 1 and Dbs have recently been shown to regulate Neurotrophin-3-induced cell migration in Schwann cells [321] and in breast cancer epithelial cells through the activation of Cdc42 and Rac1[322]. This chapter contains some preliminary experiments that demonstrate p114RhoGEF regulates migration of HCE cells and could be important in cancer metastasis.

p114RhoGEF regulates cell migration in HCE cells

To test if p114RhoGEF functions in cell migration I performed wound healing assays in HCE cells depleted of p114RhoGEF by an siRNA pool or as a control transfected with non-targeting siRNA. I discovered p114RhoGEF depleted cells failed to close the wound, 7 hours after creating the wound (Figure 5.0- and 5.1). However, p114RhoGEF depleted cells did eventually close the wound after 24 hours suggesting that absence of p114RhoGEF causes cells to migrate significantly slower. I next tested if p114RhoGEF was upregulated in different breast cancer cell lines (Figure 5.2). Immunoblotting for p114RhoGEF in total cell lysates revealed p114RhoGEF to be highly expressed in MDA-MB231 cells, a tumour cell line that is completely dedifferentiated and known to be metastatic. However expression levels of p114RhoGEF were normal in MCF7 cells, derived from a benign and partially differentiated tumour and MCF10A cells, a non-cancerous partially differentiated cell line.

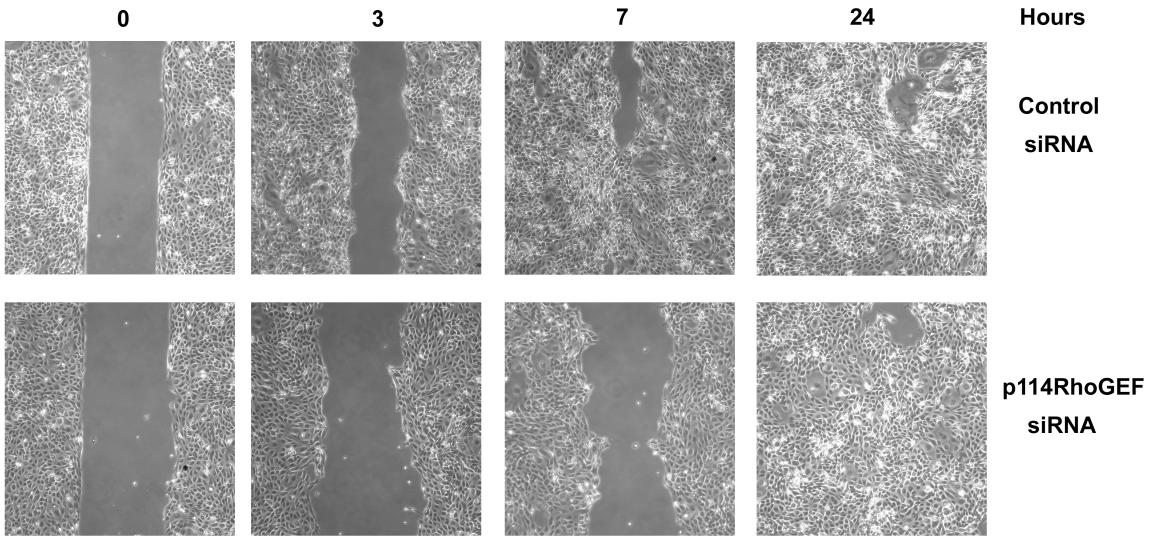

Figure 5.0 p114RhoGEF regulates cell migration during wound healing in HCE cells.

HCE cells depleted of p114RhoGEF or transfected with control on-targeting siRNA were cultured in a two chamber system until confluent. The chamber division was removed resulting in a defined cell free gap between the two monolayers. Cells were imaged 0 at 3, 7 and 24 hours after removal of the insert. Note p114RhoGEf depleted cells do eventually close the wound completely, but migrate at a slower rate.

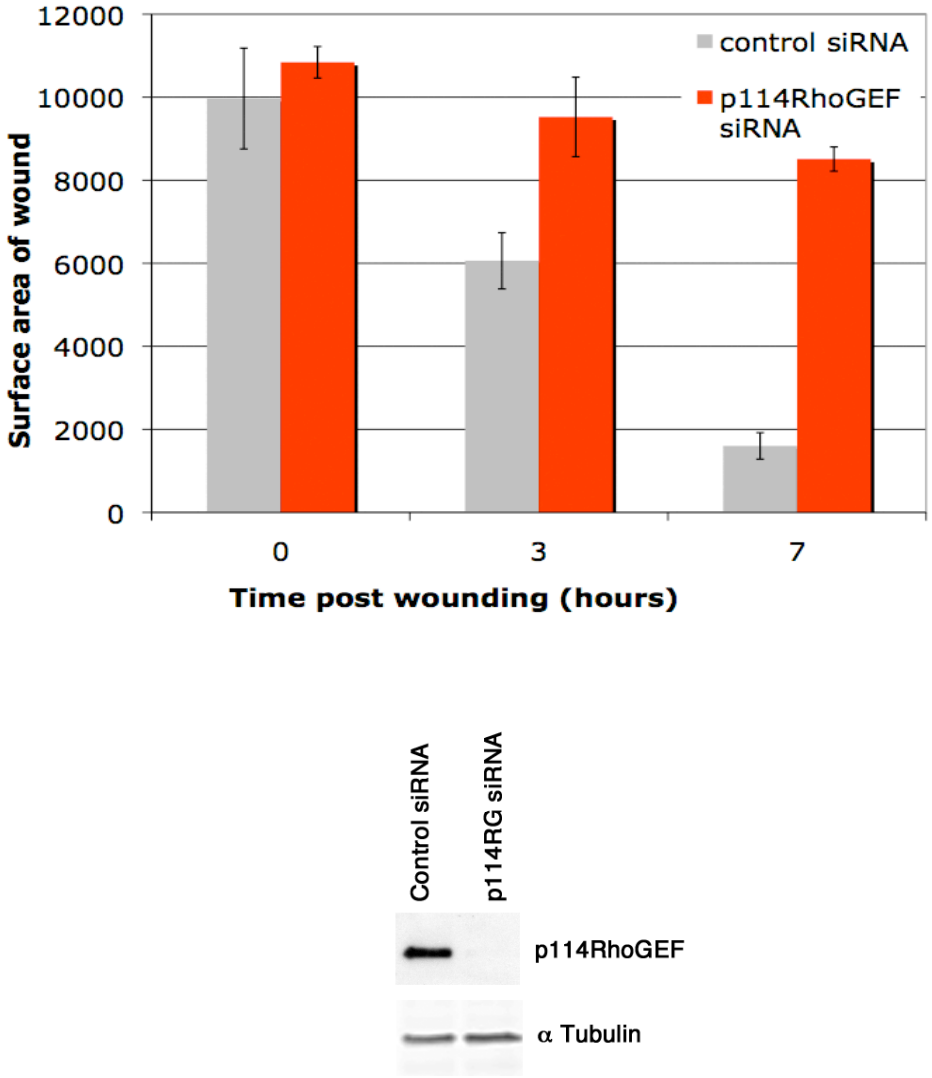

Figure 5.1 Quantification of wound healing in p114RhoGEF depleted HCE cells

From the images in figure 5.0, cell free areas were quantified at time points 0, 3 and 7 hours after removal of insert. Bars represent mean 3 experiments. Error bars +/-1 standard deviation. An Immunoblot was performed at the end of assay to observe p114RhoGEF levels, using α-tubulin as a control.

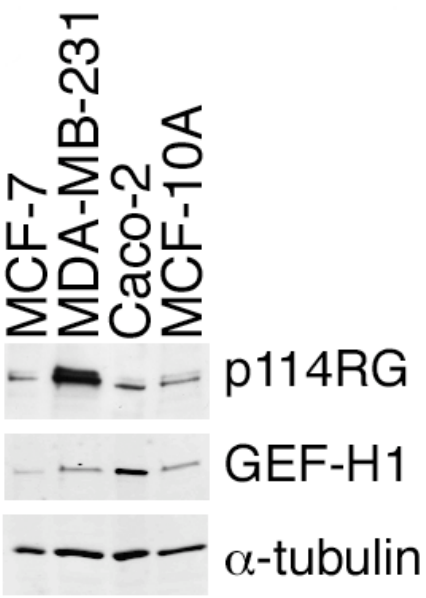

Figure 5.2 Expression levels of p114RhoGEF are upregulated in metastatic breast cancer cell lines.

Expression levels of p114RhoGEF were tested by Immunoblot, in different mammary epithelial cell types compared to caco-2 cells. MCF-7 are derived from a partially differentiated tumour, MDA-MB231 from a dedifferentiated and migratory tumour and MCF-10A from normal breast epithelium partially differentiated. Levels of GEF-H1 and α-tubulin were as measured. Note p114RhoGEF is greatly upregulated in metastatic tumour cell line MDA-MB-231.

As absence of p114RhoGEF causes HCE cells to migrate slower I investigated where p114RhoGEF localised in migrating HCE cells. I discovered 7 hours generating a wound, p114RhoGEF localised diffusely in the cytoplasm and at TJs as previously described (see Chapter 4), but interestingly, also to the tips of membrane projections of cells in front line of the migrating monolayer. E-Cadherin and ZO-1 were also present at the tips of these membrane projections in control and p114RhoGEF depleted cells. Absence of p114RhoGEF caused disruption of TJs as previously reported (see Chapter 4). However, some cells in the migrating monolayer were observed to have more long finger-like filopodia projections, perhaps indicating over activation of Cdc42.

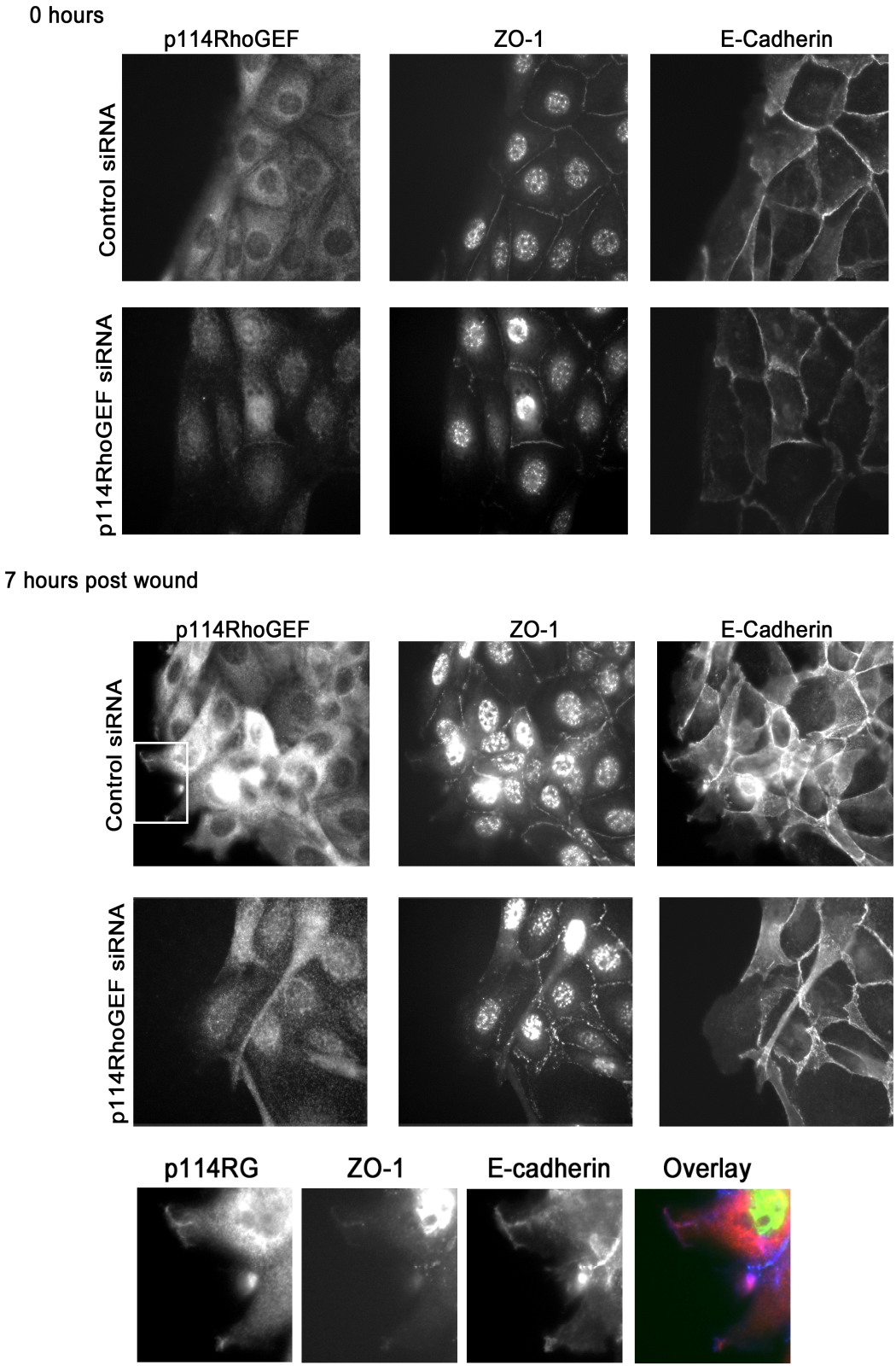

Figure 5.3 p114RhoGEF is localised to the leading edge of migrating HCE cells.

HCE cells depleted of p114RhoGEF for 72 hours were fixed after immediate removal or the chamber divider (0 hours top panel) and 7 hours after removal (bottom panel). Cells were immunostained with the indicated antibodies. Staining for p114RhoGEF was reduced in p114RhoGEF depleted cells, with cells having broken discontinuous ZO-1 distribution at junctions, as previously described. The bottom panel shows an enlarged area of marked by white box, and shows p114RhoGEF(red) is localized to the leading tips of cells, localizing with E-Cadherin (blue) and ZO-1 (green). Note in all images the wound was generated to the left of the monolayer.

Discussion

In this chapter I have discovered p114RhoGEF regulates migration of HCE cells. Evidence from breast cancer cells show expression levels of p114RhoGEF are normal in partially differentiated, normal and benign breast cancer epithelial cells. However, p114RhoGEF is highly overexpressed in a fully de-differentiated metastatic breast cancer cell line. This result correlates well with the data in migrating HCE cells during wound healing, suggesting p114RhoGEF may play an important role in migration and possibly invasion of breast cancer cells during cancer progression. Experiments involving RNAi mediated depletion and overexpression of p114RhoGEF during wound healing will need to be performed in different breast epithelial cells as well as invasion assays to further support this preliminary result. Moreover, it will be important to analyse p114RhoGEF expression in characterised cancer tissues to determine the pathological significance of its upregulation in a metastatic tumour cell line.

p114RhoGEF was discovered to localise to the tips of membrane projections of migrating HCE cells. The functional relevance for this localisation is currently unknown, but warrants further investigation, as E-Cadherin and ZO-1 also localised to membrane tips with p114RhoGEF. Interestingly a number of other studies have also identified junctional proteins such as ZO-1 the aPKC/PAR3/6 complex PatJ and Occludin at the leading edge of migrating epithelial cells during wound healing where they are known to regulate directional migration [323,

[324]. It will be interesting to test if p114RhoGEF colocalises with these components at the tips of membrane projections in HCEs and if depletion of p114RhoGEF or these components perturbs their or p114RhoGEF localisation at the leading edge.

RhoA was recently shown to be activated spatially at the leading edge of migrating cells [317, 318]. I have shown earlier that p114RhoGEF spatially activates RhoA at cell-cell contacts to drive junction formation. It could therefore be possible that p114RhoGEF spatially activates RhoA at the leading edge of migrating cells. A recent study has showed GEF-H1 is also localised to the leading edge of migrating cells where it to also spatially activates RhoA [320]. However, in this study, the spatial activation of RhoA after GEF-H1 depletion at the leading edge was examined in single randomly migrating HeLa cells. As HeLa cells are a highly transformed cancerous cell line that do not form junctions, it would be interesting to test if this result can be reproduced in a different non transformed epithelial cell type that form functional cell-cell junctions. It is intriguing to speculate if GEF-H1 together with p114RhoGEF forms part of the same RhoA signalling module or forms two distinct signalling modules to coordinate spatial activation of RhoA at the leading edge or towards the rear of migrating cells. It will also be interesting to monitor the spatial coordination of RhoA signalling by these two GEFs and the functional consequence of RhoA activation during migration during single cell migration and when cells are migrating in a monolayer during wound healing in a variety of epithelial cells types.

CHAPTER 6

Characterisation of cg10188 the putative p114RhoGEF ortholog in *Drosophila* development

Chapter 6 - Characterisation of cg10188 the putative p114RhoGEF ortholog in Drosophilla development

Overview

In this chapter I performed some preliminary experiments to investigate the function of the putative p114RhoGEF ortholog in *Drosophila* cg10188. I discovered that its absence causes lethality during development somewhere between embryogenesis and pupation. However, no effects on junction morphology were observed when cg10188 expression was ablated by RNAi in cells of larval imaginal discs.

Drosophila have just 7 RhoGTPases and 20 proteins that encode RhoGEFs and 22 RhoGAPs[325] compared to the 20 RhoGTPases and over 70 proteins that encode RhoGEFs and GAPs in mammals. However the ratio of GEFs or GAPs to RhoGTPases is still approximately 3:1 in both species, suggesting that RhoGTPases are still just as tightly regulated in *Drosophila*. Many *Drosophila* GEFs are larger than their mammalian orthologs. For example DRhoGEF2 the putative *Drosophila* ortholog of GEF-H1 contains a C1 domain followed by a DH and PH domains, but unlike GEF-H1 has a large N-terminal extension of approximately 1000 amino acids. This N-terminal extension contains a PDZ domain and an RGS like domain that is involved in binding to Gα subunits of heterotrimeric G proteins [326]. The mammalian GEFs PDZ-GEF, p115RhoGEF/lsc and LARG also contain RGS and or PDZ domains sharing

some identity to DRhoGEF2 [327]. DRhoGEF2 seems to be functionally analogous to GEF-H1 as its GEF activity is regulated by microtubule binding and it regulates processes requiring actinomyosin contractility via the activation of Rho1 the *Drosophila* ortholog of RhoA. [326] [328]. However DRhoGEF2 unlike GEF-H1 is known to be regulated by Concertina a Gα subunit of heterotrimeric G proteins [326] and therefore also shares functional orthology with p115RhoGEF, LARG and PDZ-RhoGEF, GEFs known to be regulated by Gα12 and Gα13 subunits of heterotrimeric G proteins. Thus, it appears that some GEFs in *Drosophila* are much larger and seem to be fusions of several mammalian GEFs, suggesting that a single GEF in *Drosophila* maybe performs the function of several different mammalian GEFs.

cg10188 was annotated in the *Drosophila* genome as being a putative ortholog of p114RhoGEF. I wanted to investigate how similar it was to p114RhoGEF orthlogs from different species. I aligned sequences annotated as being orthologs of p114RhoGEF in the genome sequence databases for different organisms, including the p114RhoGEF sequence of the human isoform 2, the isoform I have analysed in epithelial cells (Figure 6.0). There was a high degree of sequence conservation unsurprisingly around the DH and PH domains of all p114RhoGEF orthologs; however, the N-terminal and C-terminal regions were more divergent across species displaying less sequence identity. Indeed, the *Drosophila* ortholog, cg10188 was the most divergent having a large N terminal extension, of about 325 amino acids. The 325 extension however did not contain any known domains when run through the pfam

database. cg10188 displayed the least sequence identity to mammalian p114RhoGEF sequences, as expected from an organism more evolutionary distant to mammals.

Depletion of Cg10188 by RNAi during *Drosophila* development causes lethality

I was interested in exploring if cg10188 had a similar function to p114RhoGEF in *Drosophila*. I first tested the effect of loss of cg10188 has on fly development by using RNAi. I crossed flies that ubiquitously expressed GAL4 driven under an actin promoter and contained the CyO allele on a balancer chromosome (The CyO gene is used as a marker that produces flies with curly wings), with two different strains of fly that permitted expression of two different shRNA sequences against cg10188, under the control of a UAS element (Figure 6.1). GAL4 binds to UAS elements and activates transcription driving the expression of the shRNA and so drives cg10188 RNAi in the whole organism during development. All the progeny analysed from these crosses had the curly wing phenotype, indicating that cg10188 RNAi was lethal (Figure 6.1). The precise stage of development that is disrupted is not known, however no pupal cases were found that had flies arrested in development, suggesting development is affected somewhere between embryogenesis and larval pupation.

Based on the function of p114RhoGEF in cell junction formation and apical cell membrane constriction in mammalian cells, I hypothesised cg10188 might be

involved in developmental processes involving apical constriction. I decided to observe if cg10188 depletion by RNAi affected development of cell-cell junctions in larval imaginal discs, epithelial structures that require apical construction to bend and fold to undergo morphological changes to form eyes, antennae wings and legs in the adult fly. To investigate this I used a heat shock inducible GFP-flip-out clone system. This system allows cells that turn on cg10188 RNAi to be indentified by the lost of GFP expression (Figure 6.2). I discovered that depletion of cg10188 by RNAi did not disrupt cell-cell junctions in imaginal discs, a wing disc is shown as an example in Figure 6.3. Staining with armadillo (β-Catenin) and f-actin appeared normal in cells that had lost expression of GFP. The absence of a phenotype on junction morphology could be the result of inefficient suppression of cg10188 by RNAi, as discs were dissected only 48 hours after the induction of RNAi. Without an antibody to cg10188 it was impossible to confirm if cg10188 expression was reduced in GFP negative cells. However, areas of cells that had lost GFP expression, were quite small suggesting that cg10188 RNAi maybe inhibits proliferation or causes apoptosis.

p114 species alignment with D.melanogaster_Cg10188isoformA sequence

```
Homo_sapiens_isoform2              ------------------------------------------------
Canis_familiaris                   ------------------------------------------------
Mus_musculus                       ------------------------------------------------
Ornithorhynchus_anatinus           ------------------------------------------------
Galus_galus                        ------------------------------------------------
Xenopus_tropicalis                 ------------------------------------------------
Danio_rerio                        ------------------------------------------------
D_melanogaster_Cg10188isoform_     MDNAGEDSDNDVVTDFLNSNCSESSEALVNGGSTNRGASIESQNYCIPVI 50

Homo_sapiens_isoform2              ------------------------------------------------
Canis_familiaris                   ------------------------------------------------
Mus_musculus                       ------------------------------------------------
Ornithorhynchus_anatinus           ------------------------------------------------
Galus_galus                        ------------------------------------------------
Xenopus_tropicalis                 ------------------------------------------------
Danio_rerio                        ------------------------------------------------
D_melanogaster_Cg10188isoform_     NAPVPGPARAPIAPPPASNPASNTINNNNMIPTINVTPHSPALASKYNNI 100

Homo_sapiens_isoform2              ------------------------------------------------
Canis_familiaris                   ------------------MVTVGTNFLPSRPAVSANTVGEDAALS-RRIT 31
Mus_musculus                       ------------------------------------------------
Ornithorhynchus_anatinus           ------------------------------------------------
Galus_galus                        ------------------------------------------------
Xenopus_tropicalis                 ------------------------------------------------
Danio_rerio                        ------------------------------------------------
D_melanogaster_Cg10188isoform_     FEDTLSQLQNIRETVVQMKNSSSPSQHMQDGSLANHGLLSAAILSTSLPD 150

Homo_sapiens_isoform2              ------------------------------------------------
Canis_familiaris                   WRYKNSTARPRTALGLGAPTVNMGNTHSKSSDRDSALHGRPELSFYSSFP 81
Mus_musculus                       ------------------------------------------------
Ornithorhynchus_anatinus           ----------------GDPGVNMGNTNSKSSCRNNTIPGHPELSFYGSFS 34
Galus_galus                        ------------------------------------------------
Xenopus_tropicalis                 ------------------------------------------------
Danio_rerio                        ------------------------------------------------
D_melanogaster_Cg10188isoform_     LTGTGTGPASGGSNYAMWSSTAPQQCQFLHTDRRKSWTAVDDGSGAGDCT 200

Homo_sapiens_isoform2              ------------------------------------------------
Canis_familiaris                   RKWSENVFLDNELLTTKILSVLRPQSERGFR-------------PGHLRY 118
Mus_musculus                       ------------------------------------------------
Ornithorhynchus_anatinus           RKWNENVFLDNELLTSKILNVLRPHSERDLR-------------AGNLHC 71
Galus_galus                        -------------------------------------------------W 1
Xenopus_tropicalis                 ------------------------------------------------
Danio_rerio                        ------------------------------------------------
D_melanogaster_Cg10188isoform_     NKSVSLSSLDSEEQETIRVTEQRRRSARNSTGGISTHSLNEAELARDFER 250

Homo_sapiens_isoform2              ------------------------------------------------
Canis_familiaris                   PAHFLSTNSVFASVAASLKEHPRATLV-SDGSSALSRNVG---------- 157
Mus_musculus                       ------------------------------------------------
Ornithorhynchus_anatinus           PAHFLSTNSVFASVAASLKEQPRGSLLGSDGTPVVSRNVG---------- 111
Galus_galus                        LEQLCGTQS-----AASLKEQPRSLLLGPDGTPVLPRSLG---------- 36
Xenopus_tropicalis                 ------------------------------------------------
Danio_rerio                        ------------------------------------------------
D_melanogaster_Cg10188isoform_     IAAKRSLATEIISRIPLQKSISTSSIIAKEDIKAIARHLTDSEDENQSLL 300

Homo_sapiens_isoform2              ------------------------------MTVSQKGGPQPTPSPAGPGT 20
Canis_familiaris                   ------------------------------MTVSQKGGPQPAPSPVGTGT 177
Mus_musculus                       ------------------------------MTISQKGGLQPTPSPAGSGV 20
Ornithorhynchus_anatinus           ------------------------------MTVSQRGSPQSASNAAGTVN 131
Galus_galus                        ------------------------------MTIAQRGTSPSSFNTAGAVS 56
Xenopus_tropicalis                 ------------------------------------------------
Danio_rerio                        ------------------------------------------------
D_melanogaster_Cg10188isoform_     RAHAKIEVYDTVEKRPKRGSIFFRKKKPKAKTKSLVGGQLSACDVCGAAI 350

Homo_sapiens_isoform2              QLGPITGEMDEADSAFLKFKQ-----------TADDSLSLTSPNTESIFV 59
Canis_familiaris                   QLGPVTGEMDEADSVFLKFKQ-----------AADDSLSLTSSNAEPIFV 216
Mus_musculus                       RLGPIAGDMDEADSVFLKLKQ-----------TADDSLSLTSSNAESVFI 59
Ornithorhynchus_anatinus           RFGPITGEMDEADSGFIKLKQ-----------AADDSLSLVSSATETIFV 170
Galus_galus                        KFGLISGDMDEGDSGFIKFKQ-----------TSDDVVSLAPSTADSIFL 95
Xenopus_tropicalis                 ------------------------------------------------
Danio_rerio                        --------MDDID--YYRSKP-----------LAEESN-FQTTNYDAISI 28
```

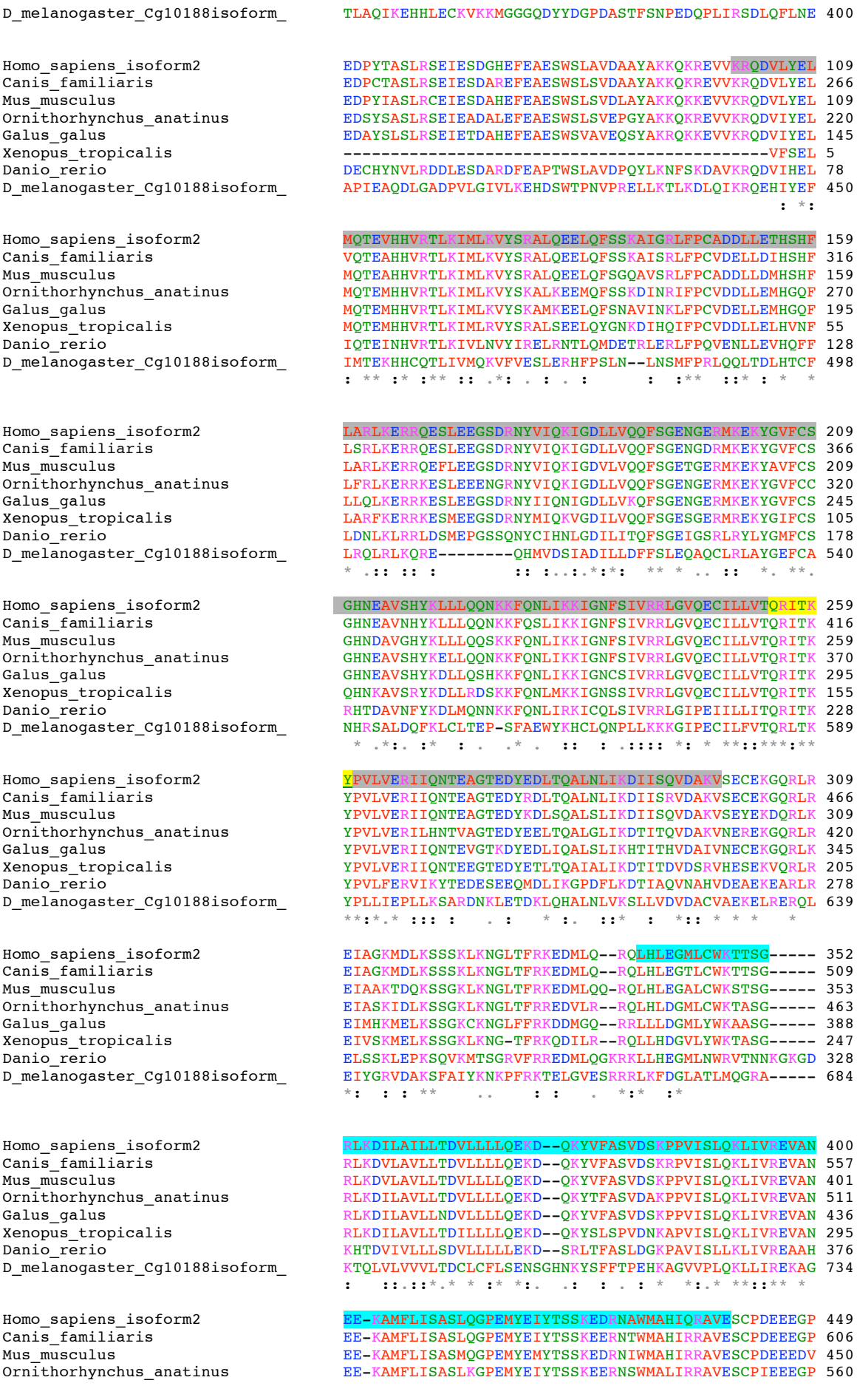
D_melanogaster_Cg10188isoform_ TLAQIKEHHLECKVKKMGGGQDYYDGPDASTFSNPEDQPLIRSDLQFLNE 400
Homo_sapiens_isoform2 EDPYTASLRSEIESDGHEFEAESWSLAVDAAYAKKQKREVVKRQDVLYEL 109
Canis_familiaris EDPCTASLRSEIESDAREFEAESWSLSVDAAYAKKQKREVVKRQDVLYEL 266
Mus_musculus EDPYIASLRCEIESDAHEFEAESWSLSVDLAYAKKQKKEVVKRQDVLYEL 109
Ornithorhynchus_anatinus EDSYSASLRSEIEADALEFEAESWSLSVEPGYAKKQKREVVKRQDVIYEL 220
Galus_galus EDAYSLSLRSEIETDAHEFEAESWSVAVEQSYAKRQKKEVVKRQDVIYEL 145
Xenopus_tropicalis ----------VFSEL 5
Danio_rerio DECHYNVLRDDLESDARDFEAPTWSLAVDPQYLKNFSKDAVKRQDVIHEL 78
D_melanogaster_Cg10188isoform_ APIEAQDLGADPVLGIVLKEHDSWTPNVPRELLKTLKDLQIKRQEHIYEF 450
Homo_sapiens_isoform2 MQTEVHHVRTLKIMLKVYSRALQEELQFSSKAIGRLFPCADDLLETHSHF 159
Canis_familiaris VQTEAHHVRTLKIMLKVYSRALQEELQFSSKAISRLFPCVDELLDIHSHF 316
Mus_musculus MQTEAHHVRTLKIMLKVYSRALQEELQFSGQAVSRLFPCADDLLDMHSHF 159
Ornithorhynchus_anatinus MQTEMHHVRTLKIMLKVYSKALKEEMQFSSKDINRIFPCVDDLLEMHGQF 270
Galus_galus MQTEMHHVRTLKIMLKVYSKAMKEELQFSNAVINKLFPCVDELLEMHGQF 195
Xenopus_tropicalis MQTEMHHVRTLKIMLRVYSRALSEELQYGNKDIHQIFPCVDDLLELHVNF 55
Danio_rerio IQTEINHVRTLKIVLNVYIRELRNTLQMDETRLERLFPQVENLLEVHQFF 128
D_melanogaster_Cg10188isoform_ IMTEKHHCQTLIVMQKVFVESLERHFPSLN--LNSMFPRLQQLTDLHTCF 498
Homo_sapiens_isoform2 LARLKERRQESLEEGSDRNYVIQKIGDLLVQQFSGENGERMKEKYGVFCS 209
Canis_familiaris LSRLKERRQESLEEGSDRNYVIQKIGDLLVQQFSGENGDRMKEKYGVFCS 366
Mus_musculus LARLKERRQEFLEEGSDRNYVIQKIGDVLVQQFSGETGERMKEKYAVFCS 209
Ornithorhynchus_anatinus LFRLKERRKESLEEENGRNYVIQKIGDLLVQQFSGENGERMKEKYGVFCC 320
Galus_galus LLQLKERRKESLEEGSDRNYIIQNIGDLLVKQFSGENGERMKEKYGVFCS 245
Xenopus_tropicalis LARFKERRKESMEEGSDRNYMIQKVGDILVQQFSGESGERMREKYGIFCS 105
Danio_rerio LDNLKLRRLDSMEPGSSQNYCIHNLGDILITQFSGEIGSRLRYLYGMFCS 178
D_melanogaster_Cg10188isoform_ LRQLRLKQRE--------QHMVDSIADILLDFFSLEQAQCLRLAYGEFCA 540
Homo_sapiens_isoform2 GHNEAVSHYKLLLQQNKKFQNLIKKIGNFSIVRRLGVQECILLVTQRITK 259
Canis_familiaris GHNEAVNHYKLLLQQNKKFQSLIKKIGNFSIVRRLGVQECILLVTQRITK 416
Mus_musculus GHNDAVGHYKLLLQQSKKFQNLIKKIGNFSIVRRLGVQECILLVTQRITK 259
Ornithorhynchus_anatinus GHNEAVSHYKELLQQNKKFQNLIKKIGNFSIVRRLGVQECILLVTQRITK 370
Galus_galus GHNEAVSHYKDLLQSHKKFQNLIKKIGNCSIVRRLGVQECILLVTQRITK 295
Xenopus_tropicalis QHNKAVSRYKDLLRDSKKFQNLMKKIGNSSIVRRLGVQECILLVTQRITK 155
Danio_rerio RHTDAVNFYKDLMQNNKKFQNLIRKICQLSIVRRLGIPEIILLITQRITK 228
D_melanogaster_Cg10188isoform_ NHRSALDQFKLCLTEP-SFAEWYKHCLQNPLLKKKGIPECILFVTQRLTK 589
Homo_sapiens_isoform2 YPVLVERIIQNTEAGTEDYEDLTQALNLIKDIISQVDAKVSECEKGQRLR 309
Canis_familiaris YPVLVERIIQNTEAGTEDYRDLTQALNLIKDIISRVDAKVSECEKGQRLR 466
Mus_musculus YPVLVERIIQNTEAGTEDYKDLSQALSLIKDIISQVDAKVSEYEKDQRLK 309
Ornithorhynchus_anatinus YPVLVERILHNTVAGTEDYEELTQALGLIKDTITQVDAKVNEREKGQRLR 420
Galus_galus YPVLVERIIQNTEVGTKDYEDLIQALSLIKHTITHVDAIVNECEKGQRLK 345
Xenopus_tropicalis YPVLVERIIQNTEEGTEDYETLTQAIALIKDTITDVDSRVHESEKVQRLR 205
Danio_rerio YPVLFERVIKYTEDESEEQMDLIKGPDFLKDTIAQVNAHVDEAEKEARLR 278
D_melanogaster_Cg10188isoform_ YPLLIEPLLKSARDNKLETDKLQHALNLVKSLLVDVDACVAEKELRERQL 639
Homo_sapiens_isoform2 EIAGKMDLKSSSKLKNGLTFRKEDMLQ--RQLHLEGMLCWKTTSG----- 352
Canis_familiaris EIAGKMDLKSSSKLKNGLTFRKEDMLQ--RQLHLEGTLCWKTTSG----- 509
Mus_musculus EIAAKTDQKSSGKLKNGLTFRKEDMLQQ-RQLHLEGALCWKSTSG----- 353
Ornithorhynchus_anatinus EIASKIDLKSSGKLKNGLTFRREDVLR--RQLHLDGMLCWKTASG----- 463
Galus_galus EIMHKMELKSSGKCKNGLFFRKDDMGQ--RRLLLDGMLYWKAASG----- 388
Xenopus_tropicalis EIVSKMELKSSGKLKNG-TFRKQDILR--RQLLHDGVLYWKTASG----- 247
Danio_rerio ELSSKLEPKSQVKMTSGRVFRREDMLQGKRKLLHEGMLNWRVTNNKGKGD 328
D_melanogaster_Cg10188isoform_ EIYGRVDAKSFAIYKNKPFRKTELGVESRRRLKFDGLATLMQGRA----- 684
Homo_sapiens_isoform2 RLKDILAILLTDVLLLLQEKD--QKYVFASVDSKPPVISLQKLIVREVAN 400
Canis_familiaris RLKDVLAVLLTDVLLLLQEKD--QKYVFASVDSKRPVISLQKLIVREVAN 557
Mus_musculus RLKDVLAVLLTDVLLLLQEKD--QKYVFASVDSKPPVISLQKLIVREVAN 401
Ornithorhynchus_anatinus RLKDILAVLLTDVLLLLQEKD--QKYTFASVDAKPPVISLQKLIVREVAN 511
Galus_galus RLKDILAVLLNDVLLLLQEKD--QKYVFASVDSKPPVISLQKLIVREVAN 436
Xenopus_tropicalis RLKDILAVLLTDILLLLQEKD--QKYSLSPVDNKAPVISLQKLIVREVAN 295
Danio_rerio KHTDVIVLLLSDVLLLLLEKD--SRLTFASLDGKPAVISLLKLIVREAAH 376
D_melanogaster_Cg10188isoform_ KTQLVLVVVLTDCLCFLSENSGHNKYSFFTPEHKAGVVPLQKLLIREKAG 734
Homo_sapiens_isoform2 EE-KAMFLISASLQGPEMYEIYTSSKEDRNAWMAHIQRAVESCPDEEEGP 449
Canis_familiaris EE-KAMFLISASLQGPEMYEIYTSSKEERNTWMAHIRRAVESCPDEEEGP 606
Mus_musculus EE-KAMFLISASMQGPEMYEMYTSSKEDRNIWMAHIRRAVESCPDEEEDV 450
Ornithorhynchus_anatinus EE-KAMFLISASLKGPEMYEIYTSSKEERNSWMALIRRAVESCPIEEEGP 560

```
Galus_galus                      EE-KAMFLISASLQGPEMYEIHTSSKEERNSWMAHIRRAVESCPDEEGGS 485
Xenopus_tropicalis               EE-KAMFLISASNTGAEMYEIHTNSKEERNFWMNIIRGAVESCPVQDAEI 344
Danio_rerio                      NE-KAMFLISASLDTPEMYEFHTSSAEERNTWTNKIWKAVECCPDVKE-- 423
D_melanogaster_Cg10188isoform_   TESRGIYIISSNPDFPEMYELKVQTPKDKNTWIQTIRQAVLDCPATDIIE 784
                                  * :.:::**:.   .****: ..: :::* *   *  **  **  .

Homo_sapiens_isoform2            FSLPEEERKVVEARATRLRDFQERLSMKDQLIAQSLLEKQQIYLEMAE-M 498
Canis_familiaris                 FSEAEEEKKGLEARALRLRDFQERLNVKDQQIAQSLGEKQQIYLEMAE-M 655
Mus_musculus                     FSEAEE-KKIAEARTMKLQEFQERLSLKDQLIAQSLLEKQQIYLEMAQ-L 498
Ornithorhynchus_anatinus         LAGLEEDRKIAEMRAAKLKEFQERLSVKDNAIAQSLYEKQQIYLEMLE-M 609
Galus_galus                      FYEPETERRMAEARAAKLREFQERLNTKDDLIVQSLTEKQQIYQEMSE-V 534
Xenopus_tropicalis               LNEAEEEKKLFTERAAKIKEFQERLNQKDYVIVQSLNEKLQTCMEMAE-L 393
Danio_rerio                      --------EEPEELSKKIWEFQRKLCVHDASIEQHLTEKLKLFSSIAASV 465
D_melanogaster_Cg10188isoform_   AEDLTAEEKLRIG--VNKRETIEKMRQKDIEQALLLEEKLMLQFNLLKEQ 832
                                         .       .  :  .::  :*      * **     .:

Homo_sapiens_isoform2            GGLEDLPQ---PRGLFRGG-DPSETLQGELILKSAMSEIEGIQSLICR-R 543
Canis_familiaris                 SGLEDVAQ---SRLLFRGG-DPSETMQGEQILKSAMSEIEDIQTLICR-Q 700
Mus_musculus                     SGLEESAQ---NRGLFRGGGDPSETLRGEQILRSAMSEIEGIQSLICQRH 545
Ornithorhynchus_anatinus         SGFEDPPQGPRSKLLFRSG-EPLENLQGEMILKSAVTEIEYLQNLICK-H 657
Galus_galus                      YGFEDHSQG--SRSRLLLG-DIPESLQGEALLKSAVVEAENLQNLIFT-H 580
Xenopus_tropicalis               YGYEDLPQE--PRITLLPRAETGENLEGKGILHSAVTILESEQSLCPAQE 441
Danio_rerio                      TGVSDTSTS--ERHPLRGN--AAEPLQGERLLTGALKDVENLQNLLVMCE 511
D_melanogaster_Cg10188isoform_   QPFGDVAG----TNSSCSAANFLAAFGSYKDLVSADCDTAELWRRVLNTV 878
                                     : .                 : .   * .*

Homo_sapiens_isoform2            LGSANGQAEDGGSSTGPPRRAETFAGYDCTNSPTKNGSFKKKVSSTDPRP 593
Canis_familiaris                 LGSANGQAEDAGGSSGLPRRAETFGGYDTVSSPSKNGILKKTCSS-DPSP 749
Mus_musculus                     LGSTSSQVEEGSVSAGLPRRAETFGGYDSVGSPSKGGSFKRKVSNSDLRP 595
Ornithorhynchus_anatinus         LANANYHSEDGSGYSLLPRRAETFGGYDSSTNTNKNGSFKKKVCSSDPRL 707
Galus_galus                      LGNGSCQSEE-SYAAGLPRRAETFGGYDSPSISNRNNSLGKSGGS-DQRQ 628
Xenopus_tropicalis               AGHNKKEQFGSSSTGYTPSRRSLGARLQRLDNPKAKSSKRRAPSPSDEES 491
Danio_rerio                      QGPTP---FTSRATDLVLKKPHAVTGLENNTHMLPENGFESSMESMGDRI 558
D_melanogaster_Cg10188isoform_   QDISQLASTIYSAATGQPVPRTLSSVGEKQSEQYASPTLPKRAETFAGFD 928
                                                         :

Homo_sapiens_isoform2            RDWRGPPN--SPDLKLSDSDI-PGSSEESPQVVEAPGTESDPRLPTVLES 640
Canis_familiaris                 RDWQGPVS--SPDLKPSNT---LGASEEAPPAGPVPGADCGPHLPAVLEL 794
Mus_musculus                     QDWQGPAS--SPDSRPCDNSAPSGCCEESPQAVEMPSTES---LPTVLEL 640
Ornithorhynchus_anatinus         KDWRSPLT--SSDSQLCDLP---GDSEEGLSTADITRPDYSSSLPATLES 752
Galus_galus                      WDWRGPAV--SSDVQLPDLP---VDAEEGSQTSDTTRQDDSSGIQPTIES 673
Xenopus_tropicalis               EDYSRAPSPILPEPNLSEGELSGSSSDQEGNKPSKHSFEAVDTLISSVLET 541
Danio_rerio                      QVANTDLDPQLRELHLSENQ---ELSADENLSVHFP------------KA 593
D_melanogaster_Cg10188isoform_   EKRGKLASKLVLTPRLQELEEKREPKSGSSSVSEQP------------L 965
                                              .  :                .

Homo_sapiens_isoform2            ELVQRIQTLSQLLLNLQAVIAHQDSYVETQRAAIQEREKQFRLQSTRGNL 690
Canis_familiaris                 ELVQRIQTLSQLLLSLQAVIAQQDSYVEMQRASIQEREKQLRLQSTRGNM 844
Mus_musculus_isoform1            ELVHRVQTLSQLLLSLQAVIAQQDSYVEMQRTAIQEREKQFRLQSTRGNL 690
Ornithorhynchus_anatinus         ELVQRIQTLLQLLLNLQAVIVHQDSYIENQRAITIEREKLYRLQSTRGNF 802
Galus_galus                      QLVQRIQTLLQLLFSLQAVISQQDSYIEVQRATMVDREKQYRLQSTRGNV 723
Xenopus_tropicalis               LHLQEPETNVMLLLFMQAVISQQDSYVEVQ----KEREKQFRQQSSRGNM 587
Danio_rerio                      EFYSTVSQLSRKLYSLQSVVQQLESHIKVQHATIEELK-----SRPRGNS 638
D_melanogaster_Cg10188isoform_   ENNYAVLQVTHHLQTLLCVISQQMTTINNLQ---------------LQLA 1000
                                              *  : .*: :  : ::

Homo_sapiens_isoform2            LLEQERQRNFEKQREERAALEKLQSQLRHEQQRWERERQWQHQELERAGA 740
Canis_familiaris                 LLEQERQRNFEKQREELAG------------------------------- 863
Mus_musculus                     LLEQERQRNFEKQREERAGVEKLQSQLRQEQQRWERERARQQQELELAGA 740
Ornithorhynchus_anatinus         LLEQEKQRNFEKQREELANMQKIQNQLKQEQQRWERERDRQQKELEYTEA 852
Galus_galus                      LLEQEKQRNFEKQREELMNVQKLQSQLKLEQQRWERERSQQQRELEISEA 773
Xenopus_tropicalis               LLEQEKQRNFEKQREELGNVQKMQDQLRLEKQKWERERERQQREAEAMEN 637
Danio_rerio                      LLEQEKHRNLHKQNEELANFQRLQNQRLQEQRQWEQERERQMLQAEAREK 688
D_melanogaster_Cg10188isoform_   LYRESPRSSAYTHKDQLEELRNLQDKQQEEKTAWQRQLKQQQEE------ 1044
                                 * .:. : .  .:.::

Homo_sapiens_isoform2            RLQEREGEARQLRERLEQERAELERQRQAYQHDLERLREAQRAVERERER 790
Canis_familiaris                 ------------------------RRAYQHDLERLREAQRAVERERERQ 887
Mus_musculus                     RLQEREGEARQMRQRLDQERTELERQRQAYQHDLERLREAQRAVDRERER 790
Ornithorhynchus_anatinus         RLQEQESESRQLRERLNQERREELDRQREAYQHDLERLRESQRAVEKEKER 902
Galus_galus                      HLQRREEETRQLKDKLIQDRKELERQREAYQHDLERLREAQRAVEKERER 823
Xenopus_tropicalis               MLRQRMGDSELQLQKLHQERDELEAQRKEYQHDLERLRESQKAVEKDRER 687
Danio_rerio                      ELRERERMACSRQEEMLAGEKQELARCREEYQQDLERLRESMRSVEKEKEK 738
D_melanogaster_Cg10188isoform_   -LAEMRAQQLQLQKQIKAEQEDVRQQREQLYKKMELLSSQGLLLSPSTP- 1092
                                              *.   :.:* * .    :. .
```

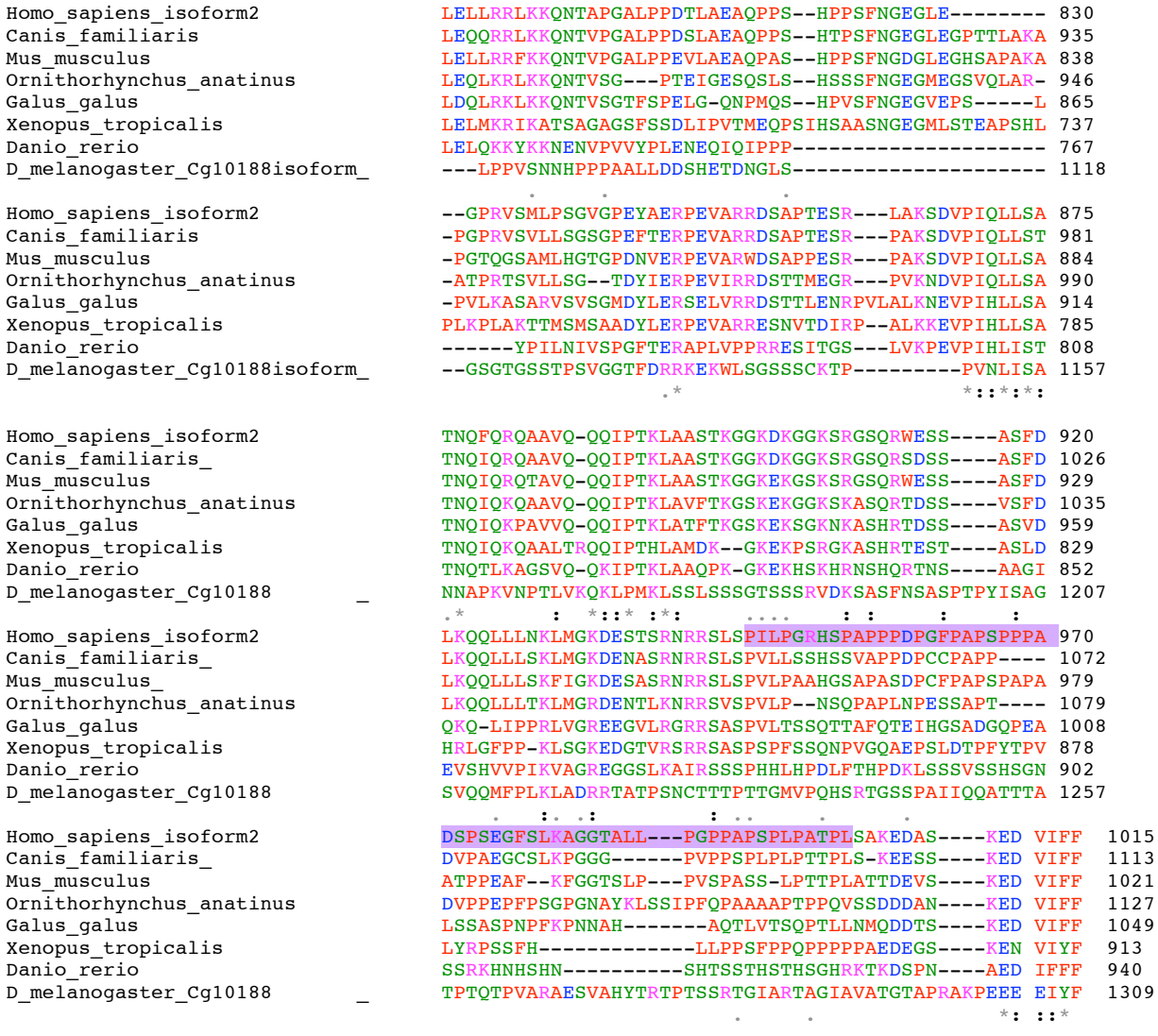

Figure 6.0 Sequence alignment of p114RhoGEF orthologs

Sequence alignment of human p114RhoGEF isoform 2 against orthologues of p114RhoGEF from other species, including the putative p114RhoGEF ortholog *cg10188* from *Drosphophila melanogaster*. In the human isoform 2 the DH domain is highlighted in grey, also highlighted in yellow within the DH domain is a conserved QRITKY motif present in all Dbl GEFs. The PH domain and proline rich regions are highlighted in light blue and purple respectively. *Homo sapiens isoform 2 Q6ZSZ5-2, Canis familiaris XP_854251, Mus musculus Q6P9R4, Ornithorhynchus anatinus(platapus*) (Ensembl), *Galus galus XP_418249.2, Xenopus tropicalis ENSXETP00000014110* (Ensembl) , *Danio rerio Q6NSP2, Drosphophila melanogaster Q9VIV.*

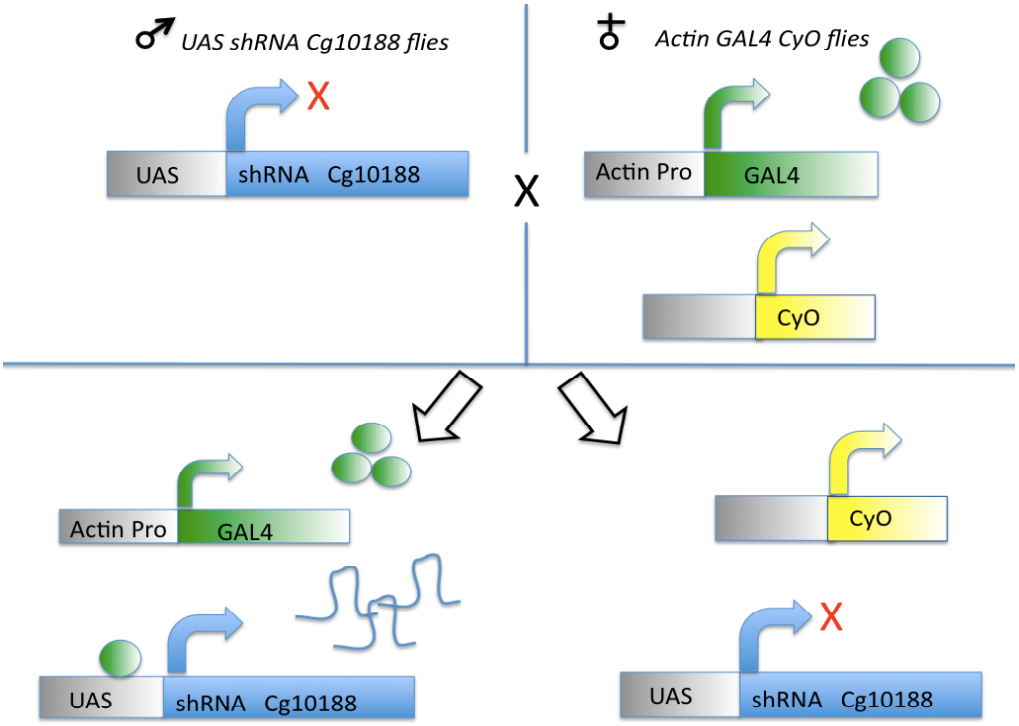

		Virgin female flies	w;Actin;GAL4/CyO			
		Chromosome	x	x	II^1	II^2
		Genetic element	w	w	Actin/ GAL4	CyO
male flies	Chromosome					
UAS-RNAi	x	\	w	w	\	\
	y	\	w	w	\	\
	II^1	UAS RNAi	\	\	UAS RNAi/Actin/GAL4	UAS RNAi/CyO
	II^2	UAS RNAi	\	\	UAS RNAi/Actin/GAL4	UAS RNAi/CyO

Figure 6.1 Depletion of cg10188 by RNAi in during development causes lethality.

Male flies containing shRNA to cg10188 driven under the control of a UAS promoter (UAS-RNAi), present on chromosome II were crossed with virgin female flies containing ubiquitously expressed GAL4 driven from an actin promoter Actin/GAL4 on chromosome II^1 . The CyO gene was present on a balancer chromosome II^2. . The resulting crosses only produced flies that all had the CyO phenotype (highlighted in yellow in table) of curly wings, indicating that files depleted of cg10188 by GAL4 dependent expression of cg10188 shRNA and causes lethality. All pupal cases observed were empty indicating that lethality occurs at any stage before pupal development. The experiment was repeated twice using two different UAS-shRNA cg10188 flies stocks containing different cg10188 specific shRNA sequences both located on chromosome II.

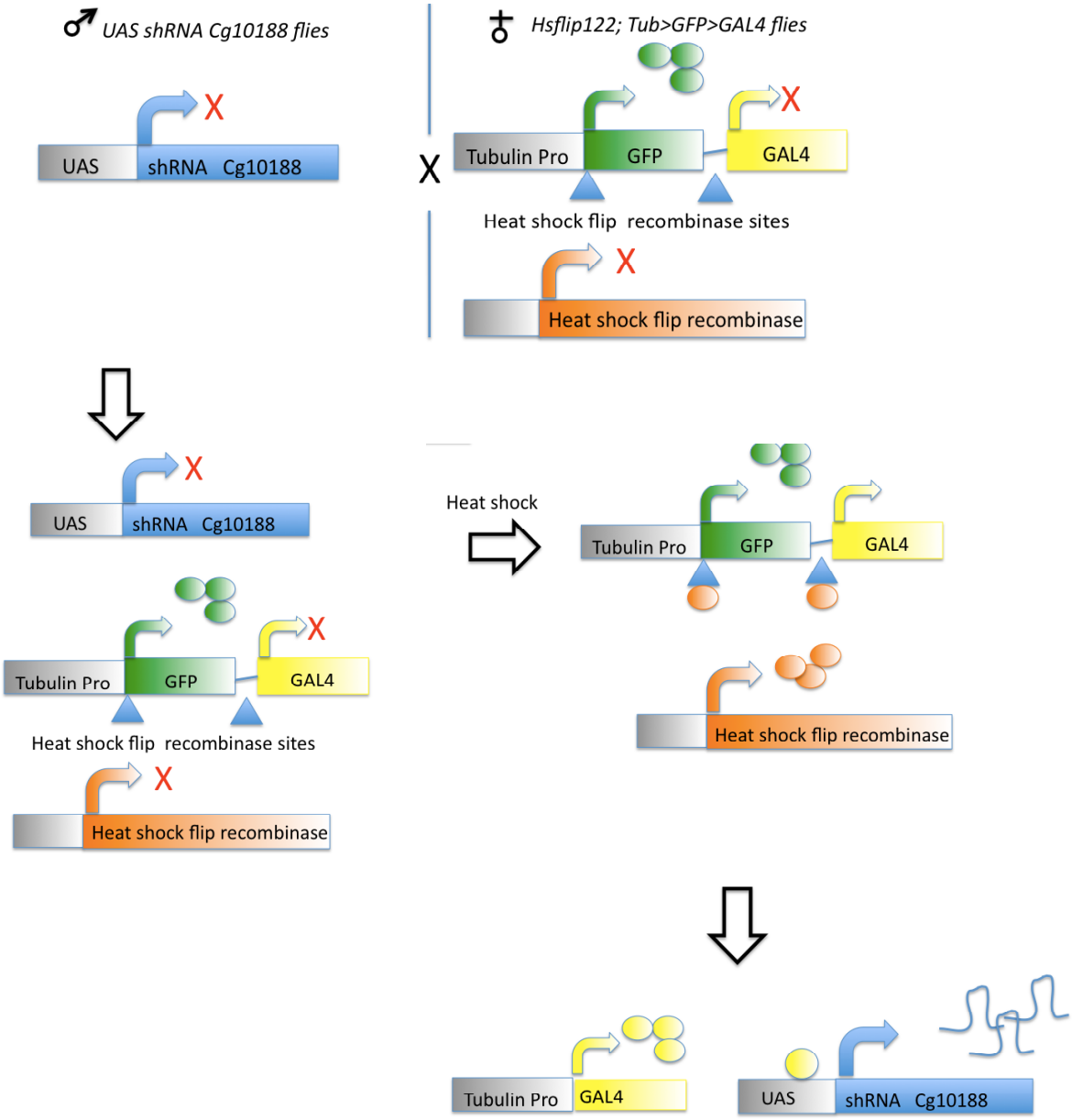

Figure 6.2 Generation of Heat shock recombinase GFP flip-out clones.

Male flies containing shRNA to cg10188 under the control of a UAS promoter were crossed with virgin female flies containing a heat shock inducible flip recombinase and expressing GFP from a minimal tubulin promoter. GFP is flanked by heat shock flip recombinase sites (blue triangles) and one of these contains a stop codon to prevent expression of GAL4. The larval progeny of this cross were heat shocked at 37°C to induce the expression of heatshock flip recombinase that causes the excision "flipping out" of GFP while simultaneously switching on ubiquitous expression of GAL4, which drives expression of shRNA to cg10188. This system produces tissues that have a mosaic expression pattern of GFP, where some cells have retained GFP expression and so do not express shRNAs, whereas some have lost GFP and express shRNAs that mediate the repression of target gene by RNAi, in this instance cg10188.

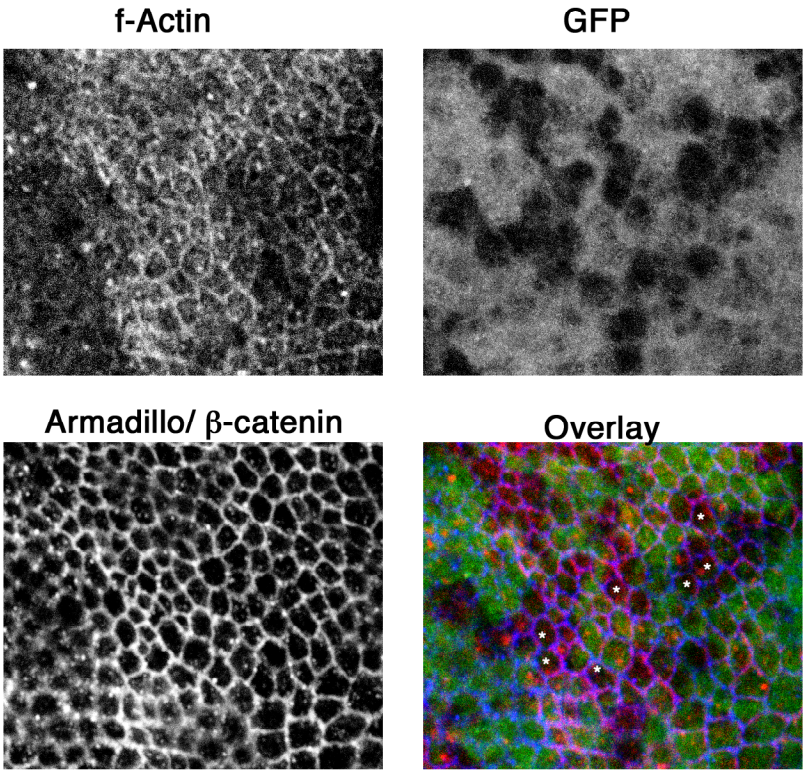

Figure 6.3 Absence of cg10188 in imaginal discs does not cause disruption of Adherens junctions or effect junctional actin organisation.

Imaginal wing discs were dissected from fly larva containing a UAS driven shRNA specific for cg10188 and a heat shock inducible flip recombinase and GFP/GAL4. Larvae were heat shocked at 37°C for 30 minutes to induce flip recombinase expression causing the excision of GFP and the expression of GAL4 to drive shRNA expression. Imaginal discs were dissected 48 hours post heat shock and immunostained for f-actin (red) and Armadillo (blue) GFP (green). Shown is a maximum intensity projection several confocal sections of the apical membrane of a section of wing disc. Cells marked with asterisk show a subset of examples where GFP expression is lost and shRNA cg10188 expression is switched on. Note no morphological changes are observed in Adherens junctions or junctional actin organisation.

Discussion

Investigation of the function of the putative p114RhoGEF ortholog in *Drosophila* cg10188 revealed its depletion by RNAi during development causes lethality. It was not determined exactly at which stage of development lethality occurred, but by the observation that no pupal cases were found occupied by flies arrested in development, indicates development is effected somewhere between embryogenesis and just before larval pupation. It will need to be investigated to find the precise stage of development affected by repeating this experiment on a larger scale to identify the defect(s) at different larval developmental stages. However, this is not conclusive data as all shRNAs have different non- specific off target effects that cannot be ruled out from this experiment. Both shRNAs sequences for cg10188 have a 19 base pair region of identity to cg15336 (VDRC database) a gene encoding a small zinc binding protein containing a C2H2 like zinc finger protein domain and therefore cg10188 shRNA could also effect cg15336 expression causing the observed lethal phenotype. Rescue by overexpression of RNAi resistant cg10188 or P-element mediated disruption of cg10188 expression will be required to support this evidence to exclude off target effects.

The absence of any phenotype in imaginal discs on junction morphology upon stimulation of cg10188 RNAi was surprising based on its lethality when cg10188 RNAi is constitutively expressed. However, areas of GFP negative cells were small suggesting that cg10188 RNAi could prevent proliferation or induce apoptosis, this will require further investigation, such as staining with markers for apoptosis (caspases). The lack of any obvious phenotype could be explained by insufficient

suppression of cg10188, as dissection was performed just 48 hours after induction of RNAi, which may not be a sufficient amount of time to allow full repression of cg10188. Overexpression of dicer an important component of the RNAi machinery [329] could increase the efficiency of RNAi in flies. The experiment could therefore be repeated in UAS-*dicer* flies that overexpress dicer under a UAS promoter to enhance the efficiency of cg10188 RNAi. Future experiments will be required to investigate if cg10188 is expressed in the imaginal discs by performing in situ hybridisation experiments and eventually developing an antibody to confirm if cg10188 protein is expressed and observe its subcellular localisation in imaginal discs and or other tissues.

Final discussion

RhoGTPases are small molecular switch proteins that are important regulators of the cytoskeleton and modulators of gene expression. RhoGTPases have thus been identified as being major signalling components associated with junctions (see Chapter 1 Pages 56-68). An important question I asked at the start of this project is how are RhoGTPases regulated to control junction formation and gene expression in the human corneal epithelium? To investigate this question I used a siRNA screening approach combined with functional assays to observe junction morphology and gene expression. This enabled the identification of components of RhoGTPase signalling that affected junction assembly and modulated NF-κB mediated gene expression in HCE cells.

Regulators and effectors of RhoGTPases that regulate junction morphology and modulate NF-κB mediated gene expression

I discovered that the RhoGTPases Cdc42 and RhoA are key regulators of junction morphology in HCE cells. I validated candidates that had various effects on junction morphology by observing if the same phenotype on junction formation could be reproduced with individual siRNAs derived from the deconvolution of the siRNA pool used in the primary screen into four different individual siRNAs. Several of the candidates chosen for validation were not identified in the primary screen in HCE cells as having any effect on junction morphology, but were discovered to have effects in a parallel screen performed in Caco-2 cells (Matter 2007 unpublished

results). These candidates were subsequently validated along with a subset of candidates identified in the primary screen to give a final total of 14 validated candidates that had effects on junction morphology in HCE cells (Chapter 3 Table 3.2). The 14 validated candidates is by no means a comprehensive list of all regulators and effectors of RhoGTPases that may potentially regulate junction formation in HCE cells as many more might have effects on junction morphology. One of the limitations of the siRNA screen is there is no guarantee that there is efficient knockdown of all target proteins. Different proteins will have different half-lives to each other, some will be more stable or the same protein may have an increased half-life and so be more stable when it is in a complex with different proteins. It might be interesting to repeat the siRNA screen with all the candidates that did not show any effect on junction morphology by disrupting cell-cell junctions after siRNA transfection. Transfecting cells with siRNAs the day after plating as before then allowing junctions to form for several days then disrupting cell-cell junctions by trypsinising with EDTA before re-plating and performing the analysis when junctions have reformed again. Disrupting cell-cell junctions after transfection of siRNA may increase the efficiency of depletion of the target protein and therefore decrease their stability and permit the identification of additional target proteins.

Many of the validated candidates identified were either GEFs and GAPs or downstream effectors of Cdc42 and or RhoA. This result correlates well with RhoA and Cdc42 having the most disruptive effects on junction formation and polarity and supports many previous studies in different cell types of the importance of these two RhoGTPases in the regulation of junctions [4, 206, 221, 245, 330]. The initial aim of this project was to fully characterise several of these validated candidate proteins and to

investigate the molecular mechanisms of how they modulate Rho signaling to regulate junction formation. One of these candidates p114RhoGEF was fully charaterised and shown to drive junction formation by activating RhoA in a spatially restricted manner (see Chapter 4). However, due to the time constraints and resources allocated to this project only p114RhoGEF could be investigated in depth. A future long-term aim is to perform a detailed analysis on a number of other candidates investigating which RhoGTPase signaling pathways they modulate, where they spatially activate RhoGTPases during junction formation and what are the downstream functional consequences of this activation on cell-cell adhesion.

In addition to candidates identified that affected junction morphology a number of components that potentially regulate NF-κB activity were also indentified in HCE cells. As the screen was performed in the presence of serum, which causes constitutive NF-κB activity I felt candidates that produced inhibitory effects, rather than stimulatory effects maybe more valid to study. The data from this NF-κB activity screen was plotted with data from the junction morphology screen and revealed a number of candidates (MAP4K1, RacGAP1 and OBSCN MCF2L(Dbs) and RhoBTB1) that had a strong inhibitory effect on NF-κB reporter activity, as well as having an effects on junction morphology. However due to limited time for this project none of these candidates were validated by repeating the NF-κB reporter activity using individual siRNAs. Future experiments will focus on validating this subset of candidates and also performing a further siRNA screens to look for RhoGTPase signaling components that regulate β-Catenin/TCF mediated gene expression. These future experiments will hopefully indentify novel RhoGTPase

signaling pathways that link intercellular cell-cell junctions to NF-κB and β-Catenin/TCF regulated gene transcription to orchestrate different epithelial cell processes, such as proliferation, cell survival, EMT and pro-inflammatory signalling.

p114RhoGEF drives junction formation and epithelial morphogenesis via the spatially restricted activation of RhoA

In this study I fully characterised p114RhoGEF, a candidate that was validated from the siRNA for junction assembly (See Chapter 4). I discovered p114RhoGEF is a novel TJ associated activator of RhoA that regulates epithelial differentiation, barrier formation and epithelial morphogenesis. I demonstrated p114RhoGEF spatially activates RhoA at cell-cell contacts activating junctional actinomyosin contractility a process that is essential for driving junction formation. I discovered mechanistic evidence for p114RhoGEF being part of a junction-associated Rho signalling module by p114RhoGEFs association with a complex containing Myosin II, Rock II and the junctional adaptor protein Cingulin. I showed the formation of this complex is dependent on the assembly of cell-cell junctions and the junctional adaptor Cingulin is required for efficient recruitment of p114RhoGEF to cell-cell junctions.

Given the physiological roles of junctional RhoA signalling, p114RhoGEF represents a regulator of central importance. Future experiments will need to focus on identifying signalling components that stimulate p114RhoGEF, to drive spatially restricted Rho signalling and Myosin activation at cell junctions. One potential candidate that may stimulate p114RhoGEF is the kinase Erk1/2. p114RhoGEF contains a putative Erk binding site within its C-terminal Proline rich region

(Scansite). Within this Erk binding site are two evolutionary conserved serine residues S952, 954 that are known to be phosphorylated in *vivo* (Phosphosite). Erk1/2 is known to stimulate the guanine nucleotide exchange activity of other GEFs; GEF-H1, for example is phosphorylated by Erk1/2 and this stimulates its exchange activity towards RhoA in response to TNFα stimulation [180] [219]. It will be important to test if p114RhoGEF is stimulated by Erk1/2. Investigating the functional relavence of phosphorylation of p114RhoGEF via Erk1/2 may permit p114RhoGEFs interaction with Cingulin and thus drive its recruitment from the cytoplasm to TJs. Phosphorylation may also function to stimulate p114RhoGEF exchange activity towards RhoA during junction formation in response to different physiological stimuli such as TNFα.

p114RhoGEF a regulator of migration ?

Based on the finding that p114RhoGEF spatially activates RhoA during junction formation I decided to investigate if it also had a function in cell migration during wound healing. I discovered p114RhoGEF does indeed regulate migration of HCE cells. p114RhoGEFs depletion causes HCE cells to migrate at a slower rate during wound healing experiments (see Chapter 5). It will be important to repeat these experiments in different breast cancer cell lines, as p114RhoGEF was shown to be upregulated in a fully de-differentiated metastatic breast cancer cell line MDA-MB231. This may link the function of p114RhoGEF to important roles in migration and invasion of breast cancer cells during cancer progression. Future experiments will need to address the question of how is p114RhoGEF regulating the rate of migration? In order in answer this question live cell imaging using FRET based

techniques will be required to observe where and when RhoA is spatially active in normal and p114RhoGEF depleted cells during cell migration. Traditionally RhoA is thought to be active only at the trailing end of migrating cells where it regulates cell body contraction and detachment of the trailing end [331]. However, recent studies demonstrated that RhoA may also be active at the leading edge of migrating cells [318], although the functional consequences of RhoA activation at the leading edge remain unknown. I discovered p114RhoGEF to be localised to the tips of protrusive membrane structures of migrating HCE cells during wound healing. It will be interesting to investigate several questions: how is p114RhoGEF recruited to these structures? Does p114RhoGEF spatially activate RhoA at these membrane tips? If so questions will need to be addressed such as: what are the functional effects of RhoA activation? How does it contribute to dynamic coordinated regulation of the cytoskeletion during cell migration?

cg10188 the putative p114RhoGEF ortholog in Drosophila melanogaster is essential during development.

I was interested in the evolutionary conservation of p114RhoGEF in different species and found it to be conserved in mammals, reptiles, amphibians, fish and flies. I explored if cg10188 the putative p114RhoGEF ortholog in the fly *Drosophila melanogaster* had a similar function to p114RhoGEF by using RNAi (Chapter 6). I discovered when cg10188 RNAi is performed during development it causes lethality, indicating cg10188 is an essential gene. The precise stage at which development was arrested remained unknown, however there were no pupal cases that were occupied by flies arrested during development indicating developmental lethality

occurred before larval pupation. However, the caveat with this result is that the observed lethality could be due to an off target effect of the shRNAs used. As demonstrated p114RhoGEF is an important regulator of junction formation and a regulator of apical membrane constriction in mammalian cells, I observed if loss of cg10188 expression by RNAi caused any defects on junctions in imaginal discs epithelial structures that require apical constriction to bend and fold to undergo morphological changes to form eyes, antennae wings and legs in the adult fly. I discovered no defect on cell-cell junctions in cells depleted of cg10188 within the imaginal discs (Chapter 6- Figure 6.3). The lack of any phenotype on cell-cell junctions could have been a result of inefficient suppression of cg10188 expression. However, as the size of clones of GFP negative cells were small, cg10188 RNAi could regulate proliferation or induce apoptosis, this will require further investigations to confirm this.

It will be important to identify the precise developmental stage affected by the loss of cg10188. Where cg10188 is expressed in the imaginal discs as well as other tissues will also be important questions to address. In situ hybridisations will have to be performed to observe expression of cg10188 while antibodies against cg10188 are developed. This will provide additional information of where to observe the effects of the loss of cg10188 expression.

Final summary

RhoGTPases are small molecular switch proteins that are important regulators of the cytoskeleton and modulators of gene expression. RhoGTPases have thus been identified as being major signalling components associated with cell-cell junctions. An Important question I asked at the start of this project was how are RhoGTPases regulated to control junction formation and gene expression in corneal epithelial cells? I have addressed this question by using a siRNA screening approach and have identifed a number of candidates that regulate or are downstream effectors of RhoGTPase signalling that affected junction formation and NF-κB regulated gene expression. I fully characterised one of these candidates p114RhoGEF, a novel TJ localised guanine nucleotide exchange factor (GEF) that drives junction formation and epithelial cell morphogenesis by spatially restricted activation of RhoA at cell-cell junctions. I discovered p114RhoGEF to have an important role in cell migration and have also started to explore the function of a putative p114RhoGEF ortholog, cg10188 in *Drosophila melanogaster* and shown it to be important in larval development.

Future studies will focus on expanding the role of p114RhoGEF in cell migration and its putative ortholog, cg10188 in *Drosophila melanogaster* during development. A long-term future aim will be discovering molecular mechanisms by which the other identified candidates in the screen regulate RhoGTPases siganlling pathways to guide junction formation and modulate gene expression.

Acknowledgements

I would first like to thank my supervisors Karl and Maria who have guided me though my PhD with their expert advice and support. I would like to especially thank Karl for giving me such an enjoyable and exciting project and for always being enthusiastic about new ideas and sharing his knowledge with me in some very insightful discussions. I have learnt a lot from you and think you are very inspiring scientist. I would also like to thank my family for their support and my lovely girlfriend Rowena who had to listen to me saying p114 a lot and Clusoe for keeping me entertained with his antics when writing at home! I would also like to thank my friends Ceniz and Ahmed for their support and all the other lab members past and present who have helped with their advice and support as well as all the staff at the Institute of Ophthalmology for making it a great place to work.

Bibliography

1. Secker, G.A. & Daniels, J.T. Limbal epithelial stem cells of the cornea. (2008).
2. Balda, M.S. & Matter, K. Tight junctions at a glance. *J Cell Sci* **121**, 3677-3682 (2008).
3. Matter, K. & Balda, M.S. Functional analysis of tight junctions. *Methods* **30**, 228-234 (2003).
4. Terry, S., Nie, M., Matter, K. & Balda, M.S. Rho signaling and tight junction functions. *Physiology (Bethesda)* **25**, 16-26.
5. Huber, D., Balda, M.S. & Matter, K. Transepithelial migration of neutrophils. *Invasion Metastasis* **18**, 70-80 (1998).
6. Popoff, M.R. & Geny, B. Multifaceted role of Rho, Rac, Cdc42 and Ras in intercellular junctions, lessons from toxins. *Biochim Biophys Acta* **1788**, 797-812 (2009).
7. Niessen, C.M. & Gottardi, C.J. Molecular components of the adherens junction. *Biochim Biophys Acta* **1778**, 562-571 (2008).
8. Goodenough, D.A., Goliger, J.A. & Paul, D.L. Connexins, connexons, and intercellular communication. *Annu Rev Biochem* **65**, 475-502 (1996).
9. Farquhar, M.G. & Palade, G.E. Junctional complexes in various epithelia. *J. Cell Biol.* **17**, 375-412 (1963).
10. Cereijido, M. Evolution of ideas on the tight junction, in *Tight junctions*. (ed. M. Cereijido) 1-13 (CRC Press, Inc., Boca Raton, FL; 1991).
11. Bazzoni, G. & Dejana, E. Endothelial cell-to-cell junctions: molecular organization and role in vascular homeostasis. *Physiol. Rev.* **84**, 869-901 (2004).
12. Wallez, Y. & Huber, P. Endothelial adherens and tight junctions in vascular homeostasis, inflammation and angiogenesis. *Biochim Biophys Acta* **1778**, 794-809 (2008).
13. Green, K.J. & Jones, J.C. Desmosomes and hemidesmosomes: structure and function of molecular components. *FASEB J* **10**, 871-881 (1996).
14. Jones, J.C., Hopkinson, S.B. & Goldfinger, L.E. Structure and assembly of hemidesmosomes. *Bioessays* **20**, 488-494 (1998).
15. Claude, P. & Goodenough, D.A. Fracture faces of zonulae occludentes from tight and leaky epithelia. *J. Cell Biol.* **58**, 390-400 (1973).
16. González-Mariscal, L., Chávez de Ramirez, B., Lázaro, A. & Cereijido, M. Establishment of tight junctions between cells from different animal species and different sealing capacities. *J. Membr. Biol.* **107**, 43-56 (1989).
17. Furuse, M. & Tsukita, S. Claudins in occluding junctions of humans and flies. *Trends Cell Biol* **16**, 181-188 (2006).
18. Matter, K. & Balda, M.S. Signalling to and from tight junctions. *Nat. Rev. Mol. Cell Biol.* **4**, 225-236 (2003).
19. Jamora, C. & Fuchs, E. Intercellular adhesion, signalling and the cytoskeleton. *Nat Cell Biol* **4**, E101-108 (2002).
20. Fanning, A.S. Organization and the regulation of the tight junction by the actin-myosin cytoskeleton, in *Tight Junctions*, Edn. 2nd. (eds. J.M. Anderson & M. Cereijido) 265-284 (CRC Press, 2001).

21. Meza, I., Sabanero, M., Stefani, E. & Cereijido, M. Occluding junctions in MDCK cells: modulation of transepithelial permeability by the cytoskeleton. *J Cell Biochem* **18**, 407-421 (1982).
22. Madara, J.L. Intestinal absorptive cell tight junctions are linked to cytoskeleton. *Am J Physiol* **253**, C171-175 (1987).
23. Blum, M.S. *et al.* Cytoskeletal rearrangement mediates human microvascular endothelial tight junction modulation by cytokines. *Am J Physiol* **273**, H286-294 (1997).
24. Kojima, T. *et al.* Disruption of circumferential actin filament causes disappearance of occludin from the cell borders of rat hepatocytes in primary culture without distinct changes of tight junction strands. *Cell Struct Funct* **24**, 11-17 (1999).
25. Turner, J.R. 'Putting the squeeze' on the tight junction: understanding cytoskeletal regulation. *Semin Cell Dev Biol* **11**, 301-308 (2000).
26. Walsh, S.V. *et al.* Rho kinase regulates tight junction function and is necessary for tight junction assembly in polarized intestinal epithelia. *Gastroenterology* **121**, 566-579 (2001).
27. Samarin, S.N., Ivanov, A.I., Flatau, G., Parkos, C.A. & Nusrat, A. Rho/Rho-associated kinase-II signaling mediates disassembly of epithelial apical junctions. *Mol Biol Cell* **18**, 3429-3439 (2007).
28. Hartsock, A. & Nelson, W.J. Adherens and tight junctions: structure, function and connections to the actin cytoskeleton. *Biochim Biophys Acta* **1778**, 660-669 (2008).
29. Garrod, D. & Kimura, T.E. Hyper-adhesion: a new concept in cell-cell adhesion. *Biochem Soc Trans* **36**, 195-201 (2008).
30. Martin-Padura, I. *et al.* Junctional adhesion molecule, a novel member of the immunoglobulin superfamily that distributes at intercellular junctions and modulates monocyte transmigration. *J. Cell Biol.* **142**, 117-127 (1998).
31. Aurrand-Lions, M., Johnson-Leger, C., Wong, C., Du Pasquier, L. & Imhof, B.A. Heterogeneity of endothelial junctions is reflected by differential expression and specific subcellular localization of the three JAM family members. *Blood* **98**, 3699-3707 (2001).
32. Ebnet, K., Suzuki, A., Ohno, S. & Vestweber, D. Junctional adhesion molecules (JAMs): more molecules with dual functions? *J. Cell Sci.* **117**, 19-29 (2004).
33. Cohen, C.J. *et al.* The coxsackievirus and adenovirus receptor is a transmembrane component of the tight junction. *Proc Natl Acad Sci U S A* **98**, 15191-15196. (2001).
34. Osler, M.E., Chang, M.S. & Bader, D.M. Bves modulates epithelial integrity through an interaction at the tight junction. *J Cell Sci* **118**, 4667-4678 (2005).
35. Van Itallie, C.M. & Anderson, J.M. Claudins and epithelial paracellular transport. *Annu Rev Physiol* **68**, 403-429 (2006).
36. Tsukita, S. & Furuse, M. Occludin and claudins in tight-junction strands: leading or supporting players? *Trends Cell Biol.* **9**, 268-273 (1999).
37. Balda, M.S., Flores-Maldonado, C., Cereijido, M. & Matter, K. Multiple domains of occludin are involved in the regulation of paracellular permeability. *J. Cell Biochem.* **78**, 85-96 (2000).
38. Ikenouchi, J., Furuse, M., Furuse, K., Sasaki, H. & Tsukita, S. Tricellulin constitutes a novel barrier at tricellular contacts of epithelial cells. *J Cell Biol* **171**, 939-945 (2005).

39. Steed, E., Rodrigues, N.T., Balda, M.S. & Matter, K. Identification of MarvelD3 as a tight junction-associated transmembrane protein of the occludin family. *BMC Cell Biol* **10**, 95 (2009).
40. Van Itallie, C.M., Colegio, O.R. & Anderson, J.M. The cytoplasmic tails of claudins can influence tight junction barrier properties through effects on protein stability. *J. Membr. Biol.* **199**, 29-38 (2004).
41. Krause, G. *et al.* Structure and function of claudins. *Biochim Biophys Acta* **1778**, 631-645 (2008).
42. Kiuchi-Saishin, Y. *et al.* Differential expression patterns of claudins, tight junction membrane proteins, in mouse nephron segments. *J. Am. So.c Nephrol.* **13**, 875-886. (2002).
43. Colegio, O.R., Van Itallie, C.M., McCrea, H.J., Rahner, C. & Anderson, J.M. Claudins create charge-selective channels in the paracellular pathway between epithelial cells. *Am. J. Physiol. Cell Physiol.* **283**, C142-147. (2002).
44. Angelow, S., Ahlstrom, R. & Yu, A.S. Biology of claudins. *Am J Physiol Renal Physiol* **295**, F867-876 (2008).
45. McCarthy, K.M. *et al.* Inducible expression of claudin-1-myc but not occludin-VSV-G results in aberrant tight junction strand formation in MDCK cells. *J Cell Sci* **113 Pt 19**, 3387-3398 (2000).
46. Yu, A.S. Claudins and epithelial paracellular transport: the end of the beginning. *Curr Opin Nephrol Hypertens* **12**, 503-509 (2003).
47. Saitou, M. *et al.* Complex phenotype of mice lacking occludin, a component of tight junction strands. *Mol Biol Cell* **11**, 4131-4142 (2000).
48. Schulzke, J.D. *et al.* Epithelial transport and barrier function in occludin-deficient mice. *Biochim. Biophys. Acta* **1669**, 34-42 (2005).
49. Schneeberger, E.E. & Lynch, R.D. The tight junction: a multifunctional complex. *Am. J. Physiol.* **286**, C1213-1228 (2004).
50. Balda, M.S. *et al.* Functional dissociation of paracellular permeability and transepithelial electrical resistance and disruption of the apical-basolateral intramembrane diffusion barrier by expression of a mutant tight junction membrane protein. *J. Cell Biol.* **134**, 1031-1049 (1996).
51. Yu, A.L. *et al.* Knock Down of Occludin Expression Leads to Diverse Phenotypic Alterations in Epithelial Cells. *Am. J. Physiol. Cell Physiol.* **288**, C1231-1241 (2005).
52. Van Itallie, C.M., Fanning, A.S., Holmes, J. & Anderson, J.M. Occludin is required for cytokine-induced regulation of tight junction barriers. *J Cell Sci* **123**, 2844-2852.
53. Willott, E. *et al.* The tight junction protein ZO-1 is homologous to the Drosophila discs-large tumor suppressor protein of septate junctions. *Proc. Natl. Acad. Sci. USA* **90**, 7834-7838 (1993).
54. Beatch, M., Jesaitis, L.A., Gallin, W.J., Goodenough, D.A. & Stevenson, B.R. The tight junction protein ZO-2 contains three PDZ (PSD-95/Discs-Large/ZO-1) domains and an alternatively spliced region. *J Biol Chem* **271**, 25723-25726 (1996).
55. Haskins, J., Gu, L., Wittchen, E.S., Hibbard, J. & Stevenson, B.R. ZO-3, a novel member of the MAGUK protein family found at the tight junction, interacts with ZO-1 and occludin. *J. Cell Biol.* **141**, 199-208. (1998).
56. Joberty, G., Petersen, C., Gao, L. & Macara, I.G. The cell-polarity protein Par6 links Par3 and atypical protein kinase C to Cdc42. *Nat. Cell Biol.* **2**, 531-539 (2000).

57. Straight, S.W. *et al.* Loss of PALS1 expression leads to tight junction and polarity defects. *Mol. Biol. Cell* **15**, 1981-1990 (2004).
58. Shin, K., Straight, S. & Margolis, B. PATJ regulates tight junction formation and polarity in mammalian epithelial cells. *J. Cell Biol.* **168**, 705-711 (2005).
59. Hamazaki, Y., Itoh, M., Sasaki, H., Furuse, M. & Tsukita, S. Multi-PDZ domain protein 1 (MUPP1) is concentrated at tight junctions through its possible interaction with claudin-1 and junctional adhesion molecule. *J. Biol. Chem.* **277**, 455-461. (2002).
60. Dobrosotskaya, I., Guy, R.K. & James, G.L. MAGI-1, a membrane-associated guanylate kinase with a unique arrangement of protein-protein interaction domains. *J Biol Chem* **272**, 31589-31597 (1997).
61. Ohnishi, H. *et al.* JACOP, a novel plaque protein localizing at the apical junctional complex with sequence similarity to cingulin. *J. Biol. Chem.* **279**, 46014-46022 (2004).
62. Guillemot, L., Paschoud, S., Jond, L., Foglia, A. & Citi, S. Paracingulin regulates the activity of Rac1 and RhoA GTPases by recruiting Tiam1 and GEF-H1 to epithelial junctions. *Mol Biol Cell* **19**, 4442-4453 (2008).
63. Cordenonsi, M. *et al.* Cingulin contains globular and coiled-coil domains and interacts with ZO-1, ZO-2, ZO-3, and myosin. *J. Cell Biol.* **147**, 1569-1582 (1999).
64. Aijaz, S., D'Atri, F., Citi, S., Balda, M.S. & Matter, K. Binding of GEF-H1 to the tight junction-associated adaptor cingulin results in inhibition of Rho signaling and G1/S phase transition. *Dev. Cell* **8**, 777-786 (2005).
65. Paris, L., Tonutti, L., Vannini, C. & Bazzoni, G. Structural organization of the tight junctions. *Biochim Biophys Acta* **1778**, 646-659 (2008).
66. Balda, M.S. & Matter, K. Tight junctions and the regulation of gene expression. *Biochim Biophys Acta* **1788**, 761-767 (2009).
67. Itoh, M. *et al.* Direct binding of three tight junction-associated MAGUKs, ZO-1, ZO-2, and ZO-3, with the COOH termini of claudins. *J Cell Biol* **147**, 1351-1363 (1999).
68. Fanning, A.S., Jameson, B.J., Jesaitis, L.A. & Anderson, J.M. The tight junction protein ZO-1 establishes a link between the transmembrane protein occludin and the actin cytoskeleton. *J Biol Chem* **273**, 29745-29753 (1998).
69. Fanning, A.S. & Anderson, J.M. The tight junction protein ZO-1 establishes a link between the membrane protein occludin and the actin cytoskeleton. *J. Biol. Chem.* **273**, 29745-29753 (1998).
70. Wittchen, E.S., Haskins, J. & Stevenson, B.R. Exogenous expression of the amino-terminal half of the tight junction protein ZO-3 perturbs junctional complex assembly. *J. Cell Biol.* **151**, 825-836 (2000).
71. Wittchen, E.S., Haskins, J. & Stevenson, B.R. Protein interactions at the tight junction. Actin has multiple binding partners, and ZO-1 forms independent complexes with ZO-2 and ZO-3. *J. Biol. Chem.* **274**, 35179-35185 (1999).
72. Itoh, M., Nagafuchi, A., Moroi, S. & Tsukita, S. Involvement of ZO-1 in cadherin-based cell adhesion through its direct binding to alpha catenin and actin filaments. *J Cell Biol* **138**, 181-192. (1997).
73. Reichert, M., Muller, T. & Hunziker, W. The PDZ domains of zonula occludens-1 induce an epithelial to mesenchymal transition of Madin-Darby canine kidney I cells. Evidence for a role of beta-catenin/Tcf/Lef signaling. *J. Biol. Chem.* **275**, 9492-9500 (2000).

74. Hoover, K.B., Liao, S.Y. & Bryant, P.J. Loss of the tight junction MAGUK ZO-1 in breast cancer: relationship to glandular differentiation and loss of heterozygosity. *Am J Pathol* **153**, 1767-1773 (1998).
75. Chlenski, A. *et al.* Tight junction protein ZO-2 is differentially expressed in normal pancreatic ducts compared to human pancreatic adenocarcinoma. *Int J Cancer* **82**, 137-144 (1999).
76. Mann, B. *et al.* Target genes of beta-catenin-T cell-factor/lymphoid-enhancer-factor signaling in human colorectal carcinomas. *Proc. Natl. Acad. Sci. U S A* **96**, 1603-1608 (1999).
77. Behrens, J. Control of beta-catenin signaling in tumor development. *Ann. N.Y. Acad. Sci.* **910**, 21-33; discussion 33-25. (2000).
78. Korinek, V. *et al.* Constitutive transcriptional activation by a beta-catenin-Tcf complex in APC-/- colon carcinoma. *Science* **275**, 1784-1787 (1997).
79. Gottardi, C.J., Arpin, M., Fanning, A.S. & Louvard, D. The junction-associated protein, zonula occludens-1, localizes to the nucleus before the maturation and during the remodeling of cell-cell contacts. *Proc. Natl. Acad. Sci. USA* **93**, 10779-10784 (1996).
80. Balda, M.S. & Matter, K. The tight junction protein ZO-1 and an interacting transcription factor regulate ErbB-2 expression. *EMBO J.* **19**, 2024-2033 (2000).
81. Traweger, A. *et al.* The tight junction protein ZO-2 localizes to the nucleus and interacts with the hnRNP protein SAF-B. *J. Biol. Chem.* **278**, 2692-2700 (2002).
82. Balda, M.S., Garrett, M.D. & Matter, K. The ZO-1 associated Y-box factor ZONAB regulates epithelial cell proliferation and cell density. *J. Cell Biol.* **160**, 423-432 (2003).
83. Sourisseau, T. *et al.* Regulation of PCNA and cyclin D1 expression and epithelial morphogenesis by the ZO-1 regulated transcription factor ZONAB/DbpA. *Mol. Cell. Biol.* **26**, 2387-2398 (2006).
84. Raleigh, D.R. *et al.* Tight junction-associated MARVEL proteins marveld3, tricellulin, and occludin have distinct but overlapping functions. *Mol Biol Cell* **21**, 1200-1213.
85. Wells, C.D. *et al.* A Rich1/Amot complex regulates the Cdc42 GTPase and apical-polarity proteins in epithelial cells. *Cell* **125**, 535-548 (2006).
86. Otani, T., Ichii, T., Aono, S. & Takeichi, M. Cdc42 GEF Tuba regulates the junctional configuration of simple epithelial cells. *J Cell Biol* **175**, 135-146 (2006).
87. Gooding, J.M., Yap, K.L. & Ikura, M. The cadherin-catenin complex as a focal point of cell adhesion and signalling: new insights from three-dimensional structures. *Bioessays* **26**, 497-511 (2004).
88. Pokutta, S., Herrenknecht, K., Kemler, R. & Engel, J. Conformational changes of the recombinant extracellular domain of E-cadherin upon calcium binding. *Eur J Biochem* **223**, 1019-1026 (1994).
89. Yap, A.S., Niessen, C.M. & Gumbiner, B.M. The juxtamembrane region of the cadherin cytoplasmic tail supports lateral clustering, adhesive strengthening, and interaction with p120ctn. *J Cell Biol* **141**, 779-789 (1998).
90. Aberle, H. *et al.* Assembly of the cadherin-catenin complex in vitro with recombinant proteins. *J Cell Sci* **107 (Pt 12)**, 3655-3663 (1994).
91. Knudsen, K.A., Soler, A.P., Johnson, K.R. & Wheelock, M.J. Interaction of alpha-actinin with the cadherin/catenin cell-cell adhesion complex via alpha-catenin. *J Cell Biol* **130**, 67-77 (1995).

92. Abe, K. & Takeichi, M. EPLIN mediates linkage of the cadherin catenin complex to F-actin and stabilizes the circumferential actin belt. *Proc Natl Acad Sci U S A* **105**, 13-19 (2008).
93. Yokoyama, S. *et al.* alpha-catenin-independent recruitment of ZO-1 to nectin-based cell-cell adhesion sites through afadin. *Mol. Biol. Cell* **12**, 1595-1609 (2001).
94. Weis, W.I. & Nelson, W.J. Re-solving the cadherin-catenin-actin conundrum. *J Biol Chem* **281**, 35593-35597 (2006).
95. Yamada, S., Pokutta, S., Drees, F., Weis, W.I. & Nelson, W.J. Deconstructing the cadherin-catenin-actin complex. *Cell* **123**, 889-901 (2005).
96. Drees, F., Pokutta, S., Yamada, S., Nelson, W.J. & Weis, W.I. Alpha-catenin is a molecular switch that binds E-cadherin-beta-catenin and regulates actin-filament assembly. *Cell* **123**, 903-915 (2005).
97. Cox, R.T., Kirkpatrick, C. & Peifer, M. Armadillo is required for adherens junction assembly, cell polarity, and morphogenesis during Drosophila embryogenesis. *J Cell Biol* **134**, 133-148 (1996).
98. Yonemura, S., Wada, Y., Watanabe, T., Nagafuchi, A. & Shibata, M. alpha-Catenin as a tension transducer that induces adherens junction development. *Nat Cell Biol* **12**, 533-542.
99. Fukuhara, A. *et al.* Role of nectin in organization of tight junctions in epithelial cells. *Genes Cells* **7**, 1059-1072 (2002).
100. Irie, K., Shimizu, K., Sakisaka, T., Ikeda, W. & Takai, Y. Roles and modes of action of nectins in cell-cell adhesion. *Semin. Cell Dev. Biol.* **15**, 643-656 (2004).
101. Tachibana, K. *et al.* Two cell adhesion molecules, nectin and cadherin, interact through their cytoplasmic domain-associated proteins. *J Cell Biol* **150**, 1161-1176 (2000).
102. Takahashi, K. *et al.* Nectin/PRR: an immunoglobulin-like cell adhesion molecule recruited to cadherin-based adherens junctions through interaction with Afadin, a PDZ domain-containing protein. *J. Cell Biol.* **145**, 539-549 (1999).
103. Takai, Y. & Nakanishi, H. Nectin and afadin: novel organizers of intercellular junctions. *J Cell Sci* **116**, 17-27 (2003).
104. Bienz, M. TCF: transcriptional activator or repressor. *Curr. Opin. Cell Biol.* **10**, 366-372 (1998).
105. Huber, O., Bierkamp, C. & Kemler, R. Cadherins and catenins in develpment. *Curr. Opin. Cell Biol.*, 685-691 (1996a).
106. Behrens, J. Cadherins and catenins: role in signal transduction and tumor progression. *Cancer Metastasis Rev.* **18**, 15-30 (1999).
107. Bienz, M. beta-Catenin: a pivot between cell adhesion and Wnt signalling. *Curr Biol* **15**, R64-67 (2005).
108. Aberle, H., Bauer, A., Stappert, J., Kispert, A. & Kemler, R. beta-catenin is a target for the ubiquitin-proteasome pathway. *Embo J* **16**, 3797-3804 (1997).
109. Shtutman, M. *et al.* The cyclin D1 gene is a target of the beta-catenin/LEF-1 pathway. *Proc. Natl. Acad. Sci. USA* **96**, 5522-5527 (1999).
110. He, T.C. *et al.* Identification of c-MYC as a target of the APC pathway. *Science* **281**, 1509-1512 (1998).
111. Karin, M. Nuclear factor-kappaB in cancer development and progression. *Nature* **441**, 431-436 (2006).

112. Guttridge, D.C., Albanese, C., Reuther, J.Y., Pestell, R.G. & Baldwin, A.S., Jr. NF-kappaB controls cell growth and differentiation through transcriptional regulation of cyclin D1. *Mol Cell Biol* **19**, 5785-5799 (1999).
113. Liu, C.A., Wang, M.J., Chi, C.W., Wu, C.W. & Chen, J.Y. Rho/Rhotekin-mediated NF-kappaB activation confers resistance to apoptosis. *Oncogene* **23**, 8731-8742 (2004).
114. Ghosh, S., May, M.J. & Kopp, E.B. NF-kappa B and Rel proteins: evolutionarily conserved mediators of immune responses. *Annu Rev Immunol* **16**, 225-260 (1998).
115. Min, C., Eddy, S.F., Sherr, D.H. & Sonenshein, G.E. NF-kappaB and epithelial to mesenchymal transition of cancer. *J Cell Biochem* **104**, 733-744 (2008).
116. Hayden, M.S. & Ghosh, S. Signaling to NF-kappaB. *Genes Dev* **18**, 2195-2224 (2004).
117. Suh, J. *et al.* Mechanisms of constitutive NF-kappaB activation in human prostate cancer cells. *Prostate* **52**, 183-200 (2002).
118. Basseres, D.S. & Baldwin, A.S. Nuclear factor-kappaB and inhibitor of kappaB kinase pathways in oncogenic initiation and progression. *Oncogene* **25**, 6817-6830 (2006).
119. Batlle, E. *et al.* The transcription factor snail is a repressor of E-cadherin gene expression in epithelial tumour cells. *Nat Cell Biol* **2**, 84-89 (2000).
120. Ikenouchi, J., Matsuda, M., Furuse, M. & Tsukita, S. Regulation of tight junctions during the epithelium-mesenchyme transition: direct repression of the gene expression of claudins/occludin by Snail. *J Cell Sci* **116**, 1959-1967 (2003).
121. Solanas, G. *et al.* E-cadherin controls beta-catenin and NF-kappaB transcriptional activity in mesenchymal gene expression. *J Cell Sci* **121**, 2224-2234 (2008).
122. Reynolds, A.B. & Roczniak-Ferguson, A. Emerging roles for p120-catenin in cell adhesion and cancer. *Oncogene* **23**, 7947-7956 (2004).
123. Park, J.I. *et al.* Kaiso/p120-catenin and TCF/beta-catenin complexes coordinately regulate canonical Wnt gene targets. *Dev Cell* **8**, 843-854 (2005).
124. Perez-Moreno, M. *et al.* p120-catenin mediates inflammatory responses in the skin. *Cell* **124**, 631-644 (2006).
125. Gonzalez-Mariscal, L., Chavez de Ramirez, B. & Cereijido, M. Tight junction formation in cultured epithelial cells (MDCK). *J. Membr. Biol.* **86**, 113-125 (1985).
126. Gumbiner, B., Stevenson, B.R. & Grimaldi, A. The role of the cell adhesion molecule uvomorulin in the formation and maintenance of epithelial junctional complex. *J. Cell Biol.* **107**, 1575-1587 (1988).
127. Fleming, T.P., Sheth, B. & Fesenko, I. Cell adhesion in the preimplantation mammalian embryo and its role in trophectoderm differentiation and blastocyst morphogenesis. *Front Biosci* **6**, D1000-1007 (2001).
128. Eckert, J.J. & Fleming, T.P. Tight junction biogenesis during early development. *Biochim Biophys Acta* **1778**, 717-728 (2008).
129. Adams, C.L., Chen, Y.T., Smith, S.J. & Nelson, W.J. Mechanisms of epithelial cell-cell adhesion and cell compaction revealed by high-resolution tracking of E-cadherin-green fluorescent protein. *J Cell Biol* **142**, 1105-1119 (1998).
130. Ehrlich, J.S., Hansen, M.D. & Nelson, W.J. Spatio-temporal regulation of Rac1 localization and lamellipodia dynamics during epithelial cell-cell adhesion. *Dev Cell* **3**, 259-270 (2002).

131. Vasioukhin, V., Bauer, C., Yin, M. & Fuchs, E. Directed actin polymerization is the driving force for epithelial cell-cell adhesion. *Cell* **100**, 209-219 (2000).
132. Asakura, T. *et al.* Similar and differential behaviour between the nectin-afadin-ponsin and cadherin-catenin systems during the formation and disruption of the polarized junctional alignment in epithelial cells. *Genes Cells* **4**, 573-581 (1999).
133. Kovacs, E.M., Goodwin, M., Ali, R.G., Paterson, A.D. & Yap, A.S. Cadherin-directed actin assembly: E-cadherin physically associates with the Arp2/3 complex to direct actin assembly in nascent adhesive contacts. *Curr Biol* **12**, 379-382 (2002).
134. Kobielak, A., Pasolli, H.A. & Fuchs, E. Mammalian formin-1 participates in adherens junctions and polymerization of linear actin cables. *Nat Cell Biol* **6**, 21-30 (2004).
135. Scott, J.A. *et al.* Ena/VASP proteins can regulate distinct modes of actin organization at cadherin-adhesive contacts. *Mol Biol Cell* **17**, 1085-1095 (2006).
136. Volkmann, N. *et al.* Structure of Arp2/3 complex in its activated state and in actin filament branch junctions. *Science* **293**, 2456-2459 (2001).
137. Zhang, J. *et al.* Actin at cell-cell junctions is composed of two dynamic and functional populations. *J Cell Sci* **118**, 5549-5562 (2005).
138. Kishikawa, M., Suzuki, A. & Ohno, S. aPKC enables development of zonula adherens by antagonizing centripetal contraction of the circumferential actomyosin cables. *J Cell Sci* **121**, 2481-2492 (2008).
139. Smutny, M. *et al.* Myosin II isoforms identify distinct functional modules that support integrity of the epithelial zonula adherens. *Nat Cell Biol* **12**, 696-702.
140. Wennerberg, K., Rossman, K.L. & Der, C.J. The Ras superfamily at a glance. *J Cell Sci* **118**, 843-846 (2005).
141. Heasman, S.J. & Ridley, A.J. Mammalian Rho GTPases: new insights into their functions from in vivo studies. *Nat Rev Mol Cell Biol* **9**, 690-701 (2008).
142. Berthold, J., Schenkova, K. & Rivero, F. Rho GTPases of the RhoBTB subfamily and tumorigenesis. *Acta Pharmacol Sin* **29**, 285-295 (2008).
143. Chardin, P. Function and regulation of Rnd proteins. *Nat Rev Mol Cell Biol* **7**, 54-62 (2006).
144. Hall, A. Rho GTPases and the actin cytoskeleton. *Science* **279**, 509-514 (1998).
145. Etienne-Manneville, S. & Hall, A. Rho GTPases in cell biology. *Nature* **420**, 629-635 (2002).
146. Sahai, E. & Marshall, C.J. RHO-GTPases and cancer. *Nat. Rev. Cancer* **2**, 133-142 (2002).
147. Tcherkezian, J. & Lamarche-Vane, N. Current knowledge of the large RhoGAP family of proteins. *Biol Cell* **99**, 67-86 (2007).
148. Rossman, K.L., Der, C.J. & Sondek, J. GEF means go: turning on RHO GTPases with guanine nucleotide-exchange factors. *Nat Rev Mol Cell Biol* **6**, 167-180 (2005).
149. Fukumoto, Y. *et al.* Molecular cloning and characterization of a novel type of regulatory protein (GDI) for the rho proteins, ras p21-like small GTP-binding proteins. *Oncogene* **5**, 1321-1328 (1990).
150. DerMardirossian, C. & Bokoch, G.M. GDIs: central regulatory molecules in Rho GTPase activation. *Trends Cell Biol* **15**, 356-363 (2005).
151. Ron, D., Tronick, S.R., Aaronson, S.A. & Eva, A. Molecular cloning and characterization of the human dbl proto-oncogene: evidence that its overexpression is sufficient to transform NIH/3T3 cells. *Embo J* **7**, 2465-2473 (1988).

152. Hart, M.J., Eva, A., Evans, T., Aaronson, S.A. & Cerione, R.A. Catalysis of guanine nucleotide exchange on the CDC42Hs protein by the dbl oncogene product. *Nature* **354**, 311-314 (1991).
153. Zheng, Y., Cerione, R. & Bender, A. Control of the yeast bud-site assembly GTPase Cdc42. Catalysis of guanine nucleotide exchange by Cdc24 and stimulation of GTPase activity by Bem3. *J Biol Chem* **269**, 2369-2372 (1994).
154. Worthylake, D.K., Rossman, K.L. & Sondek, J. Crystal structure of Rac1 in complex with the guanine nucleotide exchange region of Tiam1. *Nature* **408**, 682-688 (2000).
155. Karnoub, A.E. *et al.* Molecular basis for Rac1 recognition by guanine nucleotide exchange factors. *Nat Struct Biol* **8**, 1037-1041 (2001).
156. Cheng, L. *et al.* RhoGEF specificity mutants implicate RhoA as a target for Dbs transforming activity. *Mol Cell Biol* **22**, 6895-6905 (2002).
157. Rossman, K.L. *et al.* A crystallographic view of interactions between Dbs and Cdc42: PH domain-assisted guanine nucleotide exchange. *EMBO J* **21**, 1315-1326 (2002).
158. Das, B. *et al.* Control of intramolecular interactions between the pleckstrin homology and Dbl homology domains of Vav and Sos1 regulates Rac binding. *J Biol Chem* **275**, 15074-15081 (2000).
159. Ron, D. *et al.* A region of proto-dbl essential for its transforming activity shows sequence similarity to a yeast cell cycle gene, CDC24, and the human breakpoint cluster gene, bcr. *New Biol* **3**, 372-379 (1991).
160. Rossman, K.L. *et al.* Multifunctional roles for the PH domain of Dbs in regulating Rho GTPase activation. *J Biol Chem* **278**, 18393-18400 (2003).
161. Chen, R.H., Corbalan-Garcia, S. & Bar-Sagi, D. The role of the PH domain in the signal-dependent membrane targeting of Sos. *EMBO J* **16**, 1351-1359 (1997).
162. Baumeister, M.A. *et al.* Loss of phosphatidylinositol 3-phosphate binding by the C-terminal Tiam-1 pleckstrin homology domain prevents in vivo Rac1 activation without affecting membrane targeting. *J Biol Chem* **278**, 11457-11464 (2003).
163. Stam, J.C. *et al.* Targeting of Tiam1 to the plasma membrane requires the cooperative function of the N-terminal pleckstrin homology domain and an adjacent protein interaction domain. *J Biol Chem* **272**, 28447-28454 (1997).
164. Prag, S. *et al.* Activated ezrin promotes cell migration through recruitment of the GEF Dbl to lipid rafts and preferential downstream activation of Cdc42. *Mol Biol Cell* **18**, 2935-2948 (2007).
165. Cote, J.F. & Vuori, K. GEF what? Dock180 and related proteins help Rac to polarize cells in new ways. *Trends Cell Biol* **17**, 383-393 (2007).
166. Meller, N., Merlot, S. & Guda, C. CZH proteins: a new family of Rho-GEFs. *J Cell Sci* **118**, 4937-4946 (2005).
167. Hasegawa, H. *et al.* DOCK180, a major CRK-binding protein, alters cell morphology upon translocation to the cell membrane. *Mol Cell Biol* **16**, 1770-1776 (1996).
168. Erickson, M.R., Galletta, B.J. & Abmayr, S.M. Drosophila myoblast city encodes a conserved protein that is essential for myoblast fusion, dorsal closure, and cytoskeletal organization. *J Cell Biol* **138**, 589-603 (1997).
169. Meller, N., Irani-Tehrani, M., Ratnikov, B.I., Paschal, B.M. & Schwartz, M.A. The novel Cdc42 guanine nucleotide exchange factor, zizimin1, dimerizes via the Cdc42-binding CZH2 domain. *J Biol Chem* **279**, 37470-37476 (2004).

170. Kwofie, M.A. & Skowronski, J. Specific recognition of Rac2 and Cdc42 by DOCK2 and DOCK9 guanine nucleotide exchange factors. *J Biol Chem* **283**, 3088-3096 (2008).
171. Cote, J.F., Motoyama, A.B., Bush, J.A. & Vuori, K. A novel and evolutionarily conserved PtdIns(3,4,5)P3-binding domain is necessary for DOCK180 signalling. *Nat Cell Biol* **7**, 797-807 (2005).
172. Moon, S.Y. & Zheng, Y. Rho GTPase-activating proteins in cell regulation. *Trends Cell Biol* **13**, 13-22 (2003).
173. Rittinger, K., Walker, P.A., Eccleston, J.F., Smerdon, S.J. & Gamblin, S.J. Structure at 1.65 A of RhoA and its GTPase-activating protein in complex with a transition-state analogue. *Nature* **389**, 758-762 (1997).
174. Schmidt, A. & Hall, A. Guanine nucleotide exchange factors for Rho GTPases: turning on the switch. *Genes Dev* **16**, 1587-1609 (2002).
175. Crespo, P., Schuebel, K.E., Ostrom, A.A., Gutkind, J.S. & Bustelo, X.R. Phosphotyrosine-dependent activation of Rac-1 GDP/GTP exchange by the vav proto-oncogene product. *Nature* **385**, 169-172 (1997).
176. Han, J. *et al.* Lck regulates Vav activation of members of the Rho family of GTPases. *Mol Cell Biol* **17**, 1346-1353 (1997).
177. Fleming, I.N., Elliott, C.M., Buchanan, F.G., Downes, C.P. & Exton, J.H. Ca2+/calmodulin-dependent protein kinase II regulates Tiam1 by reversible protein phosphorylation. *J Biol Chem* **274**, 12753-12758 (1999).
178. Fleming, I.N., Elliott, C.M., Collard, J.G. & Exton, J.H. Lysophosphatidic acid induces threonine phosphorylation of Tiam1 in Swiss 3T3 fibroblasts via activation of protein kinase C. *J Biol Chem* **272**, 33105-33110 (1997).
179. Servitja, J.M., Marinissen, M.J., Sodhi, A., Bustelo, X.R. & Gutkind, J.S. Rac1 function is required for Src-induced transformation. Evidence of a role for Tiam1 and Vav2 in Rac activation by Src. *J Biol Chem* **278**, 34339-34346 (2003).
180. Fujishiro, S.H. *et al.* ERK1/2 phosphorylate GEF-H1 to enhance its guanine nucleotide exchange activity toward RhoA. *Biochem Biophys Res Commun* **368**, 162-167 (2008).
181. Zenke, F.T. *et al.* p21-activated kinase 1 phosphorylates and regulates 14-3-3 binding to GEF-H1, a microtubule-localized Rho exchange factor. *J. Biol. Chem.* **279**, 18392-18400 (2004).
182. Birkenfeld, J. *et al.* GEF-H1 modulates localized RhoA activation during cytokinesis under the control of mitotic kinases. *Dev Cell* **12**, 699-712 (2007).
183. Tcherkezian, J., Danek, E.I., Jenna, S., Triki, I. & Lamarche-Vane, N. Extracellular signal-regulated kinase 1 interacts with and phosphorylates CdGAP at an important regulatory site. *Mol Cell Biol* **25**, 6314-6329 (2005).
184. Kozasa, T. *et al.* p115 RhoGEF, a GTPase activating protein for Galpha12 and Galpha13. *Science* **280**, 2109-2111 (1998).
185. Suzuki, N., Nakamura, S., Mano, H. & Kozasa, T. Galpha 12 activates Rho GTPase through tyrosine-phosphorylated leukemia-associated RhoGEF. *Proc Natl Acad Sci U S A* **100**, 733-738 (2003).
186. Hart, M.J. *et al.* Direct stimulation of the guanine nucleotide exchange activity of p115 RhoGEF by Galpha13. *Science* **280**, 2112-2114 (1998).
187. Welch, H.C. *et al.* P-Rex1, a PtdIns(3,4,5)P3- and Gbetagamma-regulated guanine-nucleotide exchange factor for Rac. *Cell* **108**, 809-821 (2002).
188. Niu, J., Profirovic, J., Pan, H., Vaiskunaite, R. & Voyno-Yasenetskaya, T. G Protein betagamma subunits stimulate p114RhoGEF, a guanine nucleotide exchange

factor for RhoA and Rac1: regulation of cell shape and reactive oxygen species production. *Circ Res* **93**, 848-856 (2003).
189. Schmidt, A. & Hall, A. The Rho exchange factor Net1 is regulated by nuclear sequestration. *J Biol Chem* **277**, 14581-14588 (2002).
190. Tatsumoto, T., Xie, X., Blumenthal, R., Okamoto, I. & Miki, T. Human ECT2 is an exchange factor for Rho GTPases, phosphorylated in G2/M phases, and involved in cytokinesis. *J Cell Biol* **147**, 921-928 (1999).
191. Chang, Y.C., Nalbant, P., Birkenfeld, J., Chang, Z.F. & Bokoch, G.M. GEF-H1 Couples Nocodazole-induced Microtubule Disassembly to Cell Contractility via RhoA. *Mol Biol Cell* (2008).
192. Mertens, A.E., Rygiel, T.P., Olivo, C., van der Kammen, R. & Collard, J.G. The Rac activator Tiam1 controls tight junction biogenesis in keratinocytes through binding to and activation of the Par polarity complex. *J Cell Biol* **170**, 1029-1037 (2005).
193. Chen, X. & Macara, I.G. Par-3 controls tight junction assembly through the Rac exchange factor Tiam1. *Nat Cell Biol* **7**, 262-269 (2005).
194. Garcia-Mata, R. & Burridge, K. Catching a GEF by its tail. *Trends Cell Biol* **17**, 36-43 (2007).
195. Audebert, S. *et al.* Mammalian Scribble forms a tight complex with the betaPIX exchange factor. *Curr Biol* **14**, 987-995 (2004).
196. Li, Z. *et al.* Directional sensing requires G beta gamma-mediated PAK1 and PIX alpha-dependent activation of Cdc42. *Cell* **114**, 215-227 (2003).
197. Obermeier, A. *et al.* PAK promotes morphological changes by acting upstream of Rac. *EMBO J* **17**, 4328-4339 (1998).
198. Hussain, N.K. *et al.* Endocytic protein intersectin-l regulates actin assembly via Cdc42 and N-WASP. *Nat Cell Biol* **3**, 927-932 (2001).
199. Jenna, S. *et al.* The activity of the GTPase-activating protein CdGAP is regulated by the endocytic protein intersectin. *J Biol Chem* **277**, 6366-6373 (2002).
200. Balda, M.S. *et al.* Assembly and sealing of tight junctions: possible participation of G-proteins, phospholipase C, protein kinase C and calmodulin. *J. Membr. Biol.* **122**, 193-202 (1991).
201. Cereijido, M. *et al.* The making of a tight junction. *J Cell Sci Suppl* **17**, 127-132 (1993).
202. Nusrat, A. *et al.* Rho protein regulates tight junctions and perijunctional actin organization in polarized epithelia. *Proc. Natl. Acad. Sci. U S A* **92**, 10629-10633 (1995).
203. Bruewer, M., Hopkins, A.M., Hobert, M.E., Nusrat, A. & Madara, J.L. RhoA, Rac1, and Cdc42 exert distinct effects on epithelial barrier via selective structural and biochemical modulation of junctional proteins and F-actin. *Am J Physiol Cell Physiol* **287**, C327-335 (2004).
204. Jou, T.S., Schneeberger, E.E. & Nelson, W.J. Structural and functional regulation of tight junctions by RhoA and Rac1 small GTPases. *J. Cell Biol.* **142**, 101-115 (1998).
205. Wojciak-Stothard, B., Potempa, S., Eichholtz, T. & Ridley, A.J. Rho and Rac but not Cdc42 regulate endothelial cell permeability. *J. Cell Sci.* **114**, 1343-1355 (2001).
206. Takaishi, K., Sasaki, T., Kotani, H., Nishioka, H. & Takai, Y. Regulation of cell-cell adhesion by rac and rho small G proteins in MDCK cells. *J. Cell Biol.* **139**, 1047-1059 (1997).

207. Adamson, P., Etienne, S., Couraud, P.O., Calder, V. & Greenwood, J. Lymphocyte migration through brain endothelial cell monolayers involves signaling through endothelial ICAM-1 via a rho-dependent pathway. *J. Immunol.* **162**, 2964-2973 (1999).
208. Denker, B.M., Saha, C., Khawaja, S. & Nigam, S.K. Involvement of a heterotrimeric G protein alpha subunit in tight junction biogenesis. *J. Biol. Chem.* **271**, 25750-25753 (1996).
209. Meyer, T.N., Hunt, J., Schwesinger, C. & Denker, B.M. Galpha12 regulates epithelial cell junctions through Src tyrosine kinases. *Am. J. Physiol. Cell Physiol.* **285**, C1281-1293 (2003).
210. Hasegawa, H. *et al.* Opposite regulation of transepithelial electrical resistance and paracellular permeability by Rho in Madin-Darby canine kidney cells. *J. Biol. Chem.* **274**, 20982-20988 (1999).
211. Sourisseau, T. *et al.* Regulation of PCNA and cyclin D1 expression and epithelial morphogenesis by the ZO-1-regulated transcription factor ZONAB/DbpA. *Mol Cell Biol* **26**, 2387-2398 (2006).
212. Benais-Pont, G. *et al.* Identification of a tight junction-associated guanine nucleotide exchange factor that activates Rho and regulates paracellular permeability. *J. Cell Biol.* **160**, 729-740 (2003).
213. Birukova, A.A. *et al.* GEF-H1 is involved in agonist-induced human pulmonary endothelial barrier dysfunction. *Am J Physiol Lung Cell Mol Physiol* **290**, L540-548 (2006).
214. Guillemot, L. & Citi, S. Cingulin regulates claudin-2 expression and cell proliferation through the small GTPase RhoA. *Mol Biol Cell* **17**, 3569-3577 (2006).
215. Nie, M., Aijaz, S., Leefa Chong San, I.V., Balda, M.S. & Matter, K. The Y-box factor ZONAB/DbpA associates with GEF-H1/Lfc and mediates Rho-stimulated transcription. *EMBO Rep* **10**, 1125-1131 (2009).
216. Callow, M.G., Zozulya, S., Gishizky, M.L., Jallal, B. & Smeal, T. PAK4 mediates morphological changes through the regulation of GEF-H1. *J. Cell Sci.* **118**, 1861-1872 (2005).
217. Cohen, D., Rodriguez-Boulan, E. & Musch, A. Par-1 promotes a hepatic mode of apical protein trafficking in MDCK cells. *Proc. Natl. Acad. Sci. U S A* **101**, 13792-13797 (2004).
218. McKenzie, J.A. & Ridley, A.J. Roles of Rho/ROCK and MLCK in TNF-alpha-induced changes in endothelial morphology and permeability. *J Cell Physiol* (2007).
219. Kakiashvili, E. *et al.* GEF-H1 mediates tumor necrosis factor-alpha-induced Rho activation and myosin phosphorylation: role in the regulation of tubular paracellular permeability. *J Biol Chem* **284**, 11454-11466 (2009).
220. Fujita, H. *et al.* Molecular decipherment of Rho effector pathways regulating tight-junction permeability. *Biochem. J.* **346 Pt 3**, 617-622 (2000).
221. Wojciak-Stothard, B. & Ridley, A.J. Rho GTPases and the regulation of endothelial permeability. *Vascul. Pharmacol.* **39**, 187-199 (2002).
222. Van Itallie, C.M., Fanning, A.S., Bridges, A. & Anderson, J.M. ZO-1 stabilizes the tight junction solute barrier through coupling to the perijunctional cytoskeleton. *Mol Biol Cell* **20**, 3930-3940 (2009).
223. Aijaz, S., Balda, M.S. & Matter, K. Tight Junctions: Molecular Architecture and Function. *Int. Rev. Cytol.* **248**, 261-298 (2006).

224. Rao, R. Occludin phosphorylation in regulation of epithelial tight junctions. *Ann N Y Acad Sci* **1165**, 62-68 (2009).
225. Conti, M.A., Even-Ram, S., Liu, C., Yamada, K.M. & Adelstein, R.S. Defects in cell adhesion and the visceral endoderm following ablation of nonmuscle myosin heavy chain II-A in mice. *J Biol Chem* **279**, 41263-41266 (2004).
226. Ma, X., Bao, J. & Adelstein, R.S. Loss of cell adhesion causes hydrocephalus in nonmuscle myosin II-B-ablated and mutated mice. *Mol Biol Cell* **18**, 2305-2312 (2007).
227. Ivanov, A.I. *et al.* A unique role for nonmuscle myosin heavy chain IIA in regulation of epithelial apical junctions. *PLoS ONE* **2**, e658 (2007).
228. Yamazaki, Y. *et al.* ZO-1- and ZO-2-dependent integration of myosin-2 to epithelial zonula adherens. *Mol Biol Cell* **19**, 3801-3811 (2008).
229. Hirase, T. *et al.* Regulation of tight junction permeability and occludin phosphorylation by Rhoa-p160ROCK-dependent and -independent mechanisms. *J Biol Chem* **276**, 10423-10431 (2001).
230. Amano, M. *et al.* Phosphorylation and activation of myosin by Rho-associated kinase (Rho-kinase). *J Biol Chem* **271**, 20246-20249 (1996).
231. Essler, M. *et al.* Pasteurella multocida toxin increases endothelial permeability via Rho kinase and myosin light chain phosphatase. *J. Immunol.* **161**, 5640-5646 (1998).
232. Turner, J.R. *et al.* Physiological regulation of epithelial tight junctions is associated with myosin light-chain phosphorylation. *Am. J. Physiol.* **273**, C1378-C1385 (1997).
233. Turner, J.R. *et al.* PKC-dependent regulation of transepithelial resistance: roles of MLC and MLC kinase. *Am. J. Physiol.* **277**, C554-562 (1999).
234. Zolotarevsky, Y. *et al.* A membrane-permeant peptide that inhibits MLC kinase restores barrier function in in vitro models of intestinal disease. *Gastroenterology* **123**, 163-172 (2002).
235. Ma, T.Y., Boivin, M.A., Ye, D., Pedram, A. & Said, H.M. Mechanism of TNF-{alpha} modulation of Caco-2 intestinal epithelial tight junction barrier: role of myosin light-chain kinase protein expression. *Am. J. Physiol. Gastrointest. Liver Physiol.* **288**, G422-430 (2005).
236. Shen, L. *et al.* Myosin light chain phosphorylation regulates barrier function by remodeling tight junction structure. *J Cell Sci* **119**, 2095-2106 (2006).
237. Sahai, E. & Marshall, C.J. ROCK and Dia have opposing effects on adherens junctions downstream of Rho. *Nat. Cell Biol.* **4**, 408-415. (2002).
238. Gavard, J., Patel, V. & Gutkind, J.S. Angiopoietin-1 prevents VEGF-induced endothelial permeability by sequestering Src through mDia. *Dev Cell* **14**, 25-36 (2008).
239. Nonoguchi, K. *et al.* Cloning of human cDNAs for Apg-1 and Apg-2, members of the Hsp110 family, and chromosomal assignment of their genes. *Gene* **237**, 21-28 (1999).
240. Bernard, O. Lim kinases, regulators of actin dynamics. *Int J Biochem Cell Biol* **39**, 1071-1076 (2007).
241. Nagumo, Y., Han, J., Bellila, A., Isoda, H. & Tanaka, T. Cofilin mediates tight-junction opening by redistributing actin and tight-junction proteins. *Biochem Biophys Res Commun* **377**, 921-925 (2008).
242. Gorovoy, M. *et al.* LIM kinase 1 promotes endothelial barrier disruption and neutrophil infiltration in mouse lungs. *Circ Res* **105**, 549-556 (2009).

243. Miyazaki, T., Honda, K. & Ohata, H. m-Calpain antagonizes RhoA overactivation and endothelial barrier dysfunction under disturbed shear conditions. *Cardiovasc Res* **85**, 530-541.
244. Chang, Y.C., Lee, H.H., Chen, Y.J., Bokoch, G.M. & Chang, Z.F. Contribution of guanine exchange factor H1 in phorbol ester-induced apoptosis. *Cell Death Differ* **13**, 2023-2032 (2006).
245. Gopalakrishnan, S., Raman, N., Atkinson, S.J. & Marrs, J.A. Rho GTPase signaling regulates tight junction assembly and protects tight junctions during ATP depletion. *Am. J. Physiol.* **275**, C798-809 (1998).
246. Yamamoto, M. *et al.* Phosphorylation of claudin-5 and occludin by rho kinase in brain endothelial cells. *Am J Pathol* **172**, 521-533 (2008).
247. Betanzos, A. *et al.* The tight junction protein ZO-2 associates with Jun, Fos and C/EBP transcription factors in epithelial cells. *Exp. Cell Res.* **292**, 51-66 (2004).
248. Huerta, M. *et al.* Cyclin D1 is transcriptionally down-regulated by ZO-2 via an E box and the transcription factor c-Myc. *Mol Biol Cell* **18**, 4826-4836 (2007).
249. Tsapara, A., Matter, K. & Balda, M.S. The Heat Shock Protein Apg-2 Binds to the Tight Junction Protein ZO-1 and Regulates Transcriptional Activity of ZONAB. *Mol. Biol. Cell* **17**, 1322-1330 (2006).
250. Aijaz, S., Sanchez-Heras, E., Balda, M.S. & Matter, K. Regulation of tight junction assembly and epithelial morphogenesis by the heat shock protien Apg-2. *BMC Cell Biol.* (2007).
251. Frankel, P. *et al.* RalA interacts with ZONAB in a cell density-dependent manner and regulates its transcriptional activity. *EMBO J.* **24**, 54-62 (2005).
252. Sugihara, K. *et al.* The exocyst complex binds the small GTPase RalA to mediate filopodia formation. *Nat Cell Biol* **4**, 73-78 (2002).
253. Yasen, M. *et al.* The up-regulation of Y-box binding proteins (DNA binding protein A and Y-box binding protein-1) as prognostic markers of hepatocellular carcinoma. *Clin Cancer Res* **11**, 7354-7361 (2005).
254. Wang, G.R. *et al.* Upregulation of human DNA binding protein A (dbpA) in gastric cancer cells. *Acta Pharmacol Sin* **30**, 1436-1442 (2009).
255. Birkenfeld, J., Nalbant, P., Yoon, S.H. & Bokoch, G.M. Cellular functions of GEF-H1, a microtubule-regulated Rho-GEF: is altered GEF-H1 activity a crucial determinant of disease pathogenesis? *Trends Cell Biol* **18**, 210-219 (2008).
256. Quantock, A.J. & Young, R.D. Development of the corneal stroma, and the collagen-proteoglycan associations that help define its structure and function. *Dev Dyn* **237**, 2607-2621 (2008).
257. Green, K. Corneal endothelial structure and function under normal and toxic conditions. *Cell Biol Rev* **25**, 169-207 (1991).
258. Hanna, C. & O'Brien, J.E. Cell production and migration in the epithelial layer of the cornea. *Arch Ophthalmol* **64**, 536-539 (1960).
259. Goldberg, M.F. & Bron, A.J. Limbal palisades of Vogt. *Trans Am Ophthalmol Soc* **80**, 155-171 (1982).
260. Thoft, R.A. & Friend, J. The X, Y, Z hypothesis of corneal epithelial maintenance. *Invest Ophthalmol Vis Sci* **24**, 1442-1443 (1983).
261. Suzuki, K. *et al.* Cell-matrix and cell-cell interactions during corneal epithelial wound healing. *Prog Retin Eye Res* **22**, 113-133 (2003).
262. Murakami, J., Nishida, T. & Otori, T. Coordinated appearance of beta 1 integrins and fibronectin during corneal wound healing. *J Lab Clin Med* **120**, 86-93 (1992).

263. Gipson, I.K. Adhesive mechanisms of the corneal epithelium. *Acta Ophthalmol Suppl*, 13-17 (1992).
264. Stepp, M.A. Corneal integrins and their functions. *Exp Eye Res* **83**, 3-15 (2006).
265. Stepp, M.A., Spurr-Michaud, S. & Gipson, I.K. Integrins in the wounded and unwounded stratified squamous epithelium of the cornea. *Invest Ophthalmol Vis Sci* **34**, 1829-1844 (1993).
266. Fujikawa, L.S., Foster, C.S., Harrist, T.J., Lanigan, J.M. & Colvin, R.B. Fibronectin in healing rabbit corneal wounds. *Lab Invest* **45**, 120-129 (1981).
267. Suzuki, K., Tanaka, T., Enoki, M. & Nishida, T. Coordinated reassembly of the basement membrane and junctional proteins during corneal epithelial wound healing. *Invest Ophthalmol Vis Sci* **41**, 2495-2500 (2000).
268. Wang, Y., Chen, M. & Wolosin, J.M. ZO-1 in corneal epithelium; stratal distribution and synthesis induction by outer cell removal. *Exp Eye Res* **57**, 283-292 (1993).
269. Yu, F.S., Yin, J., Xu, K. & Huang, J. Growth factors and corneal epithelial wound healing. *Brain Res Bull* **81**, 229-235.
270. Grant, M.B., Khaw, P.T., Schultz, G.S., Adams, J.L. & Shimizu, R.W. Effects of epidermal growth factor, fibroblast growth factor, and transforming growth factor-beta on corneal cell chemotaxis. *Invest Ophthalmol Vis Sci* **33**, 3292-3301 (1992).
271. Wang, X., Kamiyama, K., Iguchi, I., Kita, M. & Imanishi, J. Enhancement of fibronectin-induced migration of corneal epithelial cells by cytokines. *Invest Ophthalmol Vis Sci* **35**, 4001-4007 (1994).
272. Daniels, J.T., Dart, J.K., Tuft, S.J. & Khaw, P.T. Corneal stem cells in review. *Wound Repair Regen* **9**, 483-494 (2001).
273. Anderson, S.C., Stone, C., Tkach, L. & SundarRaj, N. Rho and Rho-kinase (ROCK) signaling in adherens and gap junction assembly in corneal epithelium. *Invest Ophthalmol Vis Sci* **43**, 978-986 (2002).
274. Anderson, S.C. & SundarRaj, N. Regulation of a Rho-associated kinase expression during the corneal epithelial cell cycle. *Invest Ophthalmol Vis Sci* **42**, 933-940 (2001).
275. Yoshizaki, H. *et al.* Activity of Rho-family GTPases during cell division as visualized with FRET-based probes. *J. Cell Biol.* **162**, 223-232 (2003).
276. Matter, K., McDowell, W., Schwarz, R.T. & Hauri, H.-P. Asynchronous transport to the cell surface of intestinal brush border hydrolases is not due to differential trimming of N-linked oligosaccharides. *J. Biol. Chem.* **264** (1989).
277. Jaffe, A.B., Kaji, N., Durgan, J. & Hall, A. Cdc42 controls spindle orientation to position the apical surface during epithelial morphogenesis. *J Cell Biol* **183**, 625-633 (2008).
278. Balda, M.S. *et al.* Functional dissociation of paracellular permeability and transepithelial electrical resistance and disruption of the apical-basolateral intramembrane diffusion barrier by expression of a mutant tight junction membrane protein. *J Cell Biol* **134**, 1031-1049 (1996).
279. Seeber, J.W. *et al.* Characterisation of human corneal epithelial cell cultures maintained under serum-free conditions. *Altern Lab Anim* **36**, 569-583 (2008).
280. Yamada, S. & Nelson, W.J. Localized zones of Rho and Rac activities drive initiation and expansion of epithelial cell-cell adhesion. *J Cell Biol* **178**, 517-527 (2007).

281. Kawai, K., Kiyota, M., Seike, J., Deki, Y. & Yagisawa, H. START-GAP3/DLC3 is a GAP for RhoA and Cdc42 and is localized in focal adhesions regulating cell morphology. *Biochem Biophys Res Commun* **364**, 783-789 (2007).
282. Leung, T.H. *et al.* Deleted in liver cancer 2 (DLC2) suppresses cell transformation by means of inhibition of RhoA activity. *Proc Natl Acad Sci U S A* **102**, 15207-15212 (2005).
283. Brandt, S., Kwok, T., Hartig, R., Konig, W. & Backert, S. NF-kappaB activation and potentiation of proinflammatory responses by the Helicobacter pylori CagA protein. *Proc Natl Acad Sci U S A* **102**, 9300-9305 (2005).
284. Cao, Y. & Karin, M. NF-kappaB in mammary gland development and breast cancer. *J Mammary Gland Biol Neoplasia* **8**, 215-223 (2003).
285. Hamaguchi, M. *et al.* DBC2, a candidate for a tumor suppressor gene involved in breast cancer. *Proc Natl Acad Sci U S A* **99**, 13647-13652 (2002).
286. Espinosa, E.J., Calero, M., Sridevi, K. & Pfeffer, S.R. RhoBTB3: a Rho GTPase-family ATPase required for endosome to Golgi transport. *CELL* **137**, 938-948 (2009).
287. Morimoto, S. *et al.* Rab13 mediates the continuous endocytic recycling of occludin to the cell surface. *J. Biol. Chem.* **280**, 2220-2228 (2005).
288. Sheth, B. *et al.* Differentiation of the epithelial apical junctional complex during mouse preimplantation development: a role for rab13 in the early maturation of the tight junction. *Mech Dev* **97**, 93-104 (2000).
289. Whitehead, I., Kirk, H. & Kay, R. Retroviral transduction and oncogenic selection of a cDNA encoding Dbs, a homolog of the Dbl guanine nucleotide exchange factor. *Oncogene* **10**, 713-721 (1995).
290. Horii, Y., Beeler, J.F., Sakaguchi, K., Tachibana, M. & Miki, T. A novel oncogene, ost, encodes a guanine nucleotide exchange factor that potentially links Rho and Rac signaling pathways. *EMBO J* **13**, 4776-4786 (1994).
291. Whitehead, I.P. *et al.* Dependence of Dbl and Dbs transformation on MEK and NF-kappaB activation. *Mol Cell Biol* **19**, 7759-7770 (1999).
292. Cheng, L., Mahon, G.M., Kostenko, E.V. & Whitehead, I.P. Pleckstrin homology domain-mediated activation of the rho-specific guanine nucleotide exchange factor Dbs by Rac1. *J Biol Chem* **279**, 12786-12793 (2004).
293. Leung, T., Chen, X.Q., Tan, I., Manser, E. & Lim, L. Myotonic dystrophy kinase-related Cdc42-binding kinase acts as a Cdc42 effector in promoting cytoskeletal reorganization. *Mol Cell Biol* **18**, 130-140 (1998).
294. Nakamura, N. *et al.* Phosphorylation of ERM proteins at filopodia induced by Cdc42. *Genes Cells* **5**, 571-581 (2000).
295. Wilkinson, S., Paterson, H.F. & Marshall, C.J. Cdc42-MRCK and Rho-ROCK signalling cooperate in myosin phosphorylation and cell invasion. *Nat Cell Biol* **7**, 255-261 (2005).
296. Tan, I., Yong, J., Dong, J.M., Lim, L. & Leung, T. A tripartite complex containing MRCK modulates lamellar actomyosin retrograde flow. *CELL* **135**, 123-136 (2008).
297. Ogita, H. & Takai, Y. Activation of Rap1, Cdc42, and rac by nectin adhesion system. *Methods Enzymol* **406**, 415-424 (2006).
298. Blomquist, A. *et al.* Identification and characterization of a novel Rho-specific guanine nucleotide exchange factor. *Biochem J* **352 Pt 2**, 319-325 (2000).

299. Samarin, S.N., Ivanov, A.I., Flatau, G., Parkos, C.A. & Nusrat, A. Rho/ROCK-II Signaling Mediates Disassembly of Epithelial Apical Junctions. *Mol Biol Cell* (2007).
300. Ivanov, A.I., Hunt, D., Utech, M., Nusrat, A. & Parkos, C.A. Differential roles for actin polymerization and a myosin II motor in assembly of the epithelial apical junctional complex. *Mol. Biol. Cell* **16**, 2636-2650 (2005).
301. Zegers, M.M., O'Brien, L.E., Yu, W., Datta, A. & Mostov, K.E. Epithelial polarity and tubulogenesis in vitro. *Trends Cell Biol* **13**, 169-176 (2003).
302. Sterpetti, P. *et al.* Activation of the Lbc Rho exchange factor proto-oncogene by truncation of an extended C terminus that regulates transformation and targeting. *Mol Cell Biol* **19**, 1334-1345 (1999).
303. Krendel, M., Zenke, F.T. & Bokoch, G.M. Nucleotide exchange factor GEF-H1 mediates cross-talk between microtubules and the actin cytoskeleton. *Nat Cell Biol* **4**, 294-301 (2002).
304. Sumi, T., Matsumoto, K., Takai, Y. & Nakamura, T. Cofilin phosphorylation and actin cytoskeletal dynamics regulated by rho- and Cdc42-activated LIM-kinase 2. *J Cell Biol* **147**, 1519-1532 (1999).
305. D'Atri, F. & Citi, S. Cingulin interacts with F-actin in vitro. *FEBS Lett.* **507**, 21-24 (2001).
306. Olson, M.F., Sterpetti, P., Nagata, K., Toksoz, D. & Hall, A. Distinct roles for DH and PH domains in the Lbc oncogene. *Oncogene* **15**, 2827-2831 (1997).
307. Noren, N.K., Arthur, W.T. & Burridge, K. Cadherin engagement inhibits RhoA via p190RhoGAP. *J. Biol. Chem.* **278**, 13615-13618 (2003).
308. Abouhamed, M. *et al.* Myosin IXa regulates epithelial differentiation and its deficiency results in hydrocephalus. *Mol Biol Cell* **20**, 5074-5085 (2009).
309. Nishimura, T. & Takeichi, M. Shroom3-mediated recruitment of Rho kinases to the apical cell junctions regulates epithelial and neuroepithelial planar remodeling. *Development* **135**, 1493-1502 (2008).
310. Hildebrand, J.D. Shroom regulates epithelial cell shape via the apical positioning of an actomyosin network. *J Cell Sci* **118**, 5191-5203 (2005).
311. Dawes-Hoang, R.E. *et al.* folded gastrulation, cell shape change and the control of myosin localization. *Development* **132**, 4165-4178 (2005).
312. Lee, J.Y. & Harland, R.M. Actomyosin contractility and microtubules drive apical constriction in Xenopus bottle cells. *Dev Biol* **311**, 40-52 (2007).
313. Ivanov, A.I. *et al.* Myosin II regulates the shape of three-dimensional intestinal epithelial cysts. *J Cell Sci* **121**, 1803-1814 (2008).
314. Qin, Y., Meisen, W.H., Hao, Y. & Macara, I.G. Tuba, a Cdc42 GEF, is required for polarized spindle orientation during epithelial cyst formation. *J Cell Biol* **189**, 661-669.
315. Fukata, M., Nakagawa, M. & Kaibuchi, K. Roles of Rho-family GTPases in cell polarisation and directional migration. *Curr Opin Cell Biol* **15**, 590-597 (2003).
316. Ridley, A.J. Rho GTPases and cell migration. *J Cell Sci* **114**, 2713-2722 (2001).
317. Machacek, M. *et al.* Coordination of Rho GTPase activities during cell protrusion. *Nature* **461**, 99-103 (2009).
318. Pertz, O., Hodgson, L., Klemke, R.L. & Hahn, K.M. Spatiotemporal dynamics of RhoA activity in migrating cells. *Nature* **440**, 1069-1072 (2006).
319. Francis, S.A., Shen, X., Young, J.B., Kaul, P. & Lerner, D.J. Rho GEF Lsc is required for normal polarization, migration, and adhesion of formyl-peptide-stimulated neutrophils. *Blood* **107**, 1627-1635 (2006).

320. Nalbant, P., Chang, Y.C., Birkenfeld, J., Chang, Z.F. & Bokoch, G.M. Guanine nucleotide exchange factor-H1 regulates cell migration via localized activation of RhoA at the leading edge. *Mol Biol Cell* **20**, 4070-4082 (2009).
321. Yamauchi, J., Miyamoto, Y., Tanoue, A., Shooter, E.M. & Chan, J.R. Ras activation of a Rac1 exchange factor, Tiam1, mediates neurotrophin-3-induced Schwann cell migration. *Proc Natl Acad Sci U S A* **102**, 14889-14894 (2005).
322. Liu, Z., Adams, H.C., 3rd & Whitehead, I.P. The rho-specific guanine nucleotide exchange factor Dbs regulates breast cancer cell migration. *J Biol Chem* **284**, 15771-15780 (2009).
323. Du, D. *et al.* The tight junction protein, occludin, regulates the directional migration of epithelial cells. *Dev Cell* **18**, 52-63.
324. Shin, K., Wang, Q. & Margolis, B. PATJ regulates directional migration of mammalian epithelial cells. *EMBO Rep* **8**, 158-164 (2007).
325. Greenberg, L. & Hatini, V. Systematic expression and loss-of-function analysis defines spatially restricted requirements for DrosophilaRhoGEFs and RhoGAPs in leg morphogenesis. *Mech Dev*.
326. Rogers, S.L., Wiedemann, U., Hacker, U., Turck, C. & Vale, R.D. Drosophila RhoGEF2 associates with microtubule plus ends in an EB1-dependent manner. *Curr Biol* **14**, 1827-1833 (2004).
327. Oleksy, A. *et al.* Preliminary crystallographic analysis of the complex of the human GTPase RhoA with the DH/PH tandem of PDZ-RhoGEF. *Acta Crystallogr D Biol Crystallogr* **60**, 740-742 (2004).
328. Padash Barmchi, M., Rogers, S. & Hacker, U. DRhoGEF2 regulates actin organization and contractility in the Drosophila blastoderm embryo. *J Cell Biol* **168**, 575-585 (2005).
329. Galiana-Arnoux, D., Dostert, C., Schneemann, A., Hoffmann, J.A. & Imler, J.L. Essential function in vivo for Dicer-2 in host defense against RNA viruses in drosophila. *Nat Immunol* **7**, 590-597 (2006).
330. Jou, T.S. & Nelson, W.J. Effects of regulated expression of mutant RhoA and Rac1 small GTPases on the development of epithelial (MDCK) cell polarity. *J. Cell Biol.* **142**, 85-100 (1998).
331. Ridley, A.J., Allen, W.E., Peppelenbosch, M. & Jones, G.E. Rho family proteins and cell migration. *Biochem. Soc. Symp.* **65**, 111-123 (1999).

Websites

Bioinformatics harvester http://harvester.fzk.de/harvester/

Flybase http://flybase.org/

Pfam http://pfam.sanger.ac.uk/

Phosphosite http://www.phosphosite.org

Scan site http://scansite.mit.edu/

VDRC http://stockcenter.vdrc.at

Appendix

Antibodies

All antibodies are listed in alphabetical order and state the host species in which they were raised and were possible the clone number and the source they were obtained from, also shown are dilutions/concentrations if the antibody was used for Immunfluoresence (IF), Immunoblotting (IB) and Immunoprecipitation (IP) Zona Occludens-1,2 and 3, α Tubulin, VSV, and GEF-H1, anti GST described previously [212].

Antibody	**Host Species**	**Clone**	**Source**	**IF Dilution**	**IB Dilution**	**IP (μg)**
Alpha Tubulin	Mouse	1A2	Matter Lab	1:10	1:20	-
Alpha-Catenin	Rabbit	Poly	Sigma	1:2000	1:4000	-
ARHGEF18/p114RhoGEF	Goat	Poly	Everest	1:200	1:1000	1.5
Beta -Catenin	Goat	Poly E-17	Santa Cruz	1:100	1:1000	-
Cingulin	Rabbit	Poly	Zymed	1:2000	1:5000	1.5
Cofilin	Mouse	Mono	BD	-	1:500	-

		32/Cofilin				
E-Cadherin	Mouse	Mono 36/E-cad	BD	1:500	1:1000	-
GEF-H1	Mouse	B4/7	Matter lab	1:5	1:5	-
Giantin	Mouse	Mono	Matter lab	1:500	-	-
GST	Rabbit	Poly	Matter lab	-	1:2000	-
Myc	Mouse	Mono 9E10	Matter lab	1:200	1:1000	-
Myosin IIA	Rabbit	Poly	Sigma	1:2000	1:5000	1.5
Myosin light chain MLC	Rabbit	Poly	Cell signalling	1:200	1:500	
Myosin light chain phosphotase MYPT1	Sheep	Poly	Millipore	-	1:5000	
Occludin	Mouse	Mono OC-3F10	Invirogen	1:2000	1:5000	1.5
p115RhoGEF(Lsc)	Goat	Poly H-19	Santa Cruz	-	1:1000	1.5
Phospho	Rabbit	Mono77G2	Cell	-	1:500	-

Cofilin			signalling			
Phospho T18,S19 MLC	Rabbit	Poly	Cell signalling	1:200	1:500	-
Phospho T696 MYPT1	Sheep	Poly	Millipore	-	1:1000	-
ROCK I	Mouse	Mono	BD	-	1:1000	-
ROCK II	Mouse	Mono	BD	1:200	1:1000	-
Shroom3	Goat	T-17	Santa Cruz	-	1:1000	-
VSV	Rabbit	Poly 4921	Matter Lab	1:1000	1:2000	-
ZO-1	Rabbit	Poly 4913	Matter Lab	1:400	1:1000	1.5

siRNAs for screens

Below is a complete list of siRNAs and their target genes used in the RhoGTPase siRNA library purchased from Dhamacon. There are four individual siRNA sequences per gene used as a pool in the screen and de-convoluted into individuals siRNAs for validation.

Catalog Number	Gene Symbol	Locus ID	Accession	Sequence
D-006823-01	**INCENP**	**3619**	**NM_020238**	**CCACGAUGCUGACUAAGAA**
D-001206-13	**si*CONTROL* Non-Targeting siRNA Pool**			
D-008611-01	ABR	29	NM_001092	GAAGAUCUCUGCCCUCAAG
D-008611-02	ABR	29	NM_001092	CAACCUGGCUACCGUGUUU
D-008611-03	ABR	29	NM_001092	GAAGAGAUCUACAUUAACC
D-008611-04	ABR	29	NM_001092	CAGAGGAACUCAAAGUGAA
D-008868-05	AKAP13	11214	NM_006738	GGAAGAAGCUUGUACGUGA
D-008868-01	AKAP13	11214	NM_006738	GAAGACAUAUGGCAAGUUU
D-008868-02	AKAP13	11214	NM_006738	CGAAACAGCUGGAUUCAGA
D-008868-03	AKAP13	11214	NM_006738	UCAACAGACUCACUAAAUA
D-014168-01	ALS2	57679	NM_020919	GAAUUUAGGCUCUGAGGUA
D-014168-02	ALS2	57679	NM_020919	GGAUAAUGAUCGCGAGGAA
D-006823-02	**INCENP**	**3619**	**NM_020238**	**CAAGAAGACUGCCGAAGAG**
D-001500-01	**si*TOX* Transfection Control**			
D-014168-03	ALS2	57679	NM_020919	GCUUAGCCCUUGUACAAUG
D-014168-04	ALS2	57679	NM_020919	AGAGCCAGGUUAUGUAGUA
D-008966-01	ARHGAP1	392	NM_004308	GCCAAGUGCUCAAAUAUGA
D-008966-02	ARHGAP1	392	NM_004308	GGAGACUGUUGCCUACUUA
D-008966-03	ARHGAP1	392	NM_004308	GGCAGGAGAUGACAAGUAU
D-008966-04	ARHGAP1	392	NM_004308	GAUCUGACCUUGGAUGACA
D-009382-01	FLJ20896	79658	NM_024605	GUGAAACACUUAACAAAUG
D-009382-02	FLJ20896	79658	NM_024605	GAAGUGAAGACAAUAACAA
D-009382-03	FLJ20896	79658	NM_024605	GGAGAAUUCUGCAGAUUGG
D-009382-04	FLJ20896	79658	NM_024605	GAAUAUUGUUGUGGAAAUC
D-006823-03	**INCENP**	**3619**	**NM_020238**	**UCUGCAACAUGGAUAAUAA**
D-021122-01	ARHGAP11A	9824	NM_014783	UACAGACUCUUAUCGAUUA
D-021122-02	ARHGAP11A	9824	NM_014783	GUUCGAAGAUCUCUGCGUU
D-021122-03	ARHGAP11A	9824	NM_014783	GGUAUCAGUUCACAUCGAU
D-021122-04	ARHGAP11A	9824	NM_014783	AAGCGUACAUUGCCAGUAG
D-018019-01	ARHGAP15	55843	NM_018460	GAAAUGAGUUCCUUCUACA
D-018019-02	ARHGAP15	55843	NM_018460	GAUGCAAUAUAUCGAGUUA
D-018019-03	ARHGAP15	55843	NM_018460	GAACCUAUAUCCAGACACA
D-018019-04	ARHGAP15	55843	NM_018460	GCACUGAAUUGCUAAGUCA
D-008335-01	ARHGAP17	55114	NM_018054	GCAGACAUGUACAACUUUA
D-008335-02	ARHGAP17	55114	NM_018054	AAACAGAAGUCCUUAGUGA
D-006823-04	**INCENP**	**3619**	**NM_020238**	**GCAAAGAGCCAGAGCUGAU**
D-008335-03	ARHGAP17	55114	NM_018054	GGGAGCAGCUUGCAAGAUU

D-008335-04	ARHGAP17	55114	NM_018054	CUGAAGAGGUGGAAUUUAA
D-015110-01	ARHGAP18	93663	NM_033515	GGAAACAGAAGGCCUCUUA
D-015110-02	ARHGAP18	93663	NM_033515	UGACAGCGCUAUUAGAACA
D-015110-03	ARHGAP18	93663	NM_033515	CGAGGCAUCUAACCUUGUU
D-015110-04	ARHGAP18	93663	NM_033515	CCAUGCACUUAUUGAUUAA
D-026514-01	ARHGAP20	57569	NM_020809	GCACUCACCUGGACAACUU
D-026514-02	ARHGAP20	57569	NM_020809	GCUCAUUAAUCAGAGUUUA
D-026514-03	ARHGAP20	57569	NM_020809	GAAUUGUGCCUACUCUAAA
D-026514-04	ARHGAP20	57569	NM_020809	CCAUCCGGCUCAUCAGUAA
D-003317-05	**KIF11**	**3832**	**NM_004523**	**GCAGAAAUCUAAGGAUAUA**
D-004775-01	ARHGAP21	57584	NM_020824	UAAAGAAGCUGUCAUCCUA
D-004775-02	ARHGAP21	57584	NM_020824	GGAGACAGCUCUUCAGUUC
D-004775-03	ARHGAP21	57584	NM_020824	AAAGGAAACUUCUCAGUAA
D-004775-04	ARHGAP21	57584	NM_020824	GUAAAUCACUUGCAUCAGA
D-019080-01	ARHGAP22	58504	NM_021226	CUAGGAAGCUUGACUGUUG
D-019080-02	ARHGAP22	58504	NM_021226	GGGAUCAGCUUUUCUACUA
D-019080-03	ARHGAP22	58504	NM_021226	AUUACAACCUGCUCAGAUA
D-019080-04	ARHGAP22	58504	NM_021226	GGGAUUUAUUUCUCUACAA
D-023061-01	ARHGAP23	57636	XM_290799	GAAGACGGCCCUGCCCAUA
D-023061-02	ARHGAP23	57636	XM_290799	GGAACGAGCCGUAUUCUGG
D-003317-06	**KIF11**	**3832**	**NM_004523**	**CAACAAGGAUGAAGUCUAU**
D-023061-03	ARHGAP23	57636	XM_290799	GGGAAAGCGUCAUUGGGAA
D-023061-04	ARHGAP23	57636	XM_290799	GAAUGGAGGCCGUGGAGGA
D-014713-01	ARHGAP24	83478	NM_031305	AGAACAAGCUGGAGAGUUA
D-014713-02	ARHGAP24	83478	NM_031305	GGAGGAUACUGUUCGUUAU
D-014713-03	ARHGAP24	83478	NM_031305	CGAGAGAGGAAACACAAUA
D-014713-04	ARHGAP24	83478	NM_031305	GGUCUUUGGUCCUAAUAUC
D-021175-01	ARHGAP25	9938	XM_376060	GGACUUCCACCUACGAUAA
D-021175-02	ARHGAP25	9938	XM_376060	GAUCAGAGACCAUGAAGUC
D-021175-03	ARHGAP25	9938	XM_376060	GCAGGUUCCUACAUGAAAU
D-021175-04	ARHGAP25	9938	XM_376060	CAAGAGCUACGAAAGGAAA
D-003317-07	**KIF11**	**3832**	**NM_004523**	**CAGCAGAAAUCUAAGGAUA**
D-008426-01	ARHGAP26	23092	NM_015071	GAACAUGACUCAGAACUUU
D-008426-02	ARHGAP26	23092	NM_015071	CCAAACAGCAUCCUUAAUU
D-008426-03	ARHGAP26	23092	NM_015071	CAUAGGAGAUGCAGAAACA
D-008426-04	ARHGAP26	23092	NM_015071	GAAAGAAUCUCAGCUUCAG
D-027281-01	LOC201176	201176	NM_199282	CCGAGUCGCUGACCAGUUA
D-027281-02	LOC201176	201176	NM_199282	GAAAGCGGCUCCGGAAGAA
D-027281-03	LOC201176	201176	NM_199282	GGACUCCUCUGUUCGAUGG
D-027281-04	LOC201176	201176	NM_199282	GCACUUCCGCCAGUUCAUU
D-031016-01	ARHGAP28	79822	NM_001010000	GAAGCAAACACUCUGAUUA
D-031016-03	ARHGAP28	79822	NM_001010000	CCAUUCAACUCAACAAUCA
D-003317-08	**KIF11**	**3832**	**NM_004523**	**CUAGAUGGCUUUCUCAGUA**
D-031016-05	ARHGAP28	79822	NM_001010000	GAAUAUAUACCUGCCUUCA
D-031016-06	ARHGAP28	79822	NM_001010000	GUGAAGAACUUGAUGCCAA
D-003628-05	ARHGAP4	393	NM_001666	CGCAAGAGCUCCCUCAAGA
D-003628-01	ARHGAP4	393	NM_001666	GCUGAGAUCUGCGUUGAAA
D-003628-03	ARHGAP4	393	NM_001666	GGAGACAUGGAGAAGUUUA
D-003628-04	ARHGAP4	393	NM_001666	GACAGACCAUUGAGACAGA
D-009580-03	ARHGAP5	394	NM_001173	GUACGAAUUUGCAACCAUA
D-009580-04	ARHGAP5	394	NM_001173	UGAAAGCGCUCGUUCCAAA
D-009580-01	ARHGAP5	394	NM_001173	GAGAGCAGAUUUCCAGUUA
D-009580-02	ARHGAP5	394	NM_001173	UGAGAUCACUGCUAAAUUU

D-006823-01	**INCENP**	**3619**	**NM_020238**	**CCACGAUGCUGACUAAGAA**
D-001206-13	**si*CONTROL* Non-Targeting siRNA Pool**			
D-009304-02	ARHGAP6	395	NM_001174	AAACUUAGCCACCAUAUUU
D-009304-03	ARHGAP6	395	NM_001174	GUACACAGCUUUCAUCAAC
D-009304-01	ARHGAP6	395	NM_001174	GAAACUGGAUUCACUAGGA
D-009304-04	ARHGAP6	395	NM_001174	CAUCAUCGCUGUUGUGCAA
D-009427-01	ARHGAP8	23779	NM_181334	ACAAGGAGUUCGAUAGGAA
D-009427-02	ARHGAP8	23779	NM_181334	GAUAGGAAGUACAAGAAGA
D-009427-03	ARHGAP8	23779	NM_181334	GCAUACAAGGAGUUCGAUA
D-009427-04	ARHGAP8	23779	NM_181334	CCGUGAACUUUGACGACUA
D-010047-01	ARHGAP9	64333	NM_032496	GAACAAUGAUGUCCUGCAA
D-010047-02	ARHGAP9	64333	NM_032496	GAAGAGACCGCCCUUACAA
D-006823-02	**INCENP**	**3619**	**NM_020238**	**CAAGAAGACUGCCGAAGAG**
D-001500-01	**si*TOX* Transfection Control**			
D-010047-03	ARHGAP9	64333	NM_032496	GAAGGUCGGUUAGAUUUGG
D-010047-04	ARHGAP9	64333	NM_032496	GGGCCGAAGUUGUUUCAUG
D-016253-01	ARHGDIA	396	NM_004309	CAGGAAAGGCGUCAAGAUU
D-016253-02	ARHGDIA	396	NM_004309	GGUGUGGAGUACCGGAUAA
D-016253-03	ARHGDIA	396	NM_004309	CCGGGUUAACCGAGAGAUA
D-016253-04	ARHGDIA	396	NM_004309	AGGAUGAGCACUCGGUCAA
D-010893-05	ARHGDIB	397	NM_001175	GAUGAGAGUCUAAUUAAGU
D-010893-02	ARHGDIB	397	NM_001175	ACAGCAAGCUCAAUUAUAA
D-010893-03	ARHGDIB	397	NM_001175	GAAAGUGGAUAAAGCAACA
D-010893-04	ARHGDIB	397	NM_001175	GGAAGGUUCUGAAUAUAGA
D-006823-03	**INCENP**	**3619**	**NM_020238**	**UCUGCAACAUGGAUAAUAA**
D-012566-01	ARHGDIG	398	NM_001176	GGAAGGUGUUGAUUACAGA
D-012566-02	ARHGDIG	398	NM_001176	CCAGGAGUAUGAGUUUGUG
D-012566-03	ARHGDIG	398	NM_001176	UCAGCGGCCUCAAGUGUCU
D-012566-04	ARHGDIG	398	NM_001176	AUGAGGCUGUGCCCGAGUA
D-009421-01	ARHGEF1	9138	NM_004706	AGAACGAGCUGGAGACAAA
D-009421-02	ARHGEF1	9138	NM_004706	CAACGUCGCCUUUGAACUU
D-009421-03	ARHGEF1	9138	NM_004706	GGUGUGCUCUCAUCACUGA
D-009421-04	ARHGEF1	9138	NM_004706	UGACGUGGCGGGUGACUAA
D-013460-01	ARHGEF10	9639	NM_014629	GAACCUUACCUAAAUAAUG
D-013460-02	ARHGEF10	9639	NM_014629	GAAUACGGAUGGAGUUCGA
D-006823-04	**INCENP**	**3619**	**NM_020238**	**GCAAAGAGCCAGAGCUGAU**
D-013460-03	ARHGEF10	9639	NM_014629	GACGAUGGGAAUCACAUUA
D-013460-04	ARHGEF10	9639	NM_014629	GACCUAACCCGUUUAAAGG
D-010360-01	ARHGEF11	9826	NM_014784	GAACCUGCCUGAACUCAUA
D-010360-02	ARHGEF11	9826	NM_014784	GGAAAGACAUCUGGAAUAU
D-010360-03	ARHGEF11	9826	NM_014784	GCAAGUGGCUGCACAGUUC
D-010360-04	ARHGEF11	9826	NM_014784	GAAGAUCCCUGAGAUGCUA
D-008480-01	ARHGEF12	23365	NM_015313	AGACAGAGAUUUGGGAUUA
D-008480-02	ARHGEF12	23365	NM_015313	GGAGGAAUGUGAAGUAGAA
D-008480-03	ARHGEF12	23365	NM_015313	GAGAAGACCUGAGCUCAUU
D-008480-04	ARHGEF12	23365	NM_015313	GACAGGAAGUGAUUAAUGA
D-003317-05	**KIF11**	**3832**	**NM_004523**	**GCAGAAAUCUAAGGAUAUA**
D-009731-01	ARHGEF15	22899	NM_173728	UGAUGAAGCUCCUCAGAAU
D-009731-02	ARHGEF15	22899	NM_173728	GCAUGAAGCAGACUGAAGA
D-009731-03	ARHGEF15	22899	NM_173728	GGUUACAGGUUCUGGACUA
D-009731-04	ARHGEF15	22899	NM_173728	GAACGGUGCUCCAGAUGCU
D-010234-01	ARHGEF16	27237	NM_014448	GCGGAGAGCUGUUCUUAGU
D-010234-02	ARHGEF16	27237	NM_014448	GAUACGCUCUGCCUCAAGA
D-010234-03	ARHGEF16	27237	NM_014448	CCAACGAGGUCUACCAACA
D-010234-04	ARHGEF16	27237	NM_014448	GUUCAACGAUGUCCUGGUU

D-009751-01	ARHGEF17	9828	NM_014786	GCACCACUCUGAAGCGAAA
D-009751-02	ARHGEF17	9828	NM_014786	GAGCAAAGCAUGCGUGAGA
D-003317-06	**KIF11**	**3832**	**NM_004523**	**CAACAAGGAUGAAGUCUAU**
D-009751-04	ARHGEF17	9828	NM_014786	GCUACGAGCUUCUGGUGAA
D-009751-05	ARHGEF17	9828	NM_014786	AGUGAUGGGUUAAAUCUAA
D-009654-01	ARHGEF18	23370	NM_015318	GCACAGAGCCUCCUAGAGA
D-009654-02	ARHGEF18	23370	NM_015318	UCAGGGCGCUUGAAAGAUA
D-009654-03	ARHGEF18	23370	NM_015318	CAAGAGCGGUUGAGCAUGA
D-009654-04	ARHGEF18	23370	NM_015318	GCACUGAGGACUAUGAAGA
D-008370-05	ARHGEF19	128272	NM_153213	GGAGUGCAAUGCUAGUGUA
D-008370-06	ARHGEF19	128272	NM_153213	AAUGGAGGCUCGAAGUGUA
D-008370-01	ARHGEF19	128272	NM_153213	GAGUCUACCUGCCCUAUGU
D-008370-03	ARHGEF19	128272	NM_153213	GGACAAGCAGUGGCUGUUU
D-003317-07	**KIF11**	**3832**	**NM_004523**	**CAGCAGAAAUCUAAGGAUA**
D-009883-01	ARHGEF2	9181	NM_004723	GGACAAGCCUUCAGUGGUA
D-009883-02	ARHGEF2	9181	NM_004723	CAACAUUGCUGGACAUUUC
D-009883-03	ARHGEF2	9181	NM_004723	GAAUUAAGAUGGAGUUGCA
D-009883-05	ARHGEF2	9181	NM_004723	GUGCGGAGCAGAUGUGUAA
D-013243-01	ARHGEF3	50650	NM_019555	CAAACUAGAUCUCUGGAAU
D-013243-02	ARHGEF3	50650	NM_019555	CGAGGGAUCGUUCCUAAAU
D-013243-03	ARHGEF3	50650	NM_019555	GUGAAGGCCACGCCAUUAA
D-013243-04	ARHGEF3	50650	NM_019555	UGGCUUAACUGUAUUCGUC
D-008235-01	ARHGEF4	50649	NM_015320	GCACAAAGAUGGAGUCAAG
D-008235-02	ARHGEF4	50649	NM_015320	GAAAGGAGGCUGCACAUAG
D-003317-08	**KIF11**	**3832**	**NM_004523**	**CUAGAUGGCUUUCUCAGUA**
D-008235-03	ARHGEF4	50649	NM_015320	UCACCAAGCUCAGCAAGUA
D-008235-04	ARHGEF4	50649	NM_015320	GCUCAGAACUCAUCUACUC
D-005093-01	ARHGEF5	7984	NM_005435	GCACGGAGACUCAAAGUGA
D-005093-02	ARHGEF5	7984	NM_005435	GGACAGAGGAGCUAAUCUA
D-005093-03	ARHGEF5	7984	NM_005435	GCCAGAAGAUUGAGUUUGA
D-005093-04	ARHGEF5	7984	NM_005435	CAAUGGCUCUUCUCUCGUU
D-010231-04	ARHGEF6	9459	NM_004840	GAACGGUGGUGACUAGAUU
D-010231-01	ARHGEF6	9459	NM_004840	GAGGAUGUCUUAUAUCUUA
D-010231-02	ARHGEF6	9459	NM_004840	GGAAGAAUGUUCAAAGUUU
D-010231-03	ARHGEF6	9459	NM_004840	GGACGUUCCUCUUCUCUUA
D-006823-01	**INCENP**	**3619**	**NM_020238**	**CCACGAUGCUGACUAAGAA**
D-001206-13	**si*CONTROL* Non-Targeting siRNA Pool**			
D-009616-01	ARHGEF7	8874	NM_003899	GGAAGAAGAUGCUCAGAUU
D-009616-02	ARHGEF7	8874	NM_003899	GAAGAGCCCUCCCAAAGGA
D-009616-03	ARHGEF7	8874	NM_003899	UCAAAGAGCUCGAGAGACA
D-009616-04	ARHGEF7	8874	NM_003899	GGAGGGCGAUGACAUUAAA
D-020314-01	ARHGEF9	23229	XM_377014	UGGCUGAGCUCCUAAAGUA
D-020314-02	ARHGEF9	23229	XM_377014	GAUCUGCAAGUAUCCCUUA
D-020314-03	ARHGEF9	23229	XM_377014	CAAGCGACGUUUAGAGAAU
D-020314-04	ARHGEF9	23229	XM_377014	GAGAUUCCAUCGUUAGUGC
D-003875-02	BCR	613	NM_004327	GUAAAGCUCUCGGUCAAGU
D-003875-03	BCR	613	NM_004327	GCAUUCCGCUGACCAUCAA
D-006823-02	**INCENP**	**3619**	**NM_020238**	**CAAGAAGACUGCCGAAGAG**
D-001500-01	**si*TOX* Transfection Control**			
D-003875-06	BCR	613	NM_004327	CAGGAGCGCUUCCGCAUGA
D-003875-13	BCR	613	NM_004327	CAGAAGAAGUGUUUCAGAA
D-015006-01	C9ORF100	84904	NM_032818	CAACAGCCCUGACCAUCAA
D-015006-02	C9ORF100	84904	NM_032818	GGAGCUCUAUAACCAAUUU

D-015006-03	C9ORF100	84904	NM_032818	CGUCGUAGCUUUGGCUGAA
D-015006-04	C9ORF100	84904	NM_032818	AAAUAAAGGUUUCCGGAGG
D-005057-01	CDC42	998	NM_001791	GGAGAACCAUAUACUCUUG
D-005057-02	CDC42	998	NM_001791	GAUUACGACCGCUGAGUUA
D-005057-03	CDC42	998	NM_001791	GAUGACCCCUCUACUAUUG
D-005057-04	CDC42	998	NM_001791	CGGAAUAUGUACCGACUGU
D-006823-03	**INCENP**	**3619**	**NM_020238**	**UCUGCAACAUGGAUAAUAA**
D-003814-09	CDC42BPA	8476	NM_003607	CCAUAUAACUUGUGUAAAC
D-003814-01	CDC42BPA	8476	NM_003607	GGAAACAAAUGGUUAGAAA
D-003814-04	CDC42BPA	8476	NM_003607	GCGCAAGACUCACCAGUUU
D-003814-08	CDC42BPA	8476	NM_003607	GAAGAUAGAUUGCCUGAAG
D-004075-05	CDC42BPB	9578	NM_006035	GAAGUGGGUUGGGAUUCUA
D-004075-02	CDC42BPB	9578	NM_006035	GAAGAAUACUGAACGAAUU
D-004075-03	CDC42BPB	9578	NM_006035	GAGAAACACGGAAAUAUUA
D-004075-04	CDC42BPB	9578	NM_006035	CGAGAAGACUUUGAAAUAA
D-007691-05	HSMDPKIN	55561	XM_290516	GGAACCAUCCUUUCUUCGA
D-007691-06	HSMDPKIN	55561	XM_290516	CCACGCAUCUUUAGGGUGA
D-006823-04	**INCENP**	**3619**	**NM_020238**	**GCAAAGAGCCAGAGCUGAU**
D-007691-02	HSMDPKIN	55561	XM_290516	CAAGGACCCUGGCAUCUCA
D-007691-03	HSMDPKIN	55561	XM_290516	UAUCAAAGGUGAAAGAACU
D-017551-01	CDC42EP1	11135	NM_007061	GAAAGAGGCGGCUGACUGC
D-017551-02	CDC42EP1	11135	NM_007061	AUGAUGAGGUCAAGGUGUG
D-017551-03	CDC42EP1	11135	NM_007061	GGAAAAGCCGCAUGACCGA
D-017551-04	CDC42EP1	11135	NM_007061	GCCCAGUGGCUGAGGUGAA
D-012215-03	CDC42EP2	10435	NM_006779	CGCCACACCAUUCAUAUUG
D-012215-04	CDC42EP2	10435	NM_006779	CCAUCUAUCUGAAGCGUGG
D-012215-01	CDC42EP2	10435	NM_006779	GCAGUGACAUGUUUGGCGA
D-012215-02	CDC42EP2	10435	NM_006779	GCAUGCAGAUCCCCACAUA
D-003317-05	**KIF11**	**3832**	**NM_004523**	**GCAGAAAUCUAAGGAUAUA**
D-017358-01	CDC42EP3	10602	NM_006449	GAUGAGGUGCUGAAUGUAA
D-017358-02	CDC42EP3	10602	NM_006449	CCAAUAACAAGAAAGGAAA
D-017358-03	CDC42EP3	10602	NM_006449	GCUCUCAUGUUGCCCUUAU
D-017358-04	CDC42EP3	10602	NM_006449	CGAUGUCUUUGGAGAUAUU
D-013494-01	CDC42EP4	23580	NM_012121	CCAGUAAGCUGCCCAAGAG
D-013494-02	CDC42EP4	23580	NM_012121	CAAGACAGCCAGACAAGGA
D-013494-03	CDC42EP4	23580	NM_012121	GACACCUCCUUCCUCAAUA
D-013494-04	CDC42EP4	23580	NM_012121	CCCAUGCUCUGGAGGAUGA
D-017378-01	CDC42EP5	148170	NM_145057	CAAGGUGUGUGCCCGGAAA
D-017378-02	CDC42EP5	148170	NM_145057	CCACUUCUGUAUACAUAAA
D-003317-06	**KIF11**	**3832**	**NM_004523**	**CAACAAGGAUGAAGUCUAU**
D-017378-03	CDC42EP5	148170	NM_145057	CGUCAUCGGCCUCUAGGUU
D-017378-04	CDC42EP5	148170	NM_145057	CCAAGAAGCGGCCUGAUCG
D-013804-01	SPEC1	56882	NM_020239	CAGAUGAGAUCCAAGGGAA
D-013804-02	SPEC1	56882	NM_020239	GAAGACGGAUUGACCGGAC
D-013804-03	SPEC1	56882	NM_020239	GGACUUGCCAUGACAGGUG
D-013804-04	SPEC1	56882	NM_020239	CGAGAUAGGCCAUGGAGCA
D-020826-01	SPEC2	56990	NM_020240	UCAGUUAGCUCCAUUCAGA
D-020826-02	SPEC2	56990	NM_020240	CAGAACAGCCUCAGCCUAA
D-020826-03	SPEC2	56990	NM_020240	UGUUUCAACUGCUGUAUUG
D-020826-04	SPEC2	56990	NM_020240	GUGCAUACAGCUCAUGUUG
D-003317-07	**KIF11**	**3832**	**NM_004523**	**CAGCAGAAAUCUAAGGAUA**
D-009302-01	CENTD1	116984	NM_015230	GCAAGAAGCUUUAAAUUGA
D-009302-02	CENTD1	116984	NM_015230	GAACCCGACUGUAGUAUUA
D-009302-03	CENTD1	116984	NM_015230	GAUGGAAGCAGAAGAAUUA
D-009302-04	CENTD1	116984	NM_015230	CAAAGAGGACUUCUAUUUA

D-009136-01	CENTD2	116985	NM_015242	GAGAAGGAGUGGCCUAUUA
D-009136-02	CENTD2	116985	NM_015242	GCAGGGAUCUUACAUCUAU
D-009136-03	CENTD2	116985	NM_015242	GGAGAUCACUGCCAUUGUG
D-009136-04	CENTD2	116985	NM_015242	ACAAGAAUCUAGAGGAGUA
D-007052-01	CENTD3	64411	NM_022481	GAACUUGGCUCUGCUGUUU
D-007052-02	CENTD3	64411	NM_022481	GGAGGAGUCUGAUGUACUU
D-003317-08	**KIF11**	**3832**	**NM_004523**	**CUAGAUGGCUUUCUCAGUA**
D-007052-03	CENTD3	64411	NM_022481	GGAGAAAUAUAAAGAUGUG
D-007052-04	CENTD3	64411	NM_022481	CCAGACAGCUCCCAAAUCU
D-010251-01	CHN1	1123	NM_001822	GAAUAUAGACCUCCUGUUU
D-010251-02	CHN1	1123	NM_001822	UAUGAGAUCUCCAGAACUA
D-010251-03	CHN1	1123	NM_001822	CAAUUCCACUCAUUACAUA
D-010251-04	CHN1	1123	NM_001822	GACCUACACUUUGGCUUUA
D-003791-01	CHN2	1124	NM_004067	UCAAGAAAGUGUACUGUUG
D-003791-02	CHN2	1124	NM_004067	GAAGAGGUUUGAGUCGAUU
D-003791-03	CHN2	1124	NM_004067	UGAUAACACUGUACAUAGA
D-003791-04	CHN2	1124	NM_004067	CGAUAUAUCUGCCAAUGUC
D-006823-01	**INCENP**	**3619**	**NM_020238**	**CCACGAUGCUGACUAAGAA**
D-001206-13	**si*CONTROL* Non-Targeting siRNA Pool**			
D-004613-01	CIT	11113	NM_007174	GAUAUUAGAUGCCCUCUUU
D-004613-02	CIT	11113	NM_007174	GGACCAGUCUUCAGUAUAA
D-004613-03	CIT	11113	NM_007174	GGACAUCUAUGCUAUGAAA
D-004613-04	CIT	11113	NM_007174	GGAGCAGUCUUCCAAAUUU
D-011020-01	CYBA	1535	NM_000101	GAAGAAGGGCUCCACCAUG
D-011020-02	CYBA	1535	NM_000101	UACCAGGAAUUACUAUGUU
D-011020-03	CYBA	1535	NM_000101	GGACAGAAGCACAUGACCG
D-011020-04	CYBA	1535	NM_000101	CCAUGUGGGCCAACGAGCA
D-011021-01	CYBB	1536	NM_000397	GAAGACAACUGGACAGGAA
D-011021-02	CYBB	1536	NM_000397	GGAACUGGGCUGUGAAUGA
D-006823-02	**INCENP**	**3619**	**NM_020238**	**CAAGAAGACUGCCGAAGAG**
D-001500-01	**si*TOX* Transfection Control**			
D-011021-03	CYBB	1536	NM_000397	GUGAAUGCCCGAGUCAAUA
D-011021-04	CYBB	1536	NM_000397	GAAACUACCUAAGAUAGCG
D-017817-01	DEF6	50619	NM_022047	GCAGAGGGCUGACGAGGAU
D-017817-02	DEF6	50619	NM_022047	GGAGAAGAGUGGCAAAGUC
D-017817-03	DEF6	50619	NM_022047	GAUAGCAACGGGAACAGUA
D-017817-04	DEF6	50619	NM_022047	GGAGAUAAGCGUCCGGUCA
D-013830-01	DEPDC1B	55789	NM_018369	GUACUGGGUUUGUUACAGA
D-013830-02	DEPDC1B	55789	NM_018369	GGUACAAGCGUCACAGUAU
D-013830-03	DEPDC1B	55789	NM_018369	GAUCAUAUGGCUCUCAGGA
D-013830-04	DEPDC1B	55789	NM_018369	AGACAAUCGUCACUUAUAC
D-006823-03	**INCENP**	**3619**	**NM_020238**	**UCUGCAACAUGGAUAAUAA**
D-014602-01	DEPDC2	80243	NM_024870	GAAGCGAAUUUGUGUCAUG
D-014602-02	DEPDC2	80243	NM_024870	CUGAUAGACUGGUUAAUUG
D-014602-03	DEPDC2	80243	NM_024870	UAUGAAACAUCGACUUAUG
D-014602-04	DEPDC2	80243	NM_024870	GAACGGCGGAAAGGUUUAA
D-014602-01	DEPDC2	80243	NM_024870	GAAGCGAAUUUGUGUCAUG
D-014602-02	DEPDC2	80243	NM_024870	CUGAUAGACUGGUUAAUUG
D-014602-03	DEPDC2	80243	NM_024870	UAUGAAACAUCGACUUAUG
D-014602-04	DEPDC2	80243	NM_024870	GAACGGCGGAAAGGUUUAA
D-008713-01	DLC1	10395	NM_006094	UUAAGAACCUGGAGGACUA
D-008713-02	DLC1	10395	NM_006094	GUACGAAAGAGGAGCGUUU
D-006823-04	**INCENP**	**3619**	**NM_020238**	**GCAAAGAGCCAGAGCUGAU**

D-008713-03	DLC1	10395	NM_006094	UUAAAGAAGUCAAAGAGAA
D-008713-04	DLC1	10395	NM_006094	GCAUGUACUUAGAGGGCUU
D-026304-01	DNMBP	23268	NM_015221	GGGAUGAGCUUGAGGGAAC
D-026304-02	DNMBP	23268	NM_015221	UAGCUGAGGUUAACGGGAA
D-026304-03	DNMBP	23268	NM_015221	AAGAUAGCCUUAUGGAGAA
D-026304-04	DNMBP	23268	NM_015221	UCCACAACCUAGCAAGUUA
D-011253-01	DOCK1	1793	NM_001380	GUACCGAGGUUACACGUUA
D-011253-02	DOCK1	1793	NM_001380	UAAAUGAGCAGCUGUACAA
D-011253-03	DOCK1	1793	NM_001380	GAAAUGGUGGGCCCAAUAU
D-011253-04	DOCK1	1793	NM_001380	GGCCCAAGCCUGACUAUUU
D-003317-05	**KIF11**	**3832**	**NM_004523**	**GCAGAAAUCUAAGGAUAUA**
D-023079-01	DOCK10	55619	XM_371595	CCAGAUAACUCCUACAUUA
D-023079-02	DOCK10	55619	XM_371595	GCAGUAAGAUCAGUAUUUA
D-023079-03	DOCK10	55619	XM_371595	GAUAGCAACUCAUUACUAA
D-023079-04	DOCK10	55619	XM_371595	CAAUAUAGCUACGGAGGUU
D-015696-01	DOCK11	139818	NM_144658	UAAAUGAGCGGCUAAUUAA
D-015696-02	DOCK11	139818	NM_144658	GAUCAACACCGACAGUUUA
D-015696-03	DOCK11	139818	NM_144658	CGACAGAGUUCUACAAGGA
D-015696-04	DOCK11	139818	NM_144658	CGAAACAGAUCAGGAGUAA
D-019915-01	DOCK2	1794	NM_004946	GACAUGAGACGGCUAAUUG
D-019915-02	DOCK2	1794	NM_004946	GACCGGAAAUUUCAGCAUU
D-003317-06	**KIF11**	**3832**	**NM_004523**	**CAACAAGGAUGAAGUCUAU**
D-019915-03	DOCK2	1794	NM_004946	CAACGACACUUUGGGAAUG
D-019915-04	DOCK2	1794	NM_004946	GAAUGAGUAUCGCUCCGUU
D-012695-01	DOCK3	1795	NM_004947	GAAGAUAGGCUGCACUGUU
D-012695-02	DOCK3	1795	NM_004947	CGAGAUCACUGGCGAGUAU
D-012695-03	DOCK3	1795	NM_004947	UGACGCCCAUUCCAGAUUA
D-012695-04	DOCK3	1795	NM_004947	GACCUGUGAUGGACACGUA
D-017968-01	DOCK4	9732	NM_014705	CAAAGGGUCUGGAGCAUUA
D-017968-02	DOCK4	9732	NM_014705	CCAAAGGACUGGACUGUUA
D-017968-03	DOCK4	9732	NM_014705	UAAGAGAGCUGAUGCUUGA
D-017968-04	DOCK4	9732	NM_014705	GGAAAUAGAUGUGAUAGUG
D-003317-07	**KIF11**	**3832**	**NM_004523**	**CAGCAGAAAUCUAAGGAUA**
D-018931-01	DOCK5	80005	NM_024940	AGAACUAUCUAAUUCGUUG
D-018931-02	DOCK5	80005	NM_024940	GUAACGGGAUGCCCAAGGA
D-018931-03	DOCK5	80005	NM_024940	GAGUGGCAGUGAUGGAUAU
D-018931-04	DOCK5	80005	NM_024940	UAUCAUACAUGGGAAGGUG
D-031950-01	DOCK6	57572	NM_020812	UCACGUAUGUGGAACCGUA
D-031950-02	DOCK6	57572	NM_020812	CGACAGAACUUCGAGAUCG
D-031950-03	DOCK6	57572	NM_020812	CGGUGGAGAUGUAUAUUGA
D-031950-04	DOCK6	57572	NM_020812	CGACGCAGAACUUCAGUGA
D-031725-01	DOCK7	85440	NM_033407	GAUCGAAGUUGUAAUCGUA
D-031725-02	DOCK7	85440	NM_033407	GAGGACAGCUCGGUACGUA
D-003317-08	**KIF11**	**3832**	**NM_004523**	**CUAGAUGGCUUUCUCAGUA**
D-031725-03	DOCK7	85440	NM_033407	GGCAUGAAAUGGGUAGAUA
D-031725-04	DOCK7	85440	NM_033407	UAACCUAGGUCAAGCAUCU
D-026106-01	DOCK8	81704	NM_203447	GCAGAGCCCUACACGGUUA
D-026106-02	DOCK8	81704	NM_203447	GAUCAGAGCCUCAUUAGGA
D-026106-03	DOCK8	81704	NM_203447	GGAAAUACGUCCAGUACCA
D-026106-04	DOCK8	81704	NM_203447	CCGCUAAGCUCACAGUAAA
D-014040-01	DOCK9	23348	NM_015296	GUAAACGAACGUCUGAUUA
D-014040-02	DOCK9	23348	NM_015296	ACUCAGAAGUUUCGAGAUA
D-014040-03	DOCK9	23348	NM_015296	CAGCUUGACUACUCAUUAA
D-014040-04	DOCK9	23348	NM_015296	CGGCAUUGCUUCUCCAUAU

D-006823-01	**INCENP**	**3619**	**NM_020238**	**CCACGAUGCUGACUAAGAA**
D-001206-13	**si*CONTROL* Non-Targeting siRNA Pool**			
D-004068-05	DVL1	1855	NM_004421	GCGAGUUCUUCGUGGACAU
D-004068-06	DVL1	1855	NM_004421	CGACCAAGGCCUAUACAGU
D-004068-07	DVL1	1855	NM_004421	CGGCACACGGUCAACAAGA
D-004068-08	DVL1	1855	NM_004421	GGGAGUCAGCAGAGUGAAG
D-004069-05	DVL2	1856	NM_004422	CGCUAAACAUGGAGAAGUA
D-004069-02	DVL2	1856	NM_004422	GACAGAAACCGAGUCAGUA
D-004069-03	DVL2	1856	NM_004422	UGUGAGAGCUACCUAGUCA
D-004069-04	DVL2	1856	NM_004422	GAAACCGAGUCAGUAGUGU
D-006450-01	ECT2	1894	NM_018098	GAUAAAGGAUGAUCUUGAA
D-006450-02	ECT2	1894	NM_018098	GCACUCACCUUGUAGUUGA
D-006823-02	**INCENP**	**3619**	**NM_020238**	**CAAGAAGACUGCCGAAGAG**
D-001500-01	**si*TOX* Transfection Control**			
D-006450-03	ECT2	1894	NM_018098	GAAGGGCUCUUAUGACAUC
D-006450-04	ECT2	1894	NM_018098	CAGAGGAGAUUAAGACUAU
D-012851-01	ELMO1	9844	NM_014800	GGAUGAACCAGGAAGAUUU
D-012851-02	ELMO1	9844	NM_014800	GAAAGGACUGCCCUCAUAU
D-012851-03	ELMO1	9844	NM_014800	UGAAUGCGCUACUCGGGAA
D-012851-04	ELMO1	9844	NM_014800	GCAUUACGGAGACUUAGAA
D-008519-05	FARP1	10160	NM_005766	CAGGAAAACUCGUGUCCAU
D-008519-01	FARP1	10160	NM_005766	AAGAAGAACUCACAAGGUA
D-008519-02	FARP1	10160	NM_005766	GCACGUUGUUGUUAAGUUU
D-008519-03	FARP1	10160	NM_005766	CAGCGCAGCUCUCUUGAUU
D-006823-03	**INCENP**	**3619**	**NM_020238**	**UCUGCAACAUGGAUAAUAA**
D-009237-05	FARP2	9855	NM_014808	GGAUUUGGCUUGAACCUAU
D-009237-01	FARP2	9855	NM_014808	GAACAUACCUCAAGGAUUU
D-009237-02	FARP2	9855	NM_014808	CGAAAUUGCUCGAAAGUUG
D-009237-03	FARP2	9855	NM_014808	GCACUCGGCUGGAGAAAGA
D-009612-05	FGD1	2245	NM_004463	UCUCAAGGACUAUCUGUUA
D-009612-01	FGD1	2245	NM_004463	CCAAAGAGCUCAUAAAAGA
D-009612-02	FGD1	2245	NM_004463	CAAGAUGUAUGGUGAGUAU
D-009612-03	FGD1	2245	NM_004463	CCAAUGAGCUCCUGCAAAC
D-008431-01	FGD2	221472	NM_173558	GCUGAUGGAUGCUGAGUUU
D-008431-02	FGD2	221472	NM_173558	CGACAAGUCUCCACUCUUC
D-006823-04	**INCENP**	**3619**	**NM_020238**	**GCAAAGAGCCAGAGCUGAU**
D-008431-03	FGD2	221472	NM_173558	GGGCCGAACUGAAAUACGA
D-008431-04	FGD2	221472	NM_173558	AAGCAGCCAUUGACCAAAU
D-010371-01	FGD3	89846	NM_033086	GCACAUACAUUCAUCAUAA
D-010371-02	FGD3	89846	NM_033086	GGACGGCUCUCCAGACAUA
D-010371-03	FGD3	89846	NM_033086	CCAGAAGGCUGACAAGGAU
D-010371-04	FGD3	89846	NM_033086	GCAUGAUCCUUUACUGUGU
D-007123-01	FGD4	121512	NM_139241	GAGAAUAUGUGAAAGGAUU
D-007123-02	FGD4	121512	NM_139241	GGAGAAAGCUGCCACUCUU
D-007123-03	FGD4	121512	NM_139241	GGUAUGAGAUGCUCCUUAA
D-007123-04	FGD4	121512	NM_139241	GCAGCAAGCCAUUCUAAUA
D-003317-05	**KIF11**	**3832**	**NM_004523**	**GCAGAAAUCUAAGGAUAUA**
D-028077-02	FGD5	152273	XM_371619	GAAAGGCUGUCAAAUUGGG
D-028077-03	FGD5	152273	XM_371619	GCUCCUCACAGACUAUUUA
D-028077-04	FGD5	152273	XM_371619	AAAGUGCCCUACGCUCUAA
D-028077-01	FGD5	152273	XM_371619	GAACGUGUCUUCCUCUAGG
D-026895-01	FGD6	55785	XM_370702	GCUCAAAGAUGCCUUAAUA
D-026895-02	FGD6	55785	XM_370702	GAAGGGACCGGUUUUAUAA
D-026895-03	FGD6	55785	XM_370702	GAAUUCCGAGUCUAAAGUA

D-026895-04	FGD6	55785	XM_370702	GCUCGUCUGUUACGCCAAA
D-011281-01	GAS8	2622	NM_001481	GAACUCGACUUGCGGAGAA
D-011281-02	GAS8	2622	NM_001481	UCAAGAACCUCGUGCUAGA
D-003317-06	**KIF11**	**3832**	**NM_004523**	**CAACAAGGAUGAAGUCUAU**
D-011281-03	GAS8	2622	NM_001481	GGGACGAGCUCUAUCGGAA
D-011281-04	GAS8	2622	NM_001481	ACAGAAAGAGCACCGCAUA
D-021160-01	GMIP	51291	NM_016573	GAACUGGACUUGCGGCUCA
D-021160-02	GMIP	51291	NM_016573	GAACGUGACCCUUGAGAUG
D-021160-03	GMIP	51291	NM_016573	GAAGUGCACGGCUGAGAUA
D-021160-04	GMIP	51291	NM_016573	CGAGUGUCCUCAAGCGAUU
D-006729-01	GNE	10020	NM_005476	GGAAAUACAUAUCGAAUGA
D-006729-02	GNE	10020	NM_005476	AAACUGAACUGCAGAAUUU
D-006729-03	GNE	10020	NM_005476	CAAGAUGACUUUGACAUUA
D-006729-04	GNE	10020	NM_005476	UAACAAAACUGGCUCAUUA
D-003317-07	**KIF11**	**3832**	**NM_004523**	**CAGCAGAAAUCUAAGGAUA**
D-004158-05	GRLF1	2909	NM_024342	UCAGCGAGAUCCAAUGUAA
D-004158-02	GRLF1	2909	NM_024342	GGAGGAAUCUGUAUACAUG
D-004158-03	GRLF1	2909	NM_024342	GAACAGCGAUUUAAAGCAU
D-004158-04	GRLF1	2909	NM_024342	GAUGGGCUGUCUUUCAUUA
D-021811-05	INPP5B	3633	NM_005540	GAAGAGGAUUACACCUAUA
D-021811-06	INPP5B	3633	NM_005540	GCAUCUGCGUUGUGAAUUC
D-021811-07	INPP5B	3633	NM_005540	ACUUGGAGCUCUUCGUAAA
D-021811-08	INPP5B	3633	NM_005540	AACAGGAGCAUGCAGCUUA
D-008365-01	ITSN1	6453	NM_003024	GGACAUAGUUGUACUGAAA
D-008365-02	ITSN1	6453	NM_003024	GGAAGGAGCUGAUUAUGUG
D-003317-08	**KIF11**	**3832**	**NM_004523**	**CUAGAUGGCUUUCUCAGUA**
D-008365-03	ITSN1	6453	NM_003024	GAUAUCAGAUGUCGAUUGA
D-008365-04	ITSN1	6453	NM_003024	GGCCAUAACUGUAGAGGAA
D-009841-02	ITSN2	50618	NM_006277	GACAGGAGCUUCUCAAUCA
D-009841-03	ITSN2	50618	NM_006277	CCAAACAUGUGGGCUAUUA
D-009841-01	ITSN2	50618	NM_006277	GAUCAAACGUGACAAGUUG
D-009841-04	ITSN2	50618	NM_006277	AAACUCAGCUGGCUACUAU
D-010019-02	KALRN	8997	NM_003947	GCAAAGCACUACUUGAUGU
D-010019-03	KALRN	8997	NM_003947	GACAGGAUCUGCACCAGUA
D-010019-01	KALRN	8997	NM_003947	GAAGAGGCAUGAUGACUUU
D-010019-04	KALRN	8997	NM_003947	GGAAACUCGUGACGUAUUU
D-006823-01	**INCENP**	**3619**	**NM_020238**	**CCACGAUGCUGACUAAGAA**
D-001206-13	**si*CONTROL* Non-Targeting siRNA Pool**			
D-031982-01	LZTFL1	54585	NM_020347	GGAAAAGACUGGCACAAUA
D-031982-02	LZTFL1	54585	NM_020347	UAUAAAGGCCCAAGACUUA
D-031982-03	LZTFL1	54585	NM_020347	AAACAGCAGCUUAUCGAAA
D-031982-04	LZTFL1	54585	NM_020347	GAGAAGUGGUAUCUUAAGC
D-003577-02	MAP3K11	4296	NM_002419	GCAUGCCACUCGACUUCAA
D-003577-03	MAP3K11	4296	NM_002419	CUGGAGGACUCAAGCAAUG
D-003577-05	MAP3K11	4296	NM_002419	GAAGCCAGAAGCCAAAUAA
D-003577-07	MAP3K11	4296	NM_002419	ACACUACACUGCACAGGAA
D-003585-02	MAP3K9	4293	NM_033141	GAGCGGAACUGAACACACA
D-003585-05	MAP3K9	4293	NM_033141	CAAACGAGAUCCUAACCAA
D-006823-02	**INCENP**	**3619**	**NM_020238**	**CAAGAAGACUGCCGAAGAG**
D-001500-01	**si*TOX* Transfection Control**			
D-003585-06	MAP3K9	4293	NM_033141	GCACAGAGACGCCCAGCAA
D-003585-07	MAP3K9	4293	NM_033141	CCUAAGCCCUUUCAUGCUA
D-003904-05	MCF2	4168	NM_005369	GGUGAUAACCGCAAGUUUG

D-003904-01	MCF2	4168	NM_005369	GGUAUCAUCUGUUGAAGAA
D-003904-02	MCF2	4168	NM_005369	GGAAGAAGUUUAUAUUGUC
D-003904-04	MCF2	4168	NM_005369	GCAACAGGAUCAAUUAACA
D-010098-01	MCF2L	23263	NM_024979	AAACAGAGCUGCCCAAUGA
D-010098-02	MCF2L	23263	NM_024979	CGACAUCGCUUUCAAAUUC
D-010098-03	MCF2L	23263	NM_024979	UCAAGGAAAUGCUGAAAUA
D-010098-04	MCF2L	23263	NM_024979	CAACAGGCCUUCACAACAA
D-006823-03	**INCENP**	**3619**	**NM_020238**	**UCUGCAACAUGGAUAAUAA**
D-009313-01	MCF2L2	23101	NM_015078	GCACAUUGCUUUCUCAAGA
D-009313-02	MCF2L2	23101	NM_015078	GGAAUAGUGUUCUGUAAGA
D-009313-03	MCF2L2	23101	NM_015078	GGACCAAGCCAGAGACUUA
D-009313-04	MCF2L2	23101	NM_015078	GAAUGUAACUACCAUGGAA
D-004063-01	KIAA1804	84451	NM_032435	UGAGAUGGCUCCUACGAAU
D-004063-02	KIAA1804	84451	NM_032435	GGACAUCGAAUCAGUUUAC
D-004063-03	KIAA1804	84451	NM_032435	GAGAUGGCUCCUACGAAUA
D-004063-04	KIAA1804	84451	NM_032435	CGAAUAGUCUGAGUAGAUC
D-005352-06	MYLK2	85366	NM_033118	GGAGAAAGCCAAACGCUGU
D-005352-01	MYLK2	85366	NM_033118	GCUCGGAGGUGGCAAGUUU
D-006823-04	**INCENP**	**3619**	**NM_020238**	**GCAAAGAGCCAGAGCUGAU**
D-005352-02	MYLK2	85366	NM_033118	GACCAAAUCUCCGAUAAGA
D-005352-05	MYLK2	85366	NM_033118	AGACAGACAUGUGGAGUAU
D-006539-01	MYO9A	4649	NM_006901	GAAAGAAGCUUAGCCCUUA
D-006539-02	MYO9A	4649	NM_006901	GAUAAUACCUGCUGCAUAA
D-006539-03	MYO9A	4649	NM_006901	GAACAUACAUUACGGAUAU
D-006539-04	MYO9A	4649	NM_006901	GAACAAAGGCUAAGAGAAA
D-003915-05	NET1	10276	NM_005863	GGCAAUAUAUGAAAUGUCC
D-003915-01	NET1	10276	NM_005863	GAAGUCGCCUAGUCAAAUA
D-003915-02	NET1	10276	NM_005863	GGAGGAUGCUAUAUUGAUA
D-003915-03	NET1	10276	NM_005863	UCACGUCCUUGGCAAAUUU
D-003317-05	**KIF11**	**3832**	**NM_004523**	**GCAGAAAUCUAAGGAUAUA**
D-003916-06	NF1	4763	NM_000267	CACCGAGUCUUACAUUUAA
D-003916-01	NF1	4763	NM_000267	GGAAUAAGAUGGUAGAAUA
D-003916-02	NF1	4763	NM_000267	GAUAGAAGCUACAGUAAUA
D-003916-04	NF1	4763	NM_000267	CAACAAAGCUAAUCCUUAA
D-009354-01	NGEF	25791	NM_019850	GGAGAAACCUCAUUGAACA
D-009354-02	NGEF	25791	NM_019850	GGACCAAGUUUGUUUCGUU
D-009354-03	NGEF	25791	NM_019850	GAAAUUCCAUCUUCAAUCG
D-009354-04	NGEF	25791	NM_019850	UAAAUCGACUCUCCAAGAA
D-010193-01	NOX1	27035	NM_007052	GCACACCUGUUUAACUUUG
D-010193-02	NOX1	27035	NM_007052	GCUCUCUGCUUGAAUUUUA
D-003317-06	**KIF11**	**3832**	**NM_004523**	**CAACAAGGAUGAAGUCUAU**
D-010193-03	NOX1	27035	NM_007052	GUGGAUGCCUUCCUGAAAU
D-010193-04	NOX1	27035	NM_007052	UGAGAAGGCCGACAAAUAC
D-026087-01	NOXA1	10811	NM_006647	GAUGCCAGGUCCCUAAUCA
D-026087-02	NOXA1	10811	NM_006647	GGGAGGUGCUACACAAUGU
D-026087-03	NOXA1	10811	NM_006647	ACUUGGAGCCCGUGGAUUU
D-026087-04	NOXA1	10811	NM_006647	GGUGGAGCAAGUUGGCAAA
D-027177-05	OBSCN	84033	NM_052843	GCAGACAGCGACACCUAUA
D-027177-06	OBSCN	84033	NM_052843	AGACAUACCGCGAAGAUGA
D-027177-02	OBSCN	84033	NM_052843	GGAAGGACAUACACUCUCA
D-027177-03	OBSCN	84033	NM_052843	CAGGAGAGAUCCAAUUUGU
D-003317-07	**KIF11**	**3832**	**NM_004523**	**CAGCAGAAAUCUAAGGAUA**
D-010026-01	OCRL	4952	NM_000276	GAAAUUACCUCCCAAGUUG
D-010026-04	OCRL	4952	NM_000276	UGAAAUCCCUGAUGAGGAA
D-010026-05	OCRL	4952	NM_000276	UGACAUAGCUUCUAACAGU

D-010026-06	OCRL	4952	NM_000276	GAAAGGAUCAGUGUCGAUA
D-009444-01	OPHN1	4983	NM_002547	GAAAGAAUCUCAGUUACAA
D-009444-02	OPHN1	4983	NM_002547	GCGAGAGGCUCAAGUGUUA
D-009444-03	OPHN1	4983	NM_002547	GAACAUAGUGGUGGAAAUA
D-009444-04	OPHN1	4983	NM_002547	GCUAGUGAUUUGCUGAUUA
D-003521-01	PAK1	5058	NM_002576	GAAGAAAUAUACACGGUUU
D-003521-03	PAK1	5058	NM_002576	CAUCAAAUAUCACUAAGUC
D-003317-08	**KIF11**	**3832**	**NM_004523**	**CUAGAUGGCUUUCUCAGUA**
D-003521-05	PAK1	5058	NM_002576	CAACAAAGAACAAUCACUA
D-003521-07	PAK1	5058	NM_002576	AGAAAUACCAGCACUAUGA
D-003597-05	PAK2	5062	NM_002577	AGAAGGAACUGAUCAUUAA
D-003597-06	PAK2	5062	NM_002577	CUACAGACCUCCAAUAUCA
D-003597-07	PAK2	5062	NM_002577	GAAACUGGCCAAACCGUUA
D-003597-09	PAK2	5062	NM_002577	ACAGUGGGCUCGAUUACUA
D-003614-01	PAK3	5063	NM_002578	GACAAGAGGUGGCCAUAAA
D-003614-02	PAK3	5063	NM_002578	GGAUGGCUCUGUUAAAUUG
D-003614-03	PAK3	5063	NM_002578	GAUUAUCGCUGCAAAGGAA
D-003614-04	PAK3	5063	NM_002578	UUAAAUCGCUGUCUUGAGA
D-006823-01	**INCENP**	**3619**	**NM_020238**	**CCACGAUGCUGACUAAGAA**
D-001206-13	**si*CONTROL* Non-Targeting siRNA Pool**			
D-003615-07	PAK4	10298	NM_005884	CCAUGAAGAUGAUUCGGGA
D-003615-03	PAK4	10298	NM_005884	GGAUAAUGGUGAUUGAGAU
D-003615-05	PAK4	10298	NM_005884	GGGUGAAGCUGUCAGACUU
D-003615-06	PAK4	10298	NM_005884	AGAAUGUGGUGGAGAUGUA
D-004338-05	PAK6	56924	NM_020168	CCAAUGGGCUGGCUGCAAA
D-004338-06	PAK6	56924	NM_020168	GCACCAAUAGGCAUGGAAU
D-004338-02	PAK6	56924	NM_020168	UCAACGACAUCCAGAAGUU
D-004338-03	PAK6	56924	NM_020168	GGACAGCUACGUGAAGAUU
D-003973-09	PAK7	57144	NM_020341	CAAACUCCGUUAUGAUAUA
D-003973-10	PAK7	57144	NM_020341	GAGCACGGCUUUAAUAAGU
D-006823-02	**INCENP**	**3619**	**NM_020238**	**CAAGAAGACUGCCGAAGAG**
D-001500-01	**si*TOX* Transfection Control**			
D-003973-11	PAK7	57144	NM_020341	CAGAAGGACUCAGUACAAA
D-003973-12	PAK7	57144	NM_020341	AGGGUAACAUGUAGGAUUU
D-013859-01	PARD6A	50855	NM_016948	GCACAAGCAUGGUUCAGAC
D-013859-02	PARD6A	50855	NM_016948	CUACUUGGCUAUACGGAUG
D-013859-03	PARD6A	50855	NM_016948	GCAAAUUUGACGCCGAGUU
D-013859-04	PARD6A	50855	NM_016948	GAGUCGCAUUCGAGGAGAU
D-010681-01	PARD6B	84612	XM_030559	GGAAUAAUGUUGUGAGGAA
D-010681-02	PARD6B	84612	XM_030559	AGACAUCCAUGGAGACUUA
D-010681-03	PARD6B	84612	XM_030559	CGAAGAAGAUGACAUUAUC
D-010681-04	PARD6B	84612	XM_030559	GGGUACGUCUUUACAAAUA
D-006823-03	**INCENP**	**3619**	**NM_020238**	**UCUGCAACAUGGAUAAUAA**
D-014909-01	PARD6G	84552	NM_032510	CACCAUAUCUCCAACAGUG
D-014909-02	PARD6G	84552	NM_032510	GCAAGGCGGUUUCUAGUGC
D-014909-03	PARD6G	84552	NM_032510	UCAUAAGCCUGGGAAGUUU
D-014909-04	PARD6G	84552	NM_032510	GAACCGAAGUUUUCACAAG
D-003020-10	PIK3R1	5295	NM_181504	GAAGUAAAGCAUUGUGUCA
D-003020-11	PIK3R1	5295	NM_181504	GACGAGAGACCAAUACUUG
D-003020-12	PIK3R1	5295	NM_181504	GUUGAAGUCUCGAAUCAGU
D-003020-13	PIK3R1	5295	NM_181504	AGACCUGGAUUUAGAAUAU
D-003021-05	PIK3R2	5296	NM_005027	GGAAAGGCGGGAACAAUAA
D-003021-06	PIK3R2	5296	NM_005027	GAUGAAGCGUACUGCAAUU

D-006823-04	**INCENP**	**3619**	**NM_020238**	**GCAAAGAGCCAGAGCUGAU**
D-003021-07	PIK3R2	5296	NM_005027	GGACAGCGAAUCUCACUAC
D-003021-08	PIK3R2	5296	NM_005027	GCAAGAUCCGAGACCAGUA
D-004175-09	PRKCL1	5585	NM_002741	CCUCGAAGAUUUCAAGUUC
D-004175-10	PRKCL1	5585	NM_002741	ACAGUAAGACCAAGAUUGA
D-004175-11	PRKCL1	5585	NM_002741	ACAGCGACGUGUUCUCUGA
D-004175-12	PRKCL1	5585	NM_002741	GAGAAGCAGUUGGCCAUUG
D-004612-09	PRKCL2	5586	NM_006256	GGAGCGCUCUGAUGGACAA
D-004612-10	PRKCL2	5586	NM_006256	UAGACAGCCUGAUGUGUGA
D-004612-11	PRKCL2	5586	NM_006256	GUACGCAUCCCUCAACUAG
D-004612-03	PRKCL2	5586	NM_006256	GACAGAAGAUCUCAGCAAA
D-003317-05	**KIF11**	**3832**	**NM_004523**	**GCAGAAAUCUAAGGAUAUA**
D-004647-02	PKN3	29941	NM_013355	GAAGCCCACCGCCCUAACA
D-004647-03	PKN3	29941	NM_013355	GCGCCAAGAACGUGGUGAA
D-004647-01	PKN3	29941	NM_013355	CCAAGAACGUGGUGAAACU
D-004647-04	PKN3	29941	NM_013355	GGGCUGCGGUGCCUGGAUA
D-004201-01	PLCE1	51196	NM_016341	GAAGAGAAAUGGUCCCUUA
D-004201-02	PLCE1	51196	NM_016341	GAAAUUCCCUGACCAAAGA
D-004201-03	PLCE1	51196	NM_016341	GCAAAAGGCUCAUCAGUUA
D-004201-04	PLCE1	51196	NM_016341	GCAUAUACCUGUAAACUGA
D-009413-01	PLD1	5337	NM_002662	UAACUGAGCUUAUCUAUGU
D-009413-02	PLD1	5337	NM_002662	GAAGAACAAUUCCUUGGUA
D-003317-06	**KIF11**	**3832**	**NM_004523**	**CAACAAGGAUGAAGUCUAU**
D-009413-03	PLD1	5337	NM_002662	GAAGAUUACUUGACAAAGA
D-009413-04	PLD1	5337	NM_002662	GGUAAUCAGUGGAUAAAUU
D-005064-01	PLD2	5338	NM_002663	GGACAACCAAGAAGAAAUA
D-005064-02	PLD2	5338	NM_002663	GGACCGGCCUUUCGAAGAU
D-005064-03	PLD2	5338	NM_002663	GACCUGCACUACCGACUGA
D-005064-04	PLD2	5338	NM_002663	CAGCAUGGCGGGACUAUAU
D-009659-01	PLD3	23646	NM_012268	GGACAUCGCCUCCUUCUAC
D-009659-02	PLD3	23646	NM_012268	ACAAGUACAUGGUGACUGA
D-009659-03	PLD3	23646	NM_012268	CAACUGGUCUGGCAACUAC
D-009659-04	PLD3	23646	NM_012268	GACAAUGCCCGGAGUUUCA
D-003317-07	**KIF11**	**3832**	**NM_004523**	**CAGCAGAAAUCUAAGGAUA**
D-010295-01	LOC122618	122618	NM_138790	CCACGUGGCUUCAUACUAC
D-010295-02	LOC122618	122618	NM_138790	CCAACUGGUCGGAGGAUUA
D-010295-03	LOC122618	122618	NM_138790	CAUCUCACUUCAACCGUUU
D-010295-04	LOC122618	122618	NM_138790	GCUUGGCGCUGUCAUCUAU
D-010305-01	FLJ40773	200150	NM_152666	GCACGGGCCUUGUUAUCAA
D-010305-02	FLJ40773	200150	NM_152666	GGACUGGUAUUCACCGUAU
D-010305-03	FLJ40773	200150	NM_152666	GGCCUUAACUAUUCAGAAA
D-010305-04	FLJ40773	200150	NM_152666	GGACAAACAGCACGUGUAU
D-024745-01	PLEKHG1	57480	XM_027307	GUGAAGAGUUCCACAUUUA
D-024745-02	PLEKHG1	57480	XM_027307	GAGAUGACACGUUUACAUA
D-003317-08	**KIF11**	**3832**	**NM_004523**	**CUAGAUGGCUUUCUCAGUA**
D-024745-03	PLEKHG1	57480	XM_027307	CCAGUUGUAUGACCAGAUU
D-024745-04	PLEKHG1	57480	XM_027307	AGAAACAUCUGGACCGAUC
D-023690-01	PLEKHG2	64857	NM_022835	UGACAGCGGUUGCCUGGUA
D-023690-02	PLEKHG2	64857	NM_022835	GGAGAUUUGUUCUGAUUUC
D-023690-03	PLEKHG2	64857	NM_022835	CCGAAGAGGUGAAGUGUGU
D-023690-04	PLEKHG2	64857	NM_022835	AGCGAGAGCCCAACCAAUA
D-022051-01	PLEKHG3	26030	NM_015549	GCCAAGAGUUUGAUAUCUA
D-022051-02	PLEKHG3	26030	NM_015549	UAGACAAGAUUAAGAGCUA
D-022051-03	PLEKHG3	26030	NM_015549	GUAAGAAACUCCAUCUCCA

D-022051-05	PLEKHG3	26030	NM_015549	CCGCCCAUCUUCAGAAAUU
D-006823-01	**INCENP**	**3619**	**NM_020238**	**CCACGAUGCUGACUAAGAA**
D-001206-13	**si*CONTROL* Non-Targeting siRNA Pool**			
D-022573-01	PLEKHG4	25894	NM_015432	GGACAAGGCUGACGAGCUA
D-022573-02	PLEKHG4	25894	NM_015432	GAAUACAGGCCCUAGAGUU
D-022573-03	PLEKHG4	25894	NM_015432	GAAUAAGCCUCGCUCCGAU
D-022573-04	PLEKHG4	25894	NM_015432	GAAGUUCGCUCUCGGGCGU
D-013873-01	KIAA0720	57449	NM_020631	UCAAGUCGGUGCUGAGGAA
D-013873-02	KIAA0720	57449	NM_020631	UCAAAGGCUUCAAGAUGUU
D-013873-03	KIAA0720	57449	NM_020631	ACAGCAAGAUGGAUGUGUA
D-013873-04	KIAA0720	57449	NM_020631	GCCCAGCUCUACCGAAUCA
D-020318-01	FLJ10665	55200	NM_018173	GCUGAGACCCUGUUUGGAA
D-020318-02	FLJ10665	55200	NM_018173	GACCAUGGCUUACGCCCGA
D-006823-02	**INCENP**	**3619**	**NM_020238**	**CAAGAAGACUGCCGAAGAG**
D-001500-01	**si*TOX* Transfection Control**			
D-020318-03	FLJ10665	55200	NM_018173	GAGGAUACCCUGUGCUGGA
D-020318-04	FLJ10665	55200	NM_018173	GCGAAGAGCAAGAGAGCUU
D-016664-01	PLEKHK1	219790	NM_145307	GUGCAAUGCUCGACUAAUG
D-016664-02	PLEKHK1	219790	NM_145307	GCGAGGAGGUAAACUCUAU
D-016664-03	PLEKHK1	219790	NM_145307	UCACGACGCUAUGCCAUUU
D-016664-04	PLEKHK1	219790	NM_145307	CAACAUGUGCUGCCGACUA
D-031971-05	PLXNA1	5361	NM_032242	GAACGUGCCUGACCUCUCA
D-031971-06	PLXNA1	5361	NM_032242	GCAGAUCGAUGACGACUUC
D-031971-07	PLXNA1	5361	NM_032242	GCAGUGAACCGCAUCUAUA
D-031971-08	PLXNA1	5361	NM_032242	GCACCAACCUGGCCACUGU
D-006823-03	**INCENP**	**3619**	**NM_020238**	**UCUGCAACAUGGAUAAUAA**
D-019590-01	PLXNB1	5364	NM_002673	GAGAGGAGCCGACUACGUA
D-019590-05	PLXNB1	5364	NM_002673	GCAGAGACCUCACCUUUGA
D-019590-06	PLXNB1	5364	NM_002673	GCAAACAUCUGAUAACAUG
D-019590-07	PLXNB1	5364	NM_002673	UCACAGACCUCAUGACUGA
D-031513-01	PLXNB2	23654	XM_371474	GCAACAAGCUGCUGUACGC
D-031513-02	PLXNB2	23654	XM_371474	ACCAAUACACGCAGAAGUA
D-031513-03	PLXNB2	23654	XM_371474	UGAACACCCUCGUGGCACU
D-031513-04	PLXNB2	23654	XM_371474	CGGCAGAUGGUGCAGGUCA
D-003168-05	PTK9	5756	NM_002822	GAAGAACUACGACAGAUUA
D-003168-09	PTK9	5756	NM_002822	GAAGGAGACUAUUUAGAGU
D-006823-04	**INCENP**	**3619**	**NM_020238**	**GCAAAGAGCCAGAGCUGAU**
D-003168-10	PTK9	5756	NM_002822	GAGCGGAUGCUGUAUUCUA
D-003168-12	PTK9	5756	NM_002822	AGAGGAAUUCGAAGACUAA
D-003169-05	PTK9L	11344	NM_007284	AGAGAGAGCUCCAGCAGAU
D-003169-06	PTK9L	11344	NM_007284	UUAACGAGGUGAAGACAGA
D-003169-07	PTK9L	11344	NM_007284	ACACAGAGCCCACGGAUGU
D-003169-08	PTK9L	11344	NM_007284	GCUGGGAUCAGGACUAUGA
D-008650-01	RACGAP1	29127	NM_013277	CAAAUUAUCUCUGAAGUGU
D-008650-02	RACGAP1	29127	NM_013277	CCACAGACACCAGAUAUUA
D-008650-03	RACGAP1	29127	NM_013277	GAACAUCAGCUUCUCAAGA
D-008650-04	RACGAP1	29127	NM_013277	GUAAUCAGGUGGAUGUAGA
D-003317-05	**KIF11**	**3832**	**NM_004523**	**GCAGAAAUCUAAGGAUAUA**
D-017467-01	RAD51L3	5892	NM_002878	GCUCAAACCUGCCCUCGGA
D-017467-02	RAD51L3	5892	NM_002878	CCACAUAACUCGAGACAGG
D-017467-03	RAD51L3	5892	NM_002878	AGAAAUGUGGCUUGUCUUA
D-017467-04	RAD51L3	5892	NM_002878	GCACUCGGAUUCUCCUGGA
D-009266-01	RALBP1	10928	NM_006788	GAAUGUAACUAUCUUCUGA
D-009266-02	RALBP1	10928	NM_006788	GAUCAGCCCUACUAAGUUU

D-009266-03	RALBP1	10928	NM_006788	GAACGAAGAGCUGGAAAUA
D-009266-04	RALBP1	10928	NM_006788	GAAGGCAUCUACAGAGUAU
D-009323-01	RASGRF1	5923	NM_002891	UCAAGAAGAUUCCUUAUGA
D-009323-02	RASGRF1	5923	NM_002891	GAGAUCACCUCGUCCAUGA
D-003317-06	**KIF11**	**3832**	**NM_004523**	**CAACAAGGAUGAAGUCUAU**
D-009323-03	RASGRF1	5923	NM_002891	CCAACAAGAUUCCAGAUGA
D-009323-04	RASGRF1	5923	NM_002891	CCACUAAGCACUUCAAUGA
D-024516-05	RASGRF2	5924	NM_006909	CUGCACACCUAUCGUAUUU
D-024516-06	RASGRF2	5924	NM_006909	GCACAGUACUUGCUUGACA
D-024516-01	RASGRF2	5924	NM_006909	CAACAGAGGUGAACAUUUG
D-024516-04	RASGRF2	5924	NM_006909	GAAGGAACACCAAACUUUA
D-015163-01	RHPN1	114822	NM_052924	GGACUGCCCUGGUGCAUGU
D-015163-02	RHPN1	114822	NM_052924	CCUCAUCGCUGCCGUCAUU
D-015163-03	RHPN1	114822	NM_052924	GCGACUACAUUGUGUCAGU
D-015163-04	RHPN1	114822	NM_052924	CCAAGUAUGCGGAGCUCGA
D-003317-07	**KIF11**	**3832**	**NM_004523**	**CAGCAGAAAUCUAAGGAUA**
D-016798-01	RHPN2	85415	NM_033103	GAAGAACGACGGCUACUUU
D-016798-02	RHPN2	85415	NM_033103	GAGGAGGCAUUUACGAUUC
D-016798-03	RHPN2	85415	NM_033103	GCUUAGCCAUUGAUGAUGA
D-016798-04	RHPN2	85415	NM_033103	CGGAGUAAAUUGCAGAAUC
D-003536-05	ROCK1	6093	NM_005406	GCCAAUGACUUACUUAGGA
D-003536-01	ROCK1	6093	NM_005406	GGACACAGCUGUAAGAUUG
D-003536-02	ROCK1	6093	NM_005406	GAAGAAACAUUCCCUAUUC
D-003536-03	ROCK1	6093	NM_005406	GAGAUGAGCAAGUCAAUUA
D-004610-05	ROCK2	9475	NM_004850	GCAAAUCUGUUAAUACUCG
D-004610-01	ROCK2	9475	NM_004850	GAGGAAAGCUGAUCAUGAA
D-003317-08	**KIF11**	**3832**	**NM_004523**	**CUAGAUGGCUUUCUCAGUA**
D-004610-02	ROCK2	9475	NM_004850	GUAGAAACCUUCCCAAUUC
D-004610-03	ROCK2	9475	NM_004850	GCAACUGGCUCGUUCAAUU
D-010358-03	RRAS2	22800	NM_012250	GCACGGCAGCUUAAGGUAA
D-010358-04	RRAS2	22800	NM_012250	CGUGAUGAGUUCCCAAUGA
D-010358-05	RRAS2	22800	NM_012250	GAACCAACACGGAAAGAAA
D-010358-06	RRAS2	22800	NM_012250	UAAUAAAGCAGAUCUGGAU
D-015055-01	RTKN	6242	NM_033046	GCACAAACCUCUUCUGUUA
D-015055-02	RTKN	6242	NM_033046	GGACGGCCCUUCACCCUAA
D-015055-03	RTKN	6242	NM_033046	GAAGAGCCGCUGCUUACUA
D-015055-04	RTKN	6242	NM_033046	GAAGCUAGACCAUGAGAUC
D-006823-01	**INCENP**	**3619**	**NM_020238**	**CCACGAUGCUGACUAAGAA**
D-001206-13	**si*CONTROL* Non-Targeting siRNA Pool**			
D-015055-01	RTKN	6242	NM_033046	GCACAAACCUCUUCUGUUA
D-015055-02	RTKN	6242	NM_033046	GGACGGCCCUUCACCCUAA
D-015055-03	RTKN	6242	NM_033046	GAAGAGCCGCUGCUUACUA
D-015055-04	RTKN	6242	NM_033046	GAAGCUAGACCAUGAGAUC
D-009546-01	SH3BP1	23616	NM_018957	GACCUGUACCACUUUGUUA
D-009546-02	SH3BP1	23616	NM_018957	GAUGACAGCCACCCACUUC
D-009546-03	SH3BP1	23616	NM_018957	CAUCGAGGCCUGCGUCAUG
D-009546-04	SH3BP1	23616	NM_018957	GAGCGCAGACACCCUCUUC
D-007191-01	SMURF1	57154	NM_020429	GCACUAUGAUCUAUAUGUU
D-007191-02	SMURF1	57154	NM_020429	AAAGAGAUCUAGUCCAGAA
D-006823-02	**INCENP**	**3619**	**NM_020238**	**CAAGAAGACUGCCGAAGAG**
D-001500-01	**si*TOX* Transfection Control**			
D-007191-03	SMURF1	57154	NM_020429	GGAAGAAGGUUUGGAUUAC
D-007191-04	SMURF1	57154	NM_020429	GGACUGCAGAGGACUGUUA

D-005194-05	SOS1	6654	NM_005633	GGCAGAAAUUCGACAAUAU
D-005194-01	SOS1	6654	NM_005633	CAAAGAAGCUGUUCAAUAU
D-005194-03	SOS1	6654	NM_005633	GAAAUAGCAUGGAGAAGGA
D-005194-04	SOS1	6654	NM_005633	GAGCACCACUUCUAUGAUU
D-005195-05	SOS2	6655	NM_006939	UACUCUAGAUCGAAUGUUA
D-005195-01	SOS2	6655	NM_006939	GGACGAAGCUGUGGAAUUA
D-005195-02	SOS2	6655	NM_006939	GCACCAACCUCUCCAAAUA
D-005195-04	SOS2	6655	NM_006939	GCAAACAGCCACCUCGAUU
D-006823-03	**INCENP**	**3619**	**NM_020238**	**UCUGCAACAUGGAUAAUAA**
D-015469-01	SPATA13	221178	NM_153023	GAAGAAACUUGCCAUGUUA
D-015469-02	SPATA13	221178	NM_153023	GGAGAGCAUCGACAAGAUA
D-015469-03	SPATA13	221178	NM_153023	GGACCAACGUCAUCCGGGA
D-015469-04	SPATA13	221178	NM_153023	GCGCAGCUAGCCACUAUUU
D-009800-01	SRF	6722	NM_003131	GGACUGUGCUGAAGAGUAC
D-009800-03	SRF	6722	NM_003131	GCACCAGUGUCUGCUAGUG
D-009800-05	SRF	6722	NM_003131	GCGAGAUGGAGAUCGGUAU
D-009800-06	SRF	6722	NM_003131	UACACGACCUUCAGCAAGA
D-026974-01	SRGAP1	57522	NM_020762	CAUGAGGGCUUAGACAUUA
D-026974-02	SRGAP1	57522	NM_020762	UUAACGAUCUGAUUUCUUG
D-006823-04	**INCENP**	**3619**	**NM_020238**	**GCAAAGAGCCAGAGCUGAU**
D-026974-03	SRGAP1	57522	NM_020762	GACCAGAGUAACCAUGAUA
D-026974-04	SRGAP1	57522	NM_020762	GCAAUACACGGGCUUCAAU
D-021531-04	FNBP2	23380	XM_059095	GAGACUACCUCGGUUGAAG
D-021531-01	FNBP2	23380	XM_059095	GGAAAGGACAGGCUGAGUA
D-021531-02	FNBP2	23380	XM_059095	CCAAAGAAGGGCCAGAUAA
D-021531-03	FNBP2	23380	XM_059095	GCGGACAGAUUGCAGUCUA
D-014175-01	SRGAP2	9901	NM_014850	CCAAUGAGCUCUACACAGU
D-014175-02	SRGAP2	9901	NM_014850	GCACGGCUCUGCACGAGUU
D-014175-03	SRGAP2	9901	NM_014850	GAAUAUGAAGCCCAAAUAA
D-014175-04	SRGAP2	9901	NM_014850	CAGAACUGCUCAUGCGUUA
D-003317-05	**KIF11**	**3832**	**NM_004523**	**GCAGAAAUCUAAGGAUAUA**
D-010256-01	STARD13	90627	NM_052851	GAUGUGAACUUCCAAAGGA
D-010256-02	STARD13	90627	NM_052851	CCAAGGCACUUUCUAUUGA
D-010256-03	STARD13	90627	NM_052851	GGGCAACUUUCCACACUUA
D-010256-04	STARD13	90627	NM_052851	GAAAGUUCCCGACUACAAA
D-010254-01	STARD8	9754	NM_014725	GAAGAAGGACACUCCAUUU
D-010254-02	STARD8	9754	NM_014725	CGACGUGGCUGACCUGCUA
D-010254-03	STARD8	9754	NM_014725	GAACCUGCGUCAAAUGAAU
D-010254-04	STARD8	9754	NM_014725	GAACCCACCUUUGCCUCUA
D-012685-01	TRIP10	9322	NM_004240	GAAAGAACGCACCGAAGUG
D-012685-02	TRIP10	9322	NM_004240	GAACGGCUAGACCAGGAUA
D-003317-06	**KIF11**	**3832**	**NM_004523**	**CAACAAGGAUGAAGUCUAU**
D-012685-03	TRIP10	9322	NM_004240	CGACUCCCACGUCCUUAUA
D-012685-04	TRIP10	9322	NM_004240	CCAUUUACACGGAGUUUGA
D-008711-01	TAGAP	117289	NM_054114	UGAAACAGGUUGCAGAUAA
D-008711-02	TAGAP	117289	NM_054114	GACCAGAGCCUGUCAUUUG
D-008711-03	TAGAP	117289	NM_054114	ACACUAAACGCCAAUAAUA
D-008711-04	TAGAP	117289	NM_054114	AGAAGGACCUGAACAACAA
D-003932-01	TIAM1	7074	NM_003253	GAACCGAAGCUGUAAAGAA
D-003932-02	TIAM1	7074	NM_003253	GAAAGGAUGCACGCUAUUU
D-003932-03	TIAM1	7074	NM_003253	AACCGAAGCUGUAAAGAAA
D-003932-04	TIAM1	7074	NM_003253	GAAGUGGUCUUACCUAACG
D-003317-07	**KIF11**	**3832**	**NM_004523**	**CAGCAGAAAUCUAAGGAUA**
D-008434-05	TIAM2	26230	NM_001010927	GAACUUCAGGCGUCACAUA
D-008434-06	TIAM2	26230	NM_001010927	CGACCUAAAUUCUGUUCUA

D-008434-07	TIAM2	26230	NM_001010927	GUGUAAGGAUCGCCUGGUA
D-008434-08	TIAM2	26230	NM_001010927	UAAGAGAGCCGUCAUACUG
D-003102-06	TNK2	10188	NM_005781	GCAAGUCGUGGAUGAGUAA
D-003102-05	TNK2	10188	NM_005781	AAACGCAAGUCGUGGAUGA
D-003102-08	TNK2	10188	NM_005781	UCAGCAGCACCCACUAUUA
D-003102-09	TNK2	10188	NM_005781	GAGAACUACUGGUGGCGUG
D-005047-01	TRIO	7204	NM_007118	GAUAAGAGGUACAGAGAUU
D-005047-02	TRIO	7204	NM_007118	GGAAGUCGCUCCUUGACAA
D-003317-08	**KIF11**	**3832**	**NM_004523**	**CUAGAUGGCUUUCUCAGUA**
D-005047-03	TRIO	7204	NM_007118	CAACGGAGAGUCCAUGUUA
D-005047-04	TRIO	7204	NM_007118	GAACACCAACUUCAGAUAA
D-012685-01	TRIP10	9322	NM_004240	GAAAGAACGCACCGAAGUG
D-012685-02	TRIP10	9322	NM_004240	GAACGGCUAGACCAGGAUA
D-012685-03	TRIP10	9322	NM_004240	CGACUCCCACGUCCUUAUA
D-012685-04	TRIP10	9322	NM_004240	CCAUUUACACGGAGUUUGA
D-003935-05	VAV1	7409	NM_005428	CGACAAAGCUCUACUCAUC
D-003935-02	VAV1	7409	NM_005428	GCAGCGAGUUCUCAAAUAU
D-003935-03	VAV1	7409	NM_005428	GCAGAAAUACAUCUACUAA
D-003935-04	VAV1	7409	NM_005428	GAAGGACUGUACCGGAUCA
D-006823-01	**INCENP**	**3619**	**NM_020238**	**CCACGAUGCUGACUAAGAA**
D-001206-13	**si*CONTROL* Non-Targeting siRNA Pool**			
D-005199-01	VAV2	7410	NM_003371	GCUGAGCGCUUUGCAAUAA
D-005199-02	VAV2	7410	NM_003371	CAAGAAGUCUCACGGGAAA
D-005199-03	VAV2	7410	NM_003371	UCACAGAGGCCAAGAAAUU
D-005199-04	VAV2	7410	NM_003371	GAAAGUCUGCCACGAUAAA
D-010178-01	VAV3	10451	NM_006113	UAAUAGAUCUUCAGCAGUA
D-010178-02	VAV3	10451	NM_006113	GCAGAGACCGAACUUAUUA
D-010178-04	VAV3	10451	NM_006113	GCAAAGCACAUCAAGAUUU
D-010178-05	VAV3	10451	NM_006113	AGACCGAACUUAUUAAUAG
D-005057-01	CDC42	998	NM_001791	GGAGAACCAUAUACUCUUG
D-005057-02	CDC42	998	NM_001791	GAUUACGACCGCUGAGUUA
D-006823-02	**INCENP**	**3619**	**NM_020238**	**CAAGAAGACUGCCGAAGAG**
D-001500-01	**si*TOX* Transfection Control**			
D-005057-03	CDC42	998	NM_001791	GAUGACCCCUCUACUAUUG
D-005057-04	CDC42	998	NM_001791	CGGAAUAUGUACCGACUGU
D-003560-09	RAC1	5879	NM_018890	CGGCACCACUGUCCCAACA
D-003560-05	RAC1	5879	NM_018890	AGACGGAGCUGUAGGUAAA
D-003560-07	RAC1	5879	NM_018890	UAAGGAGAUUGGUGCUGUA
D-003560-08	RAC1	5879	NM_018890	UAAAGACACGAUCGAGAAA
D-007741-01	RAC2	5880	NM_002872	GAGAUGGGGCCGUGGGCAA
D-007741-02	RAC2	5880	NM_002872	CAGCCAAUGUGAUGGUGGA
D-007741-03	RAC2	5880	NM_002872	CCAAUGUGAUGGUGGACAG
D-007741-04	RAC2	5880	NM_002872	ACAAGGACACCAUCGAGAA
D-006823-03	**INCENP**	**3619**	**NM_020238**	**UCUGCAACAUGGAUAAUAA**
D-008836-05	RAC3	5881	NM_005052	AAACUGACGUCUUUCUGAU
D-008836-01	RAC3	5881	NM_005052	GGAGAUUGGCUCUGUGAAA
D-008836-02	RAC3	5881	NM_005052	ACGUGAUGGUGGACGGGAA
D-008836-04	RAC3	5881	NM_005052	CGAGAAUGUUCGUGCCAAG
D-003860-01	RHOA	387	NM_001664	AUGGAAAGCAGGUAGAGUU
D-003860-02	RHOA	387	NM_001664	GAACUAUGUGGCAGAUAUC
D-003860-03	RHOA	387	NM_001664	GAAAGACAUGCUUGCUCAU
D-003860-04	RHOA	387	NM_001664	GAGAUAUGGCAAACAGGAU
D-008395-07	RHOB	388	NM_004040	GCAUCCAAGCCUACGACUA

D-008395-08	RHOB	388	NM_004040	ACACCGACGUCAUUCUCAU
D-006823-04	**INCENP**	**3619**	**NM_020238**	**GCAAAGAGCCAGAGCUGAU**
D-008395-09	RHOB	388	NM_004040	CAUCCAAGCCUACGACUAC
D-008395-10	RHOB	388	NM_004040	CAACUGCUGCAAGGUGCUA
D-009389-01	RHOBTB1	9886	NM_014836	AAAUGAAGCUGCCUGUUUA
D-009389-02	RHOBTB1	9886	NM_014836	GAACUUGGCUUACCAUACU
D-009389-03	RHOBTB1	9886	NM_014836	GGACGUGACAUUUAAAUUG
D-009389-04	RHOBTB1	9886	NM_014836	GAACACCCGUUAUCCUUGU
D-009252-01	RHOBTB2	23221	NM_015178	UGACAUGGAUUAUGAAAGG
D-009252-02	RHOBTB2	23221	NM_015178	GACCGUCGCUUUGCUUAUG
D-009252-03	RHOBTB2	23221	NM_015178	CCCGAGACGUGGUAGAUGA
D-009252-04	RHOBTB2	23221	NM_015178	GGACAACGCCGUGGGUAAG
D-003317-05	**KIF11**	**3832**	**NM_004523**	**GCAGAAAUCUAAGGAUAUA**
D-020480-05	RHOBTB3	22836	NM_014899	ACAGAUGGCCGUCGAAUAU
D-020480-02	RHOBTB3	22836	NM_014899	GUAAUUACAUGGAAGCAAA
D-020480-03	RHOBTB3	22836	NM_014899	CAACCUGGCUACUUCAUUU
D-020480-04	RHOBTB3	22836	NM_014899	CAACGUUAAUGACAAGUUU
D-008555-01	RHOC	389	NM_175744	GGAGAGAGCUGGCCAAGAU
D-008555-02	RHOC	389	NM_175744	AUAAGAAGGACCUGAGGCA
D-008555-03	RHOC	389	NM_175744	GGAUCAGUGCCUUUGGCUA
D-008555-04	RHOC	389	NM_175744	GAGAGCUGGCCAAGAUGAA
D-008940-01	RHOD	29984	NM_014578	UGAACAAGCUCCGAAGAAA
D-008940-02	RHOD	29984	NM_014578	GAUUGGAGCCUGUGACCUA
D-003317-06	**KIF11**	**3832**	**NM_004523**	**CAACAAGGAUGAAGUCUAU**
D-008940-03	RHOD	29984	NM_014578	CCGAACAGCUUUGACAACA
D-008940-04	RHOD	29984	NM_014578	AGACGUCGCUGCUGAUGGU
D-008316-01	RHOF	54509	NM_019034	GGGAGAAUGUGGAGGACGU
D-008316-02	RHOF	54509	NM_019034	CGGCCGGGCAAGAAGACUA
D-008316-03	RHOF	54509	NM_019034	AGAUCGUGAUCGUGGGCGA
D-008316-04	RHOF	54509	NM_019034	ACGACAACGUCCUCAUCAA
D-008995-01	RHOG	391	NM_001665	CUACACAACUAACGCUUUC
D-008995-02	RHOG	391	NM_001665	CCAGUCCGCCGUCCUAUGA
D-008995-03	RHOG	391	NM_001665	GCAACAGGAUGGUGUCAAG
D-008995-04	RHOG	391	NM_001665	CGUCAUCUGUUUCUCCAUU
D-003317-07	**KIF11**	**3832**	**NM_004523**	**CAGCAGAAAUCUAAGGAUA**
D-008804-01	RHOH	399	NM_004310	CAAGUGGAUUGGUGAAAUU
D-008804-02	RHOH	399	NM_004310	GAGUACAGCAGGUGUUUGA
D-008804-03	RHOH	399	NM_004310	GCUCAGCCCUUAGCAAUCG
D-008804-04	RHOH	399	NM_004310	GGCCAACCAUAACUCAUUC
D-010367-01	RHOJ	57381	NM_020663	AGAAACCUCUCACUUACGA
D-010367-02	RHOJ	57381	NM_020663	CCACUGUGUUUGACCACUA
D-010367-03	RHOJ	57381	NM_020663	UCGUAAACCCUGCCUCUUA
D-010367-04	RHOJ	57381	NM_020663	CCCGUUUGCUGUAUAUGAA
D-009943-01	RHOQ	23433	NM_012249	UACCGGAACUUAAGGAAUA
D-009943-02	RHOQ	23433	NM_012249	AGAAUAGGAUCAAGAUGUA
D-003317-08	**KIF11**	**3832**	**NM_004523**	**CUAGAUGGCUUUCUCAGUA**
D-009943-03	RHOQ	23433	NM_012249	UAGCAAGACUGAAUGAUAU
D-009943-04	RHOQ	23433	NM_012249	GAACAAGGACAGAAACUAG
D-010365-01	RHOT1	55288	NM_018307	GAACUCAACUUCUUUCAGA
D-010365-02	RHOT1	55288	NM_018307	GAACCAGUAUACAGAAAUA
D-010365-03	RHOT1	55288	NM_018307	GAACAUAUCAGAGCUCUUU
D-010365-04	RHOT1	55288	NM_018307	CAGAAUACCUUGCUUAAUC
D-008340-01	RHOT2	89941	NM_138769	UCUCAGAGCUGUUCUACUA
D-008340-02	RHOT2	89941	NM_138769	ACGAAGAGCUCAACGCUUU

D-008340-03	RHOT2	89941	NM_138769	GGACGUGCGCAUCCUGUUA
D-008340-04	RHOT2	89941	NM_138769	GAGAAGAUUCGAACUAAGU
D-006823-01	**INCENP**	**3619**	**NM_020238**	**CCACGAUGCUGACUAAGAA**
D-001206-13	**si*CONTROL* Non-Targeting siRNA Pool**			
D-009882-01	RHOU	58480	NM_021205	GUACUGCUGUUUCGUAUGA
D-009882-02	RHOU	58480	NM_021205	GAACGUCAGUGAGAAAUGG
D-009882-03	RHOU	58480	NM_021205	CAGAGAAGAUGUCAAAGUC
D-009882-04	RHOU	58480	NM_021205	AAGCAGGACUCCAGAUAAA
D-006374-01	RHOV	171177	NM_133639	GAGGGACGAUGUCAACGUA
D-006374-02	RHOV	171177	NM_133639	GAAGAAACUGAAUGCCAAA
D-006374-03	RHOV	171177	NM_133639	GUAUUUGACUCGGCUAUUC
D-006374-04	RHOV	171177	NM_133639	GCUCAGCCUUGACGCAGAA
D-008929-01	RND1	27289	NM_014470	CGACUCGGAUGCAGUAUUA
D-008929-02	RND1	27289	NM_014470	GAACAGAGGGUGGAGCUUA
D-006823-02	**INCENP**	**3619**	**NM_020238**	**CAAGAAGACUGCCGAAGAG**
D-001500-01	**si*TOX* Transfection Control**			
D-008929-03	RND1	27289	NM_014470	GCCAAAAGCUGUUCCAUUA
D-008929-04	RND1	27289	NM_014470	GAACUCAUCUCUUCUACCU
D-009727-01	ARHN	8153	NM_005440	GAACUACACUGCGAGCUUU
D-009727-02	ARHN	8153	NM_005440	GACAUUAGCCGACCAGAAA
D-009727-03	ARHN	8153	NM_005440	ACACAAGGAUCGAGCCAAA
D-009727-04	ARHN	8153	NM_005440	UCAGGGAUGUCUUCCAUGU
D-007794-05	ARHE	390	NM_005168	AGAAUUACACGGCCAGUUU
D-007794-02	ARHE	390	NM_005168	GAACGUGAAAUGCAAGAUA
D-007794-03	ARHE	390	NM_005168	GAAAUUAUCCAGCAAAUCU
D-007794-04	ARHE	390	NM_005168	UAGUAGAGCUCUCCAAUCA
D-006823-03	**INCENP**	**3619**	**NM_020238**	**UCUGCAACAUGGAUAAUAA**
D-006823-04	**INCENP**	**3619**	**NM_020238**	**GCAAAGAGCCAGAGCUGAU**
D-003317-05	**KIF11**	**3832**	**NM_004523**	**GCAGAAAUCUAAGGAUAUA**
D-003317-06	**KIF11**	**3832**	**NM_004523**	**CAACAAGGAUGAAGUCUAU**
D-003317-07	**KIF11**	**3832**	**NM_004523**	**CAGCAGAAAUCUAAGGAUA**
D-003317-08	**KIF11**	**3832**	**NM_004523**	**CUAGAUGGCUUUCUCAGUA**

Table of indvidual siRNAs that gave reproducible effects during validation

Individual siRNAs sequences highlighted in red gave an effect on junction morphology that was reproducible to the pool of all four siRNAs performed in the primary screens.

Candidates that had the same reproducible effects using 2 or more individals siRNAs were scored as a validated candidate.

siRNA	1	2	3	4
Candidate				
RhoA	AUGGAAAGCAGGUAGAGUU	GAACUAUGUGGCAGAUAUC	GAAAGACAUGCUUGCUCAU	GAGAUAUGGCAAACAGGAU
P114RhoGEF	GCACAGAGCCUCCUAGAGA	UCAGGGCGCUUGAAAGAUA	CAAGAGCGGUUGAGCAUGA	GCACUGAGGACUAUGAAGA
MCF2L/Dbs	AAACAGAGCUGCCCAAUGA	CGACAUCGCUUUCAAAUUC	UCAAGGAAAUGCUGAAAUA	CAACAGGCCUUCACAACAA
DLC1	UUAAGAACCUGGAGGACUA	GUACGAAAGAGGAGCGUUU	UUAAAGAAGUCAAAGAGAA	UUAAAGAAGUCAAAGAGAA
DLC2	GAUGUGAACUUCCAAAGGA	CCAAGGCACUUUCUAUUGA	GGGCAACUUUCCACACUUA	GAAAGUUCCCGACUACAAA
DLC3	GAAGAAGGACACUCCAUUU	CGACGUGGCUGACCUGCUA	GAACCUGCGUCAAAUGAAU	GAACCCACCUUUGCCUCUA
MRCKa	CCAUAUAACUUGUGUAAAC	GGAAACAAAUGGUUAGAAA	GCGCAAGACUCACCAGUUU	GAAGAUAGAUUGCCUGAAG
MRCKb	GAAGUGGGUUGGGAUUCUA	GAAGAAUACUGAACGAAUU	GAGAAACACGGAAAUAUUA	CGAGAAGACUUUGAAAUAA
Obscurin/OBSCN	GCAGACAGCGACACCUAUA	AGACAUACCGCGAAGAUGA	GGAAGGACAUACACUCUCA	CAGGAGAGAUCCAAUUUGU
OPHN1	GAAAGAAUCUCAGUUACAA	GCGAGAGGCUCAAGUGUUA	GAACAUAGUGGUGGAAAUA	GCUAGUGAUUUGCUGAUUA
PLXNA1	GAACGUGCCUGACCUCUCA	GCAGAUCGAUGACGACUUC	GCAGUGAACCGCAUCUAUA	GCACCAACCUGGCCACUGU
PLXNB1	GAGAGGAGCCGACUACGUA	GCAGAGACCUCACCUUUGA	GCAAACAUCUGAUAACAUG	UCACAGACCUCAUGACUGA
TC10/RhoQ	UACCGGAACUUAAGGAAUA	AGAAUAGGAUCAAGAUGUA	UAGCAAGACUGAAUGAUAU	GAACAAGGACAGAAACUAG
Trio	GAUAAGAGGUACAGAGAUU	GGAAGUCGCUCCUUGACAA	CAACGGAGAGUCCAUGUUA	GAACACCAACUUCAGAUAA
Vav3	UAAUAGAUCUUCAGCAGUA	GCAGAGACCGAACUUAUUA	GCAAAGCACAUCAAGAUUU	AGACCGAACUUAUUAAUAG

Table of primary observations made in the siRNA junction assembly screen

Rack	Well	Gene Symbol	notes set 1	notes set 2
Plate 1	A01	INCENP		
Plate 1	B01	siTOX		
Plate 1	C01	siControl		
Plate 1	D01	INCENP		
Plate 1	E01	FLJ20896/ARHGAP10/Graf2		
Plate 1	F01	KIF11	large bi nuclear cells	large bi nuclear cells
Plate 1	G01	KIF11	large bi nuclear cells	large bi nuclear cells
Plate 1	H01	KIF11		large bi nuclear cells
Plate 1	A02	ABR (active BCR related); GAP		
Plate 1	B02	ARHGAP1		
Plate 1	C02	ARHGAP11A		
Plate 1	D02	ARHGAP17 / Nadrin / Rich1		
Plate 1	E02	ARHGAP21		
Plate 1	F02	ARHGAP23		
Plate 1	G02	ARHGAP26 / Graf		
Plate 1	H02	ARHGAP28		
Plate 1	A03	AKAP13; LBC	beta cat staining weaker at junctions, ruffling	occludin stain present at junctions alpha cat present at junctions looks weaker some ruffling
Plate 1	B03	ALS2 / Alsin		
Plate 1	C03	ARHGAP15		
Plate 1	D03	ARHGAP18		
Plate 1	E03	ARHGAP22 / p68RacGAP	Z0-1 staining looks patchy	occludin stain present at junctions +alpha cat looks normal
Plate 1	F03	ARHGAP24		
Plate 1	G03	LOC201176 / ARHGAP27 / CAMGAP1		
Plate 1	H03	ARHGAP4		
Plate 1	A04	ARHGAP6	cells look larger b-catenin stain shows ruffling	alpha catenin looks weaker at junctions
Plate 1	B04	ARHGAP9		
Plate 1	C04	ARHGDIG		
Plate 1	D04	ARHGEF10		
Plate 1	E04	ARHGEF15; Vsm-RhoGEF		
Plate 1	F04	ARHGEF17; p164-RhoGEF		
Plate 1	G04	ARHGEF2		
Plate 1	H04	ARHGEF4; ASEF (APC-stimulated)		
Plate 1	A05	ARHGAP8; BPGAP1		
Plate 1	B05	ARHGDIA		
Plate 1	C05	ARHGEF1 / p115-RhoGEF / Lsc		
Plate 1	D05	ARHGEF11		
Plate 1	E05	ARHGEF16	cells look larger b-catenin stain shows ruffling ZO-1 normal	cells look larger alpha cat show ruffling occludin normal
Plate 1	F05	ARHGEF18/ SA-RhoGEF / p114RhoGEF	B-catenin stain looks weaker Z01 normal	occludin absent from junctions alpha cat looks weaker
Plate 1	G05	ARHGEF3 /XPLN		
Plate 1	H05	ARHGEF5	B-catenin stain looks weaker ruffling	occludin looks weaker alpha catenin ruffling
Plate 1	A06	ARHGDIB	B-catenin stain looks weaker ruffling Z0-1 looks normal	occludin stain absent in patches alpha cat shows ruffling
Plate 1	B06	ARHGEF12, LARG	B-catenin stain looks weaker and diffuse around junctions	occludin and alpha cat stain weak or absent at junctions
Plate 1	C06	ARHGEF19		
Plate 1	D06	ARHGEF6 / a-PIX	B-catenin stain looks weaker at junctions	both stains look normal
Plate 1	E06	ARHGAP20	Z01 +b catenin look normal	occludin stain not present at junctions
Plate 1	F06	CDC42EP2 / MSE55 / Borg5	B-catenin stain looks weaker	both stains look normal
Plate 1	G06	SPEC2 (small cdc42 effector)		
Plate 1	H06	CHN2		
Plate 1	A07	ARHGEF7 b-PIX / Cool-1	B-cat stain shows membrane ruffling Z0-1 normal	Occludin stain absent from junctions a-cat looks weak
Plate 1	B07	BCR	b-cat shows membrane ruffling -Z01 normal	Occludin stain absent from junctions a-cat looks weak
Plate 1	C07	CDC42BPA; MRCKalpha	b-cat shows membrane ruffling -Z01 normal	Occludin stain absent from junctions a-cat looks weak
Plate 1	D07	HSMDPKIN CDC42 binding protein kinase gamma		
Plate 1	E07	CDC42EP3		
Plate 1	F07	CDC42EP5		
Plate 1	G07	CENTD1		
Plate 1	H07	CENTD3		
Plate 1	A08	ARHGEF9 / Collybistin / PEM-2	B-cat stain shows membrane ruffling Z01 normal	a-cat stain shows ruffling occuldin normal
Plate 1	B08	C9ORF100		
Plate 1	C08	CDC42BPB / MRCK2 (beta)	B-cat stain shows membrane ruffling Z01 normal	occludin and alpha cat stain weak or absent at junctions
Plate 1	D08	CDC42EP1		
Plate 1	E08	CDC42EP4 /		
Plate 1	F08	SPEC1		
Plate 1	G08	CENTD2	B-catenin stain show membrane ruffling	
Plate 1	H08	CHN1 / chimerin-1 / N-chimerin		
Plate 1	A09	CIT / Citron kinase		
Plate 1	B09	CYBB, cytochrome B		
Plate 1	C09	DEPDC2 / P-REX2	Very small number of cells left on coverslide	
Plate 1	D09	DLC1	B-catenin stain looks weaker	
Plate 1	E09	DOCK10	B-catenin stain looks weaker ruffles +spikes	
Plate 1	F09	DOCK2	B-catenin stain looks weaker	occludin absent at junctions a-cat weaker
Plate 1	G09	DOCK5		
Plate 1	H09	DOCK7	B-catenin stain looks weaker	
Plate 1	A10	CYBA		
Plate 1	B10	DEF6 / IBP		
Plate 1	C10	DEPDC2		
Plate 1	D10	DNMBP		
Plate 1	E10	DOCK11 / Zizimin-2		
Plate 1	F10	DOCK3		
Plate 1	G10	DOCK6		
Plate 1	H10	DOCK8		
Plate 1	A11	DEPDC1B	larger cells ruffled membrane b-catein abnormal Zo-1 and golgi stain looks like ER	
Plate 1	B11	DOCK1 / DOCK180		
Plate 1	C11	DOCK4	larger cells ruffled membrane b-catein abnormal Zo-1 and golgi stain looks like ER	occludin absent at junctions a-cat weaker
Plate 1	D11	DOCK9		
Plate 1	E11	FGD4		
Plate 1	F11	ARHGAP25	B-catenin stain looks weaker	
Plate 1	G11	GNE		
Plate 1	H11	KALRN, Karlirin		
Plate 1	A12	DVL1		
Plate 1	B12	ECT2		
Plate 1	C12	FARP2		
Plate 1	D12	FGD2		
Plate 1	E12	FGD5	B-catenin stain looks weaker	
Plate 1	F12	GAS8		
Plate 1	G12	GRLF1, p190RhoGAP-A		
Plate 1	H12	ITSN1	B-catenin stain looks weaker at junctions more diffuse	occludin stain absent from junctions -alpha cat looks weaker

Plate 2	**A01**	DVL2	more round looking cells Z0-1 stain weaker	occludin stain absent from junctions -alpha cat looks ok
Plate 2	**B01**	ELMO1	more round looking cells Z0-1 stain weaker	
Plate 2	**C01**	FGD1		
Plate 2	**D01**	FGD3		
Plate 2	**E01**	FGD6		
Plate 2	**F01**	GMIP		
Plate 2	**G01**	INPP5B	B-catenin stain more diffuse Z0-1 weaker	
Plate 2	**H01**	ITSN2	B catenin stain more diffuse	**occludin stain absent in patches alpha cat show ruffling**
Plate 2	**A02**	LZTFL1, leucineZiper .		
Plate 2	**B02**	MAP3K9, MLK1		
Plate 2	C02	MCF2L2		
Plate 2	D02	MYLK2	B-catenin stain weaker	occludin patchy
Plate 2	E02	NF1		
Plate 2	F02	NOX1		
Plate 2	G02	OCRL	B-catenin stain weak diffuse Z0-1 stain absent from junctions golgi strange	occludin patchy alpha cat ruffling
Plate 2	H02	PAK1	B-catenin stain weak Z0-1 weak golgi looks little fragmented	
Plate 2	A03	MAP3K11, MLK3		occludin stain weaker dotted alpha cat shows ruffling
Plate 2	B03	MCF2, Dbl	golgi looks little bit fragmented	
Plate 2	C03	KIAA1804, MLK4		
Plate 2	D03	MYO9A	B-catenin stain weak	occludin slighty weaker at junctions
Plate 2	E03	NGEF	ER like Z0-1 staining	very spiky cell membrane both stains present at junctions
Plate 2	F03	NOXA1		occludin looks weaker at junctions
Plate 2	G03	OPHN1		
Plate 2	H03	PAK2		
Plate 2	A04	MCF2L		
Plate 2	B04	PARD6B		
Plate 2	C04	NET1		
Plate 2	D04	PRKCL2		occludin stain patchy alpha cat ruffling
Plate 2	E04	OBSCN	weak B-catenin and weak Z0-1 staining	
Plate 2	F04	PLD3		occludin stain patchy
Plate 2	G04	PAK3	golgi looks smaller more clumped together	
Plate 2	H04	PLEKHG3	b-catenin stain shows membrane ruffling poss golgi effect ?	occludin weaker
Plate 2	A05	PAK4		
Plate 2	B05	PAK7 aka PAK5	membrane shows large spikes ruffling golgi looks abnormal	spiky membranes
Plate 2	C05	PARD6G		occludin weaker
Plate 2	D05	PIK3R2	B-catenin stain weak + zo-1 stain weak + poss golgi effect ?	weaker occludin
Plate 2	E05	PKN3		
Plate 2	F05	PLD1		
Plate 2	G05	LOC122618		
Plate 2	H05	PLEKHG1	b-catenin and Z0-1 stain weaker	occludin absent at junctions
Plate 2	A06	PAK6		
Plate 2	B06	PARD6A	Golgi looks compressed b-catenin stain +z01 stain weak	
Plate 2	C06	PIK3R1	golgi looks thin tubulated +z0-1 stain weak	
Plate 2	D06	PRKCL1 / PKN		
Plate 2	E06	PLCE1		
Plate 2	F06	PLD2		
Plate 2	G06	FLJ40773		occludin weaker
Plate 2	H06	PLEKHG2, Clg	Golgi looks bit fragmented b-cat stain weak bi nuculated cells	occludin weaker
Plate 2	A07	PLEKHG4		occludin patchy
Plate 2	B07	FLJ10665 / PLEKHG6	larger cells ruffled membrane	occludin patchy
Plate 2	C07	PLXNB1		occludin absent from junctions gaps between cells
Plate 2	D07	PTK9 / Twinfilin		occludin absent
Plate 2	E07	RAD51L3		occludin absent at junctions a-cat weaker
Plate 2	F07	RASGRF1		
Plate 2	G07	RHPN2		
Plate 2	H07	ROCK2		
Plate 2	A08	KIAA0720 / PLEKHG5	golgi looks stange tubulated z0-1 weaker	occludin weaker alpha cat weaker
Plate 2	B08	PLEKHK1		
Plate 2	C08	PLXNB2		occludin weaker at junctions
Plate 2	D08	PTK9L		occludin weak absent at junctions chromosomal segrgation
Plate 2	E08	RALBP1	possiable golgi effect Z0-1 weaker	occludin absent poss DNA effect
Plate 2	F08	RASGRF2		
Plate 2	G08	ROCK1		
Plate 2	H08	RRAS2	membrane ruffling all other stains ok	
Plate 2	A09	PLXNA1	stange golgi orientation	occludin absent from junction
Plate 2	B09	SOS2		
Plate 2	C09	RACGAP1	multi- nuclear cells about 40%	multi nuclear cells
Plate 2	D09	SRGAP2		
Plate 2	E09	RHPN1	weak B-catenin staining	
Plate 2	F09	TIAM1		
Plate 2	G09	RTKN		
Plate 2	H09	VAV1		occludin stain absent from junction
Plate 2	A10	RTKN		
Plate 2	B10	SMURF1		
Plate 2	C10	SPATA13	golgi, zo-1 b-catenin weaker	occludin stain weaker / absent from junctions
Plate 2	D10	SRGAP1		
Plate 2	E10	STARD13, DLC2	weak b-catenin compressed golgi z01 weak	weaker occludin
Plate 2	F10	TRIP10	large cells fragmented golgi weaker b-catenin + Z01	cells larger membrane ruffling
Plate 2	G10	TIAM2	Golgi looks different orientation + z0-1 weak	occludin stain weaker
Plate 2	H10	TRIO		occludin weaker at junctions
Plate 2	A11	SH3BP1		
Plate 2	B11	SOS1		
Plate 2	C11	SRF		
Plate 2	D11	FNBP2		occludin weaker alpha catenin weaker
Plate 2	E11	STARD8, DLC3	B-catenin + z0-1 weaker	occludin absent alpha cat weak
Plate 2	F11	TAGAP	weak B-catenin	
Plate 2	G11	TNK2		
Plate 2	H11	TRIP10		
Plate 2	A12	VAV2		
Plate 2	B12	CDC42	larger number of detached looking cells looks of ruffling weak b-cat stain golgi look odd	
Plate 2	C12	RAC3		
Plate 2	D12	RHOB		
Plate 2	E12	RHOBTB3	B-catenin stain looks weak +Z0-1	occuldin weak at junction in patches alpha cat look ok
Plate 2	F12	RHOD		
Plate 2	G12	RHOH		
Plate 2	H12	RHOQ		

Plate 3	**A01**	VAV3		
Plate 3	**B01**	RAC1	**B catenin weaker cell rufflin ZO-1 looks ER like golgi smaller**	
Plate 3	**C01**	RHOA	**B catenin weak at junctions Z0-1 patchy golgi look more fragmented**	
Plate 3	**D01**	RHOBTB1	**B-catenin more diffuse Z01-looks normal**	
Plate 3	**E01**	RHOC	**B-catein weaker more diffuse**	
Plate 3	**F01**	RHOF		
Plate 3	**G01**	RHOJ		
Plate 3	**H01**	RHOT1		
Plate 3	**A02**	RAC2		
Plate 3	**B02**	RHOU		
Plate 3	C02	RHOBTB2		
Plate 3	D02	RHOV		
Plate 3	E02	RHOG	**b-catenin weaker more diffuse at junctions**	
Plate 3	F02	RND1		
Plate 3	G02	RHOT2		
Plate 3	H02	ARHN		
Plate 3	A03	ARHE		
Plate 3	B03	INCENP	**larger looking cells strange tubulated golgi**	
Plate 3	C03	KIF11		
Plate 3	D03	FARP1		
Plate 3	E03	ARHGAP25		
Plate 3	F03	ARHGAP5	**b-catenin weaker more diffuse at junctions**	
Plate 3	G03	PAK3		
Plate 3	H03	MYO9A		
Plate 3	A04	FLNA	**B-catein weaker more diffuse**	
Plate 3	B04	MYH9	**more cell ruffling**	
Plate 3	C04	MYO10		
Plate 3	D04	PLEC1		
Plate 3	E04	CTNNA1	**B-catenin absent from junctions Z0-1 absent**	
Plate 3	F04	CTNNA2		
Plate 3	G04	CTNNA3	**B-catein weak Z0-1 absent from junctions**	
Plate 3	H04	CTNNAL1		
Plate 3	A05	DIAPH1	**weaker b-catenin**	
Plate 3	B05	DIAPH2		
Plate 3	C05	DIAPH3	**weaker b-catenin**	
Plate 3	D05	MAP4K1		
Plate 3	E05	MAP4K2	**weaker b-catenin at junctions weaker Z0-1**	
Plate 3	F05	MAP4K3		
Plate 3	G05	MAP4K4		
Plate 3	H05	MAP4K5	**weaker B-catenin**	
Plate 3	A06	MYH10		
Plate 3	B06	MYH11		
Plate 3	C06	MYH13		
Plate 3	D06	MYH14	**B-catenin weak in patches**	
Plate 3	E06	KIAA1000		
Plate 3	F06	MYH16		
Plate 3	G06	MYH2	**B-catenin weak at junctions golgi looks fragmented**	
Plate 3	H06	MYH3		
Plate 3	A07	MYH4		
Plate 3	B07	MYH6		
Plate 3	C07	MYH6		
Plate 3	D07	MYH7		
Plate 3	E07	MYH7B	**B-catenin still present at junctions looks more cytoplasmic /perinuclear**	
Plate 3	F07	MYH8	**cells appear larger slightly more diffuse B-catenin stain at junctions**	
Plate 3	G07	MYO15A		
Plate 3	H07	MYO18A		
Plate 3	A08	MYO18B		
Plate 3	B08	MYO1A		
Plate 3	C08	MYO1B		
Plate 3	D08	MYO1C	**weaker b-catenin and Z0-1 at junctions**	
Plate 3	E08	MYO1D		
Plate 3	F08	MYO1E		
Plate 3	G08	MYO1F		
Plate 3	H08	MYO1G		
Plate 3	A09	MYO3A		
Plate 3	B09	MYO3B		
Plate 3	C09	MYO5A		
Plate 3	D09	MYO5B		
Plate 3	E09	MYO5C		
Plate 3	F09	MYO6		
Plate 3	G09	MYO7A		
Plate 3	H09	MYO7B	**B-catenin stain looks weaker at junctions but looks increased nuclear B-catenin**	
Plate 3	A10	MYOHD1		
Plate 3	B10	PTK2		
Plate 3	C10	PTK2B		
Plate 3	D10	PTPN14		
Plate 3	E10	PTPN21		
Plate 3	F10	PTPN3		
Plate 3	G10	PTPN4		
Plate 3	H10	TNIK	**B-catenin stain absent from junctions Z0-1 absent golgi look small**	
Plate 3	A11	MYLIP		